

AFAL-TR-78-16
Volume I

①

AD-A051885

FIRE CONTROL SYSTEM ANALYSIS

Volume I - Analysis Tasks

Prepared By:

University of Dayton
Research Institute
Dayton, Ohio 45469



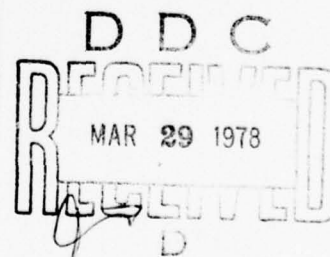
November 1977

Technical Report AFAL-TR-78-16, Vol I

Final Report for Period 1 Nov 76 - 30 Sep 77

Approved for public release; distribution unlimited.

AIR FORCE AVIONICS LABORATORY
AIR FORCE WRIGHT AERONAUTICAL LABORATORIES
AIR FORCE SYSTEMS COMMAND
WRIGHT-PATTERSON AIR FORCE BASE, OHIO 45433



NOTICE

When Government drawings, specifications, or other data are used for any purpose other than in connection with a definitely related Government procurement operation, the United States Government thereby incurs no responsibility nor any obligation whatsoever; and the fact that the government may have formulated, furnished, or in any way supplied the said drawings, specifications, or other data, is not to be regarded by implication or otherwise as in any manner licensing the holder or any other person or corporation, or conveying any rights or permission to manufacture, use, or sell any patented invention that may in any way be related thereto.

This report has been reviewed by the Information Office (OI) and is releasable to the National Technical Information Service (NTIS). At NTIS, it will be available to the general public, including foreign nations.

This technical report has been reviewed and is approved for publication.

Dennis A. Laro, Capt

Arthur G. Duke Jr

FOR THE COMMANDER

Marvin Spector

"If your address has changed, if you wish to be removed from our mailing list, or if the addressee is no longer employed by your organization please notify AEAL/RWT, W-PAFB, OH 45433 to help us maintain a current mailing list".

Copies of this report should not be returned unless return is required by security considerations, contractual obligations, or notice on a specific document.

UNCLASSIFIED

SECURITY CLASSIFICATION OF THIS PAGE (When Data Entered)

REPORT DOCUMENTATION PAGE		READ INSTRUCTIONS BEFORE COMPLETING FORM
1. REPORT NUMBER AFAL-TR-78-16, Volume I	2. GOVT ACCESSION NO.	3. RECIPIENT'S CATALOG NUMBER
4. TITLE (and Subtitle) Fire Control System Analysis Volume I - Analysis Tasks		5. TYPE OF REPORT & PERIOD COVERED Final Report 11/1/76-9/30/77
		6. PERFORMING ORG. REPORT NUMBER
7. AUTHOR(s) Lowell Ryan, Ron Reboulet, Steven Gustafson Philip Fry		8. CONTRACT OR GRANT NUMBER(s) F33615-77-C-1056
9. PERFORMING ORGANIZATION NAME AND ADDRESS University of Dayton Research Institute Dayton, Ohio 45469		10. PROGRAM ELEMENT, PROJECT, TASK AREA & WORK UNIT NUMBERS 63605F/76290359
11. CONTROLLING OFFICE NAME AND ADDRESS Air Force Avionics Laboratory Wright-Patterson AFB, Ohio 45433		12. REPORT DATE November 1977
		13. NUMBER OF PAGES 214
14. MONITORING AGENCY NAME & ADDRESS (if different from Controlling Office)		15. SECURITY CLASS. (of this report) UNCLASSIFIED
		15a. DECLASSIFICATION/DOWNGRADING SCHEDULE
16. DISTRIBUTION STATEMENT (of this Report) This document has been approved for public release and sale; its distribution is unlimited.		
17. DISTRIBUTION STATEMENT (of the abstract entered in Block 20, if different from Report)		
18. SUPPLEMENTARY NOTES		
19. KEY WORDS (Continue on reverse side if necessary and identify by block number) Kalman Filter, Target State Measurement, Radar Lag, Multiple Digital Scan Converter, Air Combat Evaluation Algorithm		
20. ABSTRACT (Continue on reverse side if necessary and identify by block number) The following three tasks are included in Volume I. Gaussian noise added to true range generated by various kinds of simulated tra- jectories served as "measurements" which were input to several kinds of Kalman filters. Filter output is compared graphically and by rms deviations. Independent methods were devised for evaluating the accuracy of target state vectors (position, velocity, and acceleration) obtained from a director fire control system. (Continued)		

DD FORM 1 JAN 73 1473

EDITION OF 1 NOV 65 IS OBSOLETE

UNCLASSIFIED

SECURITY CLASSIFICATION OF THIS PAGE (When Data Entered)

UNCLASSIFIED

SECURITY CLASSIFICATION OF THIS PAGE(When Data Entered)

20. ABSTRACT (Continued)

Attempts to find an adequate software correction to the radar lag were not successful. Analysis of data on Sight Eval tapes casts doubt on its validity.

Volume II contains reports on the following tasks. The equations used in the LCOS, TRACER, and ACE algorithms were rewritten such that they could be performed on the MDSC computer. The ACE algorithm was modified for implementation on the ROLM 16/64 computer.

ABSTRACT for	
WFO	White Section <input checked="" type="checkbox"/>
BOB	Both Section <input type="checkbox"/>
UNANNOUNCED	<input type="checkbox"/>
JUSTIFICATION	
BY	
DISTRIBUTION/AVAILABILITY CODES	
ONE	AVAIL. NO/NO SPECIAL
A	

UNCLASSIFIED

SECURITY CLASSIFICATION OF THIS PAGE(When Data Entered)

TABLE OF CONTENTS

SECTION		PAGE
1	BACKGROUND	1
2	TASK DEFINITION	3
2.1	IDENTIFY RADAR RANGE ERRORS AND DEVELOP FILTER	3
2.2	TARGET STATE MEASUREMENT	3
2.3	IDENTIFY AND CORRECT RADAR LAG PROBLEM	3
3	ANALYSIS SUPPORT	5
3.1	IDENTIFY RADAR RANGE ERRORS AND DEVELOP FILTER	5
3.1.1	INTRODUCTION	5
3.1.2	THEORY	6
3.1.3	PERFORMANCE	16
3.1.4	EVALUATION	28
3.1.5	CONCLUSIONS	35
3.2	TARGET STATE MEASUREMENT	37
3.2.1.	INTRODUCTION	37
3.2.2	FORMULATION OF THE MONTE CARLO STUDY	44
3.2.3	RESULTS OF THE MONTE CARLO STUDY	56
3.2.4	SUGGESTIONS FOR FUTURE STUDY	63
3.3	IDENTIFY AND CORRECT RADAR LAG PROBLEM	65
3.3.1	INTRODUCTION	65
3.3.1.1	BACKGROUND	65
3.3.1.2	MOTIVATION	65
3.3.1.3	SCOPE AND OBJECTIVES OF THE PROBLEM	66

TABLE OF CONTENTS (CONTINUED)

SECTION		PAGE
3	3.3.2 DATA COLLECTION	67
	3.3.2.1 GENERAL	67
	3.3.2.2 DESCRIPTION OF TEST MISSIONS	68
	3.3.2.3 INSTRUMENTATION AND RECORDED DATA	71
	3.3.3 PRELIMINARY DATA EVALUATION AND PROCESSING	74
	3.3.3.1 DESCRIPTION AND SELECTION OF DATA	74
	3.3.3.2 EVALUATION AND PRELIMINARY PROCESSING OF DATA	77
	3.3.4 ANALYSIS AND CORRECTION OF LAG PROBLEM	81
	3.3.4.1 LINEAR REGRESSION	81
	3.3.4.2 LINE-OF-SIGHT RATE OF CHANGE ANALYSIS	101
	3.3.4.3 TIME DATA PHASE SHIFT	109
	3.3.4.4 SUGGESTIONS FOR FUTURE STUDY	118
APPENDIX A	COMPARISON OF KALMAN FILTERS	119
APPENDIX B	PROGRAMS FOR KALMAN FILTERS	152
APPENDIX C	PROGRAM FOR TARGET STATE MEASUREMENT	174
APPENDIX D	RADAR LAG PROGRAM	189

LIST OF ILLUSTRATIONS

FIGURE		PAGE
1	Simulated Measurement Noise	18
2	Position Kalman Gain Component	24
3	Velocity Kalman Gain Component	25
4	Acceleration Kalman Gain Component	26
5	Simplified Block Diagram of the Director Fire Control System	38
6	Diagram of the Evaluation Method for the Acceleration of the Target Relative to the Attacker	48
7	Diagram of the Evaluation Method for the Velocity of the Target Relative to the Attacker	49
8	Diagram of the Evaluation Method for the Position of the Target Relative to the Attacker	50
9	Error Distribution of the Magnitude of the Acceleration of the Target Relative to the Attacker Obtained Using Simulated ISA and HARS Data	57
10	Error Distribution of the Magnitude of the Acceleration of the Target Relative to the Attacker Obtained Using Simulated ISA and HARS data.	58
11	Error Distribution of Components of the Acceleration of the Target Relative to the Attacker in the Attacker's Body Frame Obtained Using Simulated ISA and HARS Data	59
12	Error Distribution of the Magnitude of the Velocity of the Target Relative to the Attacker Obtained Using Simulated ADC and HARS Data	61
13	Error Distribution of the Magnitude of the Position of the Target Relative to the Attacker Obtained Using Simulated DME and SSC Data	62
14	Firing Profile for Actual Mission With a Drone Target (PQM-102)	69

LIST OF ILLUSTRATIONS (CONTINUED)

FIGURE		PAGE
15	Test Matrix	70
16	Electrical Analog Signals Recorded in Flight During Sight Eval.	72
17	Signals Recorded on Flight Film	73
18	Processing From Flight Records to the WPAFB Data Tape	75
19	Recorded Missions	76
20	RMS Range Error	80
21	Data Group I	89
22	Data Group II	90
23	Data Group III	91
24	Data Group IV	92
25	Data Group V	93
26	Data Group VI	94
27	Data Group VII	95
28	Mean EL Error Before Tracking Correction	96
29	Mean EL Error After Tracking Correction	97
30	Mean AZ Error Before Tracking Correction	98
31	Mean AZ Error After Tracking Correction	99
32	Radar Lag Angle Definition	102
33	Radar Leading Target	110
34	Radar Leading Target	111
35	Lag in Radar Azimuth	112
36	Lag in Both Radar Components	114
37	Lag in Both Radar Components	115

LIST OF TABLES

TABLE		PAGE
1	Noise Terms $v(k)$	19
2	Simulated Trajectories and Noise Variances	21
3	RMS Range Deviation	30
4	RMS Velocity Deviations	31
5	RMS Acceleration Deviations	32
6	Real and Test Inputs to the Director System	42
7	Occurrence and Accuracy Distributions for the ISA Acceleration Components	51
8	Occurrence and Accuracy Distributions for the HARS Roll, Pitch, and Yaw Angles	52
9	Occurrence and Accuracy Distributions for ADC True Air Speed and Angle of Attack	53
10	Occurrence and Accuracy Distributions for DME Range and for SSC Azimuth and Elevation Angles	54
11	Tape Data Variables	78
12	Tracking Rates (η_F, ϵ_F) vs Mean Radar Error (μ)	82
13	List of Passes Checked	105
14	Comparison of Average Lag Before and After Frame Shift	116
15	Comparison of Average Lag Before and After Frame Shift	117

SECTION 1

BACKGROUND

The recognition by the Air Force Avionics Laboratory (AFAL) of the need for improved sensors and techniques for implementing fire control director algorithms has resulted largely from the conclusions of two programs - EXPO V and Fire/Fly. EXPO V is the latest in a series of man-in-the-loop simulation studies of new fire control and gunsight concepts. The Fire/Fly program is the integrated Fire Control/Flight Control study which is investigating methods for integrating the fire control system with the flight control system to improve effectiveness while increasing survivability. Both programs have cited the necessity for improved sensors as well as improved director algorithms.

The purpose of the Fire Control Systems analysis effort, summarized in the following report, was to examine existing fire control systems test data (Sight Eval), identify error sources, evaluate and modify fire control algorithms, and perform programming for simulation, weapon system investigation, and validation.

The tasks contained in this volume were of an analytical nature.

SECTION 2

TASK DEFINITION

The broad categories of effort contained in the Statement of Work were refined by coordination with Captain J. Silverthorn, RWT-2, and resulted in the following series of tasks.

2.1 IDENTIFY RADAR RANGE ERRORS AND DEVELOP FILTER

An important input to the director gunsight computations is target range. As a result, it is desirable to have as accurate a range measurement as possible. Some type of filter (Kalman or other) is needed to produce an accurate estimate of range (and range rate). To accomplish this task, an approximate noise model is needed to aid in the filter design process. This noise model can also be used in the Air Force Flight Dynamics Laboratory (AFFDL) LAMARS simulation.

2.2 TARGET STATE MEASUREMENT

Two important subsystems of the director system are the target position sensor and Kalman angle filter. An appropriate performance measure for these subsystems is their ability to estimate target state (position, velocity, acceleration). As a result, to evaluate their performance it is necessary to independently measure these target parameters more accurately than the expected estimation errors. A technique must be developed and analyzed to accomplish this task.

2.3 IDENTIFY AND CORRECT RADAR LAG PROBLEM

The MA-1 radar was seen to lag the target by as much as 50 mrad during the Sight Eval flight test. Since this same radar is to be used during the director flight test for initial acquisition and handoff to the ASCOT sensor, it is necessary to be able to predict the lag so that the net error (difference between target true position and radar estimate) is less than ASCOT scan size (± 15 mrad).

SECTION 3
ANALYSIS SUPPORT

3.1 IDENTIFY RADAR RANGE ERRORS AND DEVELOP FILTER

3.1.1 Introduction

This report evaluates the performance of certain optimal and sub-optimal Kalman filters in yielding estimates of target state variables. The evaluation uses simulated trajectories with noise added to the true range as input to the filters, and compares filter estimates of the state variables to their true values.

A Kalman filter is often designed with respect to the coordinate system in which the target position is measured; normally the inertial or line-of-sight coordinate system. The filters considered in this report use only range information. Therefore, to give a complete specification of the target state, the relative range, relative radial velocity, and relative radial acceleration estimates yielded by these filters must be converted to a useful frame by coordinate transformations based on angular position, angular rate, and angular accelerations as measured by suitable devices and estimated by other filters.

Four Kalman range filters were compared. The first three were based on a constant relative radial acceleration model and the fourth on a constant relative radial velocity model.

To evaluate and compare these filters, trajectories of various types were generated, noise was added to each true range, and the resulting "measurement" was used as input to each filter.

Results are given graphically and as root-mean-square deviations of the filter estimate of range, (radial) velocity, and (radial) acceleration over a chosen interval.

The simulated constant acceleration trajectories assume (constant) accelerations of 0, 1g (9.8 m s^{-2}), and 6g (58.8 m s^{-2}). Two simulations assume a constant negative acceleration. The initial range and velocity were assumed to be 600 m and 200 m s^{-1} , respectively.

Two similar trajectories resulting from variable acceleration were also used as simulations. These resulted from sinusoidal accelerations of 8 sec. period and amplitudes of either 2g or 6g. The initial range was assumed to be 600 m and the initial velocity was zero.

3.1.2 Theory

Filter A: Constant Acceleration Model - Time Varying Gain

Let the state vector representing the target be denoted by

$$\underline{x}(t) = \begin{bmatrix} x_1(t) \\ x_2(t) \\ x_3(t) \end{bmatrix}$$

where $x_1(t)$, $x_2(t)$, and $x_3(t)$ represent the range, (radial) velocity, and (radial) acceleration, respectively, of the target at time t . The constant acceleration model assumes that the state vector evolves in time according to

$$\begin{aligned} \dot{x}_1 &= x_2 \\ \dot{x}_2 &= x_3 \\ \dot{x}_3 &= w(t) \end{aligned}$$

where $w(t)$ is assumed to be zero-mean, Gaussian noise uncorrelated with itself in time. This model can be written in matrix form as

$$\dot{\underline{x}}(t) = F\underline{x}(t) + Gw(t) \quad (1)$$

where

$$F = \begin{bmatrix} 0 & 1 & 0 \\ 0 & 0 & 1 \\ 0 & 0 & 0 \end{bmatrix}, \quad G = \begin{bmatrix} 0 \\ 0 \\ 1 \end{bmatrix}$$

Assuming that $w(t)$ is constant over the interval (t_0, t) , the solution of Eq. (1) is given by

$$\underline{x}(t) = \phi(t, t_0)\underline{x}(t_0) + \left[\int_{t_0}^t \phi(t, \tau) G(\tau) d\tau \right] w(t) \quad (2)$$

where

$$\phi(t, \tau) = \begin{bmatrix} 1 & t-\tau & \frac{1}{2}(t-\tau)^2 \\ 0 & 1 & t-\tau \\ 0 & 0 & 1 \end{bmatrix}$$

For successive times t_{k+1} and t_k , Eq. (2) becomes

$$\underline{x}(t_{k+1}) = \phi(t_{k+1}, t_k)\underline{x}(t_k) + \left[\int_{t_k}^{t_{k+1}} \phi(t_{k+1}, \tau) G(\tau) d\tau \right] w(t_k) \quad (3)$$

Defining

$$\underline{x}(t_{k+1}) \equiv \underline{x}(k+1)$$

$$\underline{x}(t_k) \equiv \underline{x}(k)$$

$$w(t_k) \equiv w(k)$$

$$\int_{t_k}^{t_{k+1}} \phi(t_{k+1}, \tau) G(\tau) d\tau \equiv \Gamma(k+1, k),$$

Equation (3) can be written as

$$\underline{x}(k+1) = \phi(k+1, k)\underline{x}(k) + \Gamma(k+1, k)w(k)$$

By direct integration,

$$\Gamma(k+1, k) = \int_{t_k}^{t_{k+1}} \phi(t_{k+1}, \tau) G(\tau) d\tau = \begin{bmatrix} \frac{1}{6} T^3 \\ \frac{1}{2} T^2 \\ T \end{bmatrix},$$

where

$$T = t_{k+1} - t_k$$

$$\text{and } \phi(k+1, k) = \phi = \begin{bmatrix} 1 & T & T^2/2 \\ 0 & 1 & T \\ 0 & 0 & 1 \end{bmatrix}$$

Both T and ϕ are constant given a fixed interval between successive measurements.

It is assumed that the maneuver noise term, $w(k)$, is zero-mean Gaussian noise with the autocorrelation property

$$E\{w(j)w'(k)\} = Q(k)\delta_{jk} \quad (4)$$

where

$$Q(k) = \sigma_w^2 \quad (\text{maneuver-noise variance})$$

and δ_{jk} is the Kronecker delta.

A measurement model

$$z(k+1) = H\underline{x}(k+1) + v(k+1) \quad (5)$$

is assumed where $v(k+1)$ is the (scalar) measurement noise,

$$H = [1 \quad 0 \quad 0]$$

is the measurement matrix, and $z(k+1)$ is the measurement at time t_{k+1} . Equation (5) may be written in the scalar form

$$z(k+1) = x_1(k+1) + v(k+1) \quad (6)$$

It is assumed that the measurement noise has the properties

$$E\{v(j)v(k)\} = R(k)\delta_{jk} \quad (7)$$

and

$$E\{v(j)w(k)\} = 0$$

where

$$R(k) = \sigma_v^2$$

is the measurement noise variance; also called the signal noise variance.

The "best" estimate of the state vector at time t_k is denoted by $\hat{\underline{x}}(k|k)$; this estimate based on k measurements $z(k), z(k-1), \dots, z(2), z(1)$. The covariance matrix $P(j|k)$ is defined to be

$$P(j|k) = E \{ [\underline{x}(j) - \hat{\underline{x}}(j|j)] [\underline{x}(k) - \hat{\underline{x}}(k|k)]' \},$$

where the transpose is indicated by a prime.

With these definitions, the Kalman equations are, in the logical order of their execution

$$\left. \begin{aligned} P(k+1|k) &= \phi P(k|k) \phi' + \Gamma Q(k) \Gamma' & (i) \\ \underline{K}(k+1) &= P(k+1|k) H' [H P(k+1|k) H' + \sigma_v^2]^{-1} & (ii) \\ \hat{\underline{x}}(k+1|k+1) &= \phi \hat{\underline{x}}(k|k) + \underline{K}(k+1) [z(k+1) - H \phi \hat{\underline{x}}(k|k)] & (iii) \\ P(k+1|k+1) &= [I - \underline{K}(k+1) H] P(k+1|k) & (iv) \end{aligned} \right\} \quad (8)$$

In order to use Eqs. (8), initial estimates for $\hat{\underline{x}}(k|k)$ and $P(k|k)$ for some value of k are required.

If the position of the target is known exactly at three successive times t_k , $k = 1, 2, 3$, and the target was accelerating uniformly, the velocity $\dot{x}_2(3)$ could be found from the relation

$$\dot{x}_2(k) = \frac{1}{2T} [3x_1(3) - 4x_1(2) + x_1(1)] \quad (9)$$

which may be derived from elementary kinematics. If

instead the measured values of the range in Eq. (9) are used an estimate of the velocity at $k = 3$ is given by

$$\hat{\dot{x}}_2(3|3) = \frac{1}{2T} [3z(3) - 4z(2) + z(1)]$$

Similarly, the acceleration $\ddot{x}_3(3)$ would be given by (again from

elementary kinematics)

$$\hat{\underline{x}}_3(3|3) = \frac{1}{T^2} [z(3) - 2z(2) + z(1)]$$

The first value of k for which these estimates may be formed is $k = 3$; therefore, the earliest estimate of the state vector which can be made using the above procedure is

$$\hat{\underline{x}}_3(3|3) = \begin{bmatrix} z(3) \\ \frac{1}{2T} [3z(3) - 4z(2) + z(1)] \\ \frac{1}{T^2} [z(3) - 2z(2) + z(1)] \end{bmatrix} \quad (10)$$

Because of the extreme sensitivity of $\hat{\underline{x}}_3(3|3)$ to noise, a better (and simpler) estimate is given by

$$\hat{\underline{x}}(3|3) = \begin{bmatrix} z(3) \\ \frac{1}{2T} [3z(3) - 4z(2) + z(1)] \\ 0 \end{bmatrix} \quad (11)$$

To form an initial estimate of $P(3|3)$, we will use Eq.

(10). The state vector at $k = 3$ is represented by

$$\underline{x}(3) = \begin{bmatrix} x_1(3) \\ \frac{1}{2T} [3x_1(3) - 4x_1(2) + x_1(1)] \\ \frac{1}{T^2} [x_1(3) - 2x_1(2) + x_1(1)] \end{bmatrix} \quad (12)$$

Combining Eqs. (6), (10), and (12),

$$\underline{x}(3) - \hat{\underline{x}}(3|3) = \begin{bmatrix} x_1(3) \\ \frac{1}{2T} [3x_1(3) - 4x_1(2) + x_1(1)] \\ \frac{1}{T^2} [x_1(3) - 2x_1(2) + x_1(1)] \end{bmatrix} - \begin{bmatrix} z(3) \\ \frac{1}{2T} [3z(3) - 4z(2) + z(1)] \\ \frac{1}{T^2} [z(3) - 2z(2) + z(1)] \end{bmatrix}$$

$$= - \begin{bmatrix} v(3) \\ \frac{1}{2T} [3v(3) - 4v(2) + v(1)] \\ \frac{1}{T^2} [v(3) - 2v(2) + v(1)] \end{bmatrix} \equiv - \begin{bmatrix} p_1 \\ p_2 \\ p_3 \end{bmatrix}$$

From its definition and from Eqs. (4) and (7), $P(3|3)$ is given by

$$\begin{aligned} P(3|3) &= E \left\{ \begin{bmatrix} p_1 \\ p_2 \\ p_3 \end{bmatrix} [p_1 p_2 p_3] \right\} = E \left\{ \begin{bmatrix} p_1^2 & p_1 p_2 & p_1 p_3 \\ p_1 p_2 & p_2^2 & p_2 p_3 \\ p_1 p_3 & p_2 p_3 & p_3^2 \end{bmatrix} \right\} \\ &= \frac{\sigma_v^2}{2T^4} \begin{bmatrix} 2T^4 & 3T^3 & 2T^2 \\ 3T^3 & 13T^2 & 12T \\ 2T^2 & 12T & 12 \end{bmatrix} \end{aligned} \quad (13)$$

With Eqs. (11) and (13) as initial estimates of the state vector and covariance matrix, the state vector estimate is updated with each new measurement using the Kalman Eqs. (8). [1].

Filter B: Constant acceleration model. Synthetic time-varying gain.

The Kalman gain, $\underline{K}(k)$, computed from the second equation of the set (8) of the previous section, is a function of the measurement interval T , the measurement noise variance σ_v^2 , the maneuver noise variance σ_w^2 , and the iteration number k . To apply the Kalman equations to a particular filtering problem, these parameters must be known, and the Kalman gains may be calculated for each k independent of any measurement. The components of $\underline{K}(k)$ are therefore determined a priori.

A measurement interval of $T = 0.04$ seconds has been used throughout all simulations. For Filter A values of $\underline{K}(k)$ from

$k = 3$ to $k = 200$ were computed. It was supposed that each component of the Kalman gain could be approximated by a function of the form

$$K'_i(k) = \frac{a_i}{k^i - b_i} + K_i(\infty) \quad , \quad i=1,2,3 \quad (14)$$

where the parameters a_i and b_i are found from fitting Eq. (14) to the values $K_i(5)$ and $K_i(30)$ which were computed for Filter A. $K_i(\infty)$ is the value to which $K_i(k)$ is an asymptote. Although Eqs. (14) do not purport to be the best possible fit to the optimum gain components, the advantage is that the $K_i(k)$ are easy to calculate.

If Eq. (14) is used to calculate the Kalman gain components, the state estimate is updated according to the single equation

$$\hat{\underline{x}}(k|k) = \phi \hat{\underline{x}}(k-1|k-1) + \underline{K}'(k) [z(k) - H\phi \hat{\underline{x}}(k-1|k-1)]$$

with a considerable saving in computation time.

Filter C: Constant Acceleration Model. Constant gain.

Figures (1), (2), and (3) show that each component of the Kalman gain assumes its largest value at $k = 4$, and decreases monotonically, asymptotically approaching some minimum value. The motivation of this filter is to find some particular value of k , say $k = i$, such that the constant gain $\underline{K}(i)$ may be used to update the state estimate for each iteration; i.e.,

$$\hat{\underline{x}}(k+1|k+1) = \phi \hat{\underline{x}}(k|k) + \underline{K}(i) [z(k+1) - H\phi \hat{\underline{x}}(k|k)]$$

If i is chosen to be small, the Kalman gain will be relatively large and will remain so, since $\underline{K}(i)$ is constant, by hypothesis. The resulting estimates will be very noisy and

show little tendency to converge. If the value of i chosen is large, the corresponding Kalman gain will be small and errors in the initial estimates will be slowly corrected. It is hoped that an intermediate value of i can be found such that after a reasonable number of iterations, convergence can be achieved.

Filter D: Constant Velocity Model. Time varying gain.

As its name suggests, this filter assumes that the target is moving at constant velocity. The development of the filter equations for this model is parallel to that of Filter A. It is simpler in the sense that the state vector has two components rather than three. The associated matrices are hence 2×2 , rather than 3×3 .

Let the state vector of the target be denoted by

$$\underline{x}(t) = \begin{bmatrix} x_1(t) \\ x_2(t) \end{bmatrix}$$

where $x_1(t)$ represents the range of the target and $x_2(t)$ is its (radial) velocity. This model assumes that the state vector evolves according to

$$\begin{aligned} x_1 &= x_2 \\ \dot{x}_2 &= w(t) \end{aligned}$$

where $w(t)$ is assumed to be zero-mean, Gaussian noise uncorrelated with itself in time. In matrix notation,

$$\dot{\underline{x}}(t) = F\underline{x}(t) + Gw(t) \quad (15)$$

where

$$F = \begin{bmatrix} 0 & 1 \\ 0 & 0 \end{bmatrix}, \quad G = \begin{bmatrix} 0 \\ 1 \end{bmatrix}$$

The solution of Eq. (15) is given by

$$\underline{x}(t) = \phi(t, t_0) \underline{x}(t_0) + \left[\int_{t_0}^t \phi(t, \tau) G(\tau) d\tau \right] w(t) \quad (16)$$

where

$$\phi(t, \tau) = \begin{bmatrix} 1 & t - \tau \\ 0 & 1 \end{bmatrix}$$

For successive measurement times t_{k+1} and t_k , Eq. (16)

becomes

$$\underline{x}(t_{k+1}) = \phi(t_{k+1}, t_k) \underline{x}(t_k) + \left[\int_{t_k}^{t_{k+1}} \phi(t_{k+1}, \tau) G(\tau) d\tau \right] w(t_k) \quad (17)$$

Defining, as before

$$\underline{x}(t_{k+1}) \equiv \underline{x}(k+1)$$

$$\underline{x}(t_k) \equiv \underline{x}(k)$$

$$\int_{t_k}^{t_{k+1}} \phi(t_{k+1}, \tau) G(\tau) d\tau \equiv \Gamma(k+1, k)$$

With the above definitions, Eq. (16) may be written as

$$\underline{x}(k+1) = \phi(k+1, k) \underline{x}(k) + \Gamma(k+1, k) w(k)$$

and by direct integration,

$$\Gamma(k+1, k) = \int_{t_k}^{t_{k+1}} \phi(t_{k+1}, \tau) G(\tau) d\tau = \begin{bmatrix} \frac{1}{2} T^2 \\ T \end{bmatrix}$$

where

$$T \equiv t_{k+1} - t_k$$

and

$$\phi(k+1, k) \equiv \phi = \begin{bmatrix} 1 & T \\ 0 & 1 \end{bmatrix}$$

which is constant, given a fixed interval between successive measurements.

Again, assume that

$$E \{ w(j)w(k) \} = Q(k) \delta_{jk}$$

where

$$Q(k) = \sigma_w^2 \quad (\text{maneuver noise variance})$$

The measurement model is, as before

$$z(k+1) = Hx(k+1) + v(k+1) \quad (18)$$

where $v(k+1)$ is the (scalar) measurement noise and

$$H = [1 \quad 0]$$

so that eq. (18) may be written

$$z(k+1) = x_1(k+1) + v(k+1)$$

Again, assume that the measurement noise has the properties

$$E \{ v(j)v(k) \} = R(k) \delta_{jk} \quad R(k) = \sigma_v^2$$

and

$$E \{ v(j)w(k) \} = 0$$

The Kalman equations for this model have the same form as Eq. (8), where all quantities in those equations assume the definitions given in this section. The initial state estimate and covariance matrix are initialized for $k = 2$ as follows:

$$\hat{\underline{x}}(2|2) = \begin{bmatrix} z(2) \\ \frac{1}{T} [z(2) - z(1)] \end{bmatrix} \quad (19)$$

and

$$P(2|2) = \frac{\sigma_v^2}{T^2} \begin{bmatrix} T^2 & T \\ T & 2 \end{bmatrix} \quad (20)$$

$P(2|2)$ is obtained in a manner analogous to the procedure used for Filter A.

With these initial estimates of the state vector and covariance matrix, the state vector estimate is updated with each new measurement by means of the Kalman Eqs. (8). [1].

3.1.3 Performance

Two types of trajectories were used in the simulations: those resulting from a constant acceleration (called constant acceleration trajectories) and those resulting from a sinusoidal acceleration (called sinusoidal acceleration trajectories). A constant acceleration trajectory conforms to the model of Filters A, B, and C, but is a departure from the model of Filter D, except for $x_3(k) = 0$. A sinusoidal acceleration trajectory is a departure from the models of all filters. This type of trajectory serves to determine the value of σ_w^2 (maneuver noise variance) which will optimize the response of the filter in the sense that it will track departures from the model, yet not be too sensitive to measurement noise.

A trajectory is completely determined by the form of the acceleration, $x_3(k)$, the initial range $x_1(0)$, and the initial velocity $x_2(0)$. Range, velocity, and acceleration are then

computed for each k . After generating the true values $x_1(k)$, $x_2(k)$, and $x_3(k)$, a noise term is computed as follows.

Twelve random numbers, each between 0 and 1, are generated and added. The number 6 is then subtracted from the sum. The result, when multiplied by σ_v , is an approximately zero-mean, Gaussian random variable with standard deviation σ_v . In symbols,

$$v(k) = \sigma_v \left\{ \sum_{i=1}^{12} N_i - 6 \right\} = \sigma_v n_k \quad 0 \leq N_i < 1$$

where N_i is a random number between 0 and 1.

Starting with $k = 1$, the same sequence of random variables n_k was generated for all runs. All variable acceleration simulations used the same sequence of random variables; i.e., for a given k , the value of n_k was always the same. The constant acceleration trajectories use the first 50 values of n_k of this set to compute the noise term, $v(k)$.

Figure 1 is a plot of $v(k)$ for $k = 1$ to 50 for a standard deviation $\sigma_v = 6$ m. Table I lists the values of $v(k)$ from $k = 1$ to 50 for $\sigma_v = 6$ m. Note the preponderance of negative noise terms in the last few entries. The average of the last eight noise terms is -2.59 m and the average of the last six is -2.99 m. This results in a negative bias in the estimates for the last several terms of the constant acceleration simulations.

Measurement noise characterized by $\sigma_v = \{2, 4, 6, 8, 10 \text{ m}\}$ was used in these simulations. A study by Oricon [2] suggests a value of $\sigma_v = 3$ m for radar of "medium accuracy", but $\sigma_v = 6$ m was chosen as a representative of the measurement noise encountered at range of about 600 m. Section 3.1.3 of this report shows σ_v

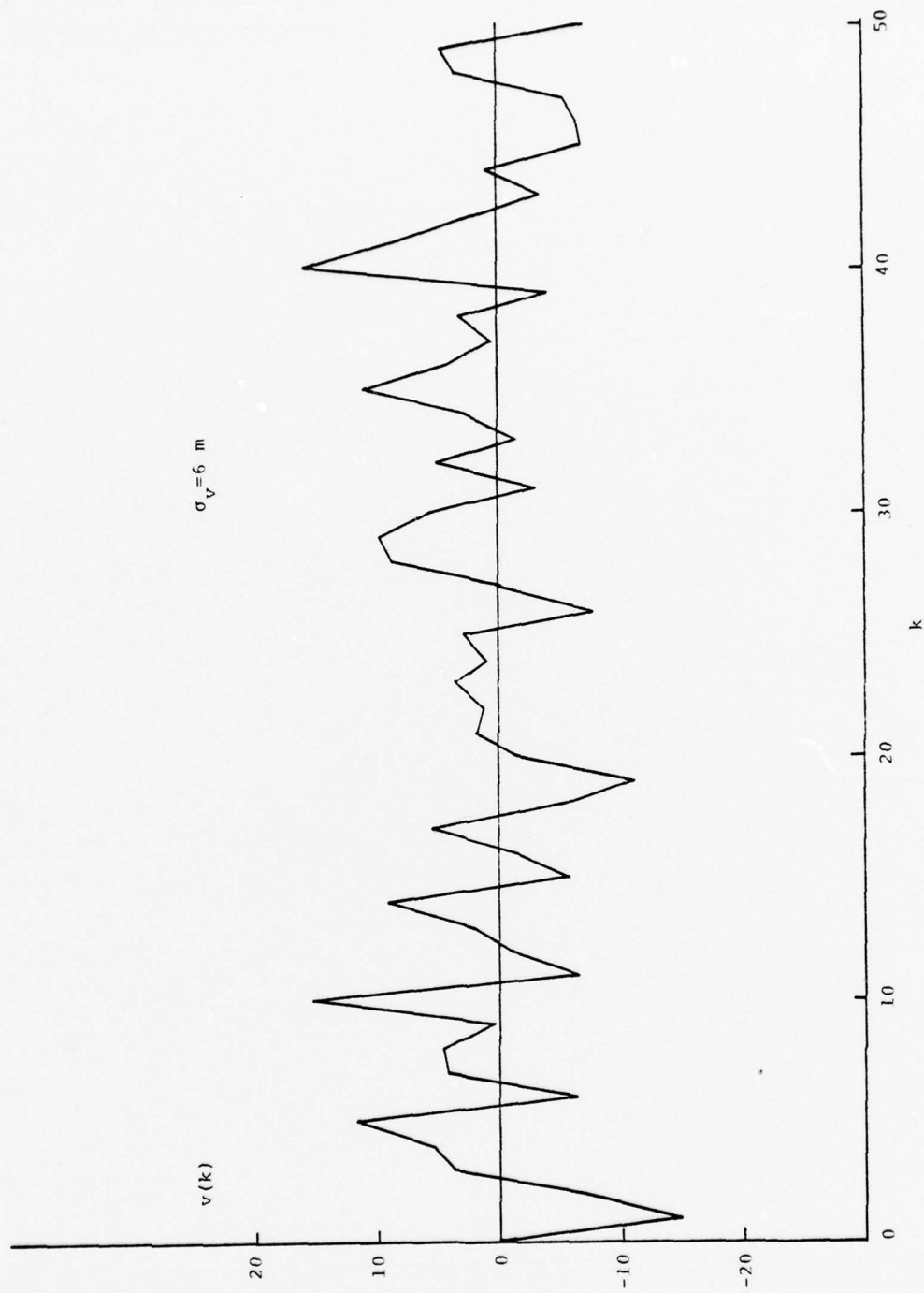


Figure 1. Simulated Measurement Noise

TABLE 1
NOISE TERMS $v(k)$
 $\sigma_v = 6m$

<u>k</u>	<u>v(k)</u>	
1	-14.75	
2	- 6.92	
3	3.74	
4	5.56	
5	11.82	
6	- 6.24	
7	4.24	
8	4.65	
9	.40	
10	15.38	
11	- 6.57	
12	- .99	
13	2.20	
14	8.97	
15	- 5.79	
16	- 1.33	
17	5.55	
18	- 5.28	
19	-10.98	
20	- 1.42	
21	1.87	
22	1.12	
23	3.37	
24	1.08	
25	2.88	
26	- 7.73	
27	- .15	
28	8.57	
29	9.49	
30	5.68	
31	- 3.06	
32	5.00	
33	- 1.37	
34	2.81	
35	11.02	
36	4.19	
37	.53	
38	3.00	
39	- 4.03	
40	15.76	
41	8.69	
42	2.81	
43	- 3.33	
44	.70	
45	- 6.93	region of negative bias
46	- 6.49	
47	- 5.18	
48	3.20	
49	4.66	
50	- 7.19	

to be about 6 m for the MA-1 radar and to be only weakly range dependent.

Table 2 is a summary of simulated trajectories and noise variances used to evaluate the filters. The line numbers at the left identify the trajectory and the filter parameters used. At the right of the table, the letter A, B, C, or D indicates the filters used to estimate state variables from the specified trajectory. A hyphen (-) indicates the filter was not used, for reasons which will be presented later.

Plots of filter performance are to be found in Appendix A. Each figure in this appendix is a plot of the true velocity and acceleration and their estimates by each of the four filters. The true velocity and acceleration are plotted with solid lines, and their corresponding estimates are plotted with dashed lines. Since Filter D does not yield an acceleration estimate, no such plot will, of course, be present. Since Filter C was used only in cases 16, 17, 18, 24, and 30, estimates from this filter will be present in these cases and absent in all others.

The format of each figure is as follows. The numerical part of the figure number is the same as the case number in Table 2. The plots in the left column of each figure show $x_2(k)$ and $\hat{x}_2(k|k)$ vs k for each filter used. There will be either three or four such plots in this column, depending on whether or not Filter C was used for that case. The right column of each figure shows plots of $x_3(k)$ and $\hat{x}_3(k|k)$ vs k for Filters A and B and for Filter C as well in those cases where this filter was used. There will be either two or three such plots in the right column.

TABLE 2

Simulated Trajectories and Noise Variances

Case	Range	Velocity	Acceleration	Measurement Noise Variance	Maneuver Noise Variance	Filter			
	$x_1(0)$ (m)	$x_2^{(0)}$ $m s^{-1}$	$x_3(k)$ $m s^{-2}$	σ_v^2	σ_w^2				
1	600	200	0	4	0	A	B	-	D
2	"	"	9.8	"	"	A	B	-	D
3	"	"	58.8	"	"	A	B	-	D
4	"	"	0	16	"	A	B	-	D
5	"	"	9.8	"	"	A	B	-	D
6	"	"	58.8	"	"	A	B	-	D
7	"	"	0	36	"	A	B	-	D
8	"	"	9.8	"	"	A	B	-	D
9	"	"	58.8	"	"	A	B	-	D
10	"	"	0	64	"	A	B	-	D
11	"	"	9.8	"	"	A	B	-	D
12	"	"	58.8	"	"	A	B	-	D
13	"	"	0	100	"	A	B	-	D
14	"	"	9.8	"	"	A	B	-	D
15	"	"	58.8	"	"	A	B	-	D
16	"	"	0	36	6000	A	B	C	D
17	"	"	9.8	"	"	A	B	C	D
18	"	"	58.8	"	"	A	B	C	D
19	"	"	-9.8	"	0	A	B	-	D
20	"	"	-58.8	"	"	A	B	-	D
21	"	"	$2g \sin \frac{\pi k}{100}$	36	0	A	B	-	D
22	"	"	"	"	2000	A	B	-	D
23	"	"	"	"	4000	A	B	-	D
24	"	"	"	"	6000	A	B	C	D
25	"	"	"	"	8000	A	B	-	D
26	"	"	"	"	10000	A	B	-	D
27	"	"	$6g \sin \frac{\pi k}{100}$	"	0	A	B	-	D
28	"	"	"	"	2000	A	B	-	D
29	"	"	"	"	4000	A	B	-	D
30	"	"	"	"	6000	A	B	C	D
31	"	"	"	"	8000	A	B	-	D
32	"	"	"	"	10000	A	B	-	D

Thus, Figure A-15 contains plots of the performance of Filters A, B, and C for the trajectory (and noise variances) listed under Case 15; i.e., $x_1(0) = 600 \text{ m}$, $x_2(0) = 200 \text{ m}$, $x_3(k) = 58.8 \text{ m s}^{-2}$, $\sigma_v^2 = 100 \text{ m}^2$, $\sigma_w^2 = 0$.

Cases 1 through 20 of Table 2 list constant acceleration simulations. These conform to the model of Filters A, B, and C. Cases 1, 4, 7, 10, 13, and 16 also conform to the model of Filter D.

In Cases 1 through 15, $\sigma_w^2 = 0$ and measurement noise variances are given the values $\sigma_v^2 = \{4, 16, 36, 64, 100 \text{ m}^2\}$. In Cases 16 through 18, $\sigma_v^2 = 36 \text{ m}^2$ and $\sigma_w^2 = 6000 \text{ m}^2 \text{s}^{-6}$; the values judged "best" to handle deviations from the model. Data supporting this conclusion are listed in Section 3.1.4. Cases 19 through 20 specify negative accelerations. Cases 21 through 26 specify sinusoidal accelerations of 2g amplitude and 8 s period. Cases 27 through 32 specify sinusoidal accelerations of the same period, but with a 6g amplitude.

Filter A: Constant Acceleration Model. Time varying gain.

Figure A-1 through A-20 contain plots of the velocity and acceleration estimates of Filter A for Cases 1 through 20 listed in Table 2. The value of σ_v^2 was used in both the noise generator and in the filter. These plots show both velocity and acceleration estimates to be extremely noisy for the first half-second, but they smooth out considerably at the end of one second, and approach the true values quite closely after about 30 iterations (1.2 s). As expected, the lower the value of σ_v^2 , the faster and closer the convergence. Note the characteristic "tail", or

negative bias, in the estimates, particularly those of higher signal noise variance. This is caused by the anomaly in the random numbers referred to earlier.

Figure A-21 through A-32 contain plots of velocity and acceleration estimates of sinusoidal acceleration simulations. Several values of the maneuver noise variance are used to find the "best" value of σ_w^2 . (See Section 3.1.4.) It is clear from Figure A-21 and A-27 that filter estimates using $\sigma_w^2 = 0$ are extremely poor, as one would expect.

Filter B: Constant Acceleration Model. Synthetic gain.

The motivation of this filter and the method of calculation of the parameters used to generate $\underline{K}'(k)$ are discussed in Section 3.1.2. Since the values of $\underline{K}(k)$, the optimum time-varying gain, depend upon the noise parameters σ_v^2 and σ_w^2 , the parameters which generate $\underline{K}'(k)$ were found by fitting Eq. (14) to $K_i(5)$ and $K_i(30)$ for each pair of noise parameters.

Figures 2, 3, and 4 are plots of $K_i(k)$ and $K_i'(k)$ vs k for the three components of the Kalman gain. The noise parameters used to generate $\underline{K}(k)$ were those judged to be optimum in a sense discussed in the next section; $\sigma_v^2 = 36 \text{ m}^2$ and $\sigma_w^2 = 6000 \text{ m}^2 \text{ s}^{-6}$. Although the fit is not a close one, this procedure yields synthetic Kalman gains such that the estimates of Filter B in Figures A-1 through A-32 are difficult to distinguish from corresponding plots of Filter A.

Filter C: Constant Acceleration Model. Constant gain.

Figures 2, 3, and 4 are plots of the components of the optimum Kalman gain vs the iteration number k . The optimum constant

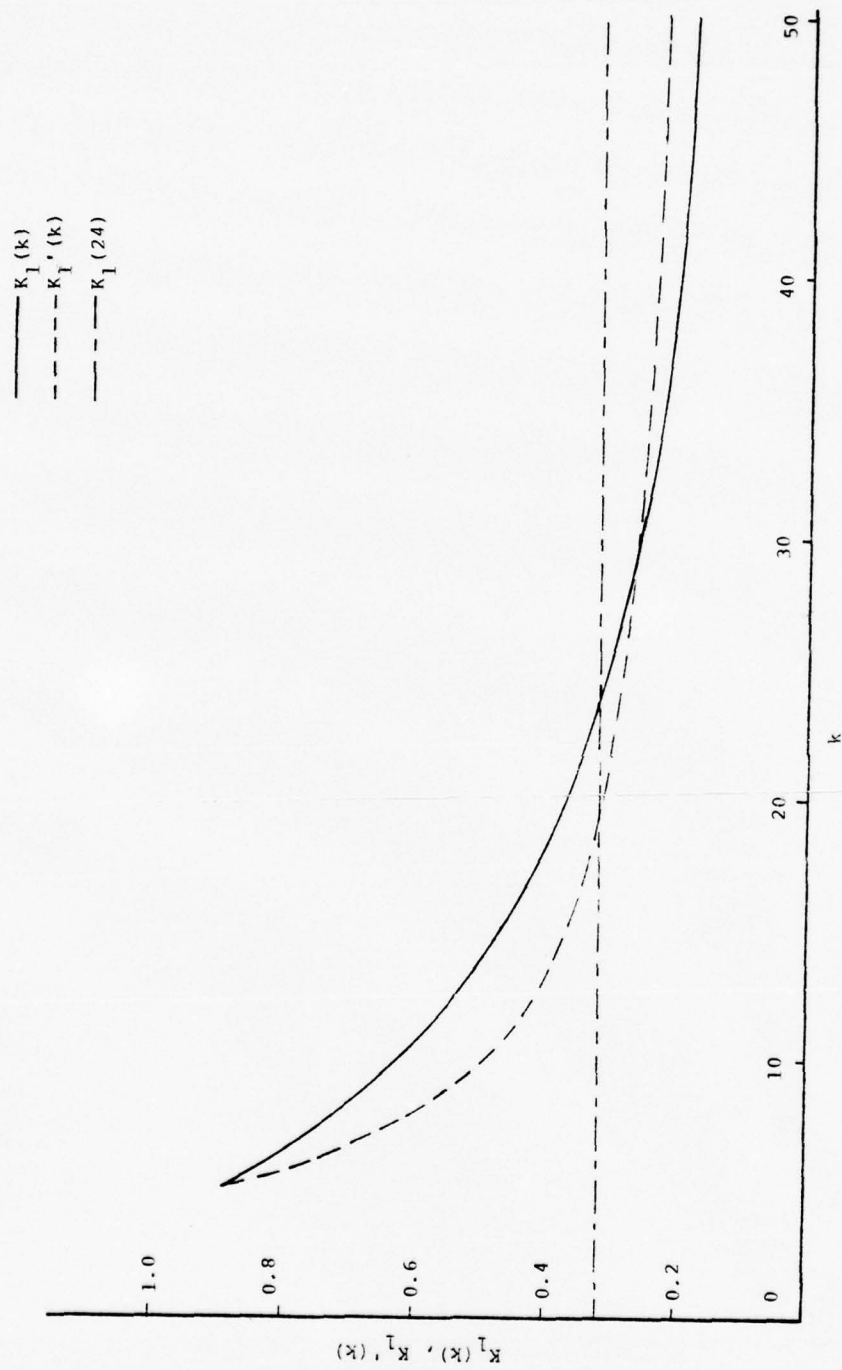


Figure 2. Position Kalman Gain Component

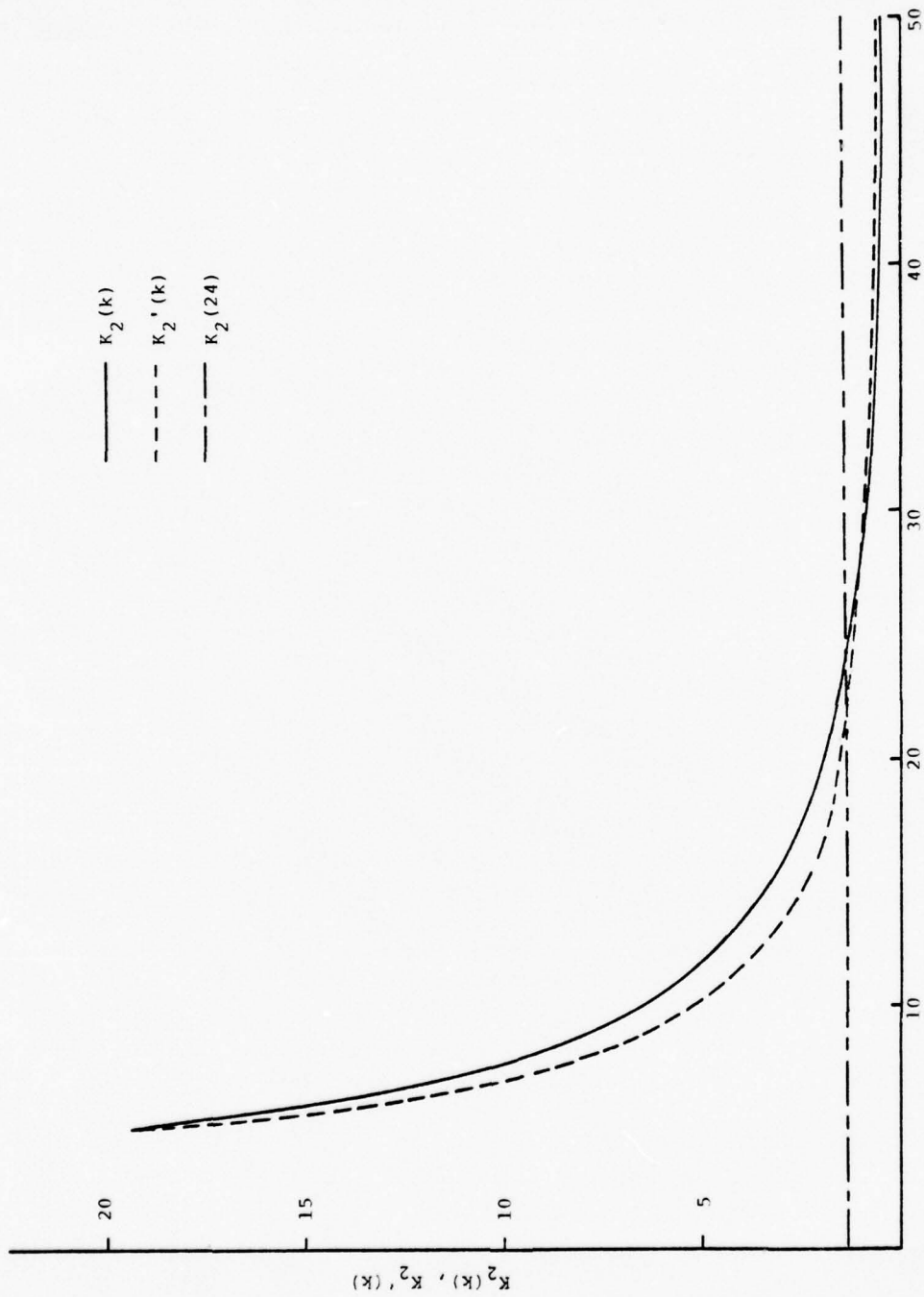


Figure 3. Velocity Kalman Gain Component

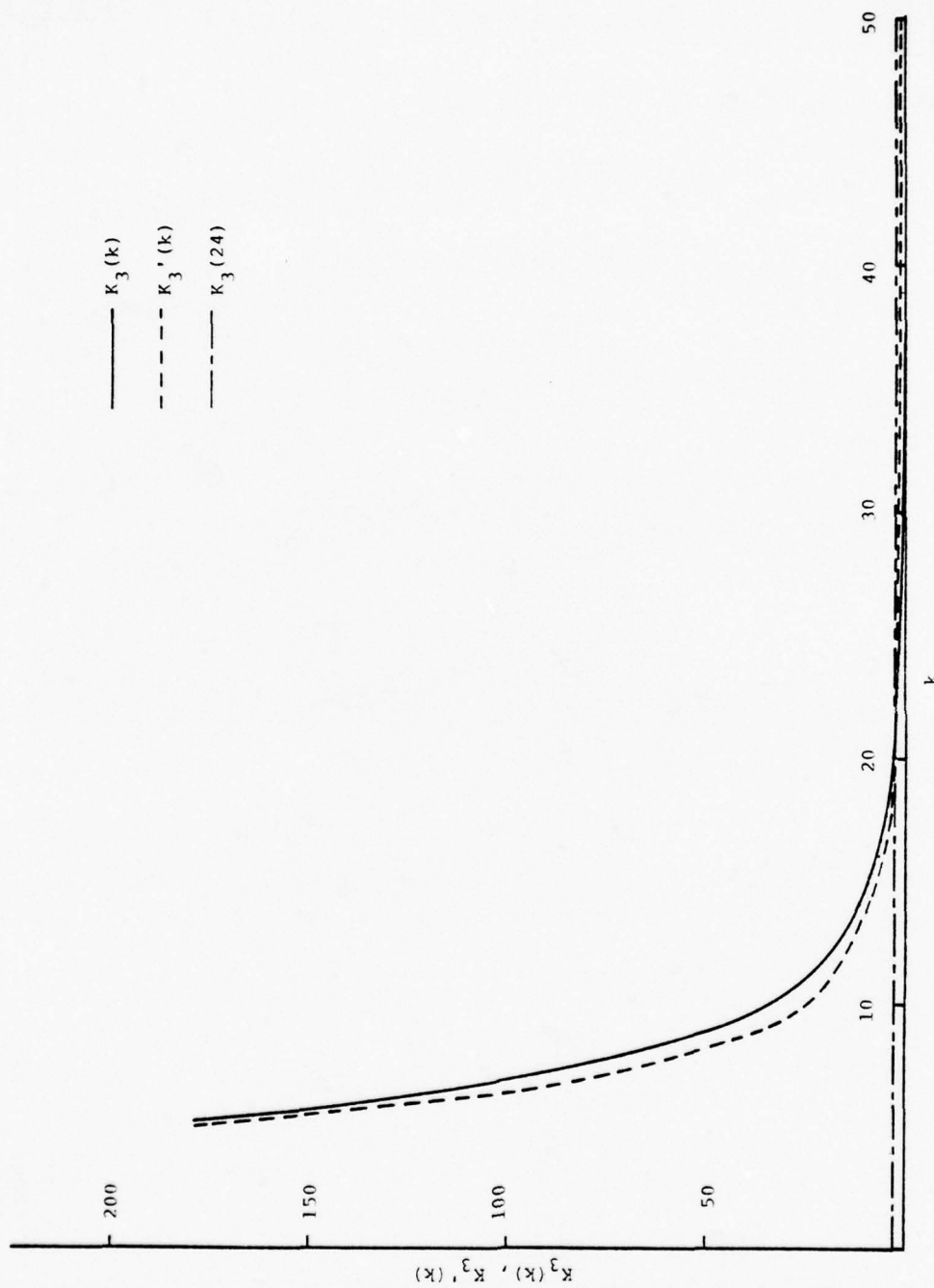


Figure 4. Acceleration Kalman Gain Component

value of the Kalman gain $\underline{K}(i)$ was determined by finding the gain which minimizes the rms deviation of the velocity. (See Section 3.1.4.) This gain was found to be $\underline{K}(24)$, and is shown in Figures 2, 3, and 4 as a dotted horizontal line. Since these values were based on optimum gains for $\sigma_v^2 = 36 \text{ m}^2$ and $\sigma_w^2 = 6000 \text{ m}^2 \text{ s}^{-6}$, we used Filter C only where appropriate; i.e., for parameters listed on lines 16, 17, 18, 24, and 30. Figure A-16, A-17, and A-18 show that velocity estimates of Filter C tend to converge to the true values, though not as quickly nor as closely as the corresponding velocity estimates of Filters A and B. Figure A-16, A-17, and A-18 show that the acceleration estimates of Filter C also show a tendency to converge, but more weakly than those of Filters A and B. Figure A-24 and A-30 show noisier velocity estimates than those shown in Figures A and B, and the acceleration estimates shown in these figures are much noisier.

Filter D: Constant Velocity Model.

This filter assumes the target to be moving with constant relative velocity. Departures from constant velocity can be treated by choosing a suitable value of σ_w^2 . This filter yields position estimates and velocity estimates only. Attempts to estimate acceleration based on some algorithm using past velocity estimates proved fruitless.

It can be seen from the figures that even for very large values of σ_w^2 , this filter yields a biased velocity estimate even for accelerations of only $1g$, which becomes considerably larger for $6g$ accelerations. The velocity estimates are quite poor for sinusoidal acceleration simulations, though better than Filter C.

3.1.4 Evaluation

Given a trajectory and a pair of noise variances (σ_v^2 and σ_w^2) we wish to characterize the performance of each filter by a single number. A root-mean-square deviation is an attractive candidate for such a characteristic number. The first difficulty with this idea, however, is that the filter output consists of three time-varying quantities $\hat{x}_1(k|k)$, $\hat{x}_2(k|k)$, and $\hat{x}_3(k|k)$; i.e., a range estimate, a velocity estimate, and an acceleration estimate. The smallest rms deviation for one component of the state estimate may not be the smallest for the others. Another difficulty can be seen by comparing plots of the estimates of Filter A with those of Filter D. Although Filter A produces noisy velocity and acceleration estimates for low k , the estimates are quite good for large k (constant acceleration trajectories), with the exception of the "tail" referred to earlier. Although Filter D yields a less noisy velocity estimate for low k , it is biased and slowly diverges from the true velocity for large k . Thus the choice of the better filter depends upon the allowable time between acquisition and when estimates are needed. For the constant acceleration trajectories, we have assumed this interval to be 1.5 sec. Thus, if the velocity rms deviation were computed over the 2 sec. interval, one would find the deviation lower for Filter D than for Filter A, due to the high noise in Filter A for small k . Such a procedure would lead to Filter D being judged "best". But if one has at least 1.5 sec. between acquisition and the time an estimate is needed, a comparison of the estimates of Filter A with those of Filter D shows that Filter A is best. Since $\hat{x}_2(k|k)$ and $\hat{x}_3(k|k)$ of Filter A smooth out in about 1.5 s.

it was decided to compute the rms estimates from $k = 39$ (1.56 s) to $k = 50$ (2.00 s). In symbols,

$$(\Delta x_i)_{\text{rms}} = \sqrt{\sum_{k=39}^{50} [x_i(k) - x_i(k|k)]^2} \quad i=1,2,3$$

where the subscript i refers to one of the three components of the state vector and the state estimate. Results are listed in Tables 3, 4, and 5.

For sinusoidal acceleration simulations, which were 8 sec. in duration or from $k = 1$ to $k = 200$, the figures show that Filters A, B, and D give reasonable estimates after about 3 sec., so the rms deviations were computed from $k = 75$ (3 sec.) to $k = 200$ (8 s); i.e.,

$$(\Delta x_i)_{\text{rms}} = \sqrt{\sum_{k=75}^{200} [x_i(k) - x_i(k|k)]^2} \quad i=1,2,3.$$

Range Estimates. $(\Delta x_1)_{\text{rms}}$

This, of course, is the most important of the three estimates, but a reasonable estimate is not difficult to obtain.

Cases 1 through 20 of Table 3 list the rms range deviations for constant acceleration trajectories. It can be seen that Filter A characteristically has the smallest deviations, with Filter B a close second. The deviations of Filter C are about 25% higher than Filter A. The deviations of Filter D are quite erratic; small for small values of the acceleration and much larger for large acceleration. This is to be expected, for Filter D is based on a constant velocity model.

TABLE 3 RMS Range Deviations

Case #	$x_1(0)$	$x_2(0)$	$x_3(k)$	σ_v^2	σ_w^2	$(\Delta x_1)_{rms}$			
						Filter			
						A	B	C	D
1	600	200	0	4	0	1.01	1.09	1.27	3.18
2			9.8			"	"	"	1.55
3			58.8			1.00	1.08	"	12.07
4			0	16		2.02	2.17	2.54	3.18
5			9.8			"	"	"	1.55
6			58.8			2.01	"	"	12.07
7			0	36		3.03	3.26	3.80	3.18
8			9.8			"	"	5.43	1.55
9			58.8			"	"	"	12.07
10			0	64		4.04	4.35	5.07	3.18
11			9.8			"	"	"	1.55
12			58.8			4.03	4.34	"	12.07
13			0	100		5.05	5.44	6.34	3.18
14			9.8			"	"	"	1.55
15			58.8			5.04	5.43	"	12.08
16			0	36	6000	3.13	4.01	3.80	3.37
17			9.8			"	"	"	2.96
18			58.8			3.12	----	3.81	3.37
19			-9.8		0	3.03	3.26	----	5.47
20			-58.8			3.04	----	----	17.63
21		0	$2gsin\frac{\pi k}{100}$	"	0	16.04	16.39	----	16.74
22			"	"	2000	1.94	1.46	----	1.92
23			"	"	4000	1.93	2.01	----	1.87
24			"	"	6000	1.97	2.06	2.98	1.95
25			"	"	8000	2.01	2.10	----	2.03
26			"	"	10000	2.05	2.13	----	2.10
27			$6gsin\frac{\pi k}{100}$	"	0	50.67	52.33	----	50.72
28			"		2000	3.81	3.43	----	4.78
29			"		4000	3.00	2.87	----	3.40
30			"		6000	2.70	2.66	2.98	2.91
31			"		8000	2.56	2.56	----	2.69
32			"		10000	2.49	2.50	----	2.58

TABLE 4 RMS Velocity Deviations

Case #	$x_1(0)$	$x_2(0)$	$x_3(k)$	σ_v^2	σ_w^2	$(\Delta x_2)_{rms}$ Filter			
						A	B	C	D
1	600	200	0	4	0	2.13	2.07	5.43	2.20
2			9.8			"	"	5.42	6.86
3			58.8			2.15	2.08	5.38	49.53
4			0	16		4.26	4.15	10.9	2.20
5			9.8			"	"	"	6.86
6			58.8			4.28	4.16	10.8	49.53
7			0	36		6.39	6.21	16.3	2.20
8			9.8			"	6.22	"	6.86
9			58.8			6.40	6.23	16.2	49.53
10			0	64		8.52	8.29	21.7	2.20
11			9.8			"	"	"	6.86
12			58.8			8.54	8.30	"	49.53
13			0	100		10.64	10.36	27.2	2.20
14			9.8			10.65	"	"	6.86
15			58.8			10.67	10.37	27.1	49.53
16			0	36	6000	7.21	9.55	16.3	6.58
17			9.8			"	"	"	8.29
18			58.8			7.22	"	16.2	2.50
19			-9.8		0	6.38	----	----	10.44
20			-58.8			6.37	----	----	53.14
21		0	$2gsin \frac{\pi k}{100}$		0	28.24	29.74	----	22.23
22			"		2000	6.03	6.36	----	7.31
23			"		4000	5.49	5.79	----	6.71
24			"		6000	5.44	5.67	12.59	6.69
25			"		8000	5.42	5.72	----	6.85
26			"		10000	5.65	5.82	----	7.06
27		$6gsin \frac{\pi k}{100}$	"		0	86.54	92.08	----	66.80
28			"		2000	16.17	17.39	----	20.50
29			"		4000	13.13	14.13	----	17.14
30			"		6000	11.71	12.52	12.99	15.53
31			"		8000	10.88	11.61	----	14.67
32			"		10000	10.34	10.95	----	14.07

TABLE 5 RMS Acceleration Deviations

Case #	$x_1(0)$	$x_2(0)$	$x_3(k)$	σ_v^2	σ_w^2	$(\Delta x_3)_{rms}$ Filter			
						A	B	C	D
1	600	200	0	4	0	2.52	2.52	9.13	
2			9.8			2.53	2.53	9.11	
3			58.8			2.58	2.58	9.06	
4			0	16		5.04	5.03	18.26	
5			9.8			5.05	5.04	18.25	
6			58.8			5.10	5.09	18.18	
7			0	36	0	7.56	7.55	27.4	
8			9.8			7.57	7.56	"	
9			58.8			7.62	7.61	27.3	
10			0	64		10.08	10.06	36.52	
11			9.8			10.09	10.07	36.51	
12			58.8			10.14	10.12	36.44	
13			0	100		12.60	12.58	45.65	
14			9.8			12.61	12.59	45.64	
15			58.8			12.66	12.64	45.57	
16			0	36	6000	9.21	11.14	27.39	
17			9.8			9.22	"	27.38	
18			58.8			9.25	"	27.31	
19			-9.8		0	7.55	-----	-----	
20			-58.8		0	7.50	-----	-----	
21	0	$2g \sin \frac{\pi k}{100}$			0	20.33	20.39	23.14	
22		"			2000	11.46	11.87	"	
23		"			4000	10.64	11.02	"	
24		"			6000	10.36	10.68	"	
25		"			8000	10.30	10.58	"	
26		"			10000	10.36	10.59	"	
27	$6g \sin \frac{\pi k}{100}$				0	61.94	62.63	28.56	
28		"			2000	33.13	34.93	"	
29		"			4000	29.83	31.24	"	
30		"			6000	28.03	29.26	"	
31		"			8000	26.86	27.99	"	
32		"			10000	26.02	27.03	"	

Lines 21 through 32 of Table 3 list $(\Delta x_1)_{\text{rms}}$ for the sinusoidal acceleration simulations. Trajectories of 6g amplitude represent a more extreme departure from the constant acceleration model than are likely to be encountered in practice, and are included to test filter response. Trajectories of 2g amplitude are more realistic, and therefore greater weight is given to these cases.

Filter B has values of $(\Delta x_1)_{\text{rms}}$ only a few per cent greater than Filter A, and the deviations of Filter D are even less than those of Filter B. Filter C contains the implicit parameters $\sigma_v^2 = 36 \text{ m}^2$ and $\sigma_w^2 = 6000 \text{ m}^2 \text{ s}^{-6}$, and was used only for trajectories listed on lines 24 and 30. The deviation is notably poorer than that of the other filters.

Velocity Estimates. $(\Delta x_2)_{\text{rms}}$

Velocity estimates are more sensitive to noise than range estimates, and $(\Delta x_2)_{\text{rms}}$ will vary more widely for different filters than $(\Delta x_1)_{\text{rms}}$. Lines 1 through 20 of Table 4 list $(\Delta x_2)_{\text{rms}}$ of the velocity estimates $\hat{x}_2(k|k)$. For nearly all cases, deviations of Filters A and B are more nearly the same. In fact, for most cases, the deviations of Filter B are slightly less than those of Filter A, but this result is most likely anomalous. Filter D yields erratic deviations; small for trajectories which match its model and much larger for those which do not. Filter C yields consistently large deviations.

Lines 21 through 32 list $(\Delta x_2)_{\text{rms}}$ for the sinusoidal acceleration simulations. As above, Filters A and B differ

but slightly and Filter C has much larger deviations, but the deviations of Filter D are surprisingly small, though not so small as those of Filter B.

Acceleration Estimates. $(\Delta x_3)_{rms}$

Lines 1 through 20 of Table 5 list $(\Delta x_3)_{rms}$ for Filter A, B, and C. There are no deviations computed for Filter D, for this filter does not provide an acceleration estimate. The deviations of Filters A and B are nearly the same, while those of Filter C are about three times greater.

Lines 21 through 32 list $(\Delta x_3)_{rms}$ for sinusoidal acceleration simulations. For the 2g amplitude trajectories, Filters A and B have deviations of about 1g and Filter C has deviations about twice as great.

Selection of Maneuver Noise Variance

As noted earlier, the maneuver noise variance (σ_w^2) is needed to allow the filter to respond to deviations from the model on which it is based. Of all simulations, only the sinusoidal trajectories (Cases 21 through 32) are deviations from the models of all filters, and so the best value of σ_w^2 is that which minimizes $(\Delta x_2)_{rms}$ and $(\Delta x_3)_{rms}$ for these cases. Since the 2g simulations are more typical of an encounter than the 6g simulations, the choice of a value of σ_w^2 will be based upon the rms deviations resulting from Cases 21 through 26 of Tables 4 and 5. For Filter A, the minimum rms deviations for both $(\Delta x_2)_{rms}$ and $(\Delta x_3)_{rms}$ occurs for $\sigma_w^2 = 8000 \text{ m}^2 \text{ s}^{-6}$.

For Filter B, the minimum $(\Delta x_2)_{\text{rms}}$ occurs for $\sigma_w^2 = 6000 \text{ m}^2 \text{ s}^{-6}$ and the minimum $(\Delta x_3)_{\text{rms}}$ occurs for $\sigma_w^2 = 8000 \text{ m}^2 \text{ s}^{-6}$. Since the differences in the rms deviations resulting from these two choices are quite small, $\sigma_w^2 = 6000 \text{ m}^2 \text{ s}^{-6}$ was chosen, for the use of the smaller value of the maneuver noise variance will result in a slightly less noisy filter.

3.1.5 Conclusion

The most striking feature of the tables of rms deviations is that in nearly all cases the deviations of Filters A and B are within a few percent of one another. Filter A computes the Kalman gain components from Eqs. (i) and (iv) of equation set (8) by matrix multiplications, whereas Filter B computes the gain components from three simple algebraic equations.

Filter A requires the parameter σ_v^2 , σ_w^2 , and T in order to give numerical results. If these parameters are given, Eqs. (8i), (8ii), and (8iv), together with Eq. (13) - initialization of the covariance matrix - can be used to calculate $\underline{K}(k)$, independently of any measurements. By following the procedure described in Section II, the parameters a_i , b_i , and $K_i(\infty)$ can be found for $i = 1, 2$, and 3. The Kalman gains can be quickly computed from Eqs. (21) and these nine parameters at a fraction of the time needed by the iterative procedure of Eqs. (8) to yield estimates of only slightly lower quality than those of the optimum filter, Filter A.

Although the calculations employed by Filter C are even simpler than those needed for Filter B, the results are much poorer and it is doubtful that the estimates would be useful.

Filter D cannot produce a useful acceleration estimate, and its performance in estimating velocities is very poor at accelerations higher than $1g$.

- [1] Stochastic Optimal Linear Estimation and Control, J.S. Meditch, McGraw-Hill(1969) .
- [2] Advanced Defensive Fire Control Processing Methods Study. ORINCON F33615-76-C-1303 Contract Status Briefing 31 Jan 77.

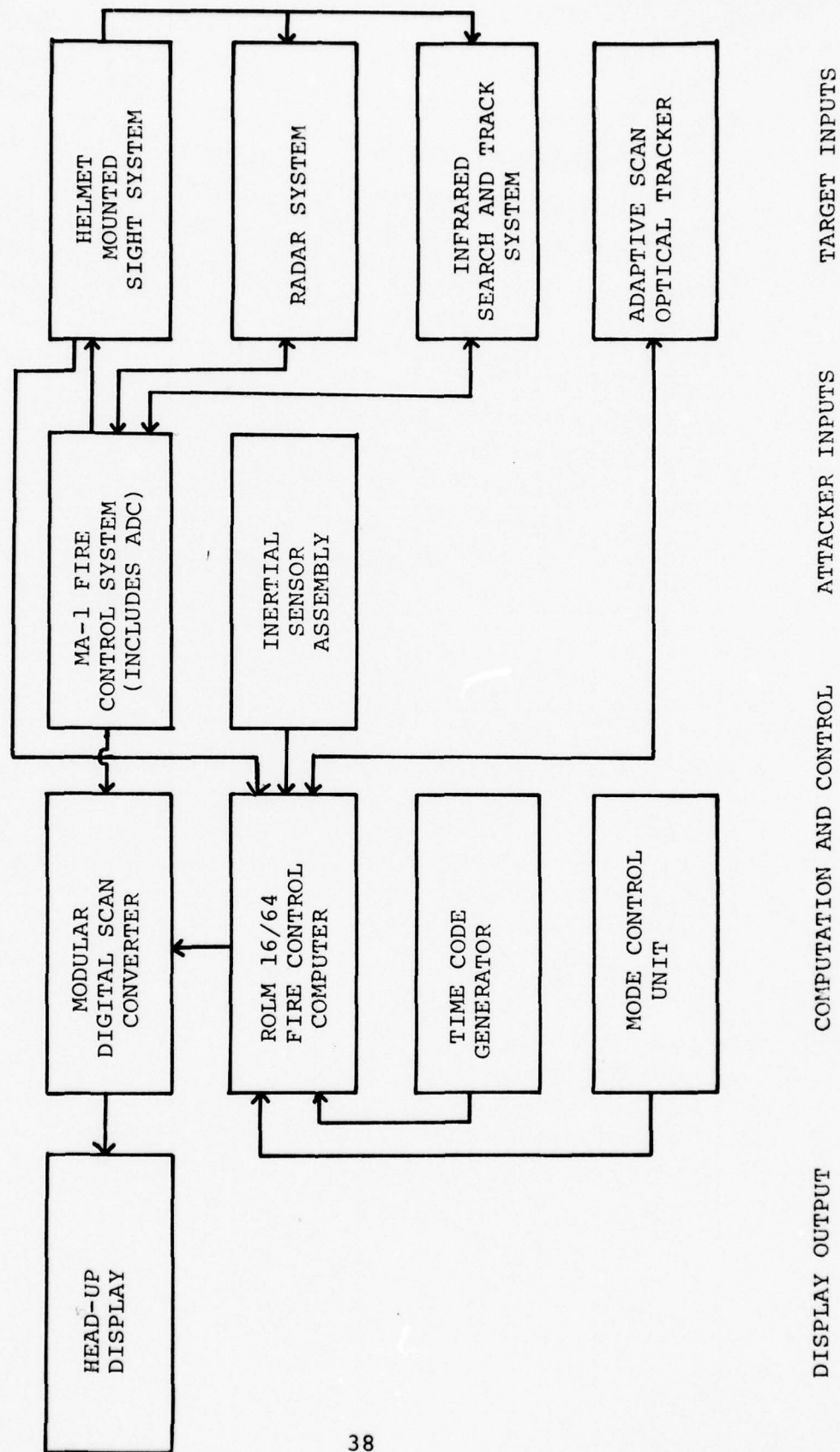
3.2 TARGET STATE MEASUREMENT

3.2.1 Introduction

The general objective of the target state measurement task is to devise independent methods for evaluating the accuracy of target state vectors (position, velocity, and acceleration) obtained from a director fire control system. The particular director system to be considered is being developed by Honeywell (the integrating contractor) for AFAL/RWT. A simplified block diagram of some essential features of this system is shown in Figure 5; components and subsystems which would not affect an actual combat encounter (e.g., the Mini-Heads-Up Display, used to obtain film records) are not included in this diagram. Director fire control systems are characterized by an extensive use of data in a line-of-sight coordinate frame rather than an aircraft body frame, and this characteristic may lead, in principle, to a more stable gunsight system. Figure 5 shows that the attacker's Inertial Sensor Assembly and Air Data Computer (via the MA-1 Fire Control System) are inputs to the director system in addition to the target sensors and the Time Code Generator and Mode Control Unit. The final output of the director system is presented on the Heads-Up Display.

The task objective stated above has several possible interpretation features. First, the stage in the director system at which target position, velocity, and acceleration are to be measured is not specified. Presumably, in order to evaluate

FIGURE 5. SIMPLIFIED BLOCK DIAGRAM OF THE
DIRECTOR FIRE CONTROL SYSTEM



the performance of the entire system, the most appropriate stage would be as close as possible to the final output of the system, i.e., the Head-Up Display. On the other hand, it may be possible to identify inadequacies in various subsystems if target state vectors are evaluated at appropriate states closer to the sensor inputs.

A second interpretation feature concerns the coordinate frame in which the "true" target state vectors are to be compared with target state vectors from the director system. There are at least three commonly used reference frames: (1) an inertial frame, fixed in the earth or in a local air mass, in which the coordinate directions are north(x), east(y), and down(z); (2) an aircraft body frame, in which the coordinate directions are forward along the aircraft axis(x)*, out the right wing(y), and the right-hand cross product of these directions(z); and (3) a line-of-sight frame, in which the coordinate directions are along the line-of-sight to the target(x), toward the front of the aircraft(y), and the right-hand cross product of these directions(z). The director system, of course, always considers the target state vectors relative to the attacker, and thus the evaluation methods to be devised should also refer to the attacker as the origin. In general, if the comparison is to be made at a stage close to the target sensor inputs of the director system, then a line-of-sight frame is probably indicated, and if this comparison is to be made at a stage close to the final output, then the attacker's body frame is probably appropriate. If only the magnitudes of the

* A "velocity" frame, in which the x direction is along the total velocity, is also used.

target state vectors are to be compared, then the orientation of the coordinate frame need not be specified.

A third interpretation feature concerns the independence of the evaluation methods. Completely independent methods would not make use of any of the sensor inputs or computational algorithms used by the director system. However, such methods, although possible in principle, would generally be difficult or expensive to implement, and thus methods which are not completely independent of the director system must be considered in practice.

A fourth and final interpretation feature concerns the relative precision of the target state vectors obtained from the director system and the "true" vectors obtained by the methods to be devised. Thus the precision required of the "true" vectors, in order that they may be considered adequate for the evaluation of the director target state vectors, is not specified.

The above considerations, which may lead to significantly different interpretations of the target state measurement task, were discussed with representatives from AFAL/RWT and from Honeywell, and some decisions were made. First, it was decided that the director system target state vectors would be evaluated at a stage close to the final output. This decision allows an assessment of the effects of error propagation and accumulation, although information on the effect of any particular stage may be lost. In a second and related decision it was determined that the target state vectors would be obtained in the attacker's body frame, since this is the coordinate frame in which these vectors are most readily available at states close to the director system output.

A third decision determined that only instrumentation planned or readily available for tests of the director system would be used to devise independent methods for the evaluation of target state vectors. Table 6 shows the real and test inputs which will be available for testing the director system. The real inputs could be used in an actual combat encounter, whereas the test inputs are available for test purposes only. Note that tracking of the target and attacker from the ground or from an observation aircraft is not available but that various test inputs transmitted from the target to the attacker are available. The test data must be used to obtain (for the evaluation methods to be devised) as much independence from the director system as possible.

In a fourth decision it was determined that unproven or unstable analysis techniques would be avoided. It is possible, for example, to obtain velocity from acceleration if the initial integration time is known, and it may be possible to identify this initial time as the time at which integration must begin to obtain known roll, pitch, and yaw angles from known roll, pitch, and yaw rates. However, this is an apparently unproven technique which may require an unacceptable amount of computer time or memory if it were implemented on the attacker's computer. Differentiation to obtain velocity from position or acceleration from velocity is an example of a generally unstable technique (in the sense that initial disturbances are accentuated), although appropriate smoothing or filtering techniques may make this procedure acceptable.

TABLE 6

REAL AND TEST INPUTS
TO THE DIRECTOR SYSTEM

REAL INPUTS

ASCOT
RADAR
IRST
HMS
ISA
ADC
TIME CODE
MODE CONTROL

TEST INPUTS

SSC
MHC
DME
HARS
TELEMETRY FROM TARGET
ISA
HARS
ADC

ASCOT - ADAPTIVE SCAN OPTICAL TRACKER
IRST - INFRARED SEARCH AND TRACK
HMS - HELMET MOUNTED SIGHT
ISA - INERTIAL SENSOR ASSEMBLY
ADC - AIR DATA COMPUTER
DME - DISTANCE MEASURING EQUIPMENT
HARS - HEADING ATTITUDE REFERENCE SYSTEM
SSC - SOLID STATE CAMERA
MHC - MINI HUD CAMERA
HUD - HEADS-UP DISPLAY

Finally, it was decided to use Monte Carlo methods to obtain error probability distributions for the target state vectors calculated according to the interpretations and decisions discussed above. These distributions could then be compared with known values for the anticipated accuracy of target state vectors from the director system. Anticipated accuracy is, at present, available only for the magnitude of the acceleration of the target relative to the attacker: a standard deviation of about $1g$. The method used to calculate an independent acceleration and an associated error distribution is determined by the decisions and interpretations discussed above, and it involves the use of simulated ISA and HARS data from both target and attacker. The mean of the error distribution for this method, in the most realistic simulation, is about 1.4 ft/sec^2 -much less than $1g$. Thus, if the various distributions assumed for the Monte Carlo simulation are appropriately conservative, and if the errors in the evaluation method are sufficiently uncorrelated with the director system, then it may be reasonable to conclude that this evaluation method is adequate for the verification of target acceleration obtained from the director system. Since anticipated accuracy figures for the director system are not available for velocity and position, no comparisons can be made for these quantities.

Note that no attempt is being made, in the current task, to locate the source of any discrepancies which may be observed between the target state vectors obtained from the director

system and the "true" vectors obtained by independent evaluation methods. An ability to identify the source of such discrepancies may form an important extension to the target state measurement task.

3.2.2 Formulation of the Monte Carlo Study

The objective of the Monte Carlo study is to obtain probability distributions for the errors in target acceleration, velocity, and position for certain evaluation methods. These methods are determined by the decisions made concerning the interpretation of the task objective, as discussed above. Referring again to Table 6, none of the real inputs should (ideally) be used for any evaluation method, but the ISA and ADC inputs, since they refer only to the attacker, may be used if necessary. The ISA units on both target and attacker are Honeywell H478 inertial sensor assemblies and are strapped-down accelerometer and gyro packages whose outputs include acceleration components and roll, pitch, and yaw rates. True air speed and angle of attack are available from the Air Data Computer on each aircraft. The Heading Attitude Reference System is part of the Stable Coordinate Reference Group (SCRGs) which in turn is part of the MA-1 Fire Control System on both target and attacker. (However, HARS is not a real input to the director system). The HARS outputs are sines and cosines of roll, pitch, and yaw angles. The Distance Measuring Equipment consists of a transmitter on the attacker and a transponder (remitter) on the target. The SSC is a Fairchild CCD solid state electronic gunsight camera

mounted with (but independent of) ASCOT on the attacker. The KB-25 Mini HUD (Head-Up Display) camera records images seen by the pilot on and through the HUD, including images of the target. Although the resolution of this camera may be high, the number of frames available during a simulated combat encounter is probably inadequate, and thus a decision was made to use only the SSC to simulate line-of-sight angle data.

Following the decisions discussed above and in the introduction, the acceleration of the target relative to the attacker is available only using ISA and HARS data from both target and attacker. Similarly, the velocity of the target relative to the attacker is available only from ADC and HARS data from both target and attacker. Finally, the position of the target relative to the attacker is available only from DME and SSC data. If the components rather than the magnitudes of the above vectors are to be obtained, then the appropriate coordinate system is the attacker's body frame.

The kinematics of the above methods may be expressed as follows. Let $u_{x/y}^f$ represent the vector u of the object x relative to the object y in the reference frame f ; e.g., $v_{t/a}^a$ is the velocity of the target relative to the attacker in the attacker's body frame. Let $T_s^e(q_x)$ represent a coordinate transformation from the initial frame s to the final frame e as a function of the quantities q for the object x ; e.g., $T_i^a(\phi_a, \theta_a, \psi_a)$ is a transformation from an inertial to a body frame as a function of the roll(ϕ), pitch(θ), and yaw(ψ) angles

of the attacker. The target state vectors to be obtained for comparison with the same vectors from the director system are

$a_{t/a}^a$, $v_{t/a}^a$, and $p_{t/a}^a$:

$$a_{t/a}^a = T_i^a(\phi_a, \theta_a, \psi_a) T_t^i(\phi_t, \theta_t, \psi_t) a_{t/i}^t - a_{a/i}^a \quad (21)$$

$$v_{t/a}^a = T_i^a(\phi_a, \theta_a, \psi_a) T_t^i(\phi_t, \theta_t, \psi_t) T_v^t(\alpha_t) v_{t/i}^v - T_v^a(\alpha_a) v_{a/i}^v \quad (22)$$

$$p_{t/a}^a = T_l^a(\epsilon_a, \eta_a) p_{t/a}^l \quad (23)$$

Here a , v , and p are acceleration, velocity, and position vectors; i , v , and l are inertial, velocity, and line-of-sight frames; t and a refer to target and attacker or to the corresponding body frame; ϕ_x , θ_x , and ψ_x are roll, pitch, and yaw angles for either target or attacker (for x -a or t), and ϵ_a and η_a are the elevation and azimuth of the target relative to the attacker. The appropriate transformation matrices are

$$T_i^x(\phi_x, \theta_x, \psi_x) = [T_x^i(\phi_x, \theta_x, \psi_x)]'$$

$$= \begin{pmatrix} C\psi_x C\theta_x & S\psi_x C\theta_x & -S\theta_x \\ -S\psi_x C\phi_x + C\psi_x S\theta_x S\phi_x & C\psi_x C\phi_x + S\psi_x S\theta_x S\phi_x & C\theta_x S\phi_x \\ S\psi_x S\phi_x + C\psi_x S\theta_x C\phi_x & -C\psi_x S\phi_x + S\psi_x S\theta_x C\phi_x & C\theta_x C\phi_x \end{pmatrix} \quad (24)$$

$$T_v^x(\alpha_x) = \begin{pmatrix} C\alpha_x & 0 & -S\alpha_x \\ 0 & 1 & 0 \\ S\alpha_x & 0 & C\alpha_x \end{pmatrix} \quad (25)$$

$$T_1^x(\epsilon_x, \eta_x) = \begin{pmatrix} C\epsilon_x C\eta_x & -S\eta_x & S\eta_x C\eta_x \\ C\epsilon_x S\eta_x & C\eta_x & S\epsilon_x S\eta_x \\ -S\epsilon_x & 0 & C\epsilon_x \end{pmatrix} \quad (26)$$

where C and S represent sin and cos and ' indicates matrix transposition. Diagrams of the methods selected for the independent evaluation of target state vectors are shown in Figures 6, 7, and 8.

In addition to the kinematic expressions, probability distributions for the occurrence of the various input quantities are required, as well as probability distributions for the measurement errors in these quantities. Tables 7 through 10 show these input quantities and their estimated occurrence and accuracy distributions. Two occurrence distributions for the ISA acceleration components (i.e., the components of $a_{t/i}^t$ or $a_{a/i}^a$) were tested. The first is a uniform distribution over the range -9g to +9g for each component, and the second is a much more realistic distribution suggested by Capt. Jerry Kendrick of AFAL/RWT: the x and y components of acceleration (in the aircraft body frame) are normally distributed with zero mean and standard deviations of 1g and 0.25g, respectively, and the z component is distributed according to the log-normal distribution $(8-4e^{\epsilon/2})g$, where $\epsilon \sim N(0,1)$. This distribution has a near cut-off at about 7.5g, a mean at about 3.5g, and a "tail" which extends to lower accelerations. Error distributions for the ISA acceleration components were obtained from a table of instrumentation signals for the F106 provided by Capt. Dave Schoor

FIGURE 6. DIAGRAM OF THE EVALUATION METHOD FOR THE
ACCELERATION OF THE TARGET RELATIVE TO THE ATTACKER

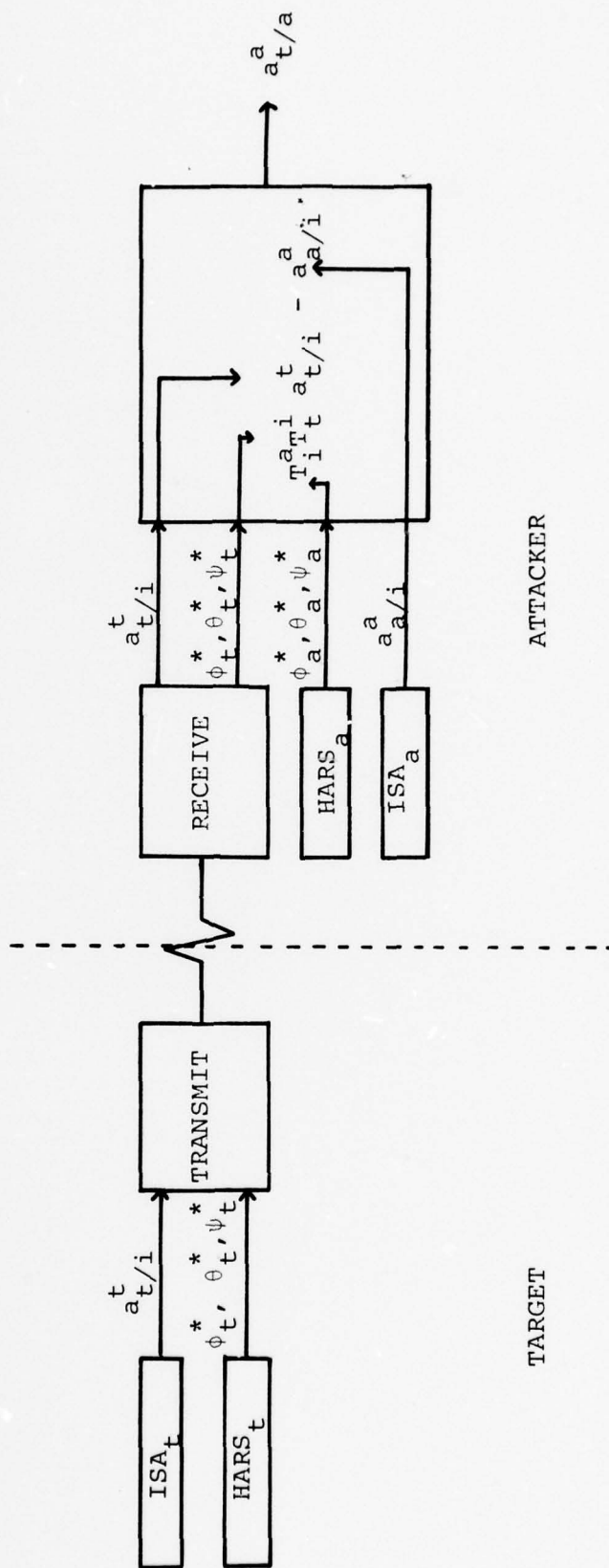


FIGURE 7. DIAGRAM OF THE EVALUATION METHOD FOR THE
VELOCITY OF THE TARGET RELATIVE TO THE ATTACKER

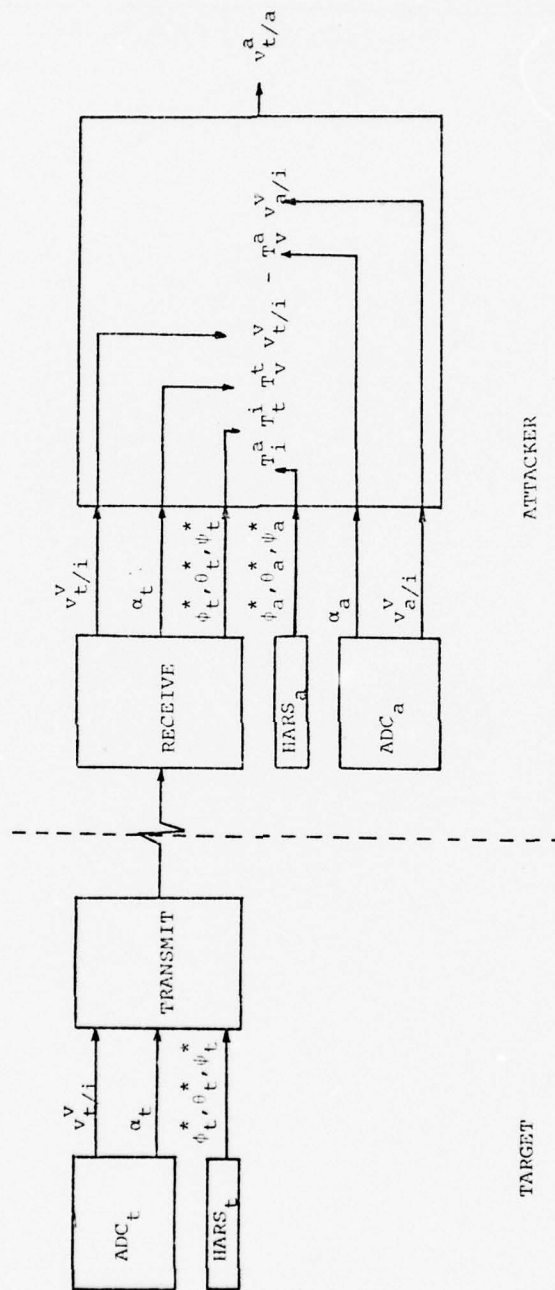


FIGURE 8. DIAGRAM OF THE EVALUATION METHOD FOR THE
POSITION OF THE TARGET RELATIVE TO THE ATTACKER

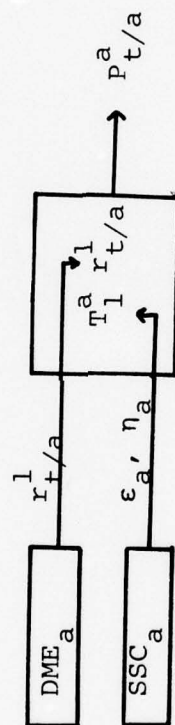


TABLE 7

OCCURRENCE AND ACCURACY DISTRIBUTIONS FOR THE
ISA ACCELERATION COMPONENTS

	OCCURRENCE	ACCURACY
BROAD DISTRIBUTION	$U(-9g, +9g)$	$N(0, 0.5 \text{ ft/sec}^2)$
NARROW DISTRIBUTION	<p>x: $N(0, 1g)$</p> <p>y: $N(0, 0.25g)$</p> <p>z: $a_z = 8-4e^{\epsilon/2}$ $\epsilon \sim N(0, 1)$</p>	(above)

TABLE 8
OCCURRENCE AND ACCURACY DISTRIBUTIONS FOR THE
HARS, ROLL, PITCH, AND YAW ANGLES

	OCCURRENCE	ACCURACY
BROAD DISTRIBUTION		
ϕ :	$U(-180^\circ, +180^\circ)$	$N(0, 0.005)$
θ :	$U(-90^\circ, +90^\circ)$	for sin or cos
ψ :	$U(-180^\circ, +180^\circ)$	of any angle
NARROW DISTRIBUTION		
ϕ :	$U(-60^\circ \rightarrow 90^\circ, +60^\circ \rightarrow +90^\circ)$	
θ :	$U(-30^\circ \rightarrow +45^\circ$ for 75% of pdf area)	(above)
ψ :	$U(-180^\circ, +180^\circ)$	

16

TABLE 9

OCCURRENCE AND ACCURACY DISTRIBUTIONS FOR
ADC TRUE AIR SPEED ANGLE OF ATTACK

	OCCURRENCE	ACCURACY
$\frac{V}{V_{X/i}}$	U(200, 600 Knots)	N(0, 4 Knots)
α	U(-5, +20°)	N(0, 0.1°)

TABLE 10
 OCCURRENCE AND ACCURACY DISTRIBUTIONS FOR DME
RANGE AND FOR SSC AZIMUTH AND ELEVATION ANGLES

	OCCURRENCE	ACCURACY
$P_{t/a}^1$	$U(0, 2500 \text{ ft})$	$N(0, 4 \text{ ft})$
η, ϵ	$U(-15^\circ, +15^\circ)$	$N(0, 0.07^\circ)$

17

at Tyndall AFB. Roll, pitch, and yaw ranges and measurement error distributions were also obtained from this table. Two different occurrence distributions were tested: uniform distributions over the permissible ranges and a more restricted piecewise uniform distribution suggested by Maj. Stewart Cranston at Tyndall AFB. Measurement errors for computed air speed and for the angle of attack were obtained from the table for the F106 mentioned above, and the occurrence distributions for these quantities were suggested by Capt. Jerry Kendrick (the side-slip angle was assumed to be zero). The occurrence and error distributions for the DME were suggested by Dr. James Yi at Honeywell. Finally, the required occurrence and accuracy distributions for the azimuth and elevation angles from the SSC were estimated from information provided by Capt. H. Woodruff and Mr. Jerry Watson of AFAL/RWT.

The procedure for the Monte Carlo calculations will now be described. Values for the components of $a_{t/i}^t$, $a_{a/i}^a$, $v_{t/i}^v$, $v_{a/i}^v$, and for the angles ϕ_a , θ_a , ψ_a , ϕ_t , θ_t , ψ_t , α_t , ϵ_a , and η_a were selected, independently, from the occurrence distributions given in Tables 7 through 10. Next measurement errors for these quantities were selected from the accuracy distributions given in these tables. The final vectors, $a_{t/a}^a$, $v_{t/a}^u$, or $p_{t/a}^a$, were then calculated according to Eqs. (21) through (26) both with and without the addition of the selected measurement errors to the selected components and angles. The resulting vectors were subtracted, and the entire procedure was repeated for 300 selection sets for each vector whose error distribution was to be

determined. Finally, probability distributions of the differences between the square root of the sum of the squares of the components (for vector magnitude), were plotted. The final result was a set of simulated error distributions for the evaluation methods defined by Eqs. (21) through (26) and diagrammed in Figures 6, 7, and 8. These evaluation methods are proposed as independent methods for evaluating the accuracy of target position, velocity, and acceleration vectors (relative to the attacker in the attacker's body frame) obtained from the director system.

3.2.3 Results of the Monte Carlo Study

Error distributions calculated according to the Monte Carlo procedure described above are given for acceleration in Figures 9 through 11. These distributions refer to the error in the acceleration of the target relative to the attacker in the attacker's body frame when this acceleration is obtained using ISA and HARS data from both target and attacker. Figure 9 shows the magnitude of this acceleration error calculated using the most realistic occurrence distributions for the ISA acceleration components and HARS angles (log-normal $(a_{x/i}^x)_z$, piecewise uniform ϕ and θ). The mean of this distribution is about 1.4 ft/sec^2 - much less than the $1g$ (32 ft/sec^2) anticipated accuracy of the magnitude of the acceleration of the target relative to the attacker from the director system. In addition, Figure 9 shows that the probability that the ISA-HARS evaluation method will approach an error of $1g$ is very small, since the "tail" of the error distribution is already small at about $0.1g$.

Figure 9. Error Distribution of the Magnitude of the Acceleration of the Target Relative to the Attacker Obtained Using Simulated ISA and HARS Data

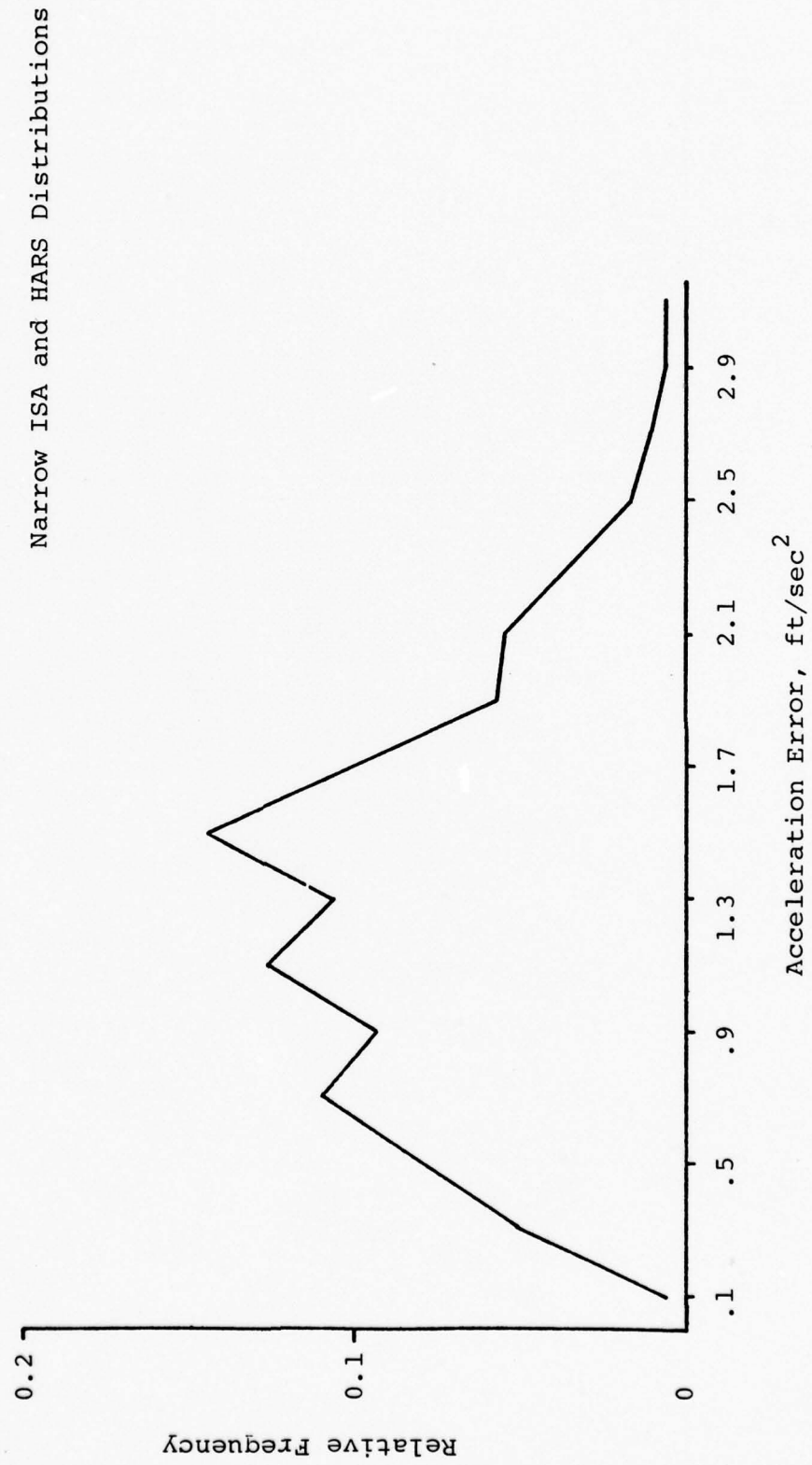


Figure 10. Error Distribution of the Magnitude of the Acceleration of the Target Relative to the Attacker Obtained Using Simulated ISA and HARS Data

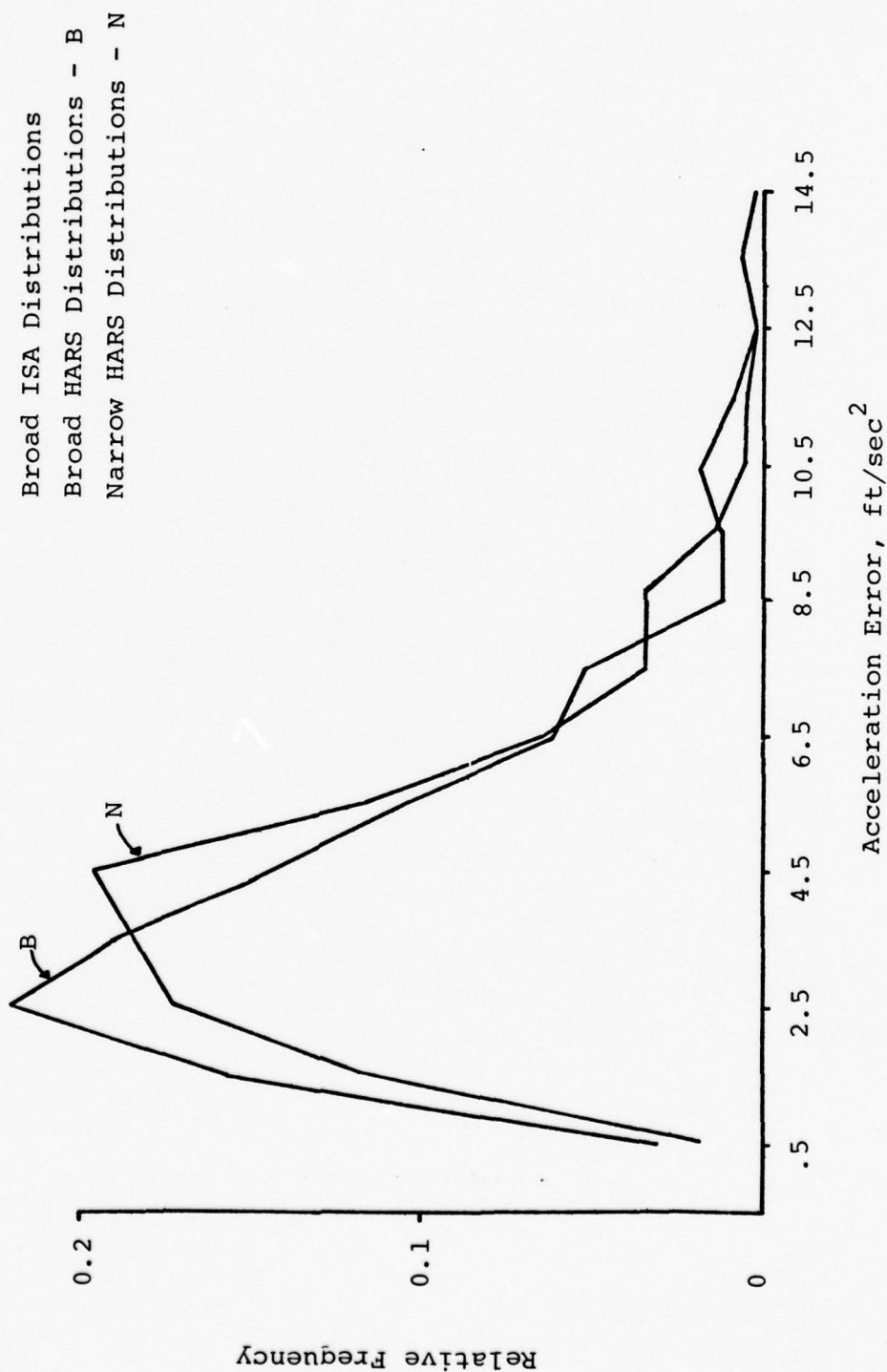
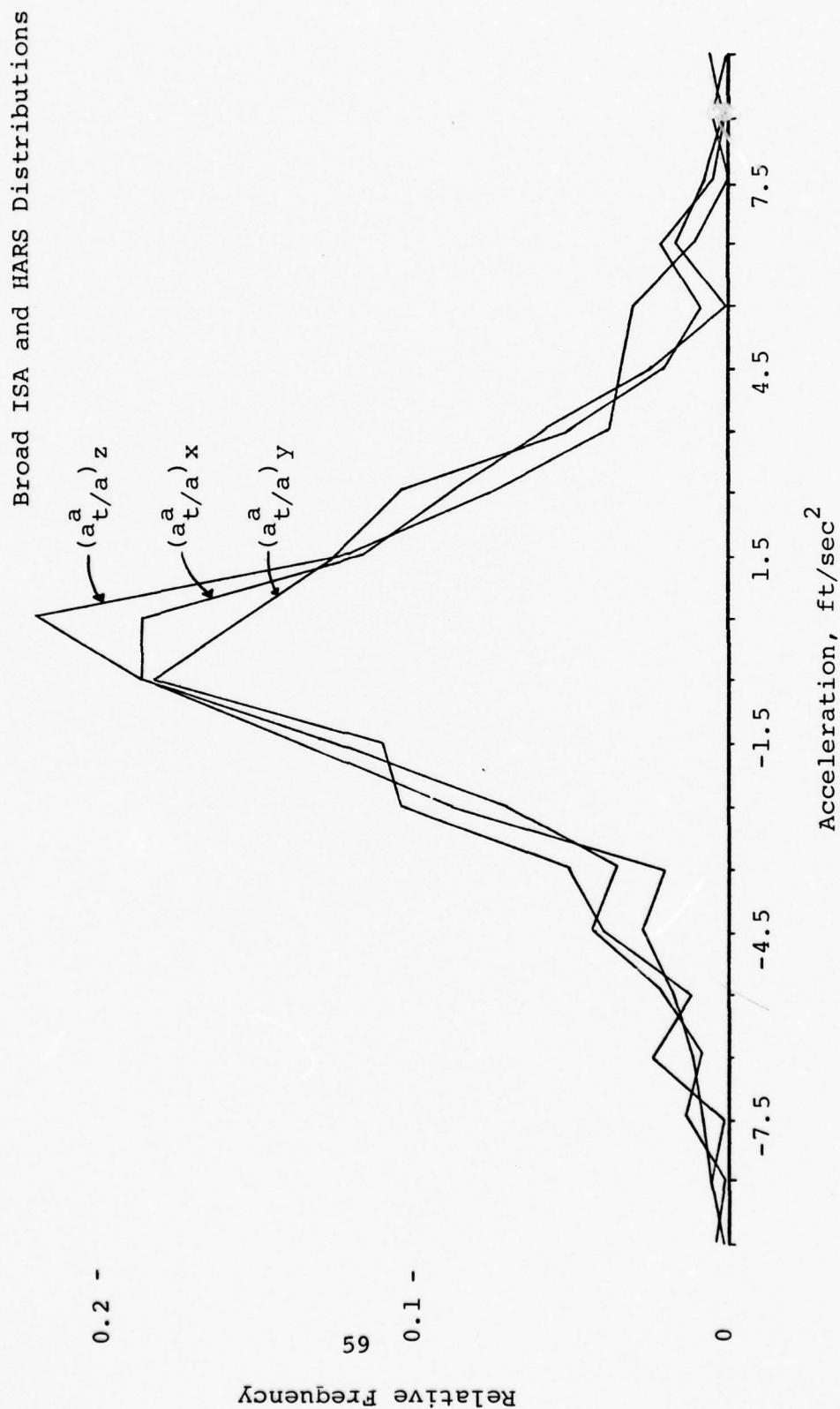


Figure 11. Error Distribution of Components of the Target Relative to the Attacker in the Attacker's Body Frame Obtained Using Simulated ISA and HARS Data



24

The error distributions for acceleration magnitude shown in Figure 10 are calculated for uniform occurrence distributions of the ISA acceleration components (from -9 to +9g.), and from uniform or piecewise uniform occurrence distributions for ϕ , θ , and ψ . These error distributions have means considerably larger (about 3 ft/sec²) than the distribution of Figure 9 because of the much greater (and probably much less realistic) probability of large acceleration. However, the use of the more restricted piecewise uniform distribution for roll and pitch angles seems to have only a minor effect on the final error distributions.

Error distributions for the x, y, and z components of the acceleration of the target relative to the attacker in the attacker's body frame are shown in Figure 11. These distributions are roughly the same since the occurrence and error distributions used in their deviation were identical (uniform distributions from -9 to 9g for the ISA acceleration components and uniform distributions for ϕ , θ , and ψ over their allowed ranges). As in Figures 9 and 10, the probability that any error in acceleration will exceed 1g is very small.

Figures 12 and 13 show error distributions for the magnitude of the velocity and position vectors of the target relative to the attacker. The restricted piecewise uniform occurrence distributions for ϕ , θ , and ψ were used for the velocity calculations. The mean error in velocity is about 8 knots and the mean error in position is about 4 ft.; both distributions are skewed toward larger magnitudes. Although these distributions

Figure 12. Error Distribution of the Magnitude of the Velocity of the Target Relative to the Attacker Obtained Using Simulated ADC and HARS Data

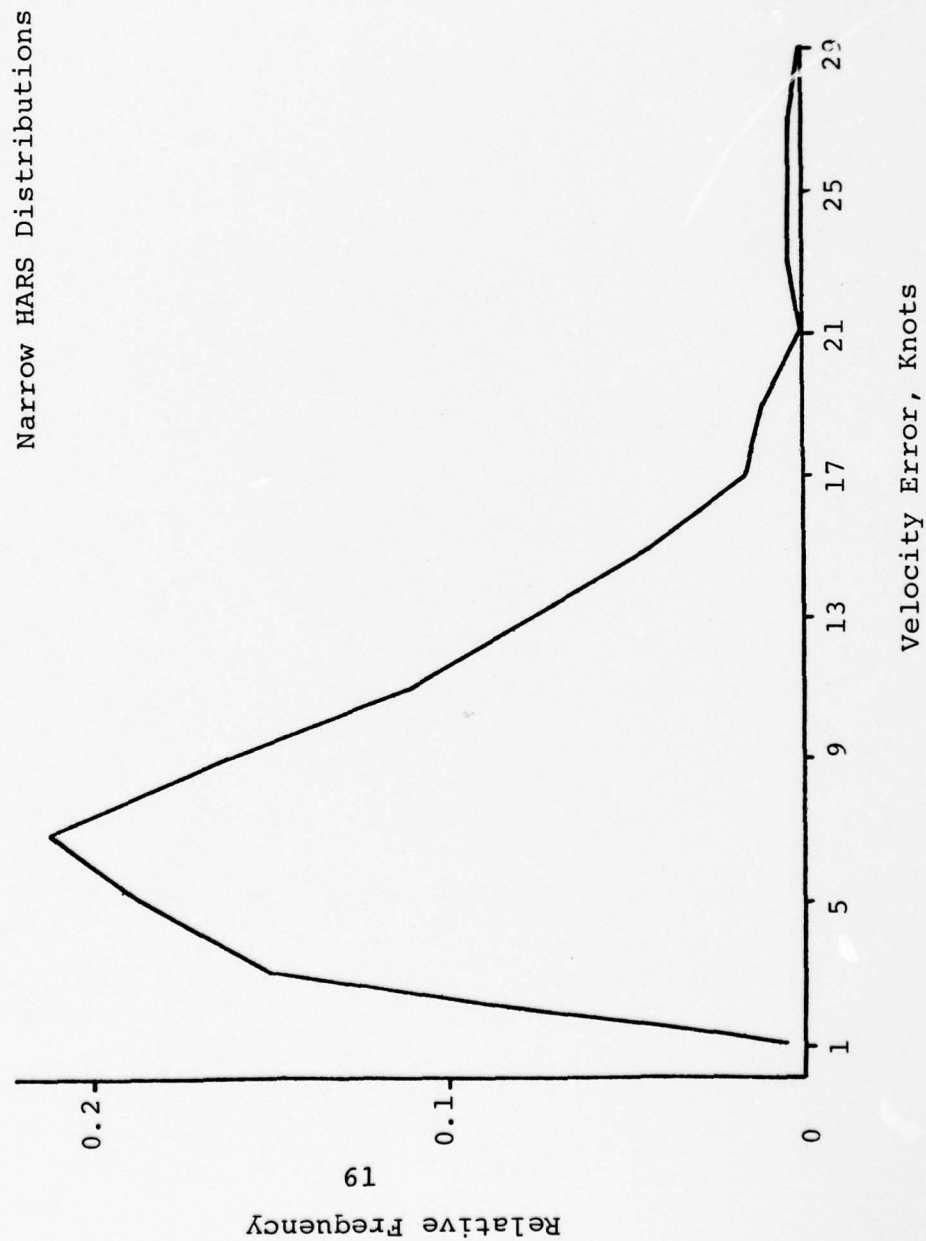
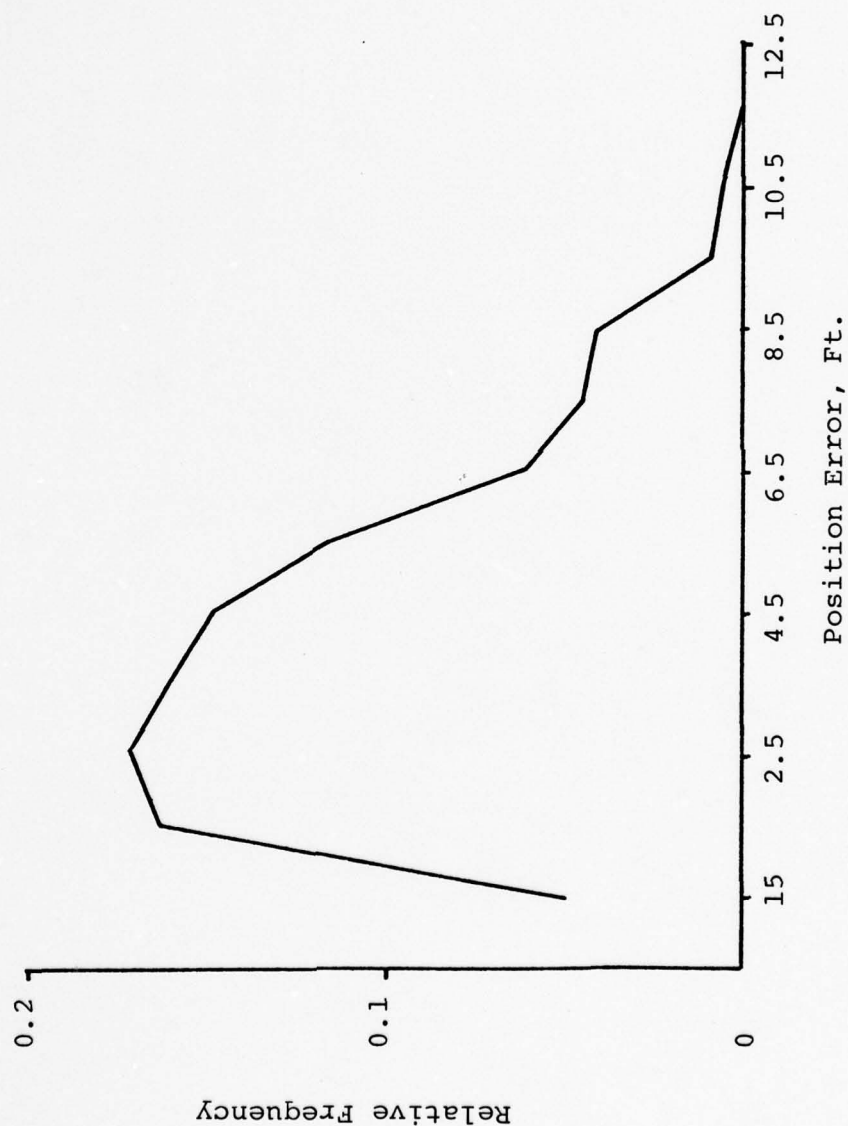


Figure 13. Error Distribution of the Magnitude of the Position of the Target Relative to the Attacker obtained using Simulated DME and SSC Data.



provide some information on the accuracy of the ADC-HARS method for velocity and the DME-SSC method for position, the anticipated accuracy of the director system for these vectors is not known at present, and thus the adequacy of these methods for the evaluation of the director system cannot be quantitatively assessed.

3.2.4 Suggestions for Future Study

As discussed in the introduction, the target state measurement task has been interpreted so that it may be said to be complete when independent methods are devised and shown to be adequate for the evaluation of target state vectors obtained from the director system. It is quite likely that unacceptable discrepancies will be found between the target state vectors from the director system and the "true" vectors from the independent evaluation methods. In the current task, no attempt is made to locate the source of these anticipated discrepancies; however, such an attempt is believed to be essential for an adequate evaluation of the complete director system.

There are at least three apparent approaches to the problem of "tracing back" observed errors in the director target state vectors. First, it may be possible to perform a sensitivity study to find the stages in the director system at which major discrepancies originate. Second, the target state measurement task, as interpreted here, might be carried out at several different stages in the director system (from the sensor inputs to the HUD output). Finally, a detailed error analysis of the entire director system, including input, processing, and output

errors, could be made. Results from any of these approaches could lead to significant performance improvements in the director system.

3.3 IDENTIFY AND CORRECT RADAR LAG PROBLEM

3.3.1 Introduction

3.3.1.1 Background

For proposed weapons systems to be effective, accurate knowledge of the target state is needed. The EXPO V and Fire/Fly programs pointed out the need for the results of improved trackers and fire control algorithms. To this end, the AFAL initiated the Gunsight Evaluation Program (Sight Eval.) to evaluate the performance of existing fire control systems. This program, conducted at Tyndall AFB using an instrumented F-106 which tracked towed and radio-controlled targets and made both live and dry firing missions, produced data which could be used for the analysis of existing fire control systems.

An important part of the instrumentation aboard the F-106 was the MA-1 radar, which measured range and range rate, elevation and elevation rate, azimuth and azimuth rate. It is the purpose of this report to analyze the performance of the MA-1 radar using the above data.

3.3.1.2 Motivation

The target state is estimated from measurements of range, azimuth, and elevation, along with the first and second derivatives of range, azimuth, and elevation. The derivatives are obtained from suitable algorithms using direct measurements of target range and angular position.

The MA-1 radar provides adequate range information, but its measurements of azimuth and elevation are

not sufficiently precise to be useful to hand off target position to an electro-optical sensor (ASCOT), whose field of view is much narrower than the MA-1, and which measures the angular position of the target with sufficient accuracy.

The major system integration problem with the above technique is that the two fields of view of the ASCOT are limited to ± 17 mrad and ± 43 mrad, whereas the MA-1 reports angular positions which are in error by as much as ± 50 mrad. It is the purpose of this analysis to improve the radar estimates of the angular position such they have a high probability of lying within the ± 17 mrad window of the ASCOT.

3.3.1.3 Scope and Objectives of the Problem

There are two different methods which can be used to do the above. The first, called the hardware approach, is to modify the design, mounting, or calibration of the MA-1 such that the desired degree of accuracy can be achieved. The second, a software approach, is to look for a suitable algorithm which will produce correction terms such that the revised radar estimates lie within the allowable error tolerances.

The principal drawback to the hardware approach is the lack of access to the design and installation data on the modified MA-1 system and to the schedules of the alignment and calibration procedures performed on the system during the Sight Eval tests.

The second approach is a possible alternative. The ROLM 16/64, a rugged, high-speed, airborne computer is a component of the proposed fire control system, and could conceivably contain provisions for correcting the angular data provided by the MA-1. It is along these lines that this study has been directed.

Two distinct efforts related to a software approach were pursued. One effort involved a relatively straightforward graphical, curve-fit attack attempting to relate tracking error to tracking rate functions. The second effort involved an analysis of the relative angular rate of change of the Line of Sight (LOS) between the aircraft body axis and the target followed by a similar analysis of angular rates between aircraft and target relative to an inertial coordinate system.

3.3.2 Data Collection

3.3.2.1 General

The original purpose of the Sight Eval program was to test and evaluate fire control systems, especially the HLGS (Hot Line Gun Sight) and the DALCOS (Digital Advanced Lead Computing Optical Sight). As mentioned previously, the objective of this study is to determine the magnitude and causes of the angular position errors in the angular position measurements of the MA-1 Fire Control System, and to develop an algorithm to reduce these errors. Of primary concern is the difference between the "true" target position, determined from a 16 mm film record, and the position reported by the MA-1 radar.

The radar target position and rates are determined by resolvers mounted on the MA-1 antenna gimbals, and by interceptor rate gyros and radar range measurements.

The data available for this study consisted of analog signals recorded on magnetic tape and target angular position recorded on 16 mm film. After each mission, the magnetic tape and film data were converted to digital form and recorded on tape.

3.3.2.2 Description of Test Missions

Ninety-five live firing missions were planned and executed for the purpose of evaluating gunsight algorithms, but only 39 of these missions were recorded.

Figure 14 shows the relationship between target and attacker in a typical firing encounter. In one mission, the target was remotely piloted PQM-102. In the remaining missions, the targets were towed. The towed targets were either the 30 ft long fiberglass FIGAT or the 15 ft long aluminum DART.

The firing tests were conducted at different ranges, altitudes, angle-off at firing, and target acceleration. The target was in either a 1g, 2g, or 4g turn. The attacker coordinated his pursuit so that firing began at prescribed angles-off (10° , 20° , 30° , or more) and ranges (1000, 1500, 2000, or 3000 ft) at altitudes of 10,000, 15,000, and 20,000 ft. Figure 15 is a matrix showing the combinations of these variables which were used in the tests.

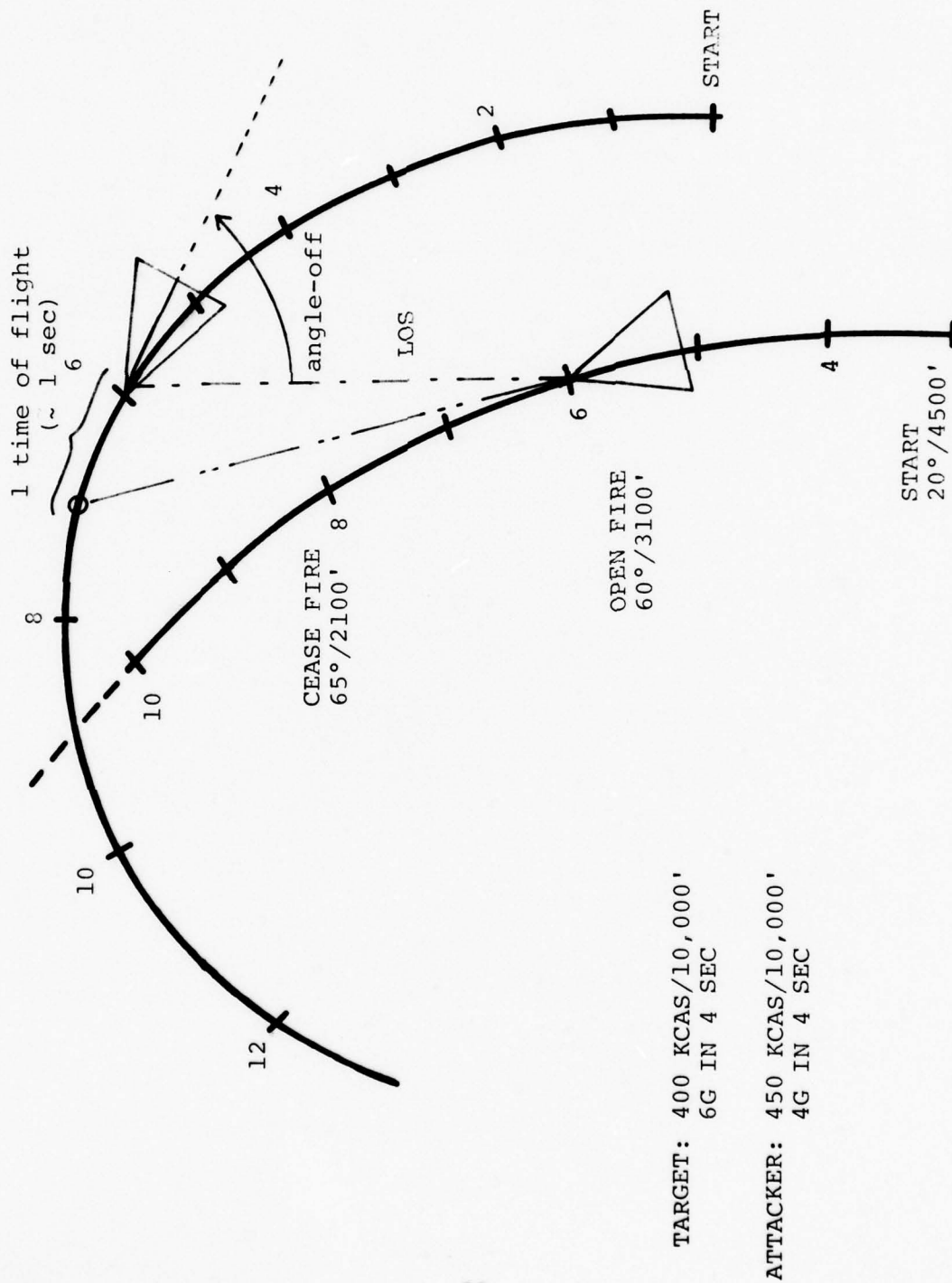


Figure 14 Firing Profile for Actual Mission
With a Drone Target (PQM-102)

Altitude	Range (1000 Feet)	1g BANNER				2g FIGAT				4g DART				Acceleration Target	Angle Off at Firing (Degrees)
		10	20	30	>30	10	20	30	>30	10	20	30	>30		
10000 ft.	3.0					X	X	X	X	X	X	X			
	2.0				X		X	X	X	X	X		X		
	1.5				X		X	X	X	X		X	X		
	1.0					X	X	X	X		X				
15000 ft.	3.0		X		X	X			X				X		
	2.0			X		X	X	X	X	X		X			
	1.5					X	X	X	X		X				
	1.0		X			X			X	X			X		
20000 ft.	3.0				X	X	X	X							
	2.0	X				X	X		X	X			X		
	1.5			X		X		X							
	1.0				X	X	X	X	X						

Figure 15 Test Matrix

3.3.2.3 Instrumentation and Recorded Data

A block diagram showing the transfer of analog data from the sensors to the recording tape is shown in Figure 16. The ISA (H 478 Inertial Sensor Assembly) measures ownship acceleration in rectangular components. The IRP (Inertial Reference Package) gives ownship pitch, yaw, and roll rates. The SCRG (Stable Coordinate Reference Group) - AHARS (Altitude Heading and Reference System) gives ownship pitch, yaw, and roll.

Radar, operating in conjunction with the CADC (Central Air Data Computer), gives range and range rate. The IR, and infra-red tracker, provides passive angular target direction for powered targets. These signals are input to an HCM-204 Fire Control Computer. The β -vane is a yaw attitude sensor.

All the signals described above are fed into a signal conditioner, whose function is to adjust the amplitude of the incoming analog signals to a 0-5 volt level, and to generate a Pulse Amplitude Modulated (PAM) train, which is an ordered sequence of all signals. The sets of data on the PAM train are separated by about 70 msec. The output of the signal conditioner is recorded on a Genesco tape recorder. The output of the IRIG - B Time Code Generator is recorded directly onto the tape, to the nearest thousandth of a second.

The conversion of data from the ISA and the MA-1 sensors into a PAM train by the signal conditioner is shown in Figure 17. The PAM train, together with ballistic

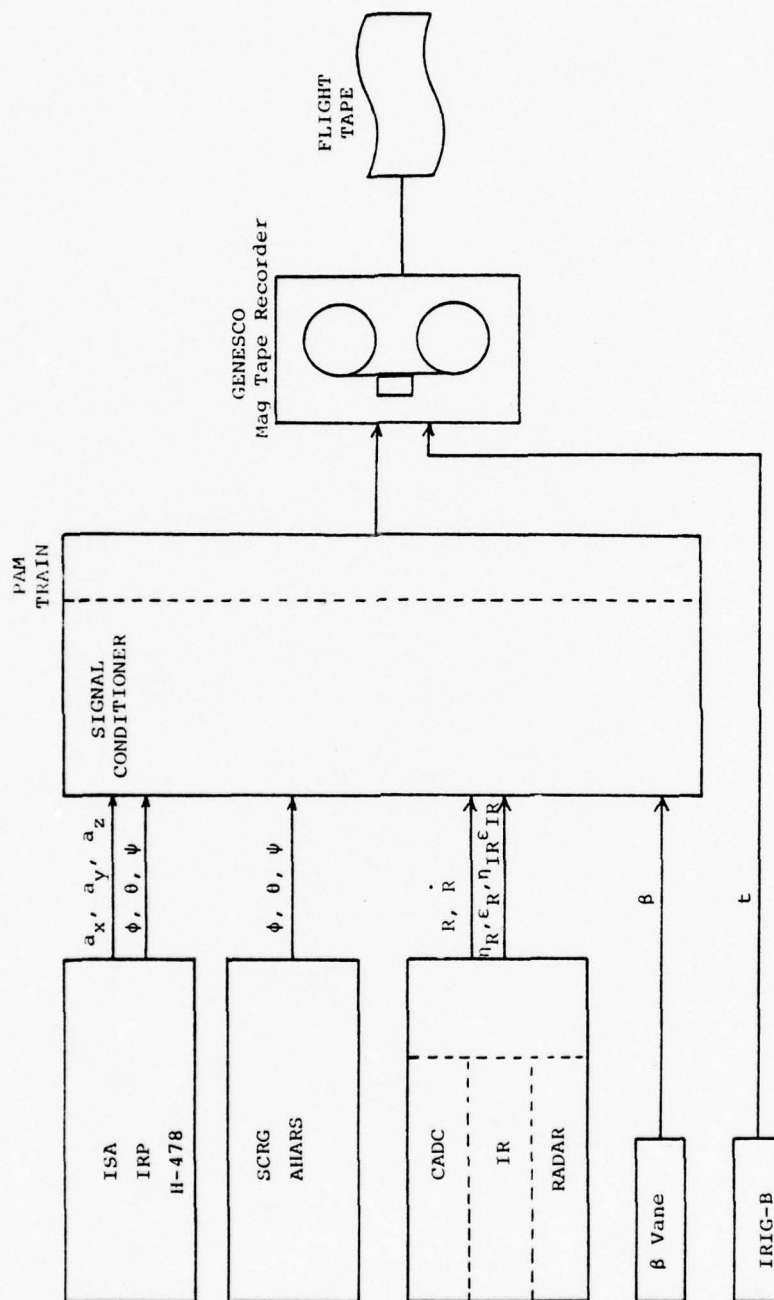


Figure 16 Electrical Analog Signals Recorded in Flight During Sight Eval

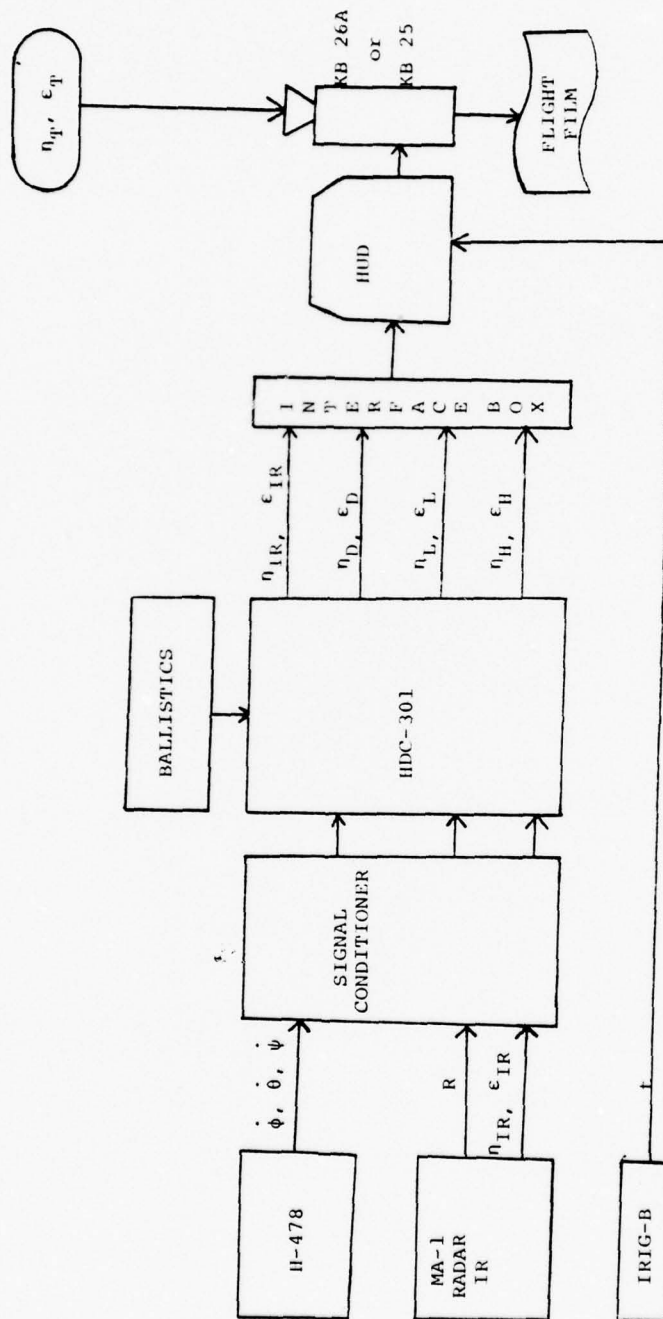


Figure 17 Signals Recorded on Flight Film

information for the type of projectile used, are fed into a HDC-301 computer. Using an algorithm peculiar to each of the gunsights to be compared, the computer determines the future azimuth and elevation of the target. An interface box converts these signals into a form such that they may be rendered as symbols on the HUD (Heads Up Display). They are simultaneously seen by the pilot and recorded on flight film by a KB 25 or KB 26A camera.

The conversion of the flight film and flight tape to digital form and the result recorded on tape in a form compatible with the CDC 6600 is shown in Figure 18. The empty box symbolizes unknown processing and transcribing operations which occurred in some cases. The result, the WPAFB tapes, were the raw material for this analysis.

3.3.3 Preliminary Data Evaluation and Processing

3.3.3.1 Description and Selection of Data

The information on the WPAFB tapes came from data recorded during test missions flown at Tyndall AFB during 1975 and 1976. Figure 19 lists the missions for which data were recorded and supplied to WPAFB. Each mission consisted of a number of passes, and only data from wet (firing) runs were recorded. A study of the data led to the classification of the missions into seven groups, two of which contain but one mission. Data from each pass were considered in the light of pilot comments. In some cases of obvious malfunction; e.g., no radar lock-on, the pass was disregarded.

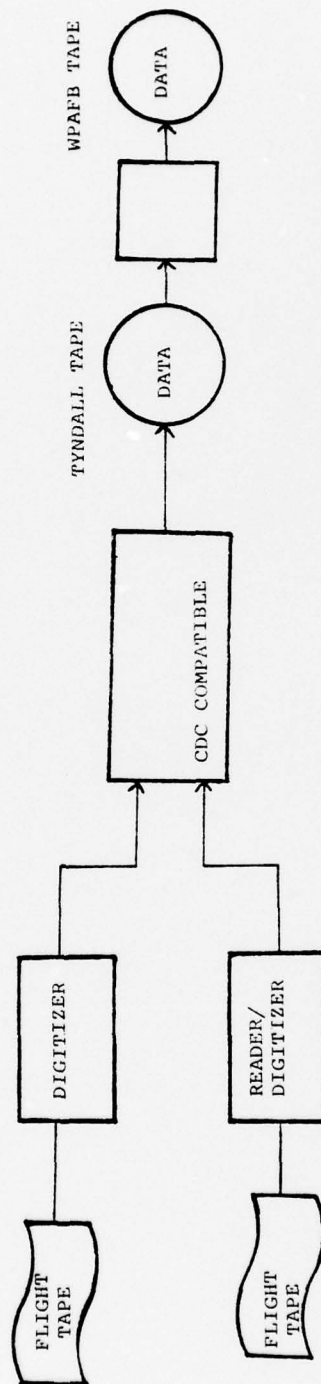
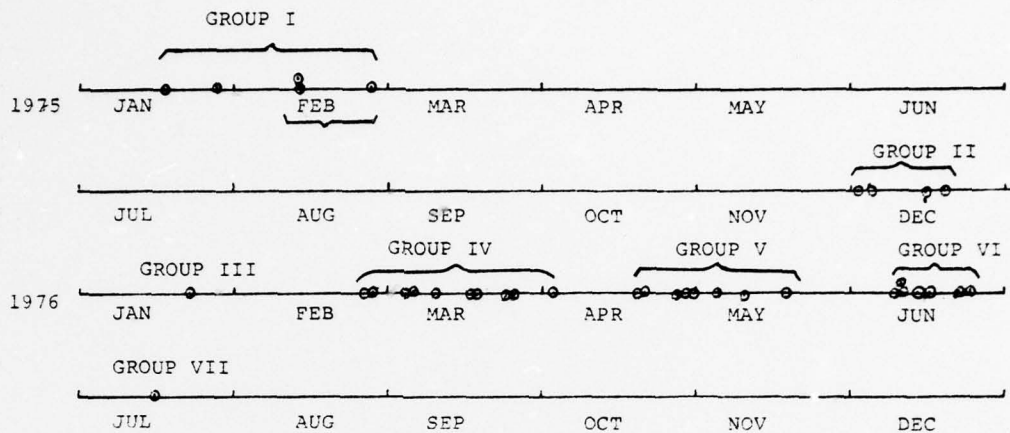


Figure 18 Processing From Flight Records to the WPAFB Data Tape



GROUP	MISSION DATE	ACTUAL DATE	TAPE	GROUP	MISSION DATE	ACTUAL DATE	TAPE
I	75017	17 JAN 75	1187	IV	76085	25 MAR 76	1183
	75027	27 JAN 75	"		(Cont.) 76092	01 APR 76	"
	95044	13 FEB 75	"		76093	02 APR 76	"
	75044	13 FEB 75	"	V	76110	19 APR 76	197
	75058	27 FEB 75	"		76111	20 APR 76	"
II	75336	02 DEC 75	719		76118	27 APR 76	"
	75338	04 DEC 75	1186		76119	28 APR 76	"
	75345	11 DEC 75	719		76121	30 APR 76	"
	75346	12 DEC 75	"		76126	05 MAY 76	301
	75349	15 DEC 75	"		76131	10 MAY 76	"
	75353	19 DEC 75	"		76139	18 MAY 76	"
III	76022	22 JAN 76	270	VI	76162 (#1)	10 JUN 76	301
IV	76057	26 FEB 76	270		76162 (32)	10 JUN 76	1186
	76058	27 FEB 76	"		76163	11 JUN 76	301
	76064	04 MAR 76	"		76166	14 JUN 76	"
	76065	05 MAR 76	"		76167	15 JUN 76	1186
	76070	10 MAR 76	"		76174	22 JUN 76	"
	76077	17 MAR 76	1183		76175	23 JUN 76	"
	76078	18 MAR 76	"	VII	76197	15 JUL 76	1186
	76083	23 MAR 76	"				

Figure 19 Recorded Missions

Each pass record consists of the PAM data plus signals from the time signal generator. Thirty-seven channels of data recorded on the WPABF tapes are listed in Table 11.

Data relevant to this analysis were the time, range, pitch rate, yaw rate, radar antenna azimuth, radar antenna elevation, film target position azimuth, and film target position elevation. When the validity of the data was in doubt, accelerometer, rate gyro, and heading information were examined as possible sources of error.

3.3.3.2 Evaluation and Preliminary Processing of Data

The film records were made on 16 mm film by a KB-25 or KB-26A camera operating at 24 frames per second. Air Force engineers have estimated a maximum error of 1 mrad due to film sensitivity. Alignment has reduced parallax to about the same magnitude. Because of the finite size of the target as seen on the film, a point on the target - usually the tail - was chosen as the target location. However, inconsistency in film reading practice could have led to variations of as much as 5 mrad in the target position.

At close range, an error of from 10 to 20 mrad could have been introduced due to differences between the point on the target selected from film reading and that which was most strongly reflecting the radar signal.

Film elevation and azimuth data and radar range data, elevation, and azimuth data were smoothed by means

TABLE 11
TAPE DATA VARIABLES

<u>WORD NO. IN RECORD</u>	<u>VARIABLE</u>	<u>UNITS</u>
1	IRIG TIME	MSEC
2	TRACKER MODE (0=Range, 1=IR)	—
3	MACH NUMBER	—
4	IMPACT TEMPERATURE	°R
5	STATIC PRESSURE	LES/FT ²
6	ANGLE OR ATTACK	RAD
7	RANGE	FT
8	RANGE RATE	FT/SEC
9	MANUAL RANGE	FT
10	TRIGGER #1 (1.= ON)	—
11	TRIGGER #2 (1.= ON)	—
12	RANGE ON TARGET (1.=LOCK)	—
13	DELAYED RANGE ON TET (1.=LOCK)	—
14	ROLL RATE	RAD/SEC
15	PITCH RATE	RAD/SEC
16	YAW RATE	RAD/SEC
17	X ACCELEROMETER	FT/SEC ²
18	Y ACCELEROMETER	FT/SEC ²
19	Z ACCELEROMETER	FT/SEC ²
20	SIDESLIP ANGLE	RAD
21	EVENT (1.= ON)	—
22	HEADING	RAD
23	ROLL	RAD
24	PITCH	RAD
25	RADAR ANTENNA AZIMUTH	RAD
26	RADAR ANTENNA ELEVATION	RAD
27	—	—
28	—	—
29	IR GIMBAL, AZIMUTH	RAD
30	IR GIMBAL, ELEVATION	RAD
31	AMMO TEMPERATURE (UNCALIB.)	—
32	FILM TARGET POSITION, AZIMUTH	MRAD
33	FILM TARGET POSITION, ELEVATION	MRAD
34	FILM LCOS POS, AZIMUTH	MRAD
35	FILM LCOS POS, ELEVATION	MRAD
36	FILM HLES POS, AZIMUTH	MRAD
37	FILM HLES POS, ELEVATION	MRAD
38	FILM DESIGNATOR POS, AZIMUTH	MRAD
39	FILM DESIGNATOR POS, ELEVATION	MRAD
40-50	(BLANK)	—

of a polynomial function, although the raw film data were reasonably smooth.

The rms error between the radar range data and the fitting function was calculated for 90 passes and the results plotted in Figure 20. The rms variation in radar range lies between 12 and 53 ft (4 to 16 m) and shows no strong dependence on range. If one assumes that the maximum rms deviation of 53 ft corresponds to 3σ , then the noise in the radar range measurements has a standard deviation of less than 6 m.

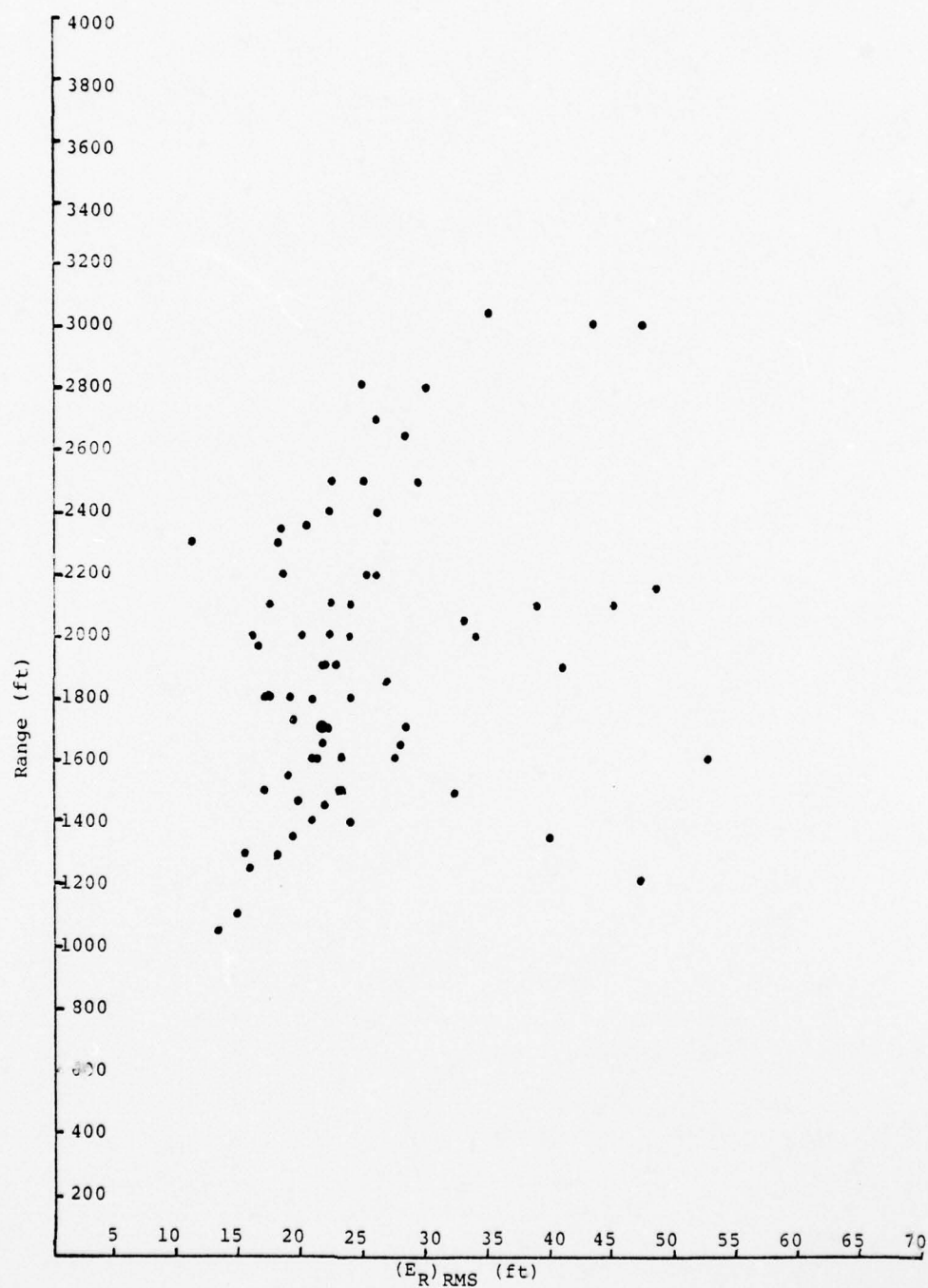


Figure 20 RMS Range Error

3.3.4 Analysis and Correction of Lag Problem

3.3.4.1 Linear Regression

Preliminary plots of radar and film data indicated that the radar data was usually lagging the film data. To use the radar to predict the target position at a future time point or to aim the ASCOT, it is necessary to compensate for the lag. The ideal system adjustment would be a software correction if a functional relationship could be identified which consistently reduced the radar lag. This functional relationship also had to reduce the radar lag to ± 15 MRAD, the ASCOT lock-on constant. Average radar lag was calculated by subtracting film position from radar position for each pass. It was noted that the average radar lag varies considerably between passes on the same mission.

If it is assumed that radar tracking error is a function of line-of-sight rate, the general form of the error is:

$$E_{\epsilon} = A_1 + B_1 \dot{\epsilon}_R + C_1 q$$

$$E_{\eta} = A_2 + B_2 \dot{\eta}_R + C_2 r$$

where

E - Error

$\dot{\epsilon}_R$ - Target elevation rate of change with respect to interceptor airframe axis

$\dot{\eta}_R$ - Target azimuth rate of change with respect to interceptor airframe axis

q - Interceptor pitch angle rate

r - Interceptor yaw angle rate

A, B, C - Constants derived by regression program

The target crossing and consequent radar tracking error was assumed to be a combination of a bias, A , plus a constant, B , times the azimuth or elevation tracking rate

TABLE 12

Tracking Rates (η_F, ϵ_F) vs Mean Radar Error (μ)

MD	DATE	PASS#	AZIMUTH				ELEVATION				Lock-On	ϵ	η
			TURN	TRACK RATE	YAW	AVERAGE RADAR ERROR	STAND. DEVIATION	TRACK RATE	PITCH	AVERAGE RADAR ERROR	STAND. DEVIATION		
75017	17 Jan. 1975	1	R L	-.233	-.003	-51.1	18.3	.049	.124	87.8	10.7	1	OK
		2	L R	.120	.036	38.8	10.8	.209	.191	121	10.3	1	OK
		3	R L	-.150	-.044	-17.9	10.7	.144	.127	85.6	12.7	1	OK
		4	L R	.114	.039	41.5	9.24	.137	.024	92.1	11.0	1	OK
		5	R L	-.150	-.045	-26.2	10.7	.127	.159	81.8	9.36	1	OK
		6	L R	.066	.052	27.1	7.16	.240	.074	148	8.42	1	OK
		7	R L	-.151	-.048	-36.9	9.80	.273	.180	138	9.57	1	OK
		9	R L	-.200	-.043	-38.0	7.37	.240	.055	105	9.73	1	OK
75027	27 Jan.	2	R L	-.082	-.036	-3.0	11.1	.168	.054	28.5	15.6	1	OK
		3	L R	.163	.054	55.5	14.1	.092	.138	31.1	12.5	1	OK
		5	R L	-.161	-.030	-18.8	12.2	.168	.026	51.3	18.0	1	OK
		6	L R	.103	.054	43.8	15.0	.061	.118	36.2	15.3	1	OK
		7	R L	-.180	-.029	-27.1	12.5	.171	.097	56.8	12.7	1	OK
		8	L R	.097	.027	40.0	12.4	.020	.072	27.1	15.2	1	OK
		9	L R	.095	.056	48.4	16.0	.069	.075	35.1	16.6	1	OK
		10	R L	-.023	-.020	10.3	13.4	.027	.052	27.0	15.0	1	OK
95044	13 Feb.	3	R L	-.101	-.035	-53.7	8.92	.076	.042	-3.3	11.1	1	OK
		4	L R	.085	.020	6.2	8.58	.031	.034	-11.0	10.7	1	OK
		5	L R	.111	.028	6.1	10.2	.042	.016	-3.8	9.50	1	OK
		6	R L	-.099	-.027	-55.3	9.16	.057	.022	-10.7	8.80	1	OK
		8	R L	-.198	-.018	-128	17.3	.081	.041	-6.4	8.95	1	OK
		9	R L	-.232	-.030	-152	10.9	.121	-.006	3.5	12.2	1	OK
		2	L R	.078	.04	-9.2	8.29	.092	.016	-1.0	8.56	1	OK
		3	R L	-.035	-.047	-52.1	9.59	.066	.048	-14.5	7.29	1	OK
75044	13 Feb.	5	R L	-.059	-.044	-54.7	7.97	.052	.082	-21.0	8.48	1	OK
		6	L R	.047	.046	-17.7	6.55	.088	-.001	-8.0	7.50	1	OK
		7	R L	.053	.050	-15.9	6.68	.130	.045	2.9	9.54	1	OK
		9	R L	.008	.070	-42.3	10.0	.045	.091	-17.8	7.87	1	OK
		10	L R	.116	.044	49.4	26.0	.063	.081	22.0	18.0	1	OK
		1	R L	-.135	-.018	-79.8	14.6	.073	.006	-10.5	16.2	1	OK
		2	L R	.165	.024	1.2	14.0	.062	.02	-8.8	12.6	1	OK
		4	L R	.162	.023	-5.7	13.3	.092	-.008	-5.9	15.2	1	OK
75058	27 Feb.	6	R L	-.126	-.024	-79.0	15.0	.069	.070	-12.2	14.0	1	OK
		7	L R	.218	.023	-10.6	18.0	.049	.071	-12.8	17.1	1	OK
		9	R L	-.1	-.022	-103	22.8	.088	.053	-14.7	23.4	1	OK
		1	L R	.059	.044	7.97	3.15	.011	.078	4.93	4.12	1	OK
		2	R L	-.055	-.042	-20.3	3.99	.035	.083	11.6	2.91	1	OK
		3	L R	.076	.039	8.56	3.10	.022	.087	5.8	3.01	1	OK
		4	R L	-.100	-.033	-22.5	2.91	.076	.048	10.13	2.54	1	OK
75336	2 Dec.	1	L R	.059	.044	7.97	3.15	.011	.078	4.93	4.12	1	OK
		2	R L	-.055	-.042	-20.3	3.99	.035	.083	11.6	2.91	1	OK
		3	L R	.076	.039	8.56	3.10	.022	.087	5.8	3.01	1	OK
		4	R L	-.100	-.033	-22.5	2.91	.076	.048	10.13	2.54	1	OK
		1	L R	.059	.044	7.97	3.15	.011	.078	4.93	4.12	1	OK
		2	R L	-.055	-.042	-20.3	3.99	.035	.083	11.6	2.91	1	OK
		3	L R	.076	.039	8.56	3.10	.022	.087	5.8	3.01	1	OK
		4	R L	-.100	-.033	-22.5	2.91	.076	.048	10.13	2.54	1	OK
75338	4 Dec.	1	L R	.059	.044	7.97	3.15	.011	.078	4.93	4.12	1	OK
		2	R L	-.055	-.042	-20.3	3.99	.035	.083	11.6	2.91	1	OK
		3	L R	.076	.039	8.56	3.10	.022	.087	5.8	3.01	1	OK
		4	R L	-.100	-.033	-22.5	2.91	.076	.048	10.13	2.54	1	OK
		1	L R	.059	.044	7.97	3.15	.011	.078	4.93	4.12	1	OK
		2	R L	-.055	-.042	-20.3	3.99	.035	.083	11.6	2.91	1	OK
		3	L R	.076	.039	8.56	3.10	.022	.087	5.8	3.01	1	OK
		4	R L	-.100	-.033	-22.5	2.91	.076	.048	10.13	2.54	1	OK

* See explanation of numbers at end of Table.

TABLE 12

Tracking Rates (η_F, ϵ_F) vs Mean Radar Error (μ) (Continued)

MD	DATE	PASS#	AZIMUTH			ELEVATION					Lock-On	ϵ	η
			TURN	TRACK RATE	YAW	AVERAGE RADAR ERROR	STAND. DEVIATION	TRACK RATE	PITCH	AVERAGE RADAR ERROR	STAND. DEVIATION		
75345 F	11 Dec.	1	R L	-.032	-.008	-12.2	3.33	.018	.126	2.0	4.48	2.6	OK
		2	L R	.007	.012	1.4	4.28	-.011	.097	7.3	3.24	2.6	OK
		3	R L	-.019	-.017	-10.4	3.66	.036	.104	4.34	3.57	2.6	OK
		4	L R	-.004	.026	-4.7	3.63	-.008	.114	6.45	3.77	2.6	OK
		5	R L	-.020	-.0005	-11.56	3.60	.020	.109	5.37	4.52	2.6	OK
75346 F	12 Dec.	1	L R	.050	-.009	5.2	7.64	-.025	.138	4.5	8.49	2.6	OK
		2	R L	-.022	-.008	-8.8	9.90	.013	.156	3.5	4.95	2.6	OK
		4	L R	-.029	-.002	-10.96	7.41	.018	.171	5.93	6.21	2.6	OK
		5	R L	.018	.023	-0.4	8.41	-.006	.156	4.02	8.49	2.6	OK
		6	L R	-.026	.060	47.2	24.3	.006	.182	9.57	16.6	2.6	OK
		7	L R	.008	.027	-4.42	15.0	.003	.157	3.98	17.2	2.6	OK
		1	L R	.020	.053	.06	3.59	.007	.105	5.41	2.30	2.6	OK
75353 F	19 Dec.	1	L R	.192	.025	48.4	5.04	.011	.055	6.92	7.74	6	OK
		2	R L	-.048	-.055	-4.1	6.94	.070	.071	22.3	4.64	6	OK
		3	L R	.106	.035	10.1	4.66	.036	.053	8.8	5.80	6	OK
		4	R L	-.096	-.037	-24.1	3.62	.051	.070	19.2	4.65	6	OK
		5	L R	.087	.045	16.85	3.69	.022	.106	16.76	5.00	6	OK
		6	L R	.104	.033	20.9	3.27	.014	.072	9.74	4.62	6	OK
		7	R L	-.193	-.045	-48.3	5.39	.081	.173	30.55	10.83	6	OK
76022 F	22 Jan. 1976	1	L R	.156	.042	127.5	19.6	.131	.040	123	27.3	7a1	OK
		4	L R	.022	.030	-13.9	5.95	.033	.040	-13.4	7.67	OK	OK
		2	L R	.006	.033	-31	7.34	.010	.111	16.6	6.4	6	OK
76057	26 Feb.	3	L R	.052	.042	6.92	6.54	.036	.155	30.7	4.00	OK	OK
		4	L R	.058	.040	9.60	5.38	.067	.094	40.6	7.39	OK	OK
		5	R L	-.005	.041	-11.6	13.7	.074	.112	39.8	6.18	OK	OK
		6	R L	-.016	.004	-20.6	30.6	.005	.105	6.97	18.1	OK	OK
		7	R L	-.026	.028	-24.9	10.3	-.038	.182	1.67	12.1	OK	OK
		1	R L	-.097	-.042	-41.3	3.97	.009	.150	13.0	6.24	OK	OK
		3	R L	-.044	-.054	-29.5	4.55	.030	.087	18.4	5.24	OK	OK
D		4	L R	.080	.042	7.74	2.55	.122	.030	25.7	2.85	OK	OK
		7	R L	-0.59	-.039	-33.1	4.48	.052	.113	16.2	6.93	OK	OK
		8	L R	.136	-.033	-5.82	47.3	.088	.076	-39.7	17.0	OK	OK
		9	R L	-.060	-.042	-91.5	27.5	.091	.071	79.9	40.1	7a1	OK
		1	L R	.046	.046			.017	.055			OK	OK
76064 F	4 Mar.	2	R L	-.014	-.023			.041	.055			OK	OK
		4	R L	-.048	-.055			.104	.046			OK	OK
		5	L R	.102	.038			.069	.092			OK	OK
		6	R L	-.006	-.022			.040	.097			OK	OK
		1	L R	.048	.042	-4.55	9.66	.028	.059	14.8	7.01	OK	OK
		2	R L	-.018	-.026	-24.3	4.24	.031	.073	8.45	5.12	OK	OK
D	5 Mar.	3	L R	.053	.036	-3.73	9.86	.069	.120	33.2	5.33	OK	OK
		4	R L	-.072	-.055	-56.0	7.10	.047	.093	33.8	4.00	OK	OK
		6	R L	-.066	-.043	-36.3	4.26	.068	.081	19.2	5.38	OK	OK
		1	L R	.048	.042	-4.55	9.66	.028	.059	14.8	7.01	OK	OK

TABLE 12

Tracking Rates (η_F, ϵ_F) vs Mean Radar Error (μ) (Continued)

			AZIMUTH				ELEVATION								
MD	DATE	PASS#	TURN	TRACK RATE	AVERAGE RADAR YAW ERROR	STAND. DEVIATION	TRACK RATE	PITCH	AVERAGE RADAR ERROR	STAND. DEVIATION	Lock-On	ϵ	η		
76065	5 Mar.	7	L R	.162	.042	104	26.5	.159	.222	141	28.4	1	7		
		8	R L	-.116	-.045	-53.3	3.96	.127	.080	34.1	5.46	1	OK		
76070	10 Mar.	2	R L	-.003	0.17	-2.28	13.5	.030	.139	-8.68	4.69	1	OK		
		3	L R	-.091	-.052	12.2	14.2	.084	.154	7.77	4.69	1	OK		
		4	R L	0.081	-.024	-9.29	20.2	.050	.097	-1.13	5.05	1	OK		
		5	L R	.101	.057	.01	14.6	.149	.029	11.9	5.26	1	OK		
76077	17 Mar.	6	R L	-.164	-.017	-1.85	28.5	.121	.075	11.3	5.83	1	OK		
		1	L R	.035	.035	3.54	3.40	.041	.074	9.8	4.41	1	OK		
76078	18 Mar.	2	R L	-.030	-.034	-10.5	3.36	.065	.047	10.5	3.58	1	OK		
		3	L R	-.036	-.041	-12.7	6.74	.086	.061	16.4	5.69	1	OK		
		5	L R	.118	.037	3.0	4.05	.086	.093	6.4	7.12	1	OK		
		6	R L	-.131	-.024	-27.4	3.28	.101	.105	12.7	3.93	1	OK		
76083	23 Mar.	7	L R	.164	.037	9.8	4.09	.144	.106	13.1	5.79	1	OK		
		1	R L	-.024	-.017	-7.1	3.02	.034	.066	3.4	3.47	1	OK		
		2	L R	.073	.017	16.6	4.55	.065	.105	16.6	4.90	1	OK		
		3	L R	-.006	.051	5.9	6.14	.007	.101	13.7	9.59	1	OK		
76085-F	25 Mar.	4	L R	-.025	.024	10.5	3.55	.017	.094	13.4	3.84	1	OK		
		5	R L	-.046	-.013	-16.8	11.4	.026	.087	-6.4	9.59	1	OK		
		6	L R	.170	.025	35.9	6.75	.122	.101	30.3	7.36	1	OK		
		7	R L	-.139	-.029	-33.4	3.67	.118	.079	11.4	7.95	1	OK		
76092	1 Apr.	8	R L	-.169	-.021	-41.8	3.58	.101	.056	17.6	2.96	1	OK		
		1	L R	.168	.040	26.2	4.42	.105	.087	27.0	3.19	1	OK		
		2	R L	-.162	-.022	-29.7	7.89	.103	.034	2.9	7.47	1	OK		
		3	L R	.179	.036	24.4	2.59	.130	.065	23.3	2.51	1	OK		
79093	2 Apr.	4	R L	-.116	-.031	-35.0	9.16	.114	.049	15.7	6.35	1	OK		
		5	L R	.303	.032	58.6	38.3	.257	.069	59.1	28.9	1	OK		
		2	L R	.016	.055	4.4	7.74	.020	.09	25.2	5.82	1	OK		
		1	R L	-.033	-.0007	-26.8	16.4	.005	.102	20.0	7.54	1	OK		
76110	19 Apr	3	R L	-.005	.046	4.3	1.91	.053	.120	12.3	3.76	1	OK		
		1	R L	-.030	.012	-17.1	10.7	-.004	.121	9.8	14.1	1	OK		
		2	L R	.002	-.038	-32.0	4.03	-.080	.207	56.1	4.42	1	OK		
		3	L R	.005	.039	167.5	3.11	-.055	.135	-83.4	28.6	1	OK		
76110	19 Apr	5	R L	.0003	-.041	211.1	3.82	-.030	.099	-90.6	21.5	1	OK		
		1	R L	-.030	.012	-17.1	10.7	-.004	.121	9.8	14.1	1	OK		
		2	L R	.002	-.038	-32.0	4.03	-.080	.207	56.1	4.42	1	OK		
		3	L R	.005	.039	167.5	3.11	-.055	.135	-83.4	28.6	1	OK		
76110	19 Apr	5	R L	.0003	-.041	211.1	3.82	-.030	.099	-90.6	21.5	1	OK		
		1	R L	-.030	.012	-17.1	10.7	-.004	.121	9.8	14.1	1	OK		
		2	L R	.002	-.038	-32.0	4.03	-.080	.207	56.1	4.42	1	OK		
		3	L R	.005	.039	167.5	3.11	-.055	.135	-83.4	28.6	1	OK		
76110	19 Apr	5	R L	.0003	-.041	211.1	3.82	-.030	.099	-90.6	21.5	1	OK		
		1	R L	-.030	.012	-17.1	10.7	-.004	.121	9.8	14.1	1	OK		
		2	L R	.002	-.038	-32.0	4.03	-.080	.207	56.1	4.42	1	OK		
		3	L R	.005	.039	167.5	3.11	-.055	.135	-83.4	28.6	1	OK		
76110	19 Apr	5	R L	.0003	-.041	211.1	3.82	-.030	.099	-90.6	21.5	1	OK		
		1	R L	-.030	.012	-17.1	10.7	-.004	.121	9.8	14.1	1	OK		
		2	L R	.002	-.038	-32.0	4.03	-.080	.207	56.1	4.42	1	OK		
		3	L R	.005	.039	167.5	3.11	-.055	.135	-83.4	28.6	1	OK		
76110	19 Apr	5	R L	.0003	-.041	211.1	3.82	-.030	.099	-90.6	21.5	1	OK		
		1	R L	-.030	.012	-17.1	10.7	-.004	.121	9.8	14.1	1	OK		
		2	L R	.002	-.038	-32.0	4.03	-.080	.207	56.1	4.42	1	OK		
		3	L R	.005	.039	167.5	3.11	-.055	.135	-83.4	28.6	1	OK		
76110	19 Apr	5	R L	.0003	-.041	211.1	3.82	-.030	.099	-90.6	21.5	1	OK		
		1	R L	-.030	.012	-17.1	10.7	-.004	.121	9.8	14.1	1	OK		
		2	L R	.002	-.038	-32.0	4.03	-.080	.207	56.1	4.42	1	OK		
		3	L R	.005	.039	167.5	3.11	-.055	.135	-83.4	28.6	1	OK		
76110	19 Apr	5	R L	.0003	-.041	211.1	3.82	-.030	.099	-90.6	21.5	1	OK		
		1	R L	-.030	.012	-17.1	10.7	-.004	.121	9.8	14.1	1	OK		
		2	L R	.002	-.038	-32.0	4.03	-.080	.207	56.1	4.42	1	OK		
		3	L R	.005	.039	167.5	3.11	-.055	.135	-83.4	28.6	1	OK		
76110	19 Apr	5	R L	.0003	-.041	211.1	3.82	-.030	.099	-90.6	21.5	1	OK		
		1	R L	-.030	.012	-17.1	10.7	-.004	.121	9.8	14.1	1	OK		
		2	L R	.002	-.038	-32.0	4.03	-.080	.207	56.1	4.42	1	OK		
		3	L R	.005	.039	167.5	3.11	-.055	.135	-83.4	28.6	1	OK		
76110	19 Apr	5	R L	.0003	-.041	211.1	3.82	-.030	.099	-90.6	21.5	1	OK		
		1	R L	-.030	.012	-17.1	10.7	-.004	.121	9.8	14.1	1	OK		
		2	L R	.002	-.038	-32.0	4.03	-.080	.207	56.1	4.42	1	OK		
		3	L R	.005	.039	167.5	3.11	-.055	.135	-83.4	28.6	1	OK		
76110	19 Apr	5	R L	.0003	-.041	211.1	3.82	-.030	.099	-90.6	21.5	1	OK		
		1	R L	-.030	.012	-17.1	10.7	-.004	.121	9.8	14.1	1	OK		
		2	L R	.002	-.038	-32.0	4.03	-.080	.207	56.1	4.42	1	OK		
		3	L R	.005	.039	167.5	3.11	-.055	.135	-83.4	28.6	1	OK		
76110	19 Apr	5	R L	.0003	-.041	211.1	3.82	-.030	.099	-90.6	21.5	1	OK		
		1	R L	-.030	.012	-17.1	10.7	-.004	.121	9.8	14.1	1	OK		
		2	L R	.002	-.038	-32.0	4.03	-.080	.207	56.1	4.42	1	OK		
		3	L R	.005	.039	167.5	3.11	-.055	.135	-83.4	28.6	1	OK		
76110	19 Apr	5	R L	.0003	-.041	211.1	3.82	-.030	.099	-90.6	21.5	1	OK		
		1	R L	-.030	.012	-17.1	10.7	-.004	.121	9.8	14.1	1	OK		
		2	L R	.002	-.038	-32.0	4.03	-.080	.207	56.1	4.42	1	OK		
		3	L R	.005	.039	167.5	3.11	-.055	.135	-83.4	28.6	1	OK		
76110	19 Apr	5	R L	.0003	-.041	211.1	3.82	-.030	.099	-90.6	21.5	1	OK		
		1	R L	-.030	.012	-17.1	10.7	-.004	.121	9.8	14.1	1	OK		
		2	L R	.002	-.038	-32.0	4.03	-.080	.207	56.1	4.42	1	OK		
		3	L R	.005	.039	167.5	3.11	-.055	.135	-83.4	28.6	1	OK		
76110	19 Apr	5	R L	.0003	-.041	211.1	3.82	-.030	.099	-90.6	21.5	1	OK		
		1	R L	-.030	.012	-17.1	10.7	-.004	.121	9.8	14.1	1	OK		
		2	L R	.002	-.038	-32.0	4.03	-.080	.207	56.1	4.42	1	OK		
		3	L R	.005	.039	167.5	3.11	-.055	.135	-83.4	28.6	1	OK		
76110	19 Apr	5	R L	.0003	-.041	211.1	3.82	-.030	.099	-90.6	21.5	1	OK		
		1	R L	-.030	.012	-17.1	10.7	-.004	.121	9.8	14.1	1	OK		
		2	L R	.002	-.038	-32.0	4.03	-.080	.207	56.1	4.42	1	OK		
		3	L R	.005	.039	167.5	3.11	-.055	.135	-83.4	28.6	1	OK		
76110	19 Apr	5	R L	.0003	-.041	211.1	3.82	-.030	.099	-90.6	21.5	1	OK		
		1	R L	-.030	.012	-17.1	10.7	-.004	.121	9.8	14.1	1	OK		
		2	L R	.002	-.038	-32.0	4.03	-.080	.207	56.1	4.42	1	OK		
		3	L R	.005	.039	167.5	3.11	-.055	.135	-83.4	28.6	1	OK		
76110	19 Apr	5	R L	.0003	-.041	211.1	3.82	-.030	.099	-90.6	21.5	1	OK		
		1	R L	-.030	.012	-17.1	10.7	-.004	.121	9.8	14.1	1	OK		
		2	L R	.002	-.038	-32.0	4.03	-.080	.207	56.1	4.42	1	OK		
		3	L R	.005	.039	167.5	3.11	-.055	.135	-83.4	28.6	1	OK		
76110	19 Apr	5	R L	.0003	-.041	211.1	3.82	-.030	.099	-90.6	21.5	1	OK		
		1	R L	-.030	.012	-17.1	10.7	-.004	.121	9.8	14.1	1	OK		
		2	L R	.002	-.038	-32.0	4.03	-.080	.207	56.1	4.42	1	OK		
		3	L R	.005	.039	167.5	3.11	-.055	.135	-83.4	28.6	1	OK		
76110	19 Apr	5	R L	.0003	-.041	211.1	3.82	-.030	.099	-90.6	21.5	1	OK		
		1	R L	-.030	.012	-17.1	10.7	-.004	.121	9.8	14.1	1	OK		
		2	L R	.002	-.038	-32.0	4.03	-.080	.207	56.1	4.42	1	OK		
		3	L R	.005	.039	167.5	3.11	-.055	.135	-83.4	28.6	1	OK		
76110	19 Apr	5	R L	.0003	-.041	211.1	3.82	-.030	.099	-90.6	21.5	1	OK		
		1	R L	-.030	.012	-17.1	10.7	-.004	.121	9.8	14.1	1	OK		
		2	L R	.002	-.038	-32.0	4.03	-.080	.207	56.1	4.42	1	OK		
		3	L R	.005	.039	167.5	3.11	-.055	.135	-83.4	28.6	1	OK		
76110	19 Apr	5	R L	.0003	-.041	211.1	3.82	-.030	.099	-90.6	21.5	1	OK		
		1	R L	-.030	.012	-17.1	10.7	-.004	.121	9.8	14.1	1	OK		
		2	L R	.002	-.038	-32.0	4.03	-.080	.207	56.1	4.42	1	OK		
		3	L R	.005	.039	167.5	3.11	-.055	.135	-83.4	28.6	1	OK		
76110	19 Apr														

TABLE 12

Tracking Rates (η, ϵ_F) vs Mean Radar Error (μ) (Continued)

MD	DATE	PASS#	AZIMUTH			ELEVATION					Lock-On	ϵ	η
			TURN	TRACK RATE	YAW	AVERAGE RADAR ERROR	STAND. DEVIATION	TRACK RATE	PITCH	AVERAGE RADAR ERROR	STAND. DEVIATION		
76111 F	20 Apr.	1	R L	-.090	-.033	-18.9	4.14	.103	.012	12.6	5.21	OK	OK
		2	L R	-.059	.033	19.2	2.50	.064	-.026	10.6	2.86	OK	OK
		3	R L	-.181	-.029	-38.8	4.36	.077	.076	11.9	3.84	OK	OK
		4	R L	-.151	-.038	-28.4	4.75	.134	-.069	22.5	6.49	OK	OK
		5	L R	.180	.027	40.9	4.53	.092	.117	20.4	4.62	OK	OK
76118 F	27 Apr.	1	R L	-.085	-.031	-23.1	2.64	.081	.019	16.9	4.75	OK	OK
		2	L R	-.074	.054	20.4	7.18	.130	.0005	21.8	6.15	OK	OK
		3	R L	-.123	-.032	-33.1	3.57	.104	-.055	25.4	6.76	OK	OK
		4	L R	.129	.030	13.9	3.24	.105	.035	6.6	5.84	OK	OK
		5	L R	.110	.043	27.7	2.89	.110	.007	19.1	4.03	OK	OK
		6	R L	-.164	-.036	-52	9.23	.182	-.040	51.7	16.3	OK	OK
		7	L R	.186	.042	-57	3.23	.172	.015	34.2	6.47	OK	OK
		8	R L	-.132	-.037	-75	23.3	.128	.118	130	58.0	OK	OK
76119 F	28 Apr.	4	L R	.044	.016	-229	53.6	.007	.070	-295	56.5	OK	OK
		5	L R	.037	.037	9.0	3.13	.019	-.042	3.3	3.97	OK	OK
		6	L R	.052	.052	7.72	3.28	.064	.034	13.8	5.58	OK	OK
		7	R L	-.034	-.040	-12.9	4.22	.077	.055	22.2	5.60	OK	OK
		8	L R	.042	.033	16.8	12.4	-.004	.084	9.7	11.4	OK	OK
		9	L R	.093	.039	27.9	5.53	.021	.085	23.0	6.42	OK	OK
		10	L R	.103	.042	35.1	5.37	.105	.043	29.1	8.14	OK	OK
		1	L R	-.003	.035	-4.9	4.28	.033	.054	2.2	3.61	OK	OK
		2	R L	-.022	-.022	-11.6	3.79	.035	.048	.3	3.51	OK	OK
		3	L R	.025	.039	9.9	2.83	.022	.058	2.9	2.59	OK	OK
76121 F	30 Apr.	4	L R	.031	.043	10.3	6.20	.050	.091	6.4	11.9	OK	OK
		5	L R	.135	.040	42	3.88	.115	.012	27.6	4.60	OK	OK
		6	R L	-.098	-.035	-24	3.31	.159	.036	22	3.39	OK	OK
		7	L R	.082	.042	-18.8	5.11	.088	.065	15.5	6.29	OK	OK
		8	R L	-.090	-.036	-17.7	4.27	.106	.012	-6	4.06	OK	OK
		9	L R	.140	.047	39.5	4.46	.161	.042	37.6	6.80	OK	OK
		1	L R	.034	.036	-11.3	2.82	.033	.084	4.9	4.21	OK	OK
		2	R L	-.062	-.029	-23.7	2.90	.059	.020	-2.6	3.36	OK	OK
		3	L R	.060	.030	11.7	3.73	.045	.039	4.7	3.75	OK	OK
		4	L R	.032	.043	15.4	20.5	.055	.067	11.4	11.6	OK	OK
76126 D	5 May	1	L R	-.030	.043	-14.5	2.65	.059	.032	-3.5	3.30	OK	OK
		2	R L	.117	.050	24.8	5.37	.102	.138	39.5	17.7	OK	OK
		3	L R	-.057	-.026	-21.1	5.22	.060	.105	10.8	4.17	OK	OK
		4	R L	.115	.035	22.7	2.30	.117	.085	17.1	5.98	OK	OK
		5	L R	-.039	.049	12.0	3.75	.045	.073	5.2	3.92	OK	OK
		6	R L	.143	-.035	-49	5.47	.121	.093	33.9	9.04	OK	OK
		7	L R	-.104	.104	23.9	5.06	.182	.103	66.1	11.5	OK	OK
		8	R L	.007	.029	-4.6	5.85	.020	.090	-3.1	3.25	OK	OK
		9	L R	-.064	-.027	-18.1	4.39	.148	.104	9.1	5.82	OK	OK
		10	R L	.032	.043	15.4	20.5	.055	.067	11.4	11.6	OK	OK

TABLE 12

Tracking Rates (η_F, ϵ_F) vs Mean Radar Error (μ) (Continued)

			AZIMUTH				ELEVATION							
MD	DATE	PASS#	TURN	TRACK RATE	YAW	AVERAGE RADAR ERROR	STAND. DEVIATION	TRACK RATE	PITCH	AVERAGE RADAR ERROR	STAND. DEVIATION	Lock-On	ϵ	η
76139	18 May	1	R L	.105	-.033	-299	54.8	.087	.054	150	27.1	0	1	1
		2	L R	-.160	-.049	227	25.2	.173	.147	121	27.1	0	1	1
		3	R L	.241	-.033	-333	37.0	.125	.066	152	21.8	0	1	1
		4	L R	-.141	-.054	267	37.7	.087	.108	176	22.6	0	1	1
		5	R L	.410	-.031	-340	22.8	.401	.197	177	23.7	0	1	1
		6	L R	-.218	-.070	55.1	38.3	.284	.170	155	39.8	0	1	1
		7	L R	.008	.053	12.9	17.9	.057	.082	73.8	81.3	0	1	6
76162	10 Jun.	1	R L	-.065	-.078	31.2	126	.086	.013	39.2	53.3	OK	OK	8
		2	R L	-.068	-.017	-32.5	10.3	.125	.139	28.5	15.7	OK	OK	OK
		3	R L	-.072	-.033	-26.3	7.13	.175	.059	30.0	6.72	OK	OK	OK
		4	R L	-.015	-.049	-7.2	46.2	.119	.090	28.7	28.4	OK	OK	OK
		5	R L	-.073	-.027	-34.6	2.66	.250	.056	55.3	11.8	OK	OK	OK
		6	R L	-.121	-.017	-50.3	8.96	.129	.190	33.9	14.2	OK	OK	OK
		7	R L	-.101	-.053	6.7	100	.110	.076	24.2	25.5	OK	OK	8
76162	10 Jun.	11	R L	-.065	-.048	-22.7	18.5	.087	.068	25.6	22.2	OK	OK	OK
		12	R L	-.070	-.026	-25.2	12.1	.127	.129	36.3	15.4	OK	OK	OK
		13	R L	-.072	-.043	-19.5	8.01	.176	.049	37.7	8.02	OK	OK	OK
		14	R L	-.017	-.050	-6.5	11.0	.119	.093	32.2	16.9	OK	OK	OK
		15	R L	-.073	-.032	-27.5	7.14	.246	.045	60.3	17.8	OK	OK	OK
		16	R L	-.121	-.025	-41.1	10.0	.130	.183	40.2	14.6	OK	OK	OK
		17	R L	-.103	-.031	24.1	10.2	.110	.112	32.1	16.6	OK	OK	OK
76163	11 Jun.	1	L R	.055	.031	29.6	5.93	.057	.042	18.3	7.08	OK	OK	OK
		2	R L	-.131	-.034	-27.1	5.56	.117	.129	23.4	6.75	OK	OK	OK
		3	L R	.115	.030	41.9	7.36	.104	.026	25.7	8.69	OK	OK	OK
		4	L R	-.163	-.043	-32.0	5.25	.090	.019	28.2	8.52	OK	OK	OK
		5	R L	-.040	-.051	2.1	6.52	.051	.045	13.2	5.29	OK	OK	OK
		6	L R	.136	.025	44.6	6.49	.092	.034	26.8	6.18	OK	OK	OK
		9	L R	.094	.038	37.6	4.88	.130	.006	30.3	8.72	OK	OK	OK
76166	14 Jun.	1	R L	-.034	-.016	-12.0	6.18	.009	.079	-5.1	6.84	12	12	12
		2	L R	.004	.045	2.0	2.01	.023	.059	2.2	7.22	OK	OK	OK
		3	R L	-.050	-.052	-18.6	8.35	.115	.020	11.6	6.81	OK	OK	OK
		4	L R	.049	.015	27.1	46.8	.056	.101	17.8	37.0	OK	OK	OK
		5	R L	-.074	-.038	-26.1	23.7	.060	.087	2.3	5.70	OK	OK	OK
		6	L R	.182	.042	23.7	7.51	.060	.151	6.0	6.98	OK	OK	OK
		7	L R	.096	.048	12.6	5.97	.086	.090	7.3	6.49	OK	OK	OK
76167	15 Jun.	8	L R	.100	.031	23.0	5.71	.134	.113	21.6	5.05	OK	OK	OK
		1	L R	.181	.032	-81	29.5	.087	.062	-87	20.6	OK	OK	OK
		2	L R	-.013	.028	-8.2	5.17	-.071	.092	-33.2	27.6	OK	OK	OK

TABLE 12

Tracking Rates (η_F, ϵ_F) vs Mean Radar Error (μ) (Continued)

MD	DATE	PASS#	AZIMUTH			ELEVATION					ϵ	η
			TURN	TRACK RATE	YAW	AVERAGE RADAR ERROR	STAND. DEVIATION	TRACK RATE	PITCH	AVERAGE RADAR ERROR	STAND. DEVIATION	Lock-On
76174 D	22 Jun.	1	R L	-.041	-.006	-14.6	6.47	.039	.053	-6.5	5.77	OK
		2	L R	-.248	.016	65.8	11.4	.199	.041	48.5	11.3	OK
		3		-.000005	.036	129	296	.191	.054	-41.1	29.8	OK
		4	R L	-.149	.603	50.6	28.7	.171	.146	23.1	9.66	OK
		5	R L	-.133	-.033	-52.1	6.68	.396	.027	52.9	8.71	OK
76175 F	23 Jun.	1	R L	-.034	-.069	19.9	95.1	.082	-.00003	25.4	78.9	2.8
		2	R L	-.804	-.041	-42.1	9.11	.135	.107	13.1	13.9	OK
		3	R L	-.033	-.033	-21.9	6.44	.128	.028	8.3	5.24	OK
		4	R L	-.116	-.034	-46.3	4.87	.208	.063	26.9	14.2	OK
		5	R L	-.025	-.074	32.5	104	.079	-.020	40.0	76.8	2
		6	L R	-.097	.042	23.4	6.38	.133	.016	14.5	7.28	OK
		7	R L	-.121	-.029	-53.5	3.27	.176	.028	20.0	3.64	OK
		8	L R	.235	.052	42.8	4.12	.064	.142	14.5	2.32	OK
		9	L R			47.5	5.85			13.8	4.18	OK
76197 F	15 Jul.	1	L R	.083	.040	7.1	2.52	.081	.055	4.8	4.12	OK
		2	R L	-.049	-.057	-14.1	55.8	.093	.056	11.9	48.1	2.8
		3	R L	-.064	-.104	38.6	125	.188	-.041	56.5	67.5	2.8
		4		.048	-.250	194	13.0	.086	-.284	134	24.3	2.8
		5	R L	-.051	-.036	-32.0	3.90	.099	.031	1.5	6.06	OK
		6	L R	-.082	.045	7.4	3.56	.094	.030	5.8	3.28	OK
		7	L R	.169	.034	23.0	4.95	.111	.066	14.1	3.46	OK
		8		.133	.032	-22.8	30.9	.126	.135	15.1	4.57	OK
		9		-.128	-.026			.145	.111			OK

1. No radar lock-on - or lock-on lost.
2. Poly curve fit to radar data was not adequate for calculation of crossing rates.
3. No radar data at all.
4. Tape not read due to parity errors.
5. Suspect tape (data out of chronological order).
6. AZ rate or EL rate changed sign.
7. Radar not tracking properly (1)
8. Erratic radar data.
9. Film data too short (6 pts or less)
10. No radar motion
11. No film data
12. Radar data appears descretized.

of the radar antenna, plus a constant, C, times the pitch or yaw angle rates of the interceptor. The missions were divided into seven chronological groupings and a regression analysis was performed on each group to determine the coefficients A, B, and C. The data groupings (as defined in Section 3.3.3.1) are shown in Figures 21 thru 27.

The results of the regression indicated that the significant contribution was always the $B_1 \dot{\epsilon}_R$ term. This is not surprising as the pitch and yaw rates were small compared with $\dot{\epsilon}$ as was the C coefficient. The total contribution of Cq or Cr was thus negligible. The A coefficient defines the bias in the radar. The bias contribution while small, varied between data groups indicating a negligible constant bias. Ideally if the radar lag is a true function of crossing rate, a zero crossing rate implies no radar lag. For these reasons the functional relationship for all missions was simply expressed as

$$E_{\epsilon} = B_1 \dot{\epsilon}_R ; B_1 = -135$$

$$E_{\eta} = B_2 \dot{\epsilon}_R ; B_2 = -250$$

The mean radar error components were then calculated for each pass. The tracking error correction was applied and the mean radar error was again calculated. Histograms of the mean radar errors are shown in Figures 28 thru 31. The mean error plotted can be expressed as

$$\epsilon_R - \epsilon_F - E_{\epsilon} = E_{\epsilon c}$$

$$\eta_R - \eta_F - E_{\eta} = E_{\eta c}$$

where ϵ_R Radar Elevation

ϵ_F Film Elevation

η_R Radar Azimuth

E_{ϵ} Elevation Tracking Corrector

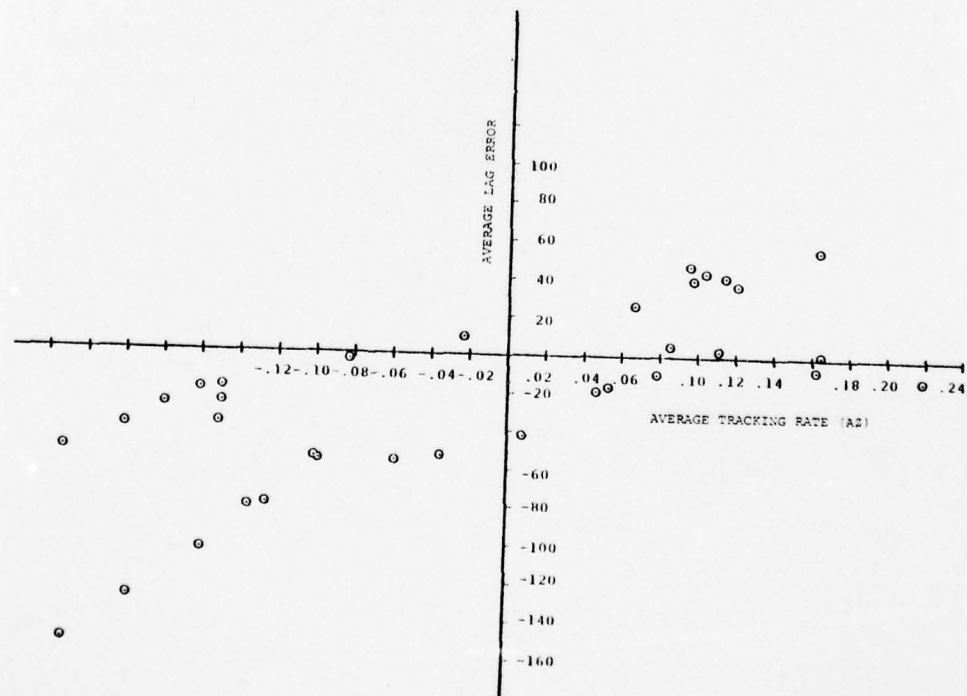
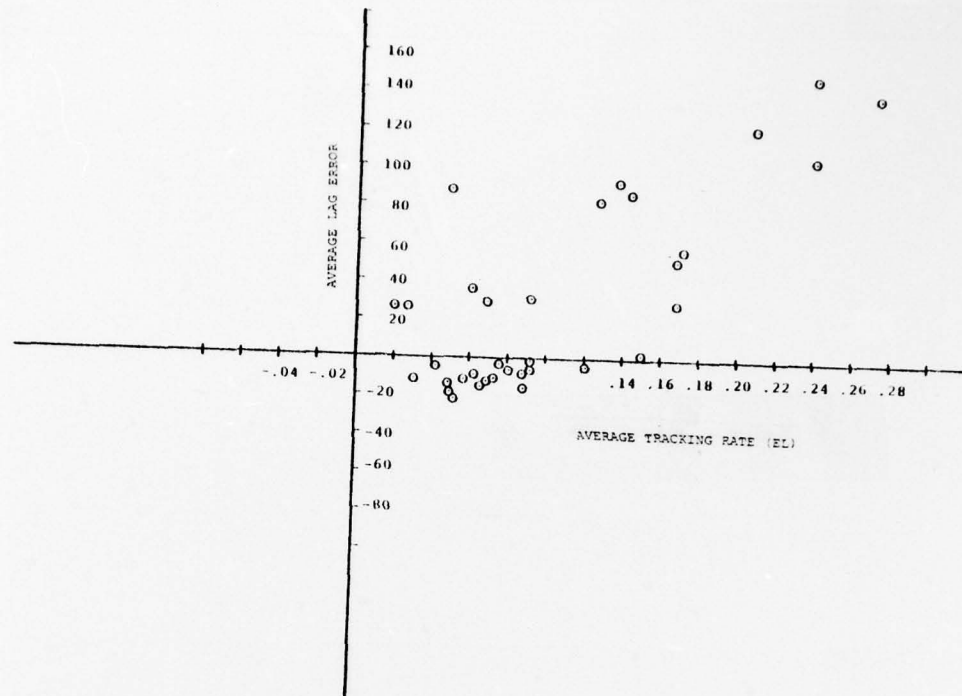


Figure 21 Data Group I

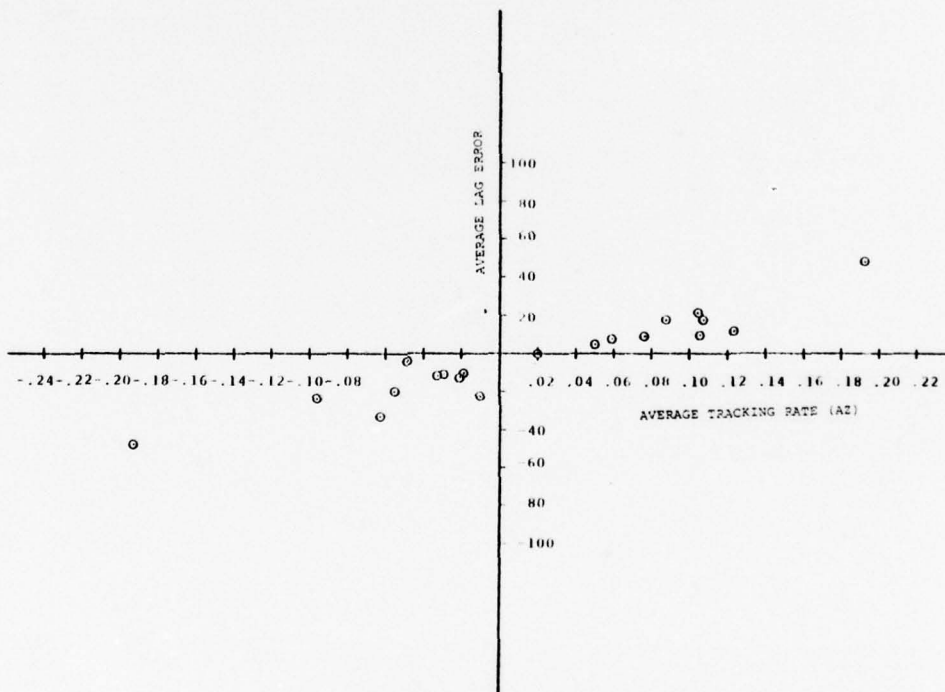
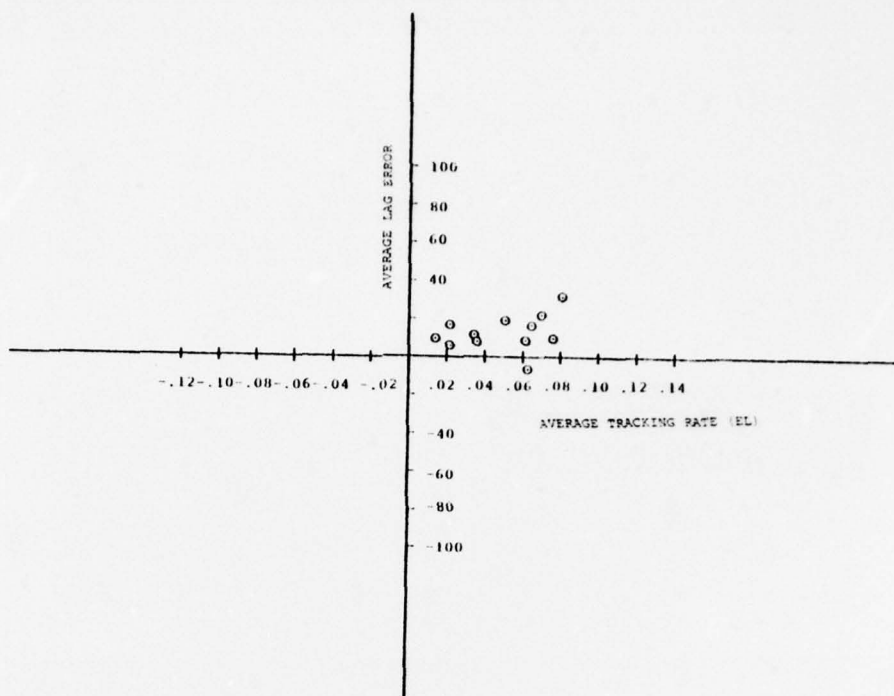


Figure 22 Data Group II

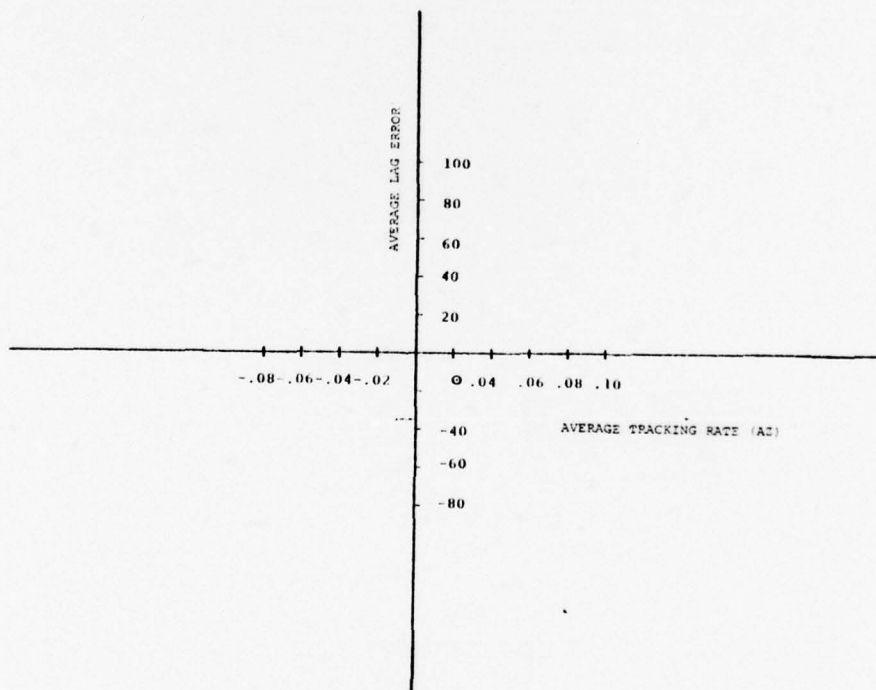
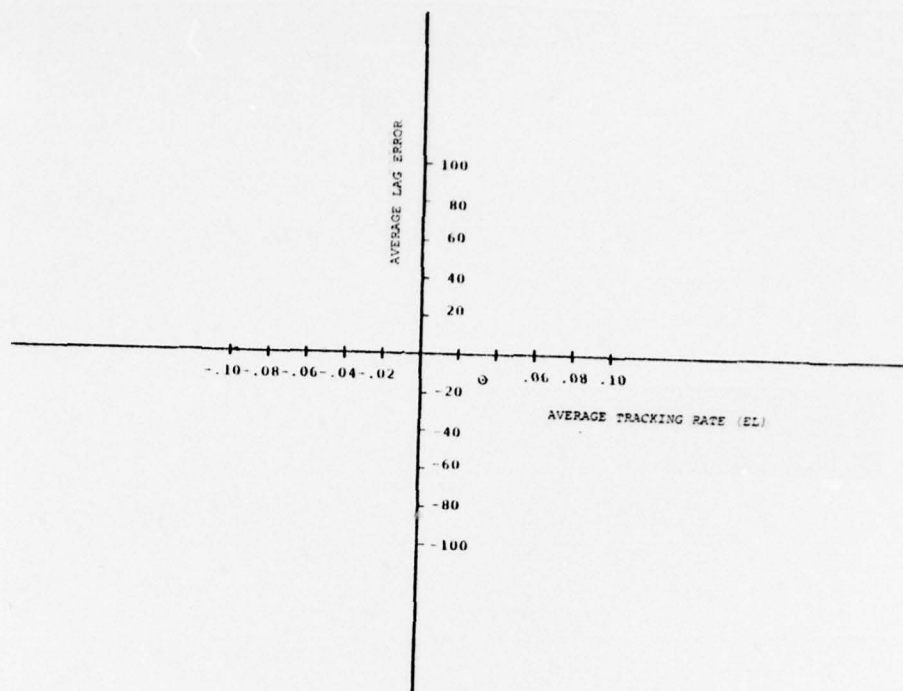


Figure 23 Data Group III

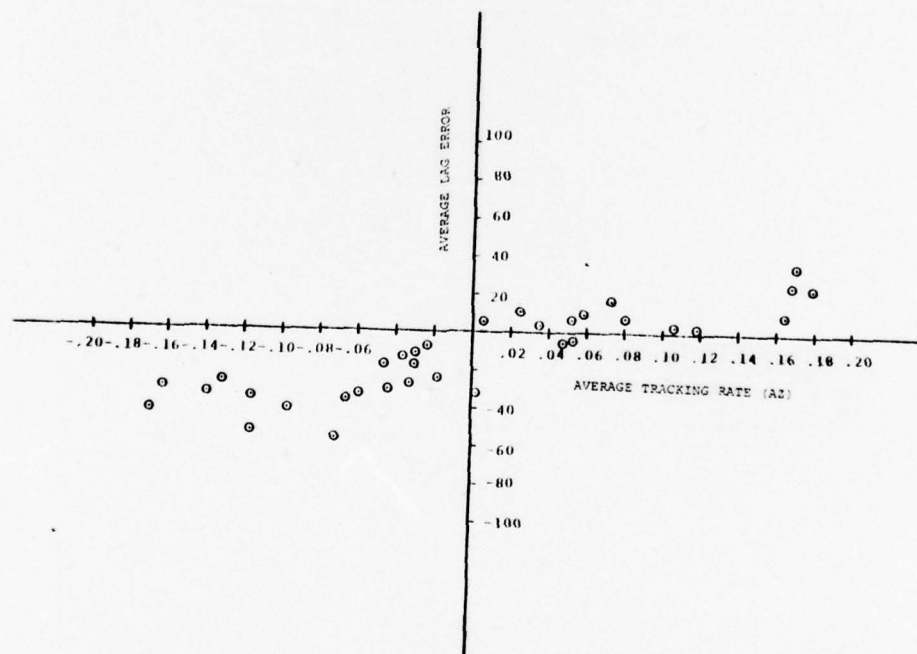
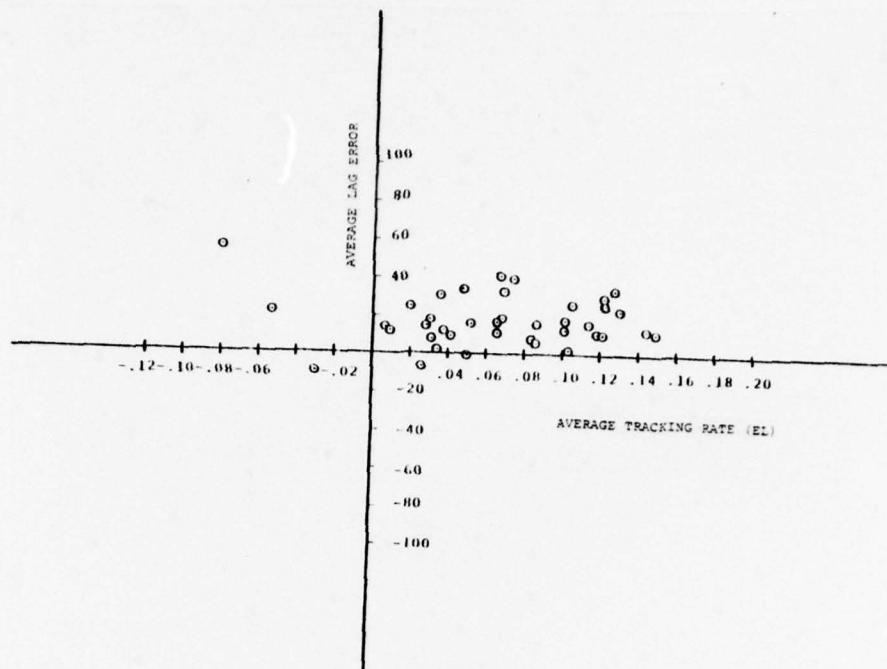


Figure 24 Data Group IV

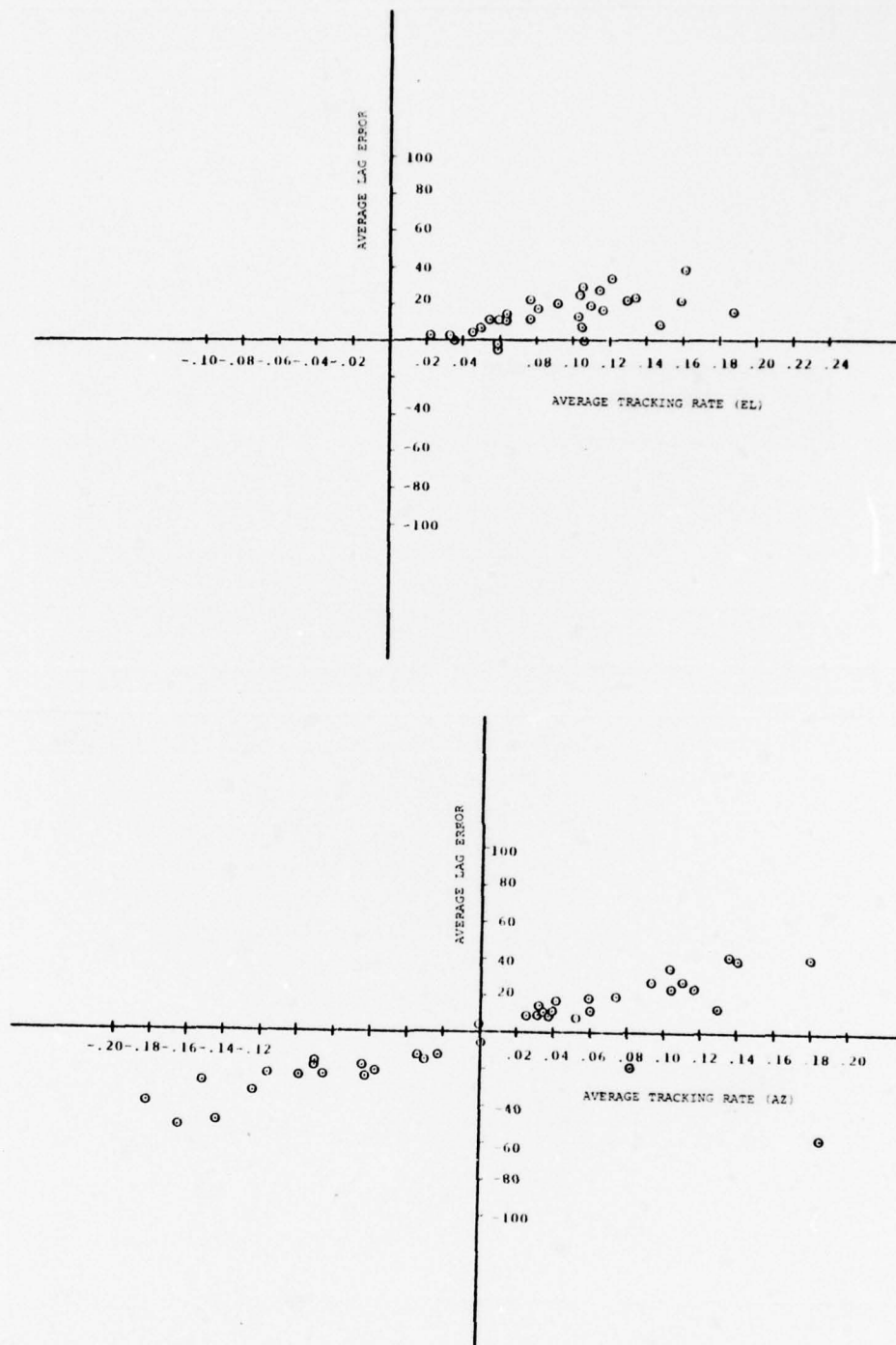


Figure 25 Data Group V

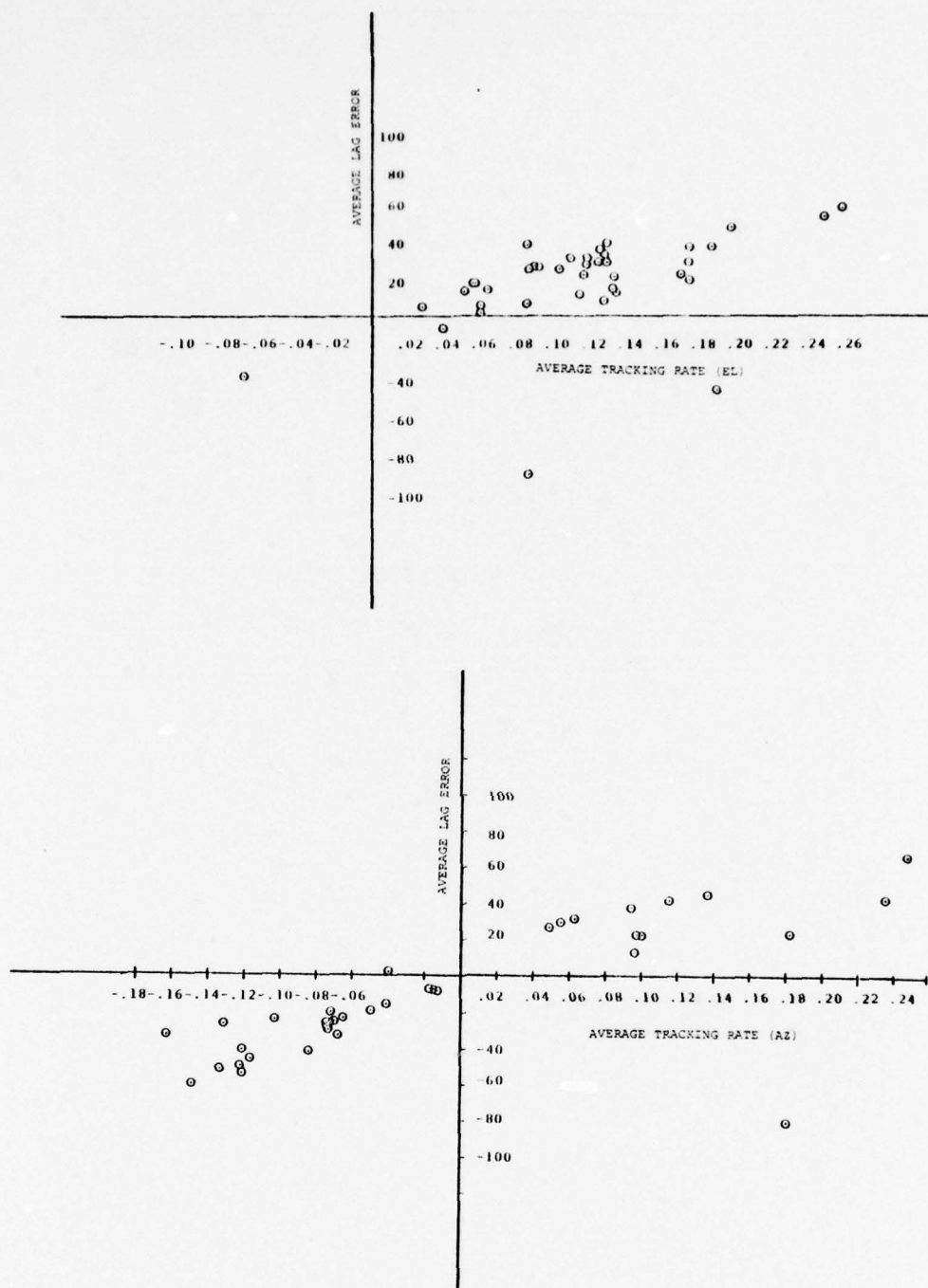


Figure 26 Data Group VI

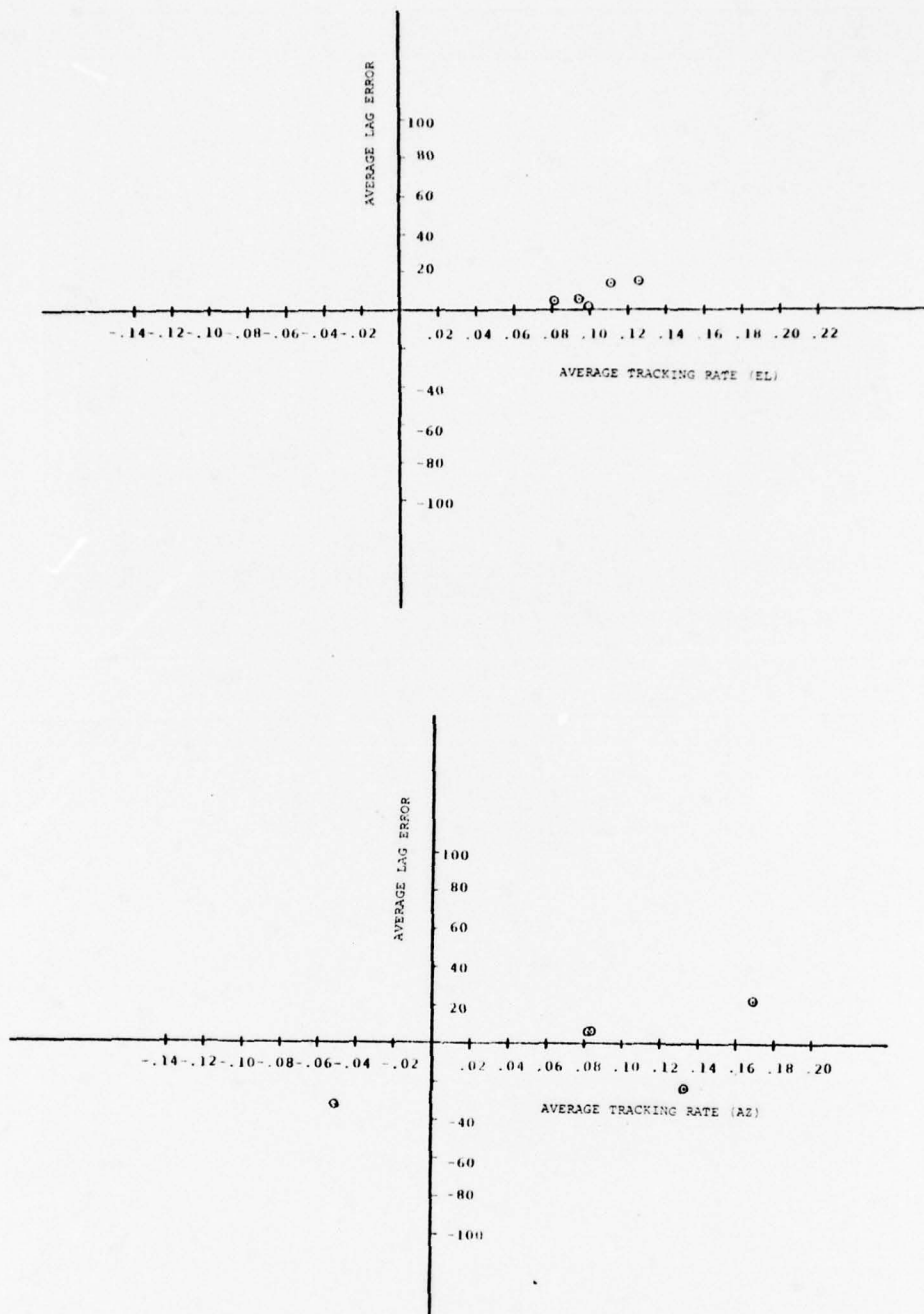


Figure 27 Data Group VII



Figure 28 Average EL Error Before Tracking Correction

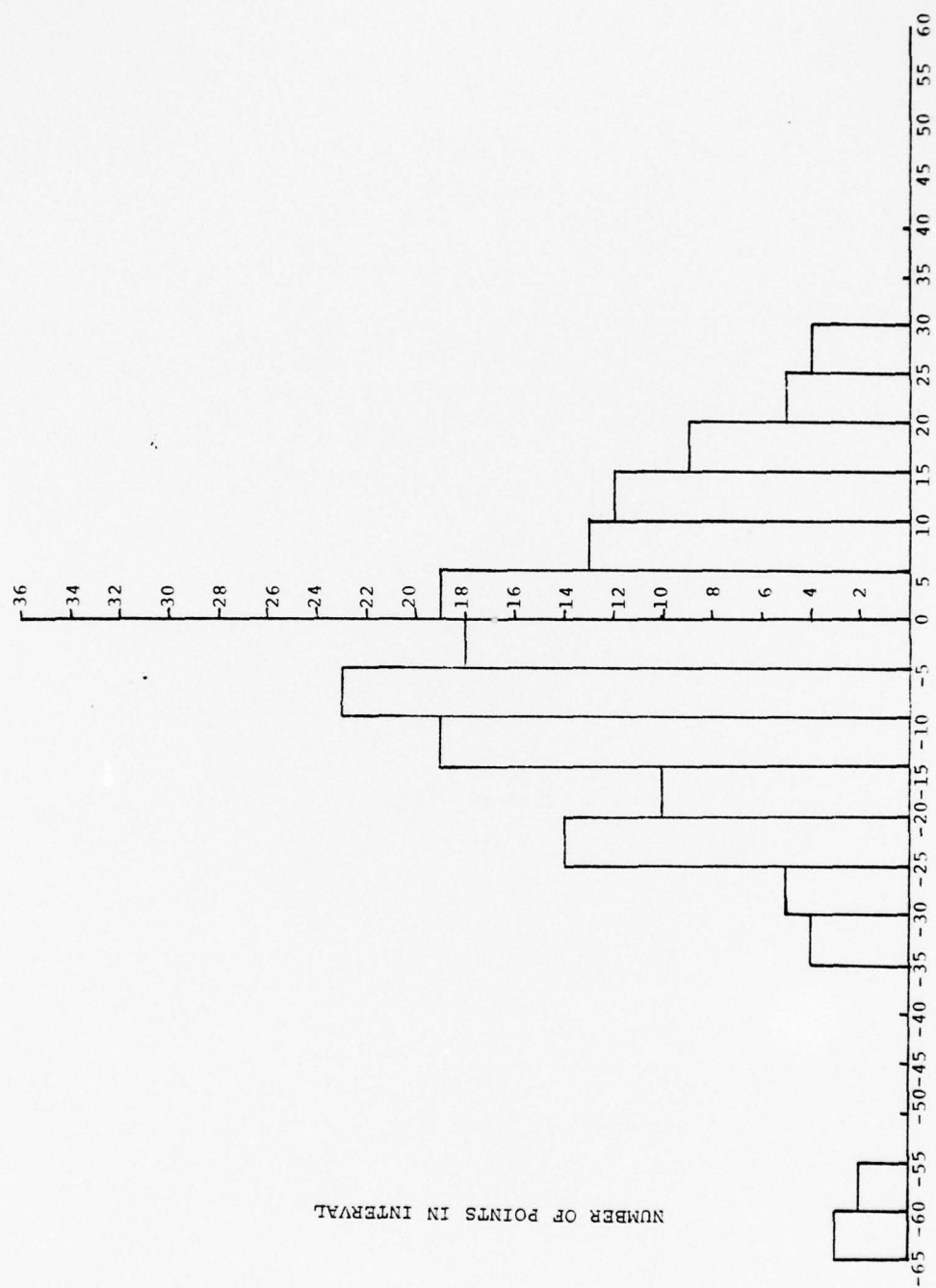


Figure 29 Average EL Error After Tracking Correction

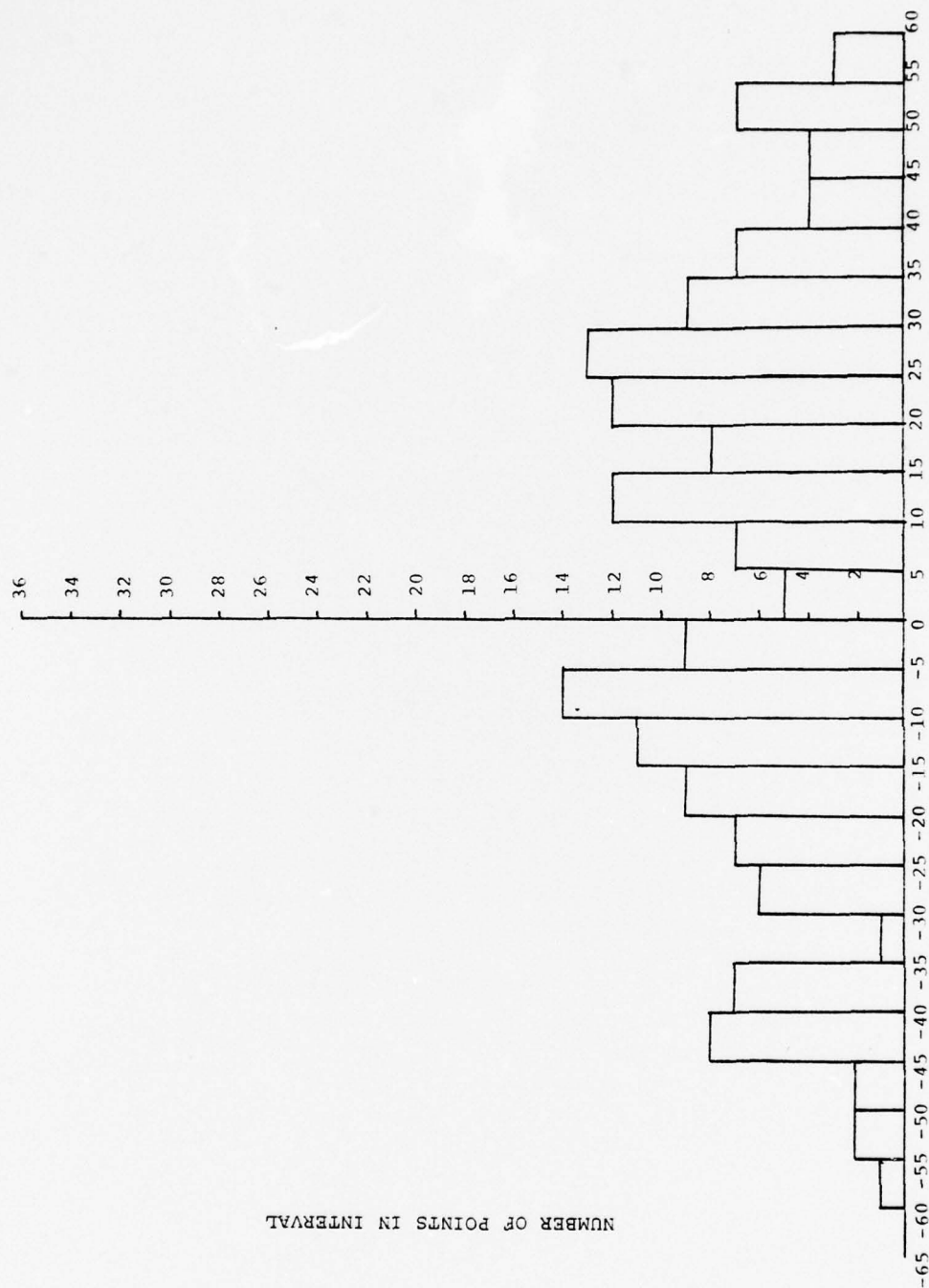


Figure 30 Average AZ Error Before Tracking Correction

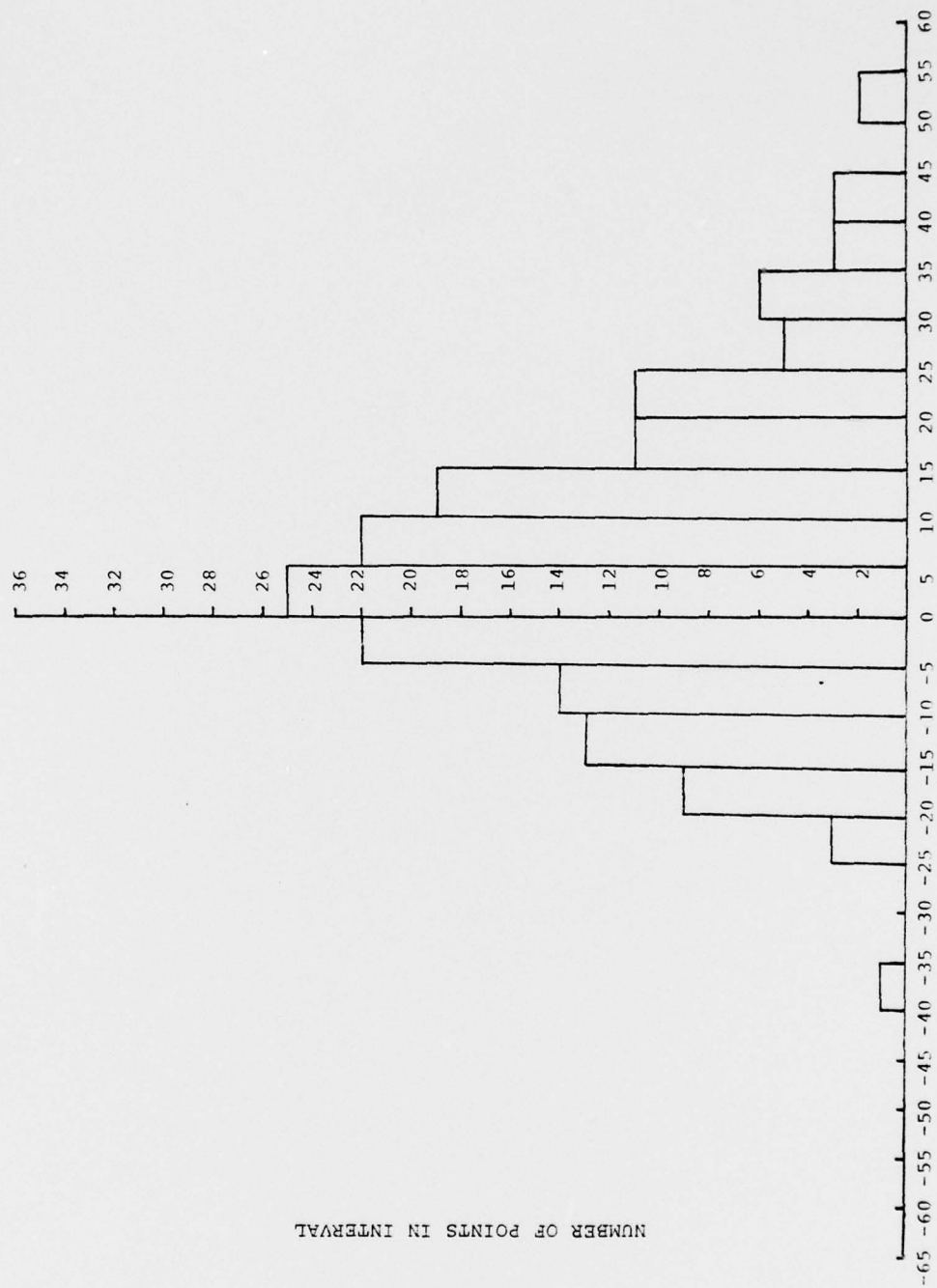


Figure 31 Average AZ Error After Tracking Correction

E_{η} Azimuth tracking Correction

$E_{\epsilon c}$ Elevation error

$E_{\eta c}$ Azimuth error

The tracking error correction did reduce the radar mean lag for a number of the passes. However, a significant number of the passes were still greater than the 17 MRAD constraint. This suggests that error sources other than crossing rates are contributing to the radar lag.

3.3.4.2 Line-of-Sight Rate of Change Analysis

Validity of Sight Eval Data

To provide an alternative to graphical methods of studying the radar lag problem, a program, SDATA, was written to reduce the Sight Eval data. SDATA first smooths the Sight Eval data and then uses an Euler parameter integration scheme to compute the principal variables during each engagement. The important variables computed are range, range rate, pursuer and target positions and velocities, the absolute LOS turn rate and the LOS turn rate relative to the pursuer, pursuer turn rate, headings of both pursuer and target.

The program SDATA had a second purpose which was to determine if the Sight Eval data was invalid. Once the SDATA integration scheme is initialized, it is possible to compare the computed values of pursuer roll, pitch, and yaw angles and pursuer speed with those values obtained from smoothed Sight Eval data. These comparisons indicate that the Sight Eval data, although much noisier than would be hoped, does furnish a reasonable basis for a study of the radar lag problem, assuming, of course, that none of the scaling or other operations, performed on the tapes prior to our effort, introduced significant error. Documentation has not been obtained on some aspects of these operations. Two other qualifications are in order. The geometry of most of the engagements or passes in the Sight Eval data are very similar in geometry. This raises the question of the confidence one could have in a derived fit for a fundamentally different engagement geometry. Another problem is that most passes are of short duration, often less than a second, rarely over 2 seconds. Would a fit be valid for larger periods of time?

It was hoped that an analysis of a large number of engagements would allow the derivation of an equation giving radar lag angle as some function of the various engagement turn rates. Three turn rates that seem likely candidates are true

LOS turn rate with respect to inertial coordinates, pursuer ownship turn rate, and the relative LOS turn rate with respect to the pursuer.

With this goal in mind, a number of fitting equations were derived and added to SDATA. A large number of engagements were then analyzed in SDATA and the results of each of the fits for each engagement was tabulated. Two different types of fit were utilized and their deviation and intent will now be outlined.

In the following discussion all turn rates and the vector radar lag angle itself are expressed in terms of their components in the SDATA inertial x y z coordinate system.

Radar lag angle is represented as a vector as follows:

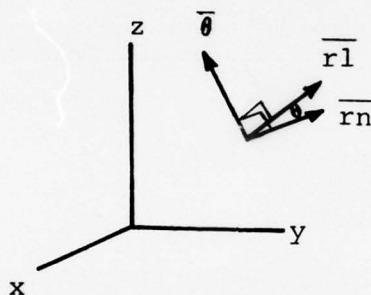


Figure 32

In Figure 32 \bar{r}_n and \bar{r}_l are unit vectors along the radar axis and along the true line of sight to the target respectively, both vectors emanating from the pursuing aircraft. Then by definition $\bar{\theta} = \theta \frac{\bar{r}_n \times \bar{r}_l}{|\bar{r}_n \times \bar{r}_l|}$. This procedure is valid since θ is of relatively small magnitude and it has the advantages of eliminating many annoying sign convention problems as well as simplifying the formulation of fit equations.

Let \bar{w}_a be the true LOS turn rate, \bar{w}_b the pursuer ownship turn rate, and \bar{w}_c the angular rate of change of the LOS with respect to the pursuing aircraft. Let the number of time points in an engagement be n . The first fit equations are of the type

$$\bar{\alpha}_i = a \bar{w}_{a_i} + b \bar{w}_{b_i} + c \bar{w}_{c_i}$$

where the constants a , b , and c are chosen so as to minimize

$$E = \sum_{i=1}^n (\bar{\theta}_i - \bar{\alpha}_i) \cdot (\bar{\theta}_i - \bar{\alpha}_i)$$

by requiring that $\frac{\delta E}{\delta a} = \frac{\delta E}{\delta b} = \frac{\delta E}{\delta c} = 0$ a, b, and c are readily computed. Some fits of this type attempted were

$$\bar{\alpha}_i = b \bar{w}b_i + c \bar{w}c_i$$

$$\bar{\alpha}_i = a \bar{w}a_i$$

$$\bar{\alpha}_i = b \bar{w}b_i$$

$$\bar{\alpha}_i = c \bar{w}c_i$$

The second type of fit tried included a bias vector term \bar{b} which was intended to eliminate variations between engagements caused by differing initial conditions at radar lockon. This equation is of the form

$$\bar{\alpha}_i = a \bar{w}a_i + \bar{b}$$

where both the constant a and the three constant components of \bar{b} , b_x , b_y , and b_z must be found. Again, setting

$$\frac{\delta E}{\delta a} = \frac{\delta E}{\delta b_x} = \frac{\delta E}{\delta b_y} = \frac{\delta E}{\delta b_z} = 0$$

allows a straightforward computation of these constants.

To obtain a measure of the reduction in lag angle for a given fit, a sample mean and a sample standard deviation calculation is performed on both the lag angle $\bar{\theta}_i$ and on the "unexplained" part of lag angle $\bar{\theta}_i - \bar{\alpha}_i$ as follows:

$$\theta_{av} = \frac{1}{n} \sum_{i=1}^n |\bar{\theta}_i|$$

$$\theta_{sd} = \left[\frac{\sum_{i=1}^n |\bar{\theta}_i|^2 - n \theta_{av}^2}{n-1} \right]^{\frac{1}{2}}$$

$$\text{fit}_{\text{av}} = \frac{1}{n} \sum_{i=1}^n |\bar{\theta}_i - \bar{\alpha}_i|$$

$$\text{fit}_{\text{sd}} = \left[\frac{\sum_{i=1}^n |\bar{\theta}_i - \bar{\alpha}_i|^2 - n \text{fit}_{\text{av}}^2}{n-1} \right]^{\frac{1}{2}}$$

Fit-Equation Validation

Each of the above fits reduces the average lag angle, sometimes quite dramatically, but of course the key question is "Is there a fit whose constants remain relatively stable from engagement to engagement?" Apparently, there is not. Each of the fits tried exhibits a randomness in its constants over a number of passes even within the same mission.

Of the fits examined, the two giving the best overall reduction in the mean radar lag angle while at the same time having the least variation in the fitting constants were $\bar{\alpha}_i = a \bar{w}a_i$, the fit to lag angle as a constant times the true LOS turn rate, and $\bar{\alpha}_i = c \bar{w}c_i$, the fit as a constant times the LOS turn rate relative to the pursuing aircraft. The following data are based on 106 passes from the latest tape data. No pass was included that had a mean lag angle in excess of 90 mils. The average lag angle over these passes was 34.8 mils with an average standard deviation of 7.45 mils.

Reference Table 13, list of passes checked, using the fit $\alpha_i = a \bar{w}a_i$ gave an average fitted lag angle of 11.8 mils with an average standard deviation of 5.04 mils. But the constant a varied between 0.028 to 0.432 with the bulk of the a 's falling between 0.10 and 0.26. The c 's varied between the extremes of 0.140 and 0.325. This large variation in fit constants shows clearly the difficulty of attempting to correct for lag angle in this manner. This variation in the two best performing fits tried is a result of the fact that large lag angles occur with both high and low turn rates as do the small lag angles. Assuming

TABLE 13 LIST OF PASSES CHECKED

Mission	Pass	a(sec)	c(sec)	Fit _{av}			Fit _{sd}		
				$\theta_{av}(\text{mils})$	a(mils)	c(mils)	$\theta_{sd}(\text{mils})$	a(mils)	c(mils)
76077	1	0.072	0.146	10.7	4.0	5.6	2.3	2.2	2.9
"	2	0.108	0.187	14.9	5.2	5.6	2.8	2.0	2.5
"	3	0.125	0.212	21.6	6.1	6.0	3.3	3.3	1.7
"	4	0.028	0.044	8.3	5.5	5.8	4.0	2.8	3.1
"	5	0.101	0.177	30.2	14.9	7.3	1.6	3.4	2.2
"	6	0.048	0.068	15.9	3.1	4.2	3.0	2.2	3.6
76078	1	0.051	0.129	8.3	5.7	5.6	1.8	2.1	2.2
"	2	0.114	0.220	23.4	7.3	5.7	3.8	3.2	3.5
"	3	0.041	0.294	15.9	14.9	11.8	4.5	5.1	4.7
"	4	0.138	0.419	17.5	3.4	6.4	3.1	1.5	4.5
"	5	0.029	0.215	18.8	18.3	15.3	13.7	13.9	11.3
"	6	0.159	0.228	47.5	9.3	8.0	8.9	4.7	2.6
"	7	0.120	0.180	35.9	17.5	12.5	3.2	5.0	3.1
"	8	0.170	0.223	45.0	15.3	8.6	1.9	4.0	3.9
76083	1	0.130	0.183	37.5	4.1	9.2	3.7	1.4	1.7
"	2	0.113	0.140	30.2	15.8	14.2	4.8	2.8	2.0
"	3	0.120	0.150	33.7	1.7	4.9	2.0	1.2	0.5
"	4	0.158	0.217	37.6	15.2	13.7	2.3	1.0	1.1
76085	1	0.054	0.555	26.5	24.4	13.6	4.7	8.5	6.1
76092	1	0.240	0.248	35.0	21.1	29.5	14.7	13.7	12.1
76093	1	0.082	0.365	25.1	22.0	11.3	7.4	9.0	4.9
76110	1	0.432	0.728	87.1	50.5	59.2	27.2	21.7	19.3
"	4	0.366	0.561	82.2	41.0	29.6	39.0	14.4	12.5
"	6	0.422	0.851	78.9	41.8	19.5	39.4	18.6	9.3
76111	1	0.134	0.161	23.2	5.5	6.3	4.0	2.2	2.8
"	2	0.171	0.246	21.8	7.1	8.2	1.6	1.5	1.3
"	3	0.145	0.202	40.6	12.9	4.6	3.6	2.4	1.4
"	4	0.130	0.180	36.8	6.8	4.5	5.9	3.4	2.1
"	5	0.149	0.229	45.8	14.7	2.0	5.0	1.8	0.6
76118	1	0.188	0.243	28.8	3.9	4.2	2.6	2.1	1.8
"	2	0.170	0.191	30.8	6.5	9.8	1.5	3.4	3.8
"	3	0.184	0.258	42.0	8.5	5.6	4.5	3.6	3.0
"	4	0.067	0.084	15.4	5.4	5.2	2.5	3.4	3.5
"	5	0.174	0.207	33.6	3.8	7.2	1.8	1.6	2.0
"	6	0.251	0.301	74.9	14.7	8.7	12.1	4.7	4.7
"	7	0.221	0.251	66.5	12.1	14.3	2.9	6.7	1.2
76119	2	9.120	0.306	11.8	4.7	4.4	3.3	2.0	3.1
"	3	0.114	0.168	16.5	5.1	7.2	3.7	2.8	4.7
"	4	0.166	0.278	25.8	4.3	7.5	1.9	1.3	3.2
"	5	0.097	0.312	20.6	16.3	14.0	6.5	8.0	5.6
"	6	0.201	0.291	36.4	7.6	17.0	2.7	3.2	10.2
"	7	0.223	0.306	45.9	9.7	7.2	3.0	6.3	2.7
76121	1	0.037	0.088	5.7	4.9	4.7	3.2	2.4	2.3
"	2	0.069	0.160	11.8	9.8	9.7	3.0	2.5	1.5
"	3	0.080	0.243	10.7	7.3	6.4	1.6	1.5	2.1
"	4	0.079	0.215	14.6	7.2	6.7	4.5	4.7	4.8
"	5	0.236	0.282	50.3	4.5	9.8	3.5	1.2	1.1
"	6	0.132	0.163	32.3	8.3	3.9	2.4	1.9	0.8
"	7	0.119	0.198	24.1	6.1	13.9	2.6	1.6	2.0
"	8	0.072	0.075	17.6	12.4	7.5	1.9	2.8	2.8
"	9	0.202	0.256	55.1	7.1	5.8	5.7	2.5	3.0
76126	1	0.066	0.210	12.2	8.3	18.7	1.5	1.9	1.4
"	2	0.135	0.179	24.3	18.0	7.4	1.5	3.4	1.8
"	3	0.113	0.246	11.5	7.6	18.3	3.9	2.3	2.9

TABLE 13 LIST OF PASSES CHECKED (CONTINUED)

Mission	Pass	a(sec)	c(sec)	θ_{av} (mils)	Fit _{av}		θ_{sd} (mils)	Fit _{sd}	
					a(mils)	c(mils)		a(mils)	c(mils)
76131	1	0.115	0.243	19.4	18.2	18.3	21.4	15.2	15.7
"	2	0.042	0.050	14.9	14.2	14.5	2.1	2.6	2.5
"	3	0.166	0.302	47.8	14.1	18.2	17.1	6.2	6.9
"	4	0.105	0.253	24.1	14.7	11.6	5.0	3.1	3.3
"	5	0.107	0.171	28.4	9.8	6.0	2.9	2.2	2.1
"	6	0.059	0.206	12.1	8.3	6.4	2.8	2.8	2.9
"	7	0.194	0.305	58.8	19.5	6.8	5.8	1.4	4.6
"	8	0.229	0.345	72.5	14.2	18.0	12.1	4.4	2.6
"	10	0.059	0.091	21.6	15.4	15.8	4.8	2.3	2.0
76162	1	0.065	0.243	81.0	76.7	71.0	60.0	63.5	65.6
"	2	0.143	0.278	44.1	22.7	15.1	16.7	4.0	2.2
"	3	0.151	0.205	40.0	14.7	12.6	5.2	3.5	2.8
"	4	0.120	0.281	36.8	21.3	20.2	23.9	27.6	18.0
"	5	0.198	0.243	66.3	16.9	18.1	8.7	1.9	1.4
"	6	0.151	0.326	61.2	32.5	14.1	15.3	1.8	1.7
"	7	0.194	0.225	65.4	54.5	49.8	58.7	31.2	63.3
76163	1	0.260	0.386	34.5	12.4	11.3	2.8	4.7	4.3
"	3	0.119	0.209	36.1	9.7	3.1	2.3	3.3	1.5
"	4	0.249	0.306	49.0	9.8	10.1	3.2	3.7	3.1
"	5	0.293	0.376	42.8	9.7	10.2	4.2	4.0	2.9
"	6	0.169	0.201	51.3	9.2	6.1	4.8	5.0	3.1
"	7	0.069	0.146	14.5	11.1	10.0	2.4	2.5	3.2
"	8	0.251	0.312	52.3	8.2	4.8	4.3	4.7	3.4
"	9	0.260	0.285	48.9	10.4	13.2	5.4	3.8	3.1
76166	1	0.031	0.174	13.8	13.5	10.0	6.2	5.6	4.4
"	2	0.032	0.183	5.7	4.9	3.5	3.1	2.9	1.4
"	3	0.119	0.144	22.6	11.0	12.7	4.9	4.8	5.2
"	5	0.092	0.216	26.6	20.7	15.6	6.4	5.4	7.2
"	6	0.070	0.128	25.2	12.4	5.5	3.9	5.1	2.7
"	7	0.059	0.112	15.2	6.5	4.0	2.0	3.0	2.0
"	8	0.108	0.185	31.9	10.6	5.6	3.8	1.9	2.0
76174	1	0.055	0.130	16.6	15.3	14.4	3.7	3.7	3.0
"	2	0.234	0.257	82.5	11.9	8.4	5.4	3.8	3.3
76175	2	0.103	0.187	46.2	35.3	29.6	3.9	8.8	4.9
"	3	0.088	0.102	23.4	17.8	19.0	4.8	6.1	4.5
"	4	0.151	0.181	54.2	28.4	27.8	11.1	2.6	3.5
"	6	0.128	0.152	28.4	10.9	10.7	4.9	6.3	3.6
"	7	0.191	0.223	57.1	31.9	32.3	2.6	1.8	2.3
"	8	0.124	0.187	45.5	13.8	3.7	4.1	1.4	2.0
"	9	0.151	0.245	49.8	20.0	4.3	3.6	3.6	2.0
76197	1	0.046	0.074	8.8	3.6	2.8	2.7	2.0	1.3
75338	1	0.125	0.304	32.9	21.5	9.7	3.7	3.4	3.4
"	2	0.070	0.105	15.1	2.8	4.3	2.8	1.4	1.8
"	3	0.115	0.277	33.1	26.1	20.6	4.6	5.9	2.7
"	4	0.094	0.171	21.9	10.4	10.0	14.3	14.0	10.8
76162	1	0.160	0.303	39.5	17.2	15.5	9.5	13.8	9.0
"	2	0.165	0.194	45.2	12.2	8.0	17.3	3.9	3.1
"	3	0.172	0.226	43.3	7.9	5.6	5.3	2.7	2.1
"	4	0.157	0.287	34.7	8.9	10.4	14.5	8.1	7.7
"	5	0.218	0.259	68.0	7.3	9.9	11.6	2.9	2.9
"	6	0.159	0.317	58.4	20.1	5.9	15.0	3.9	2.8
"	7	0.150	0.268	41.3	9.0	6.6	14.2	6.2	5.2

that the Sight Eval data does indeed present a substantially true picture of the system performance, the data conveys a strong impression of erratic system performance.

It seems reasonable to conclude that whatever the causes of the radar lag problem, the lag angle is not a function of the engagement geometry. This conclusion can be criticized on the basis that a higher order fit should have been tried or some conceptually different type of fit involving different engagement variables might have been successful, etc. Perhaps. But the fact remains that the various turn rates used all have roughly the same direction as the vector lag angle and most of the engagement variables are involved in computing these turn rates. There should have been some perceivable trend in the fit constants somewhere. After all, the lag angle problem is caused largely by an incorrect axis turn rate with perhaps an initial misorientation problem added for good measure.

There does exist the possibility of taking one of the fits and working up those values of its constants which yield the best overall statistical decrease in radar lag angle for a large number of engagements. But there are two obvious hazards in the procedure. First, if the true source of the problem remains undiscovered, what assurance is there that there will not be radical changes in system performance in the future? Second, since the engagements are so similar and so brief, would the correction be valid in engagements having a different geometry or a greater duration?

One further comment is necessary. It may seem that the more direct approach of doing a system analysis, on the MA-1 system and its subsequent modifications, was ignored. After all, the original applications of the MA-1 system radar did not require it to produce the highly accurate target angular direction data now being asked of it. An analysis of the MA-1 system design and performance was initiated. This analysis required detailed system design theory and performance data as well as systems

modification and modified system performance data of the MA-1 used in Sight Eval testing. The extensive period since the original design and test of the MA-1 materially reduced the availability of pertinent design and performance data, leaving the geometrical approach as the only analysis alternative.

3.3.4.3 Time Data Phase Shift

An examination of the plots of radar antenna position in azimuth and elevation versus film target position shows an apparent data phase shift which varies up to .5 seconds and averages approximately .25 seconds. There are a number of reasons why such a phase shift could exist. Delay in instrumentation circuitry is a function of the number of processing and amplification stages through which an electronic signal must pass. However, this category of delay results in less than a microsecond per stage and will seldom reach the .25 second delay observed. A more likely possibility is a discrepancy in the synchronization of magnetic tape and film data during the merger into a single data tape. Of course, the probability is high that the phase shift does indeed exist, and, if so, the direct modification to the correction algorithm is obvious. Graphs of passes that illustrate the data shift are shown in Figures 33 thru 37.

The most obvious example of a data shift is shown in Figure 33. On this pass the radar was leading the film data in azimuth. This immediately suggests a data merging or calibration problem as the radar can never constantly lead the target. The occurrence of radar lead was not often obvious, but Figure 34 strongly suggests that the radar was leading the elevation for approximately $1\frac{1}{2}$ of the 3 seconds of available data. The radar data follows the film data profile very closely and the differences between film and radar are small, and rarely exceed 10 MRAD. If not closely inspected, this pass would have been accepted as an ideal pass.

The third example of a possible data shift in azimuth is seen in Figure 35. The elevation radar data closely follows the film data with the radar occasionally overshooting the target, but immediately being corrected. This is how one would expect the radar to behave, and the component differences rarely exceed 15 MRAD. Inspection of the azimuth data reveals a

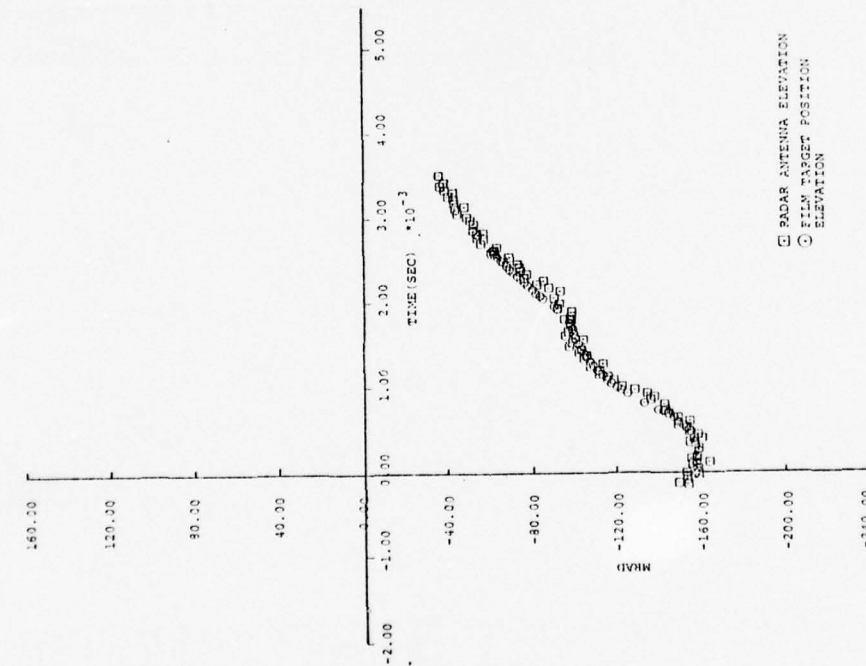
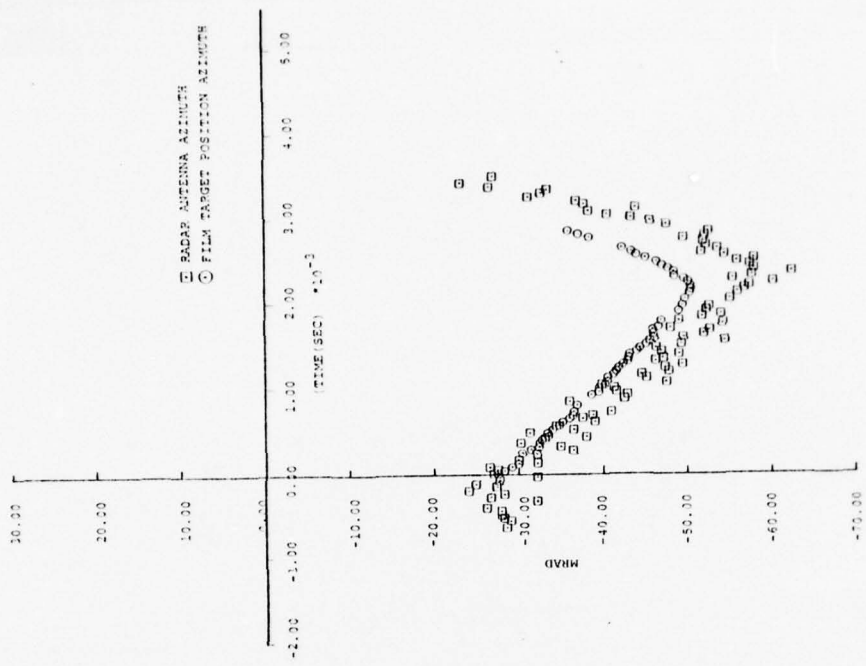


Figure 33 Radar Leading Target

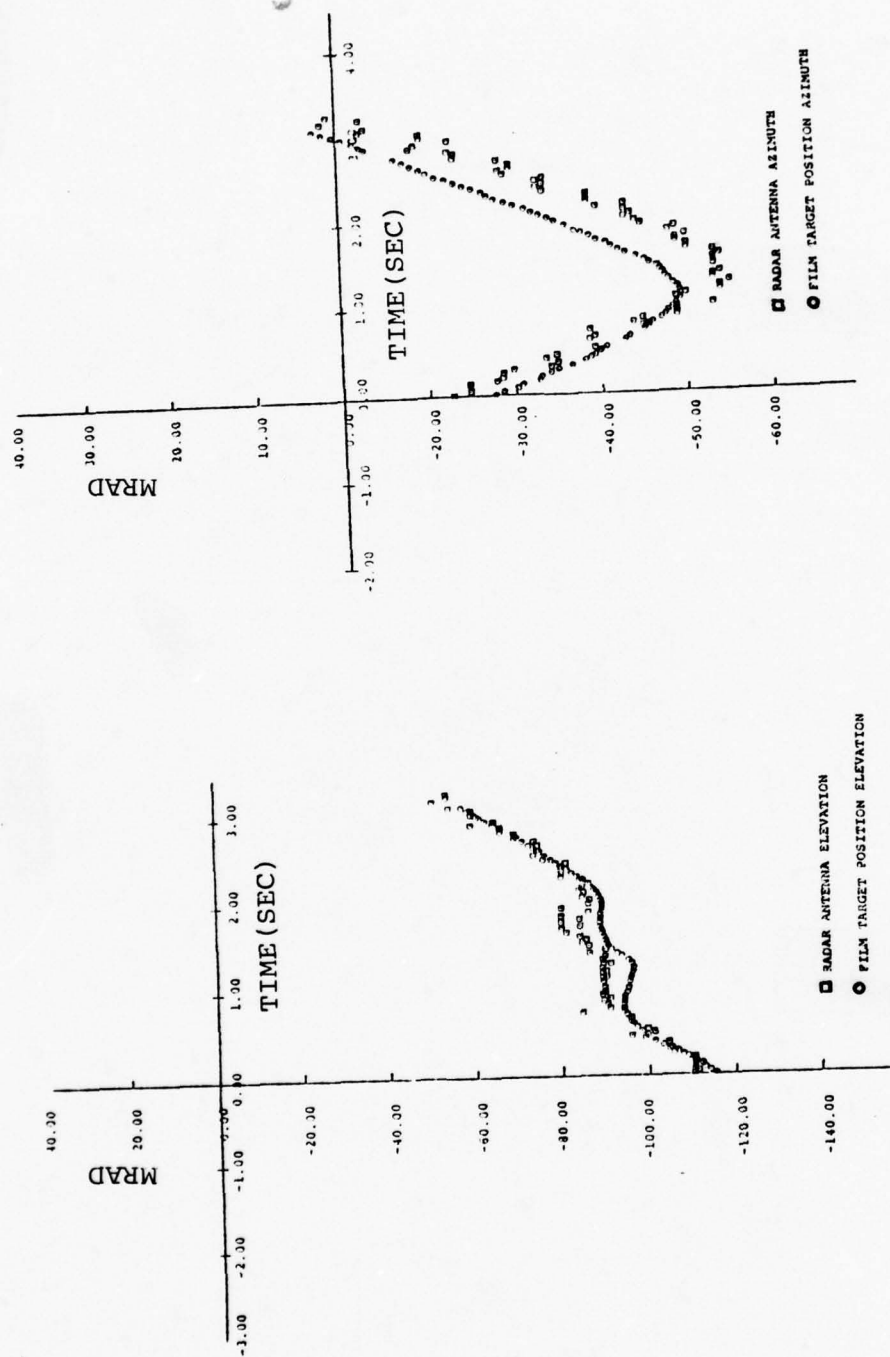


Figure 34 Radar Leading Target

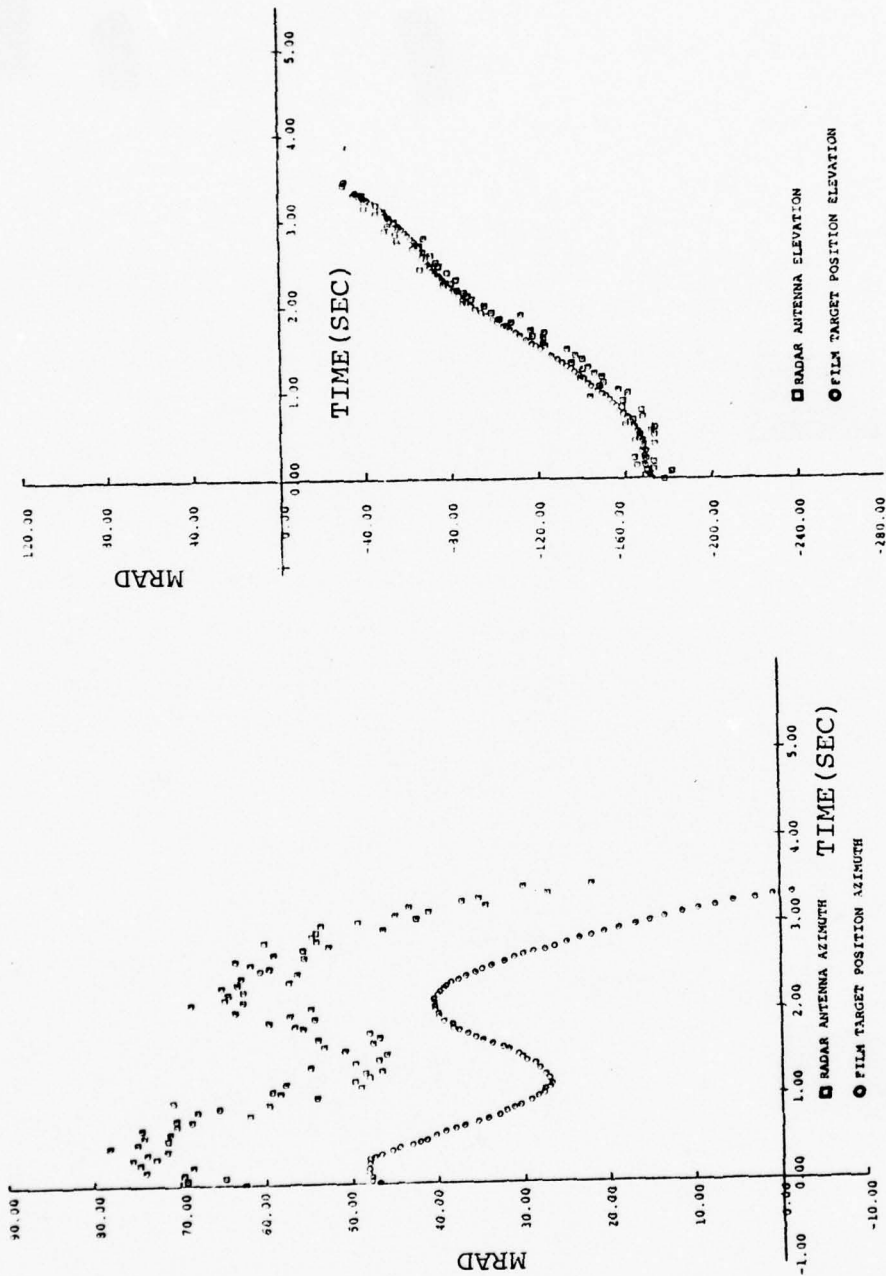


Figure 35 Lag in Radar Azimuth

very poor tracking job by the radar. The same basic profile is observed by radar and film but the radar is lagging the film by approximately 25-30 MRAD. Also the radar profile, if smoothed, seems to be about 1/4 second out of synchronization with the film.

The above examples are extremes noted in reviewing the data. The largest percentage of the passes showed the radar lagging the film data. This lag time was felt to be excessive in most cases. The radar profiles in Figures 36 and 37 suggest the radar is roughly 1/4 second behind the film data and are typical of many passes. Being unable to isolate the true radar lag from a data shift, it was decided to try a variety of time shifts. It was felt that the radar should respond with a correction in less than a tenth of a second. Accordingly, time corrections of 4 to 8 frames were selected to see if the total lag angle could be consistently corrected.

Program SDATA described in detail in Section 3.3.4.2 was modified to perform all lag angle calculations in the program inertial coordinate system, with the film target direction being transformed to inertial coordinates by that transformation consistent with the lag time assumed. Two tapes were run with this correction. The results of the data shift are shown in Tables 14 and 15.

In many passes the lag angle is reduced below the 15 MRAD requirement. In Table 14, 5 of the 29 passes had lag angles less than 15 MRAD. After the frame shift, 24 of 29 had lag angles less than 15 MRAD. In Table 15, 4 of the 26 passes had lag angles less than 15 MRAD. After the frame shift, 14 of 24 had lag angles less than 15 MRAD. Of the 54 passes tried for this data shift, only 2 that would have been accepted were made unacceptable by the shift. However, there appears to be a definite contribution to lag angle from this data shift. Further, an error in synchronization is the only possible explanation for those few passes which show the radar leading the film.

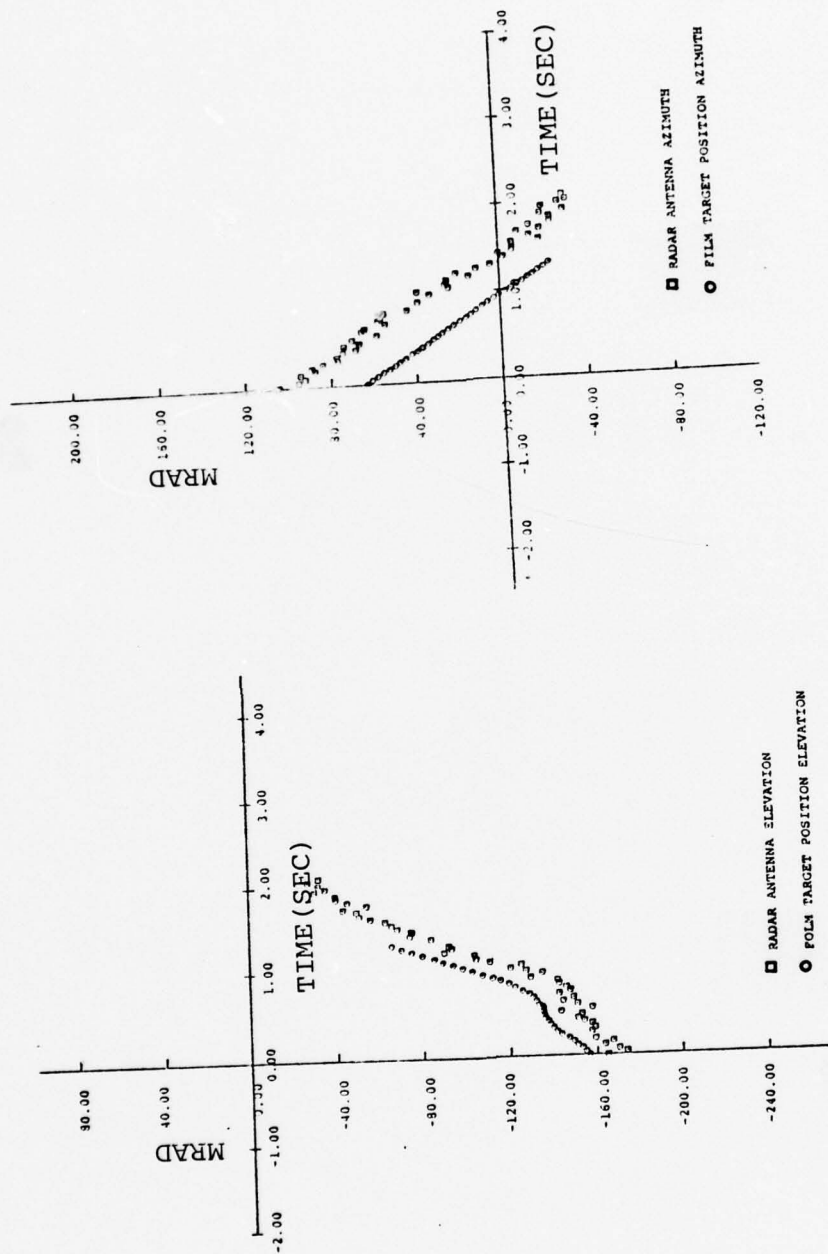


Figure 36 Lag in Both Radar Components

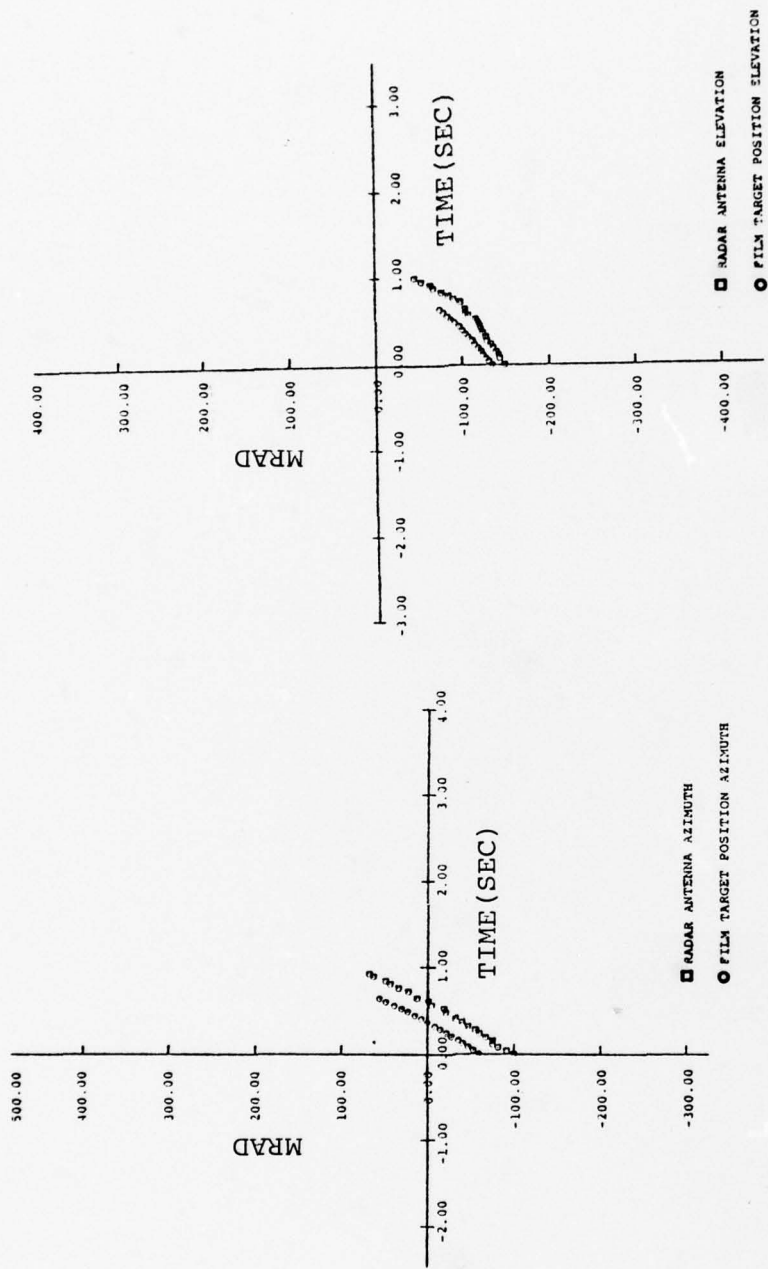


Figure 37 Lag in Both Radar Components

TABLE 14 Comparison of Average Lag Before and After Frame Shift

MISSION	PASS	AVERAGE LAG MRAD	BEST FRAME SHIFT (No of Frames)	ADJUSTED LAG MRAD	FRAMES ERROR < 15 MRAD	COMMENTS
76111	1	23.2	4	6.12	4-6	
	2	21.8	6	7.73	4-8	
	3	40.6	5	4.50	4-7	
	4	36.8	5	4.34	4-6	
	5	45.8	6	2.07	5-7	
76118	1	28.8	6	3.93	4-8	
	2	30.8	5	6.65	4-6	
	3	42.0	6	5.44	5-8	
	4	15.4	4	14.89	4	
	5	33.6	5	7.23	4-6	
	6	74.9	6	5.97	5-6	
	7	66.5	6	15.03	---	
	8	135.5	8	130.48	---	No Radar Lock
76119	1	383.5	4	388.14	---	No Radar Lock
	2	11.8	8	4.02	4-8	
	3	16.5	4	6.18	4-7	
	4	25.8	6	7.96	4-8	
	5	20.6	6	16.81	---	
	6	36.4	8	12.85	7-8	
	7	45.9	6	5.59	5-8	
76121	1	5.7	4	7.28	4-8	
	2	11.8	4	10.11	4-8	
	3	10.7	6	6.79	4-8	
	4	14.6	4	9.99	4-6	
	5	50.3	6	6.71	5-8	
	6	32.3	4	11.29	4	
	7	24.1	4	3.92	4-6	
	8	17.6	4	19.33	---	
	9	55.1	6	4.57	5-8	

TABLE 15 Comparison of Average Lag Before and After Frame Shift

MISSION	PASS	AVERAGE LAG MRAD	BEST FRAME SHIFT (No of Frames)	ADJUSTED LAG MRAD	FRAMES ERROR < 15 MRAD	COMMENTS
76077	1	10.7	4	6.19	4-8	
	2	14.9	4	6.34	4-8	
	3	21.6	5	10.33	4-6	
	4	8.3	4	18.75	---	
	5	30.2	5	7.88	4-6	
	6	15.9	4	25.61	---	
76078	1	8.3	4	6.13	4-8	
	2	23.4	5	6.25	4-8	
	3	15.9	4	14.73	4-6	
	4	17.5	8	8.19	4-8	
	5	18.8	4	16.02	---	
	6	47.5	7	8.99	5-8	
	7	35.9	5	11.92	4-6	
	8	45.0	6	8.07	4-7	
76083	1	37.5	5	8.81	4-7	
	2	30.2	4	16.64	---	
	3	33.7	4	6.45	4-5	
	4	37.6	5	13.88	4-5	
76085	1	26.5	7	20.78	---	
76092	1	35.0	4	34.22	---	
	2	13.01	4	24.07	---	Radar Lead (Elevation)
76093	1	25.1	8	15.52	---	
	2	63.5	4	78.92	---	No Radar Lock
	3	185.3	8	181.59	---	No Radar Lock
	4	226.6	8	225.84	---	No Radar Lock

Again reaching a general conclusion is made difficult by the lack of detailed documentation on the experimental design and on the data reduction procedures. This procedure did not give a great improvement in all passes, but the results do indicate that the radar may be considerably more accurate in determining target angular direction, than was previously thought.

3.3.4.4 Suggestions for Future Study

It is evident that a time lag occurred between the times the film and radar data were recorded. This lag may be an actual interval introduction by real radar error or it may be an artificial interval caused by instrumentation or data merger into a single tape. This time lag which results in radar error is of sufficient importance that a follow-on study should determine the true source of the delay.

In connection with the current analysis, the availability of a detailed instrumentation and test plan, maintenance, calibration, and modification logs for the aircraft and fire control system, and details of data processing would have been of material assistance. In future testing, the close coordination between analysis and test planning should be emphasized, with consideration given to a single analysis/Test Manager. A sample analysis exercise concurrently with initial flight tests will eliminate many later analysis snags.

APPENDIX A
COMPARISON OF KALMAN FILTERS

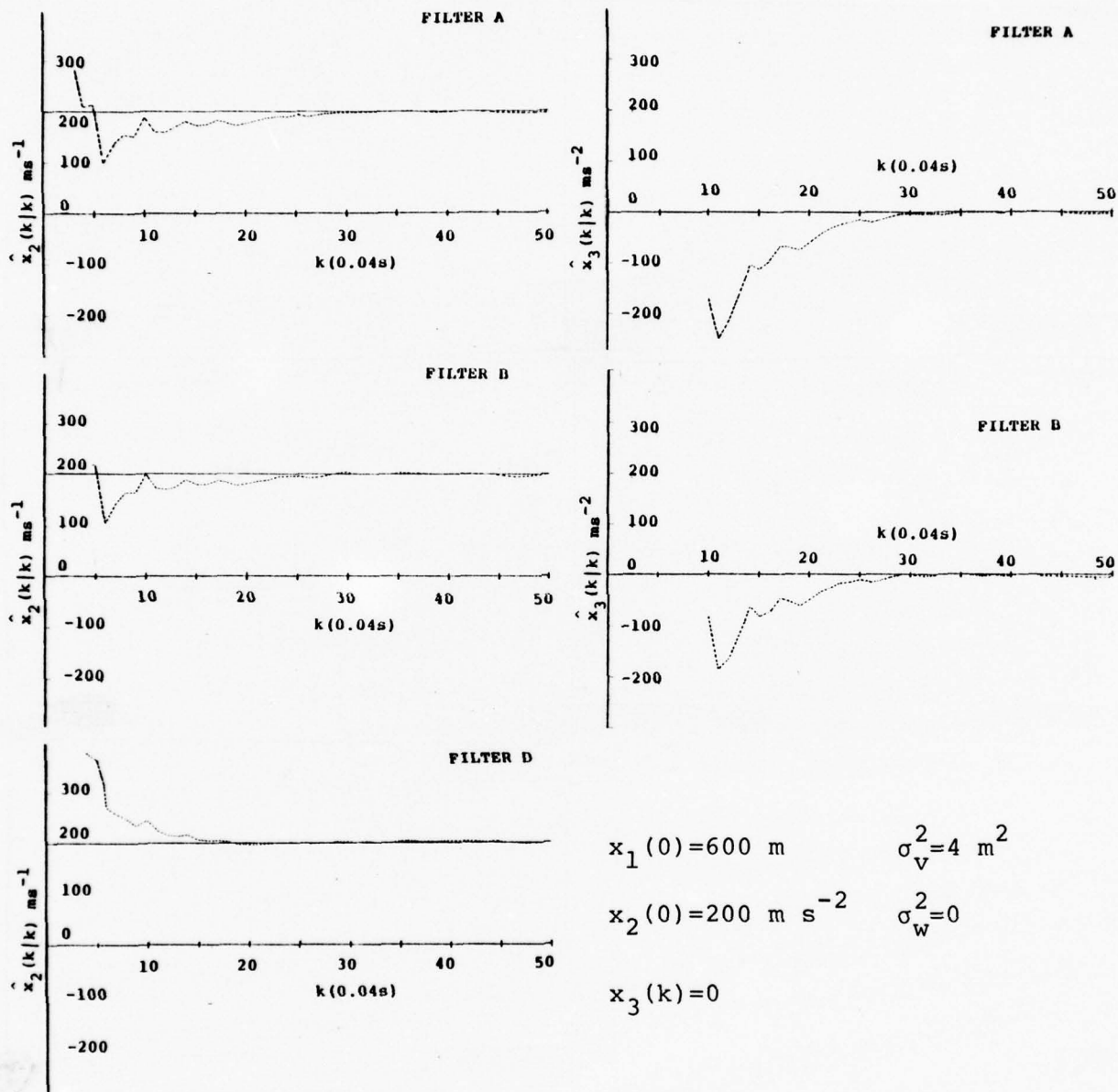


Figure A-1

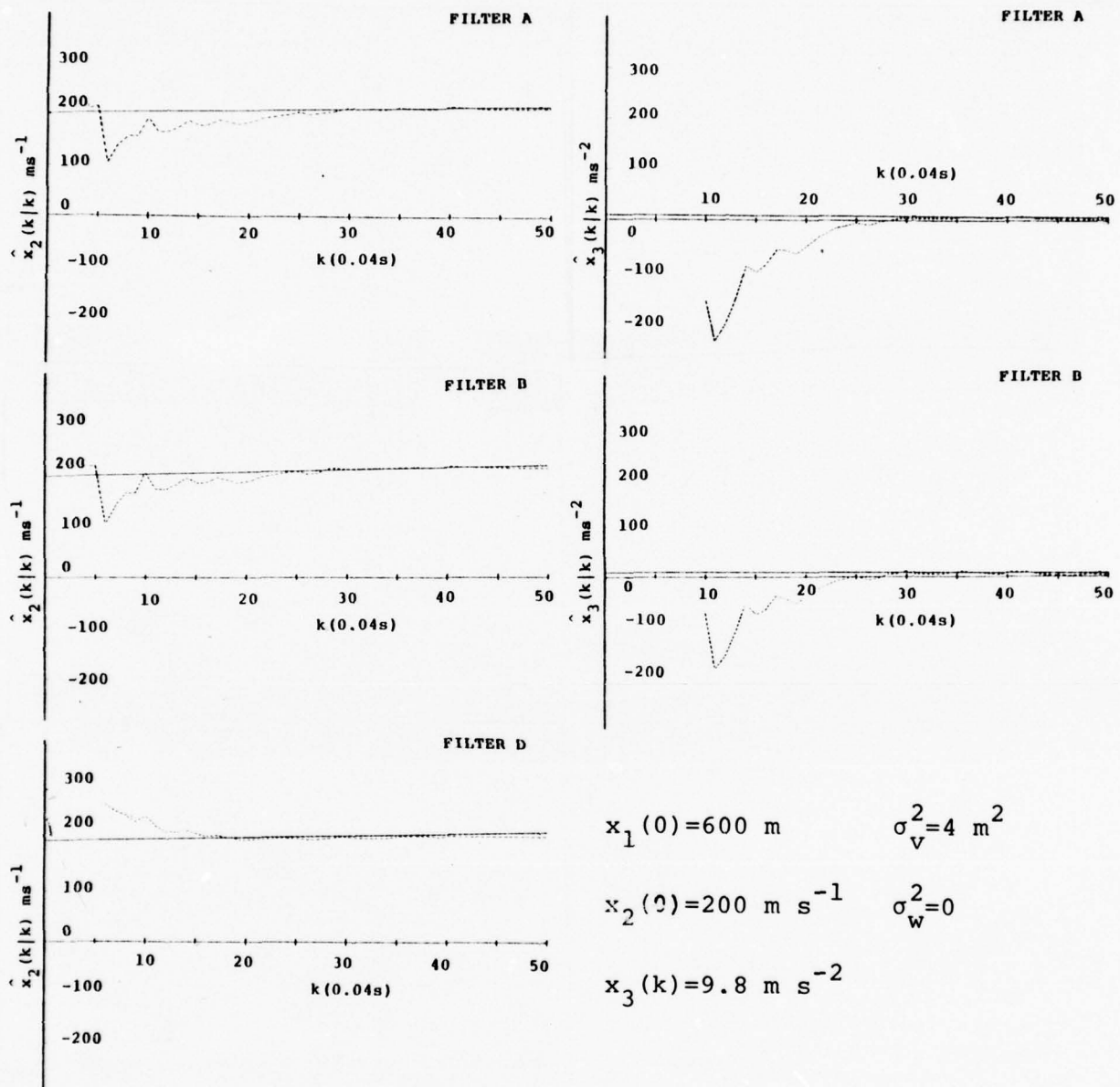


Figure A-2

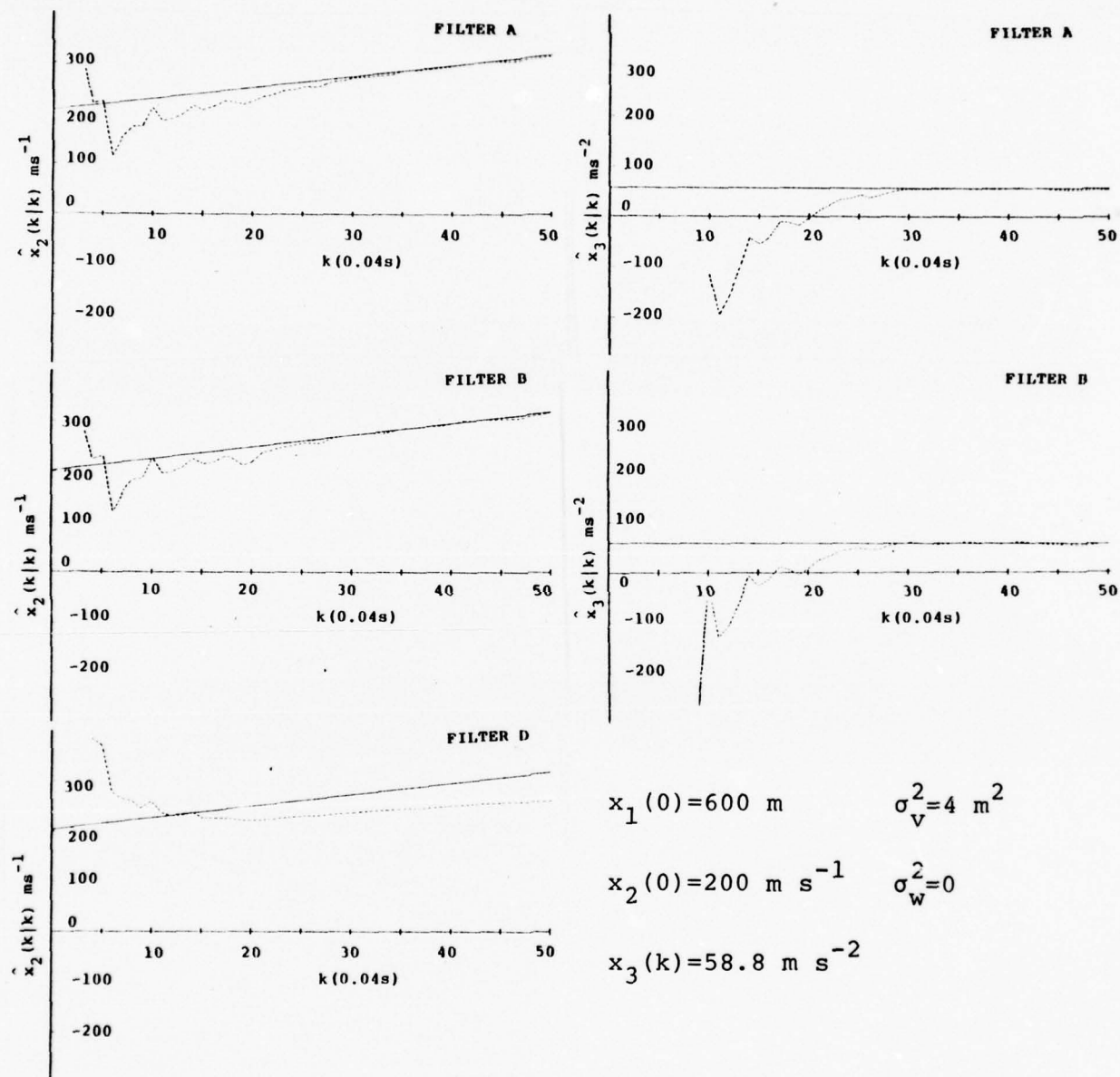


Figure A-3

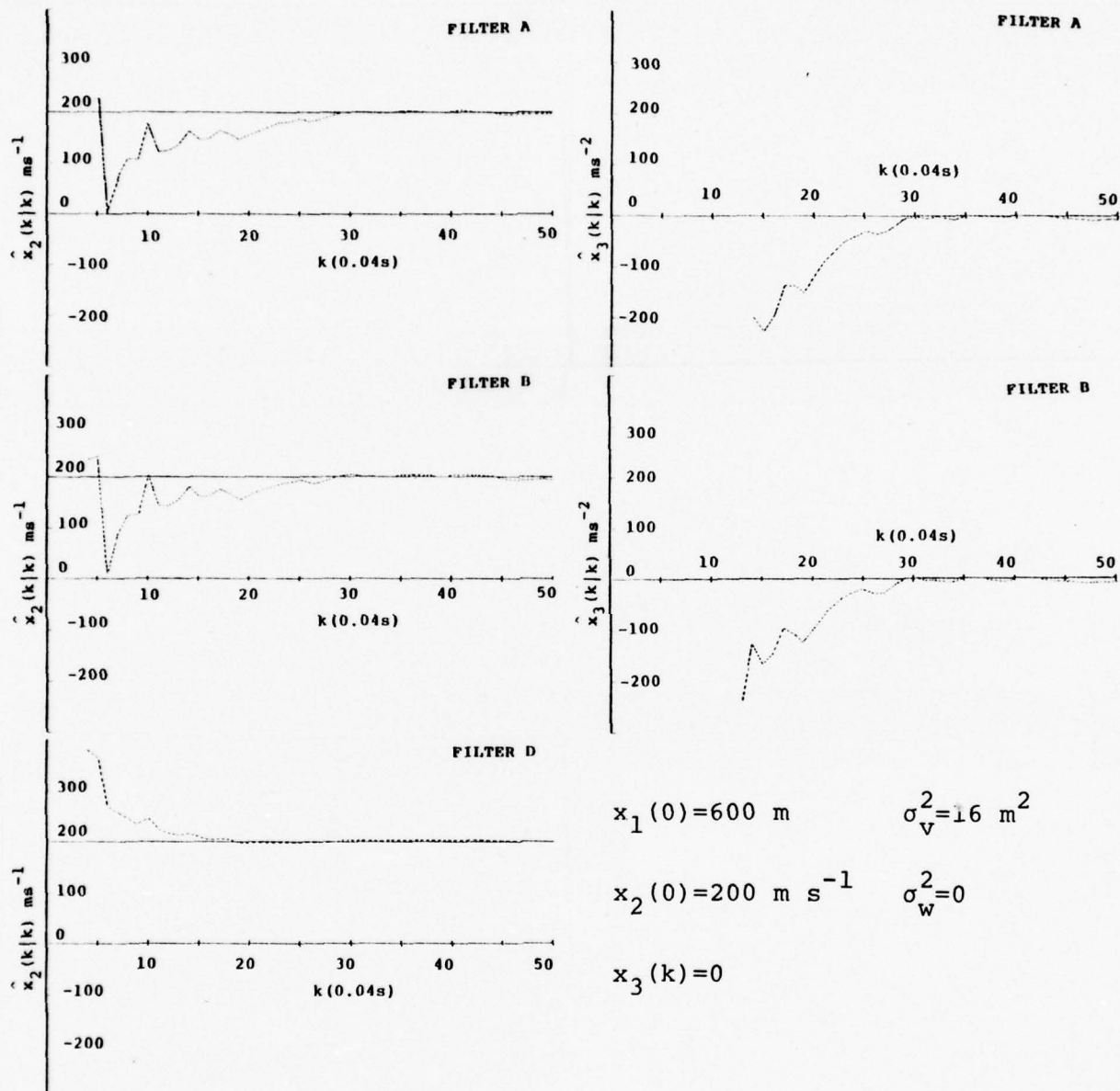


Figure A-4

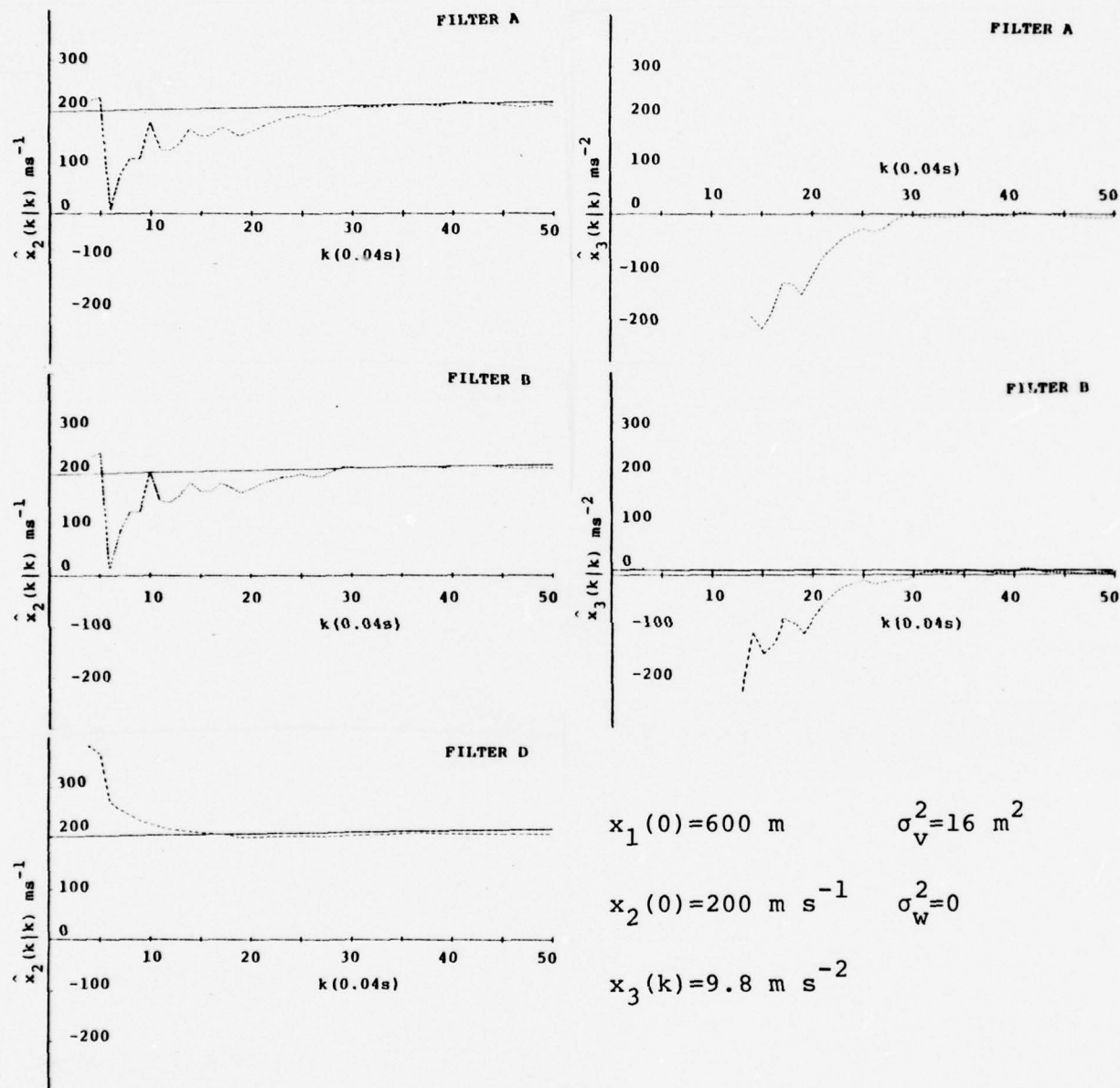


Figure A-5

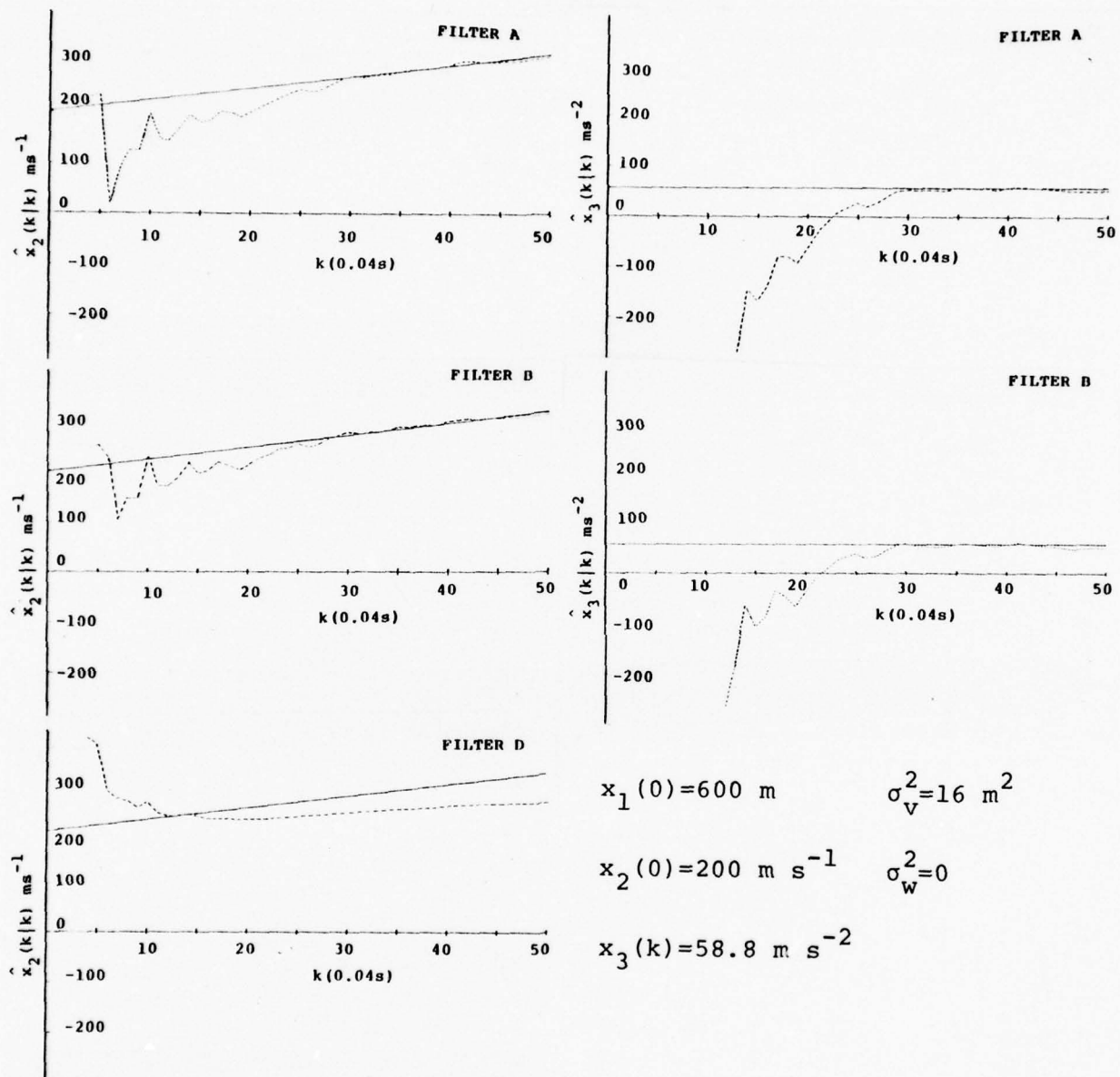


Figure A-6

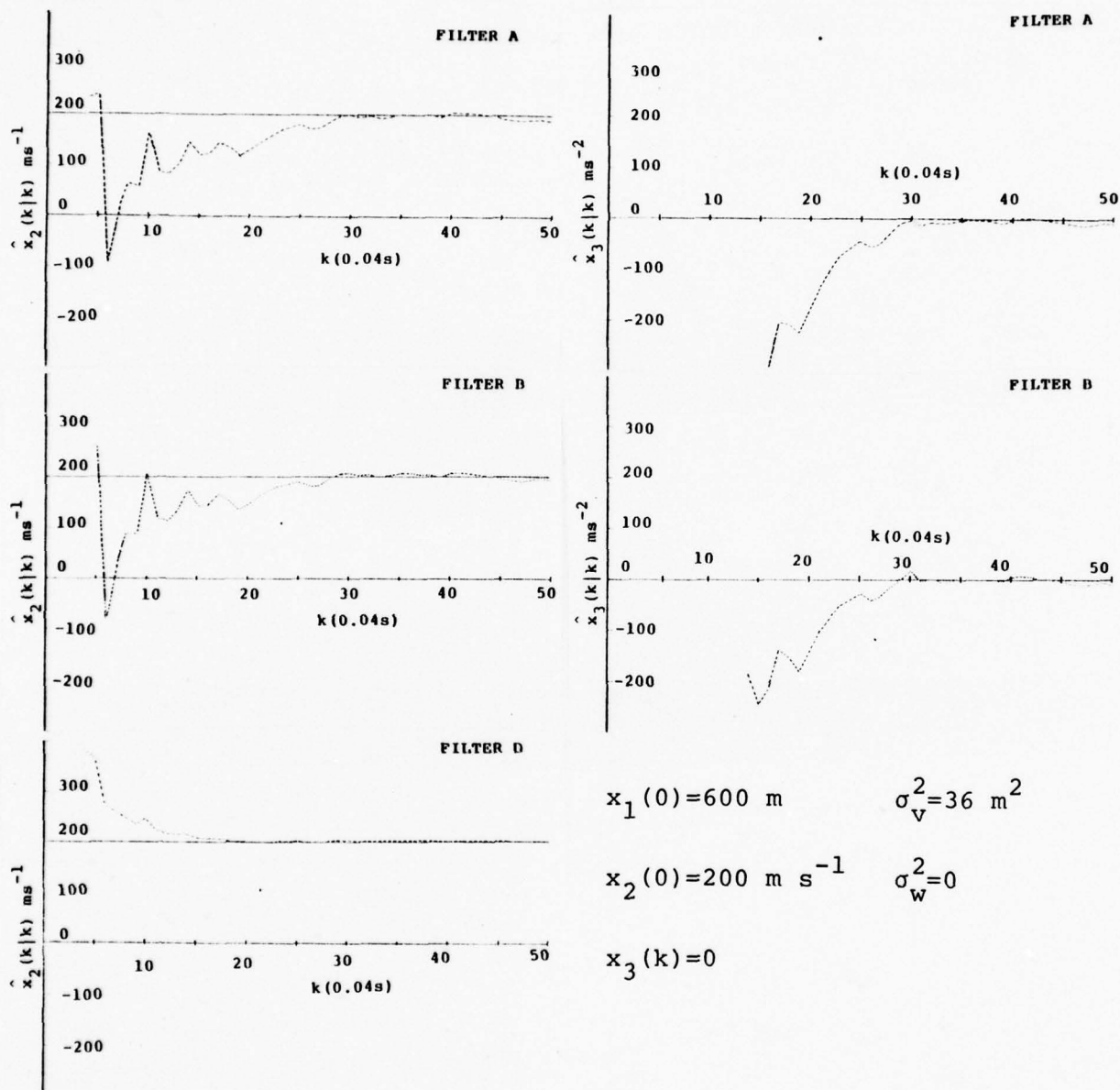


Figure A-7

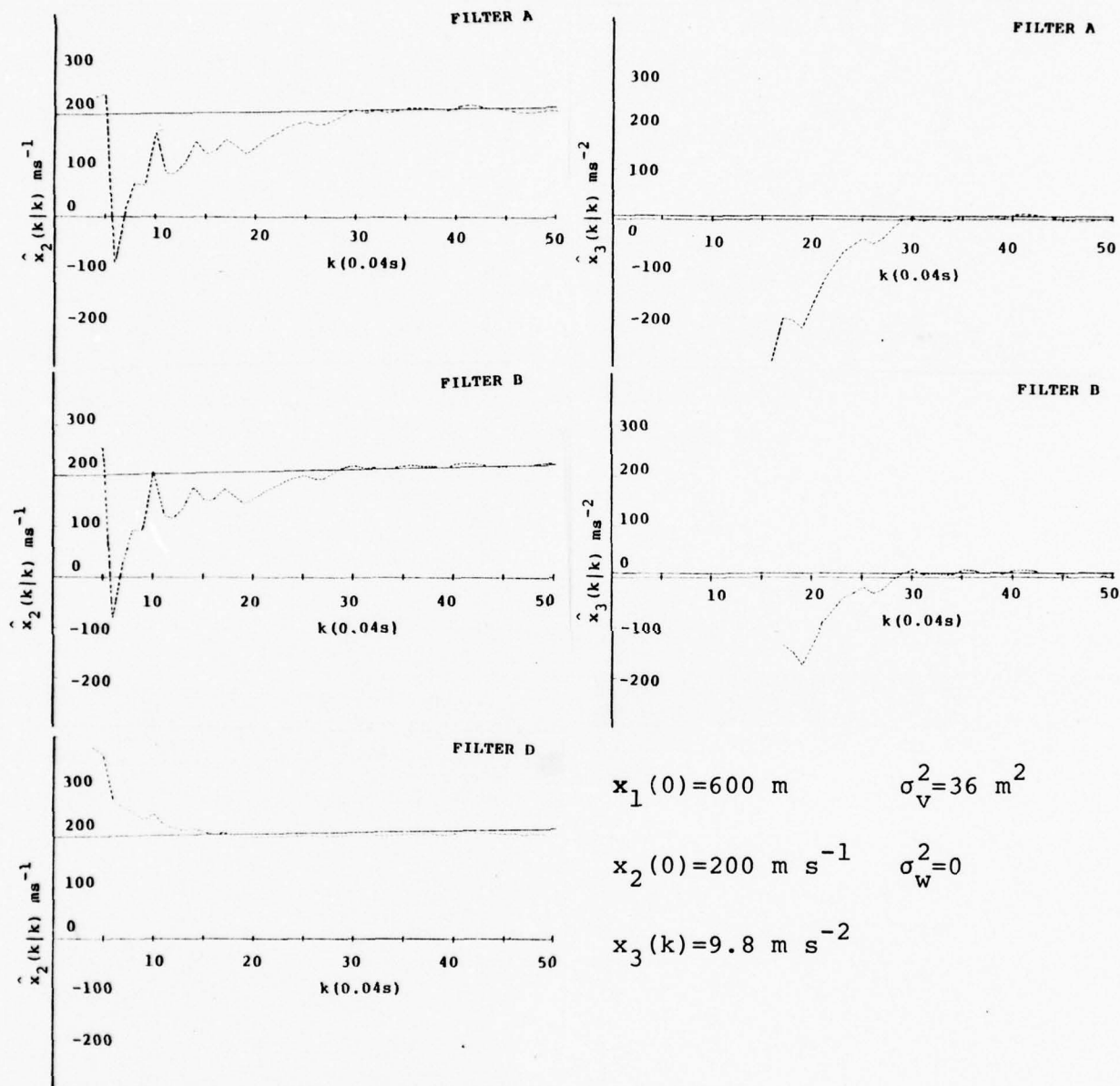


Figure A-8

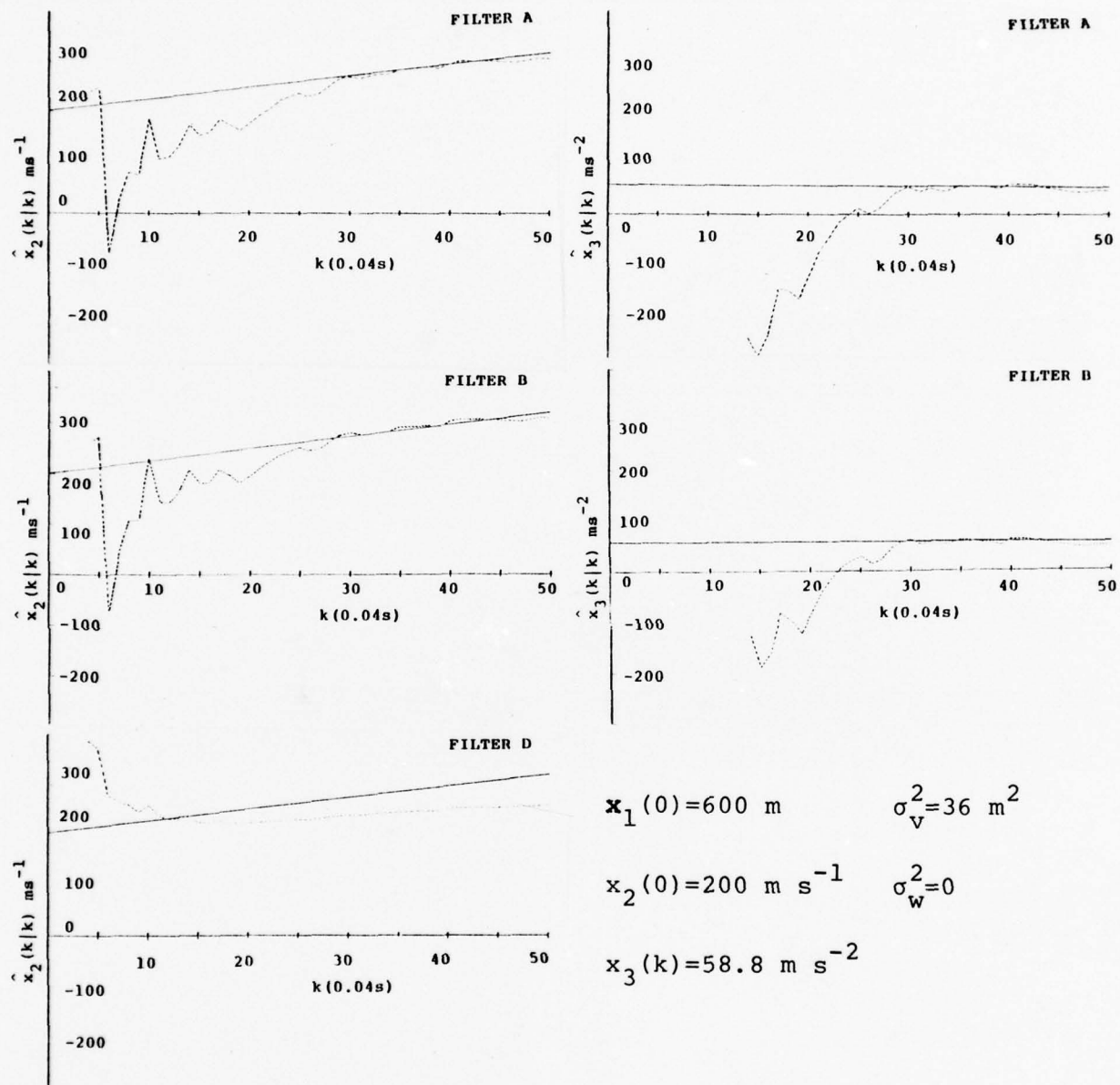


Figure A-9

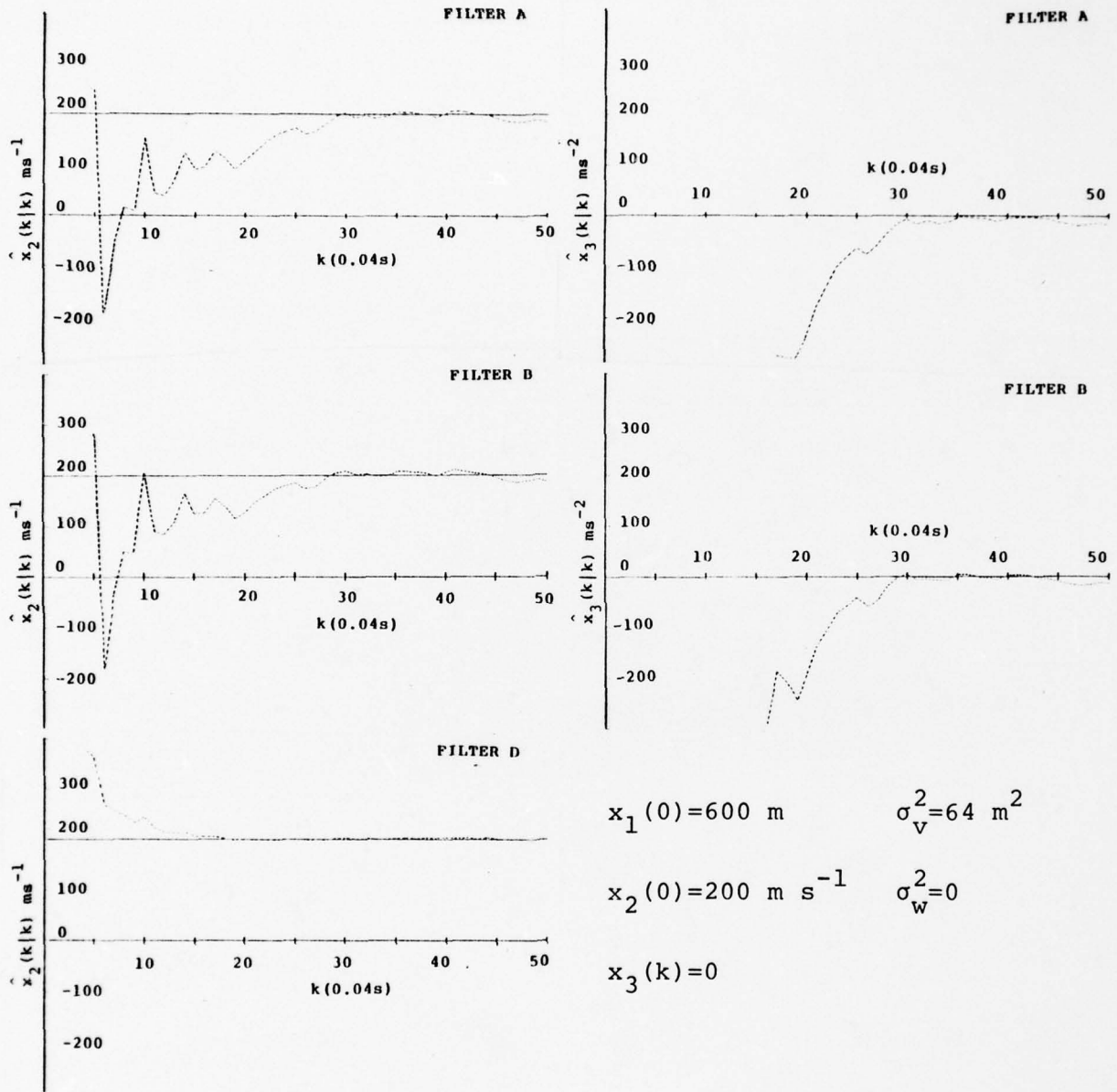


Figure A-10

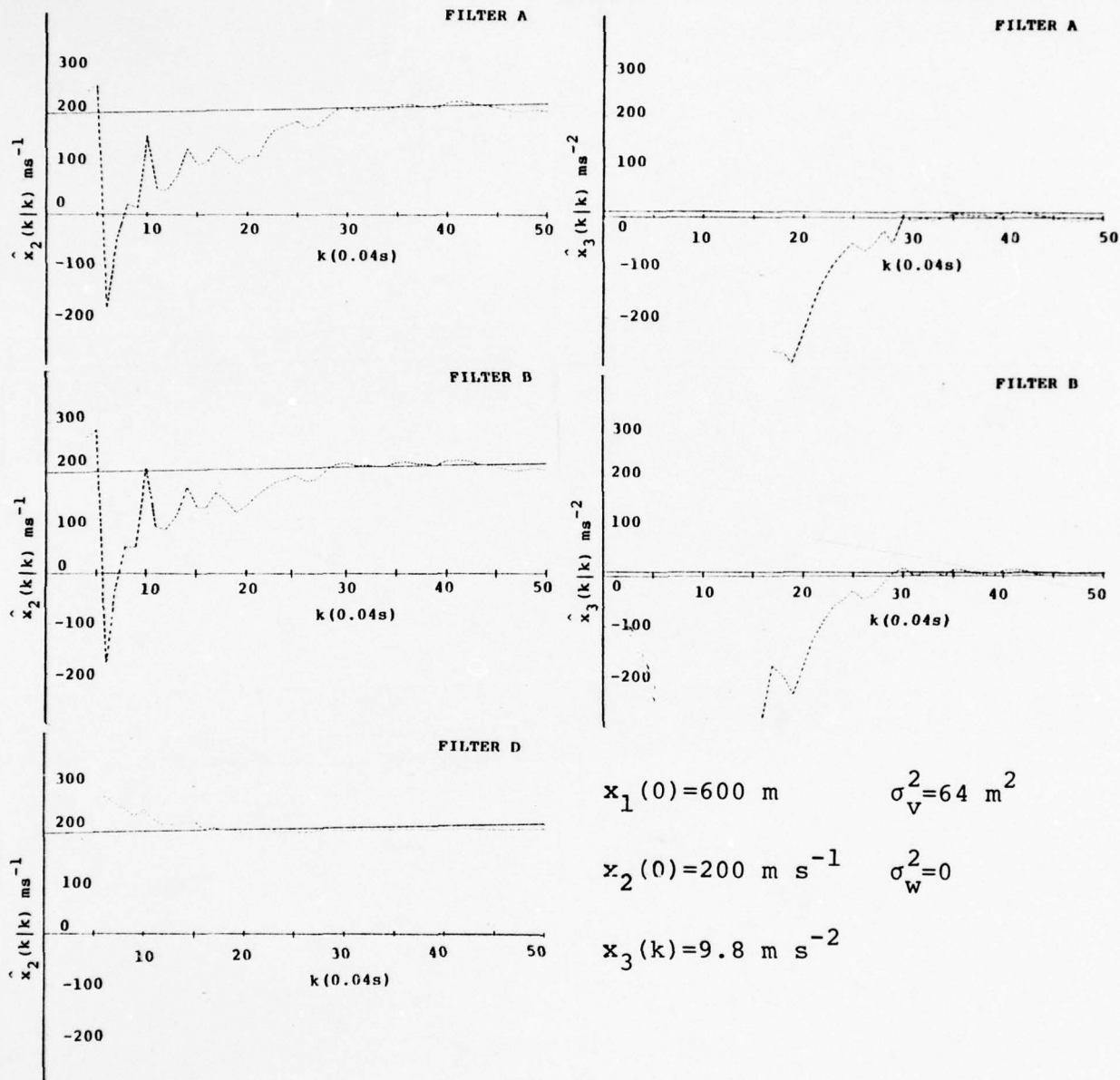


Figure A-11

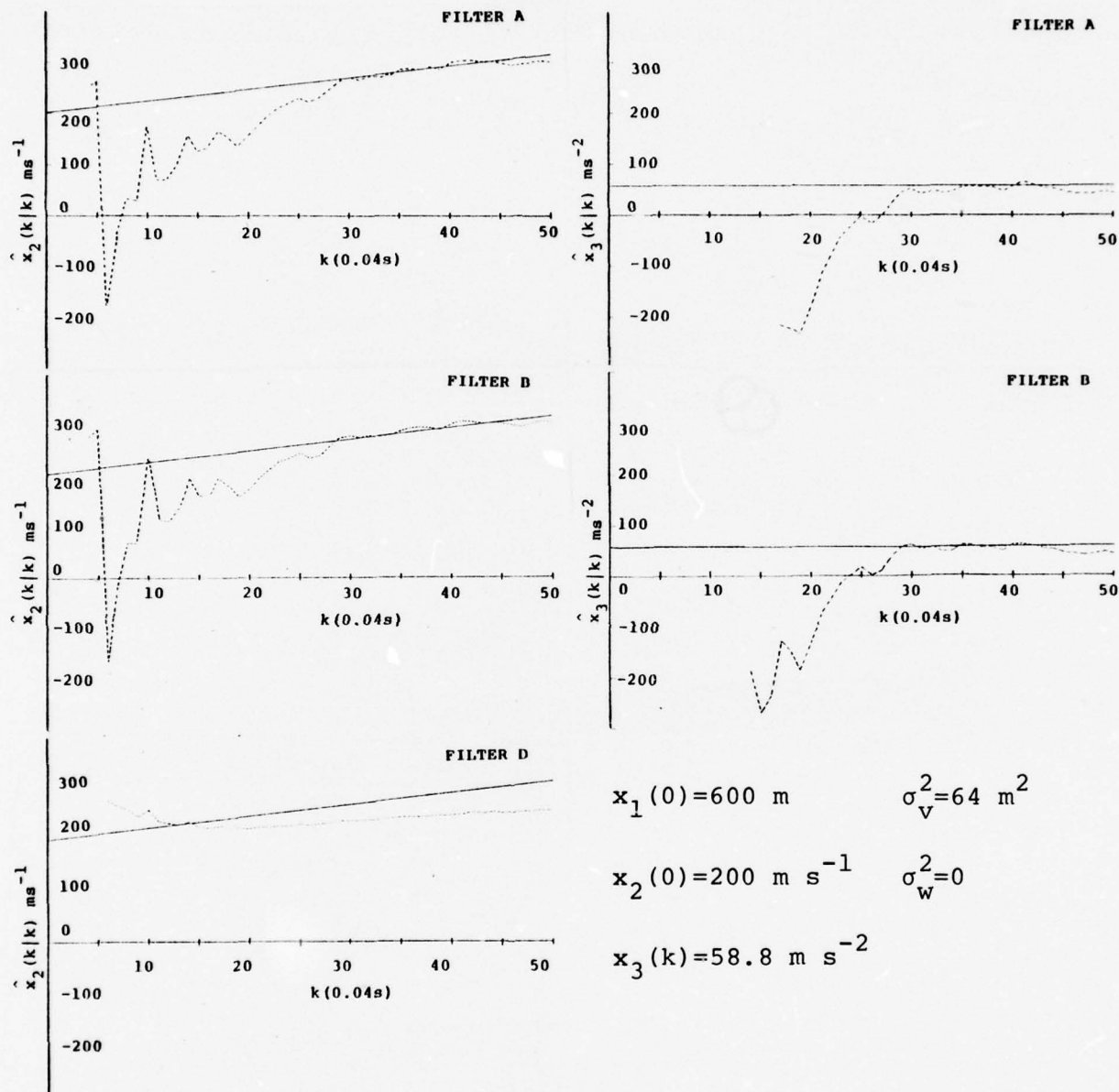


Figure A-12

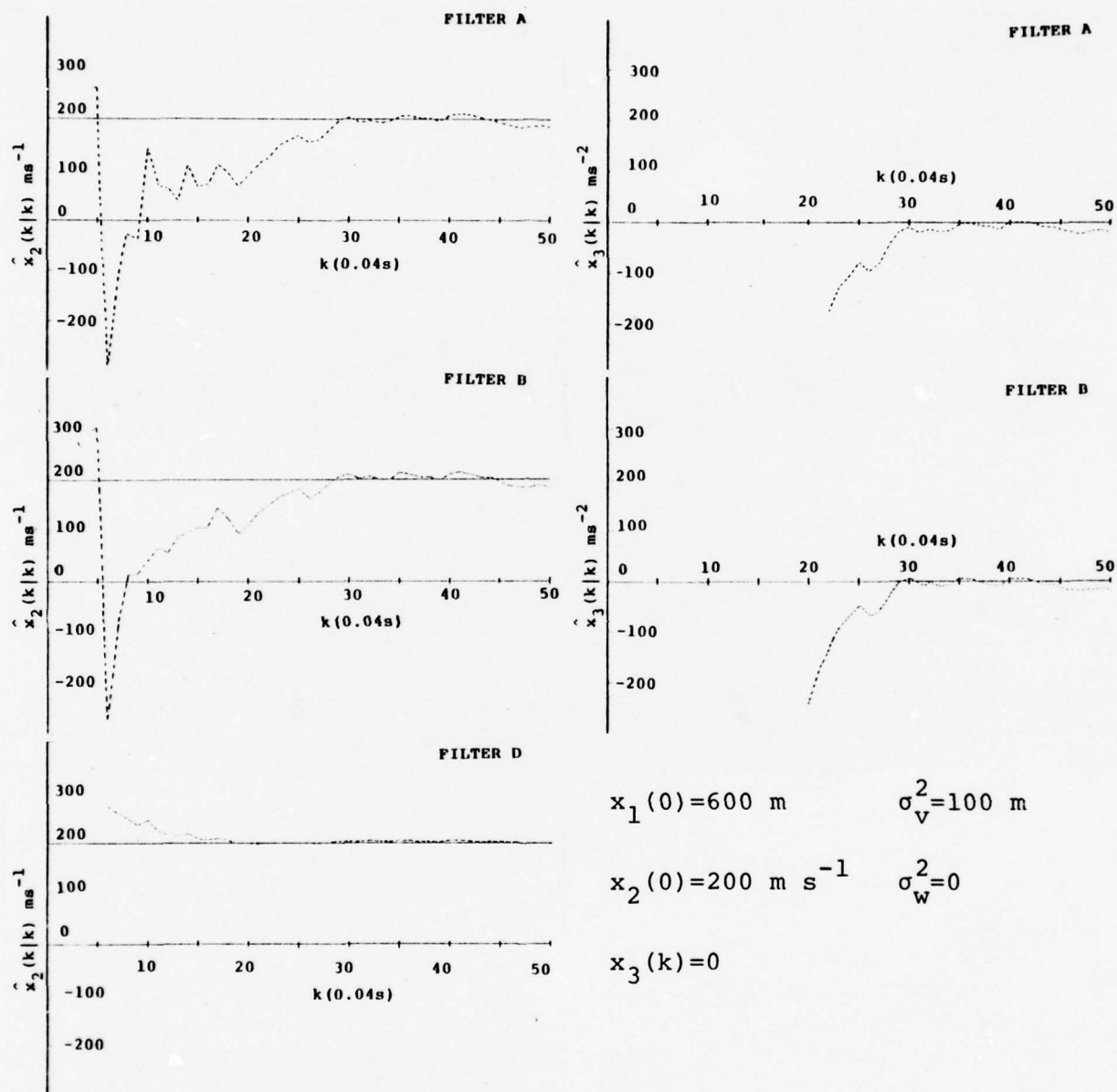


Figure A-13

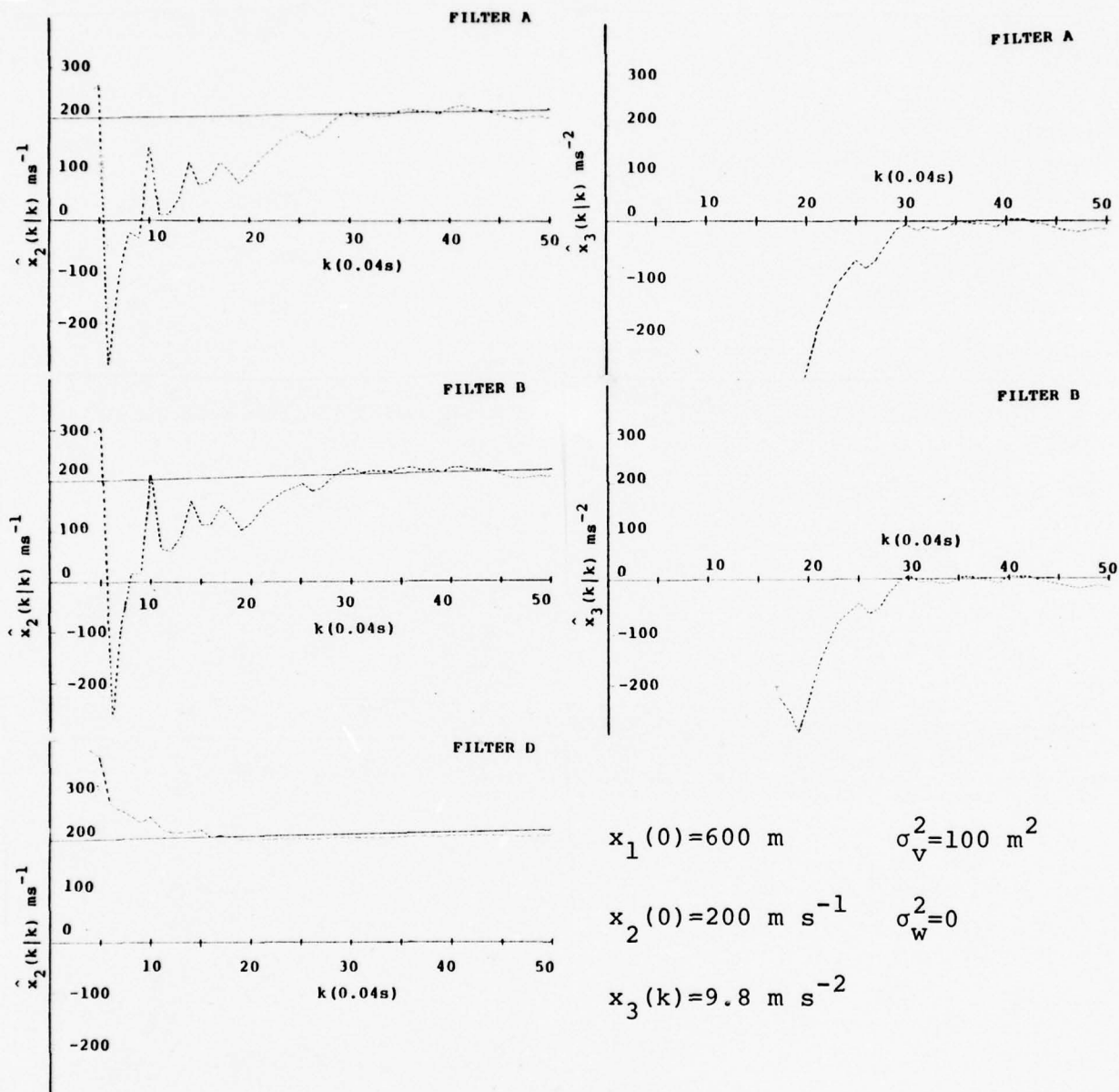


Figure A-14

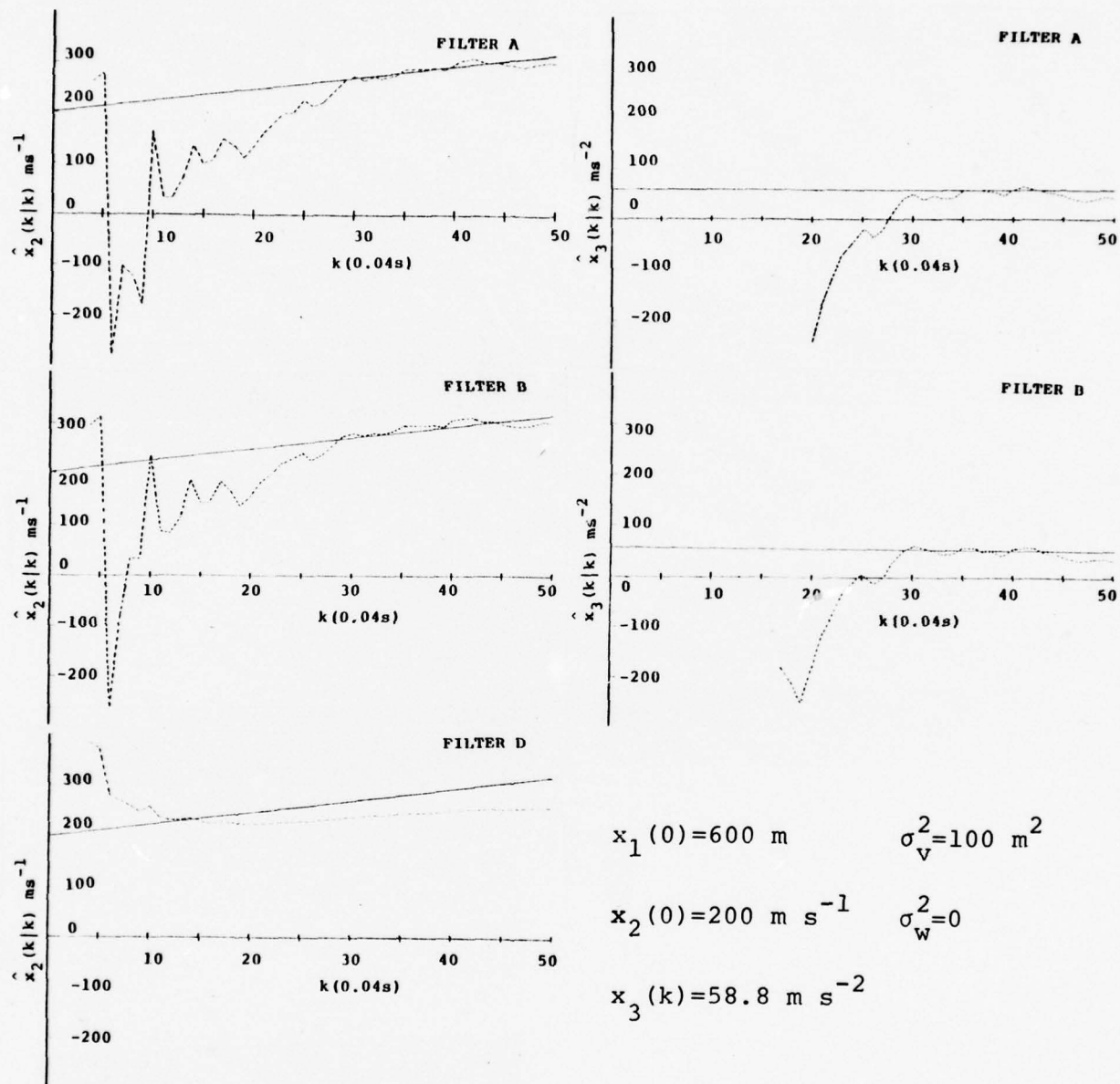


Figure A-15

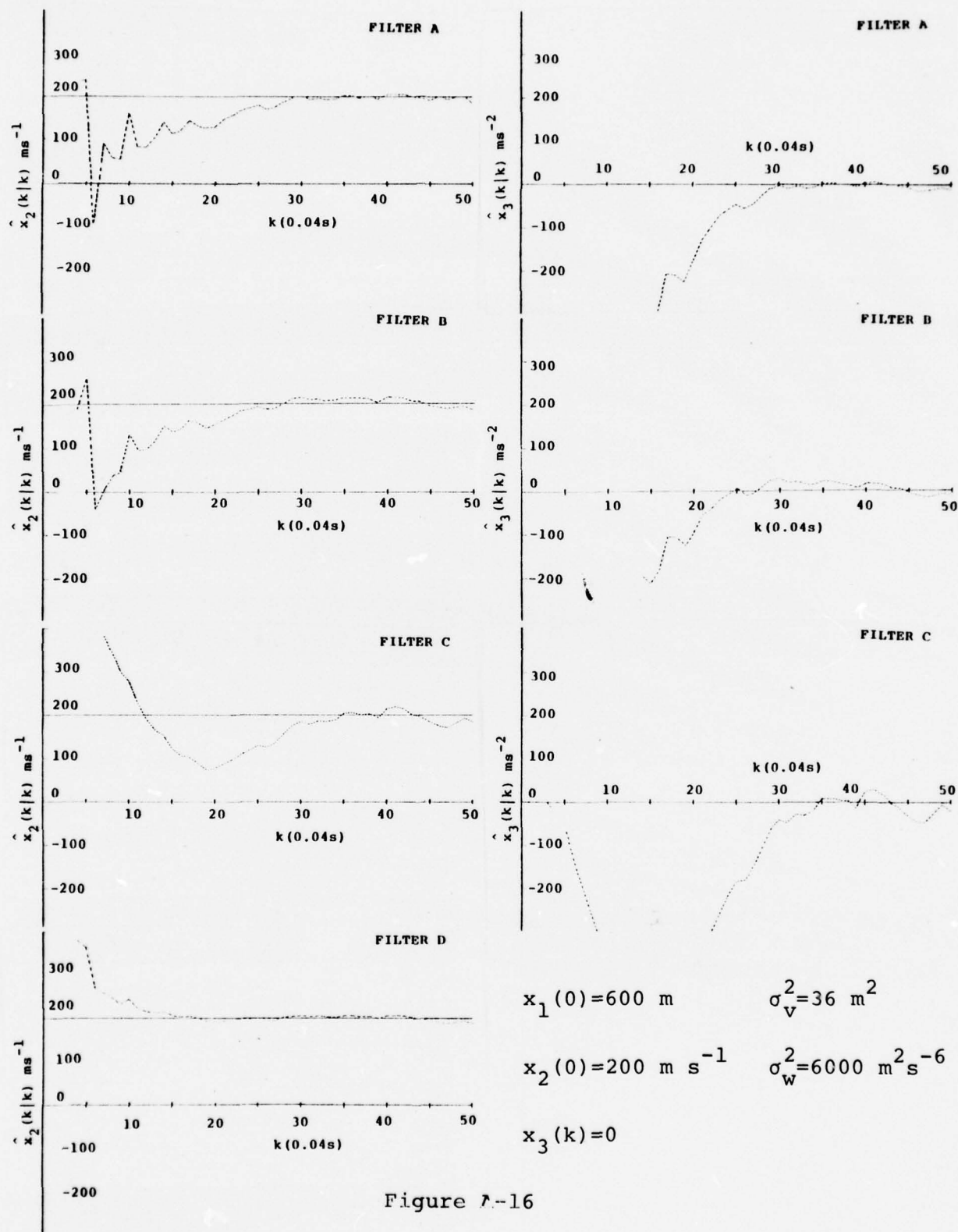


Figure 7-16

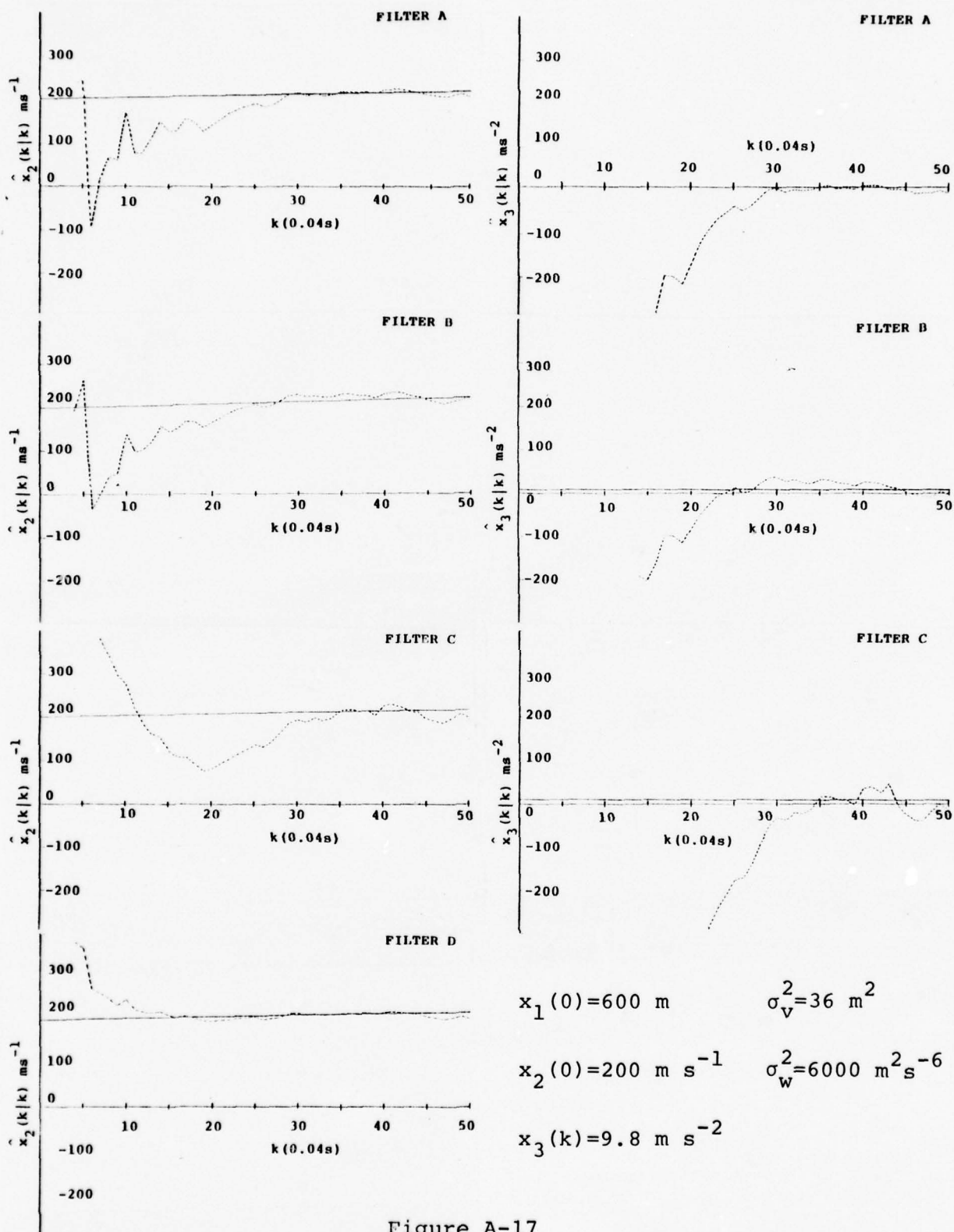


Figure A-17

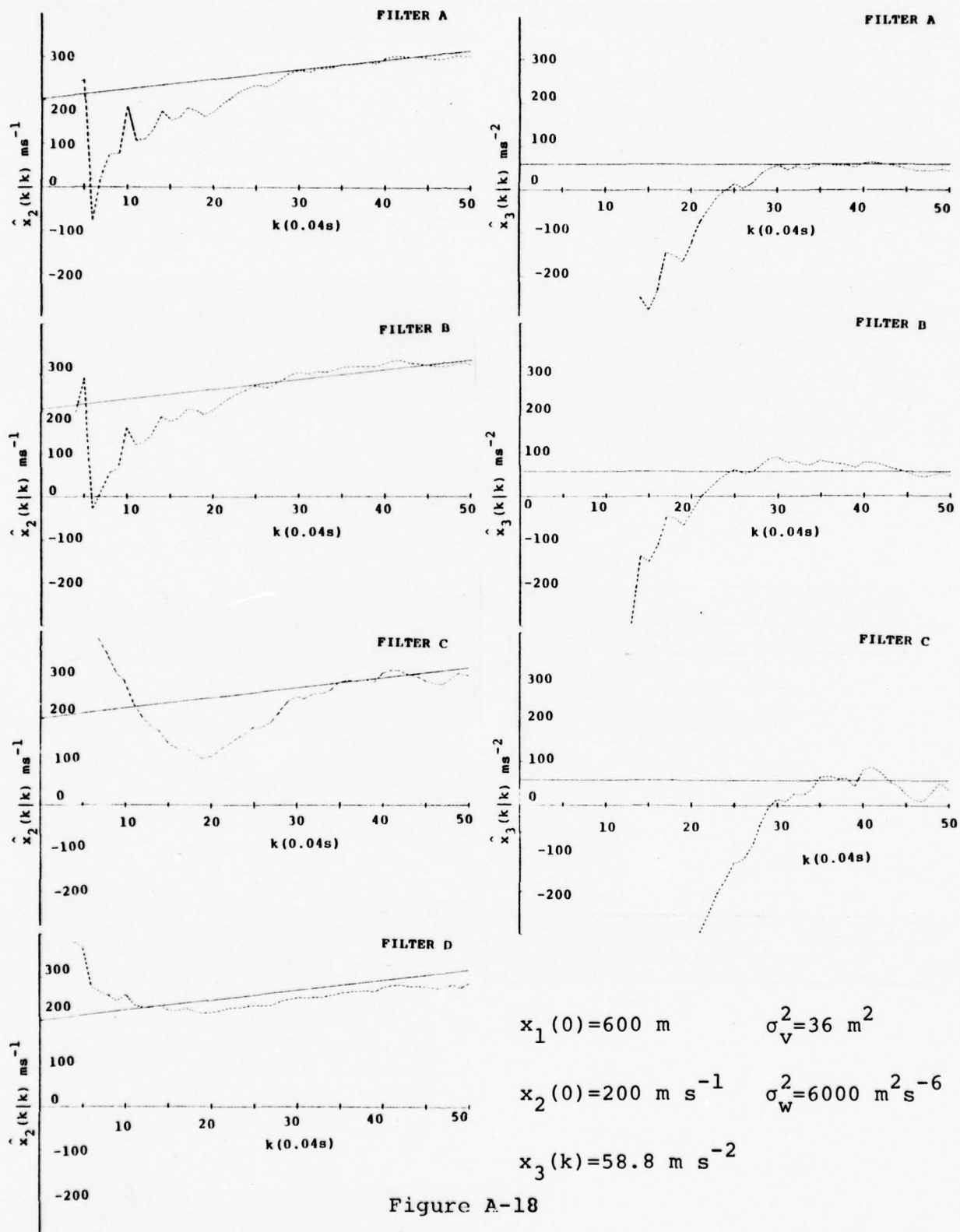


Figure A-18

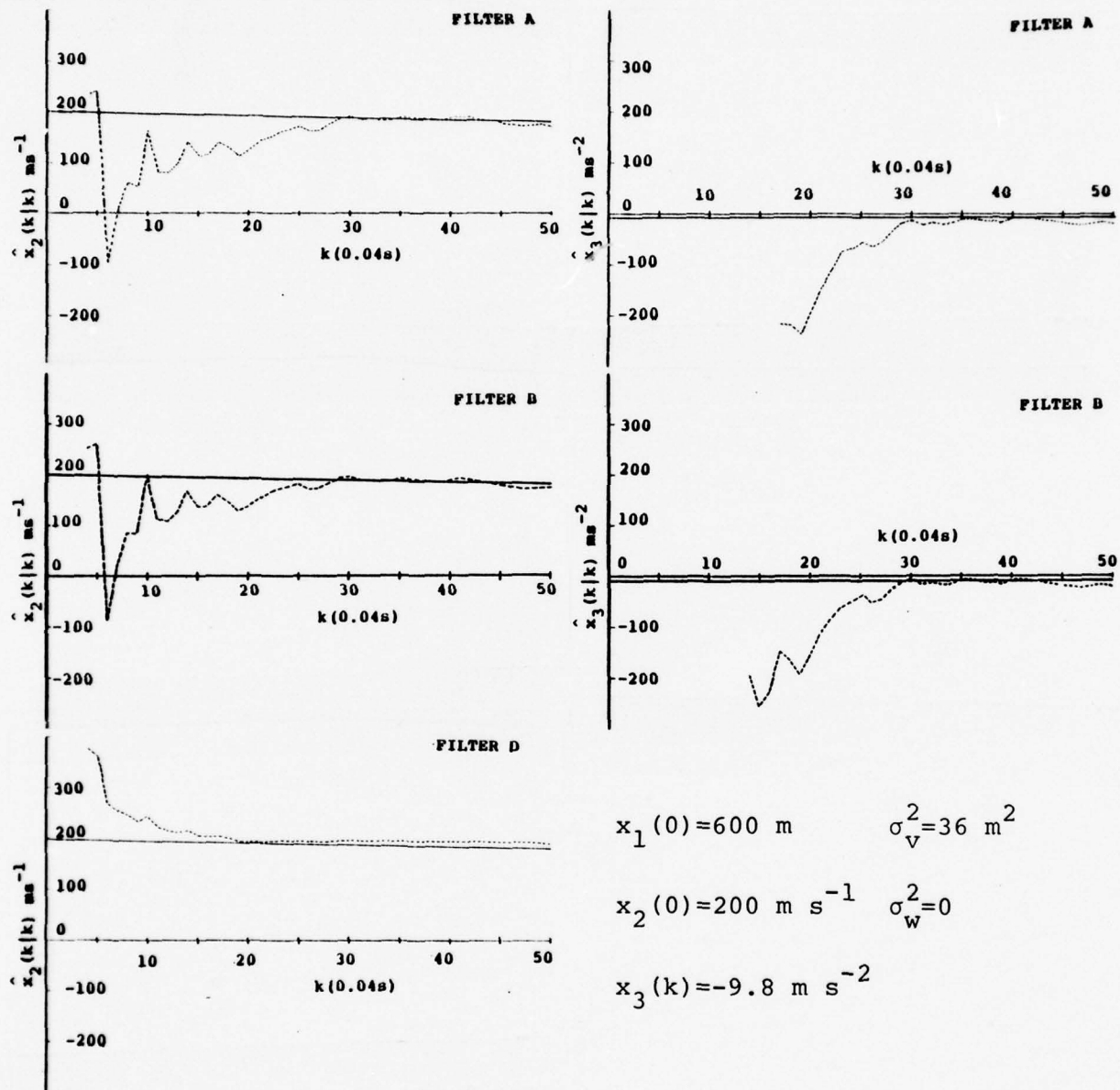


Figure A-19

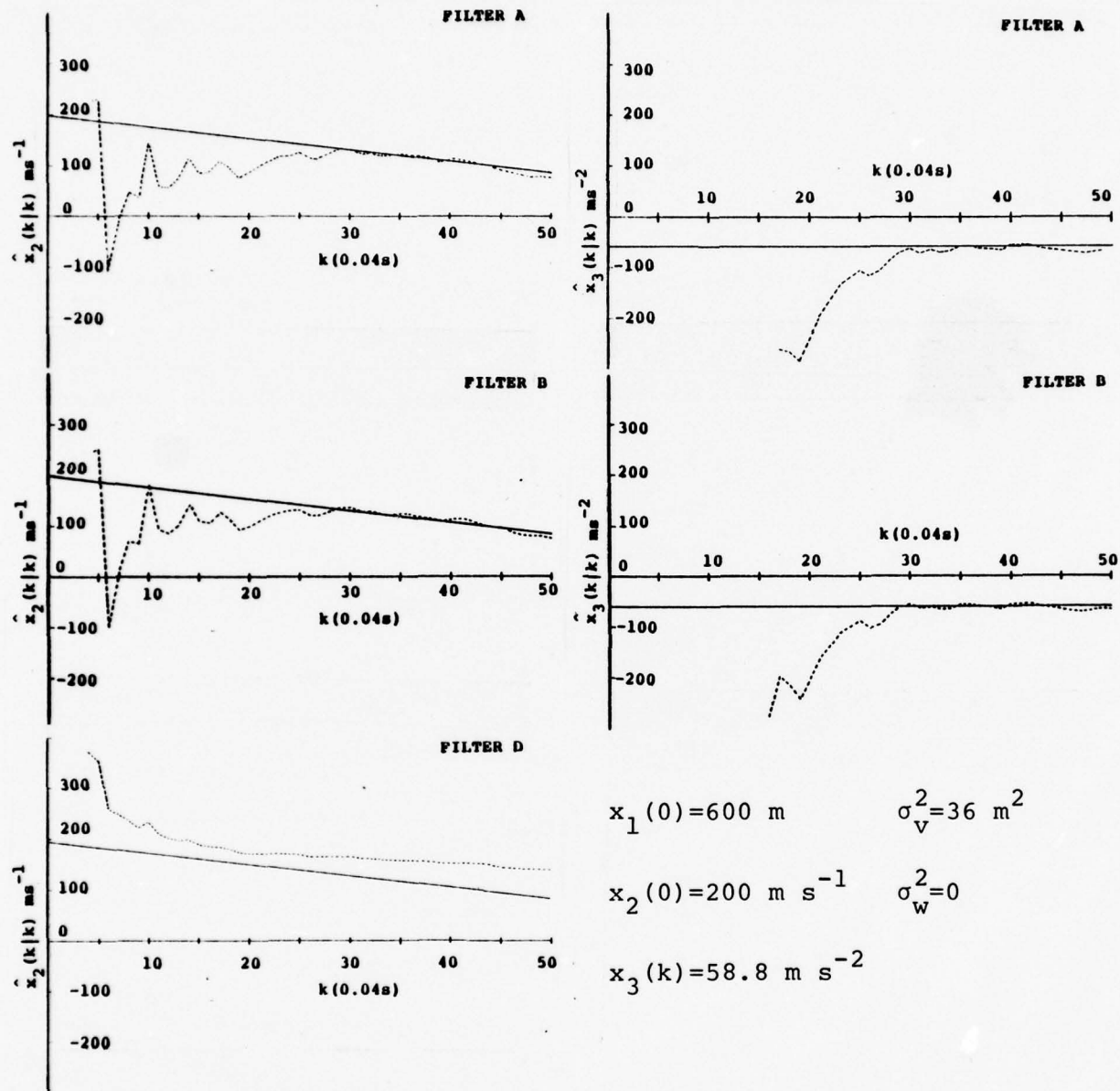


Figure A-20

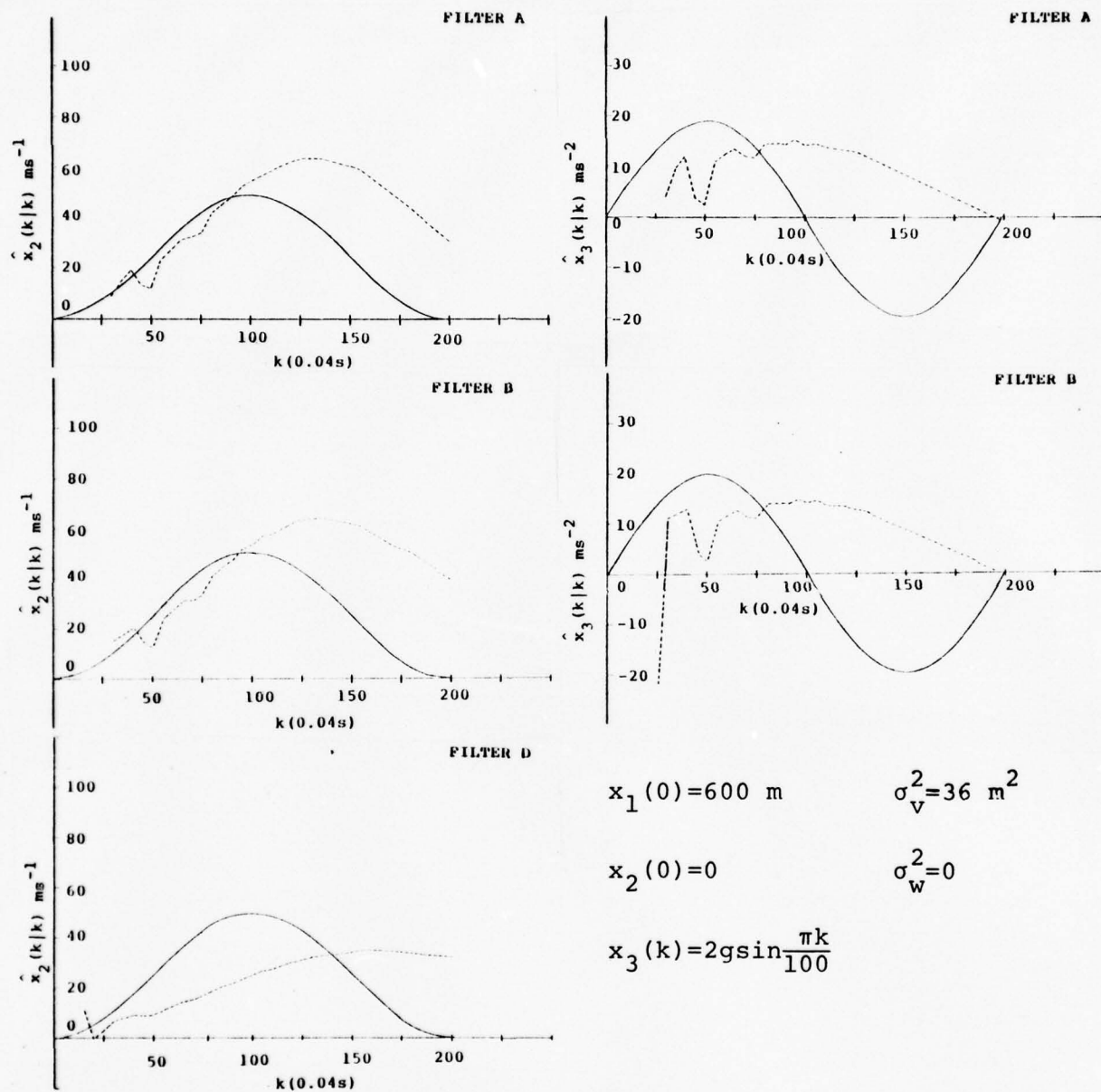


Figure A-21

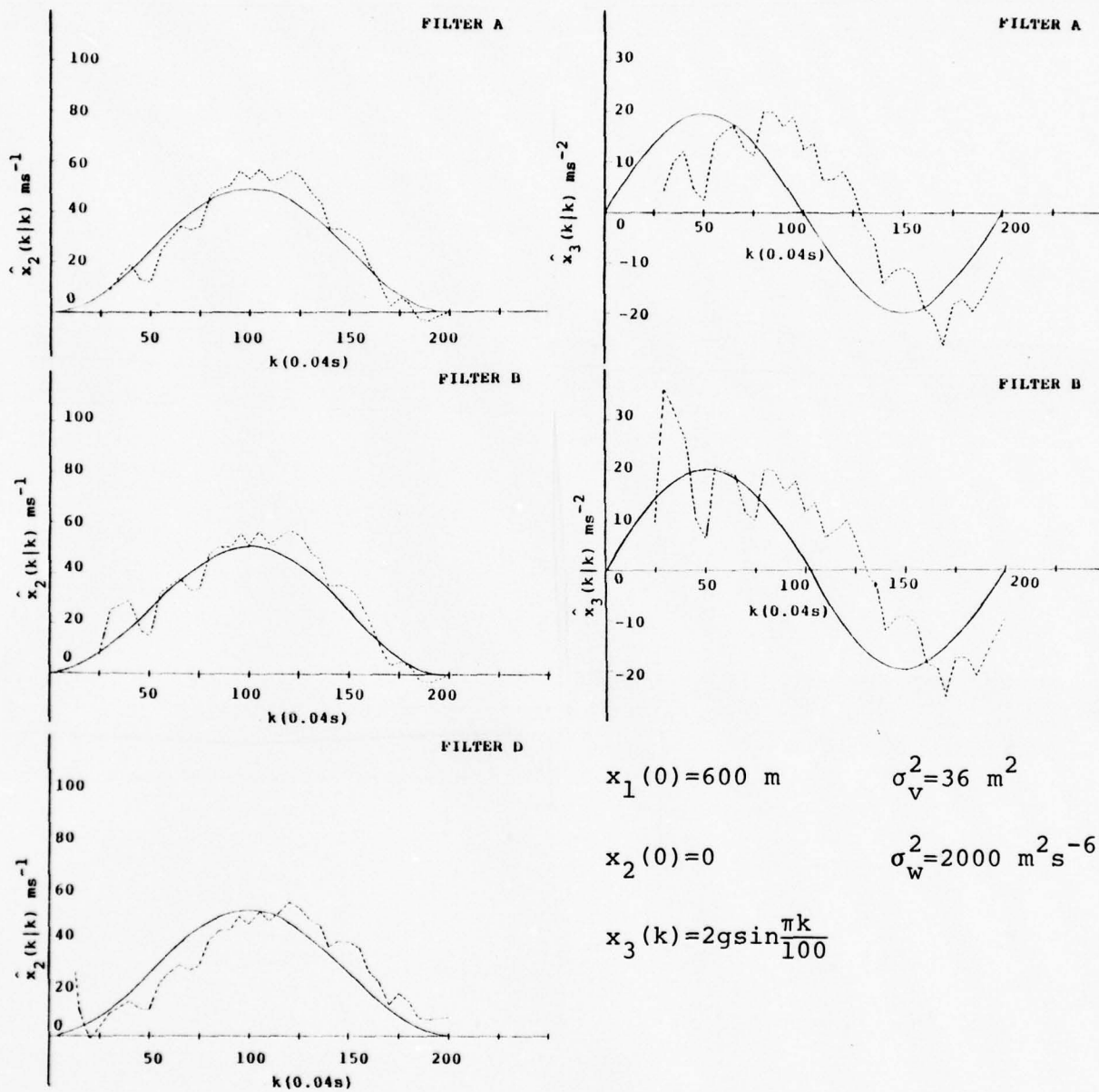


Figure A-22

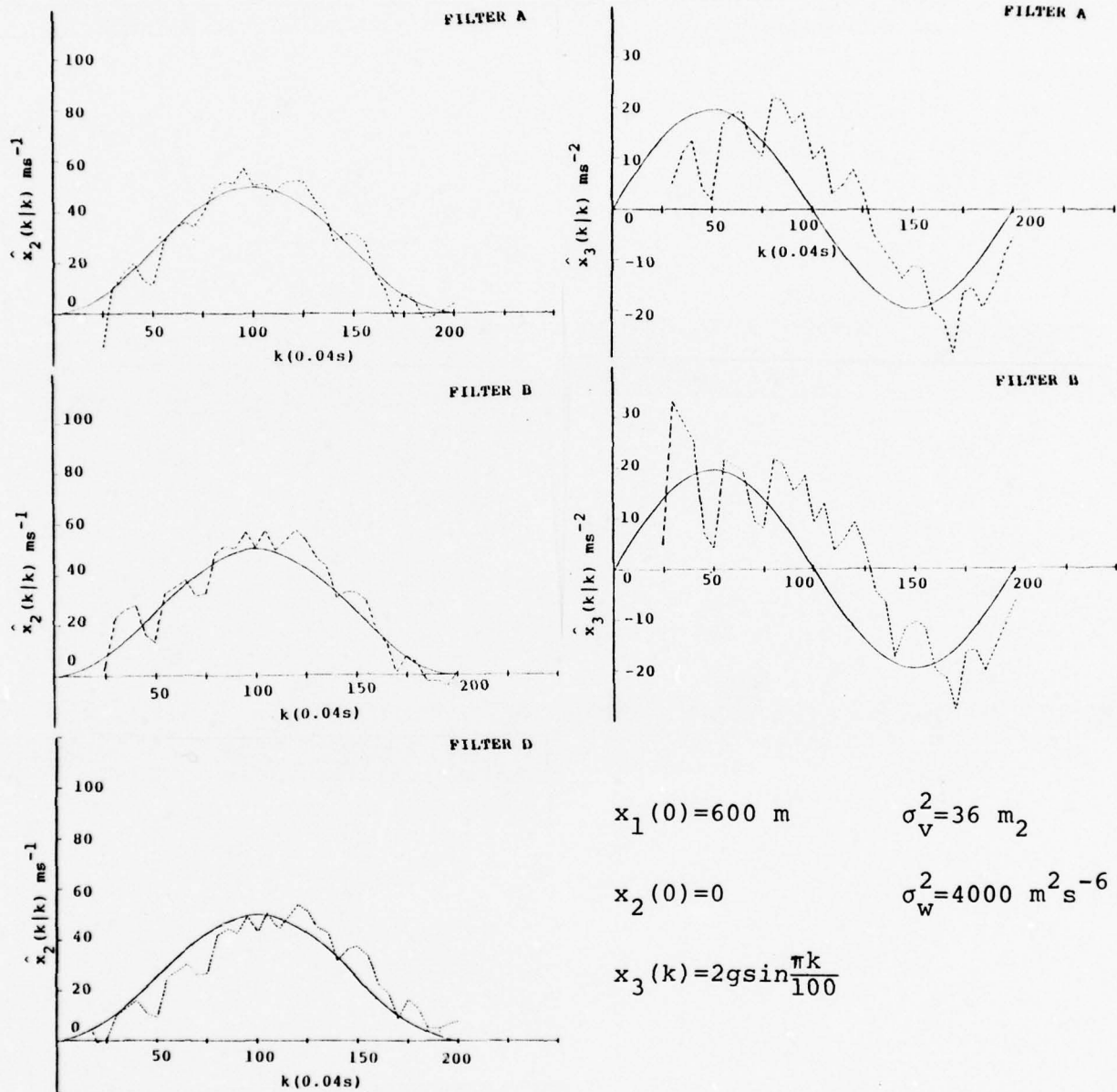


Figure A-23

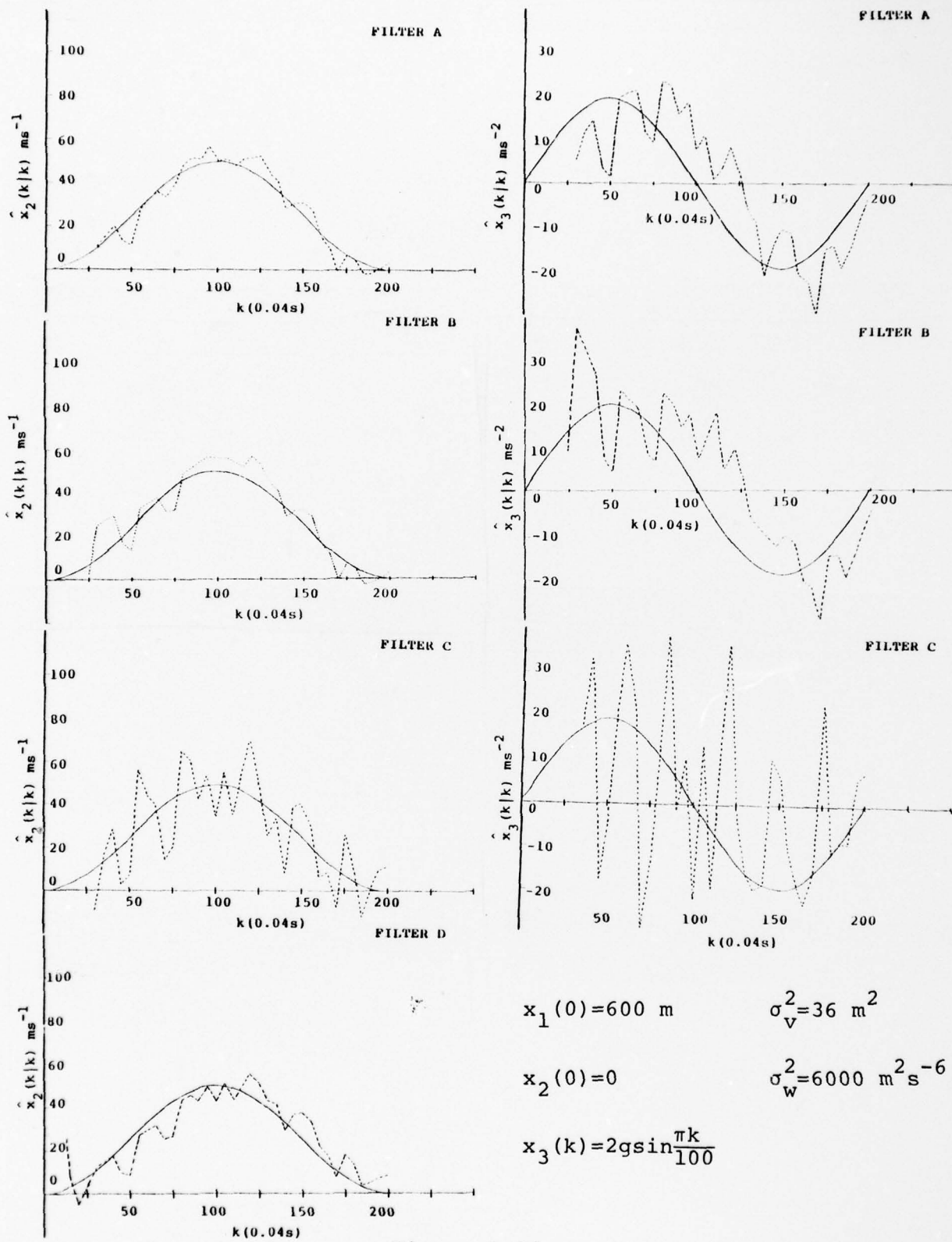


Figure A-24

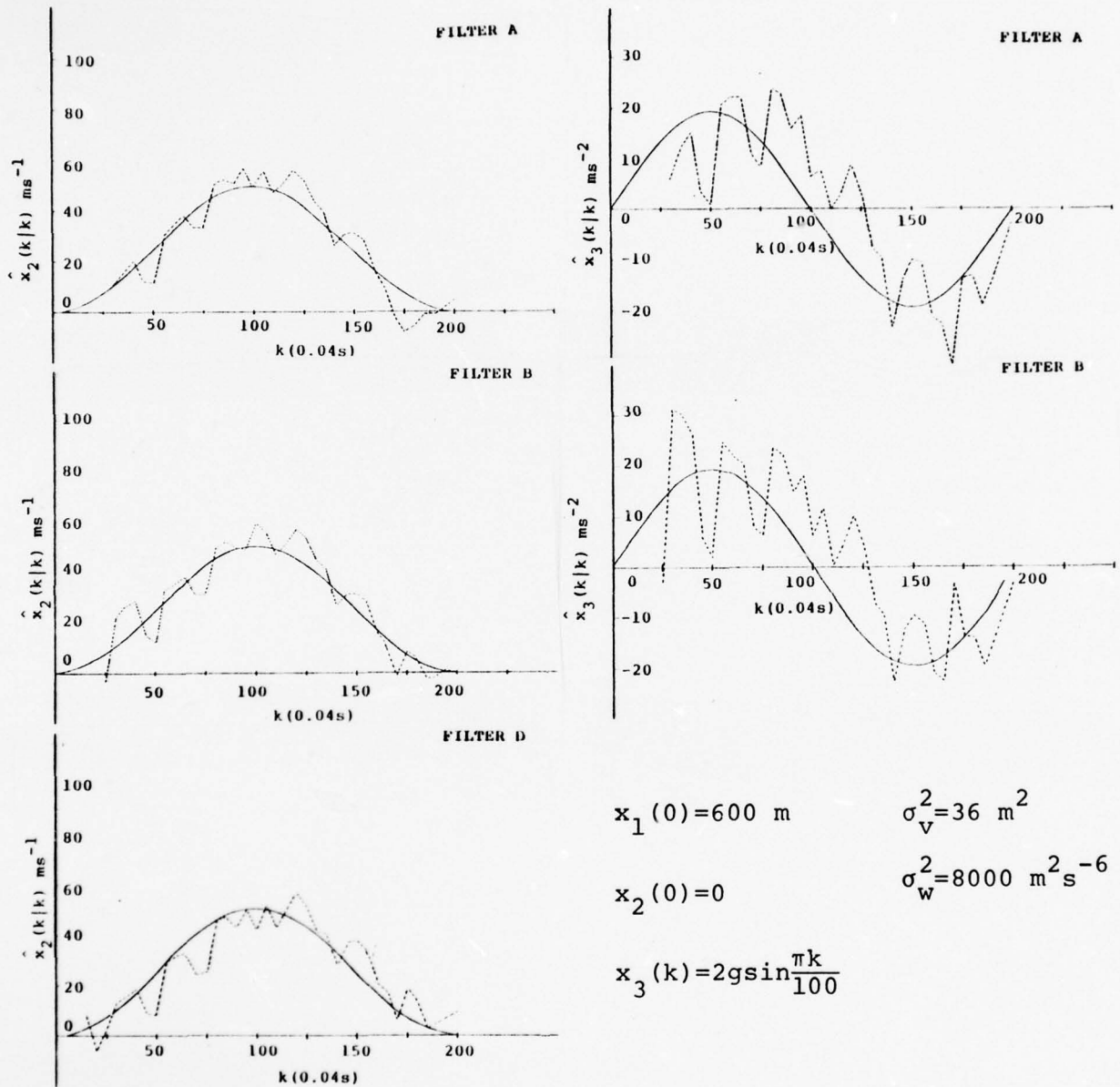


Figure A-25

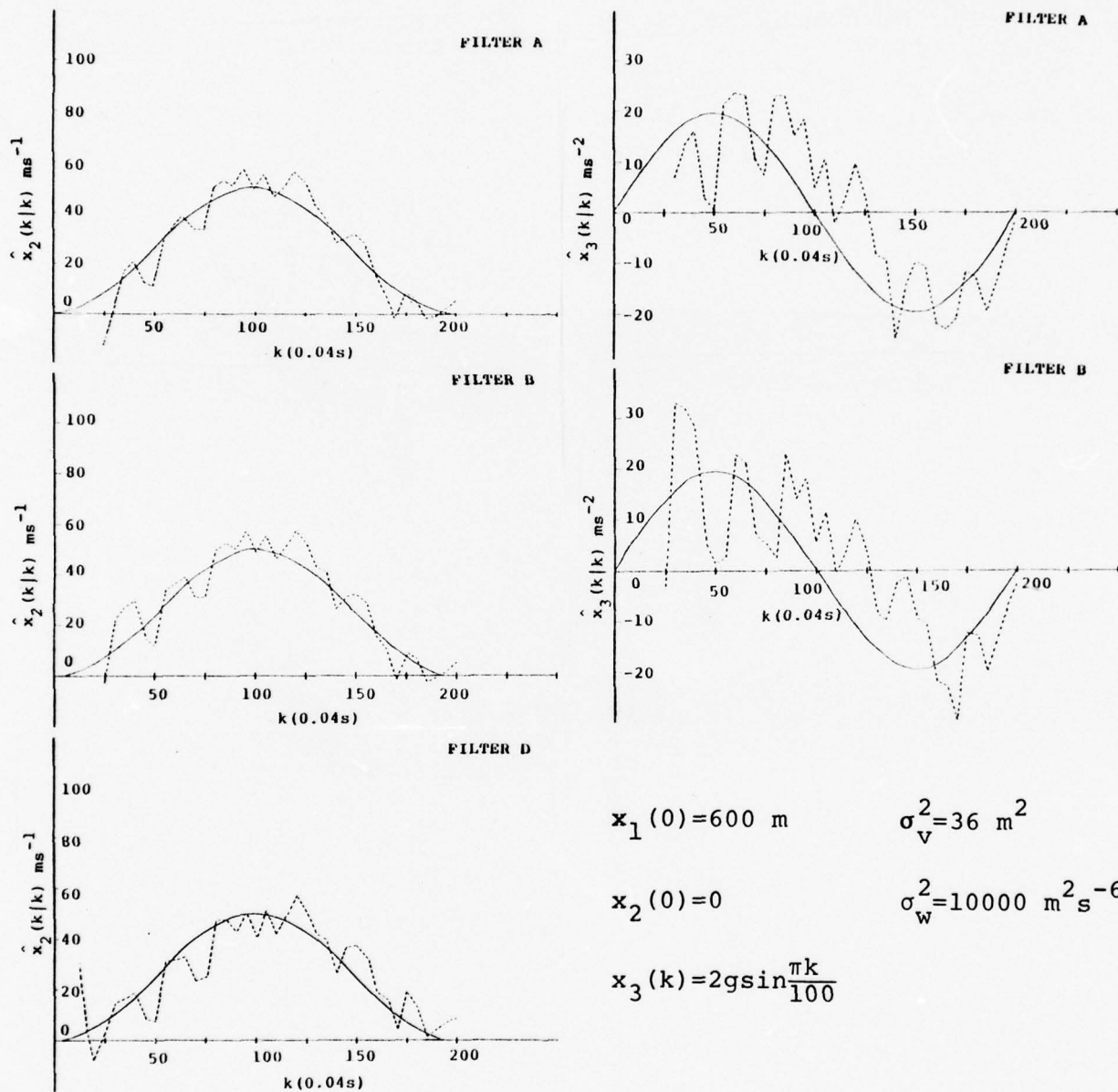


Figure A-26

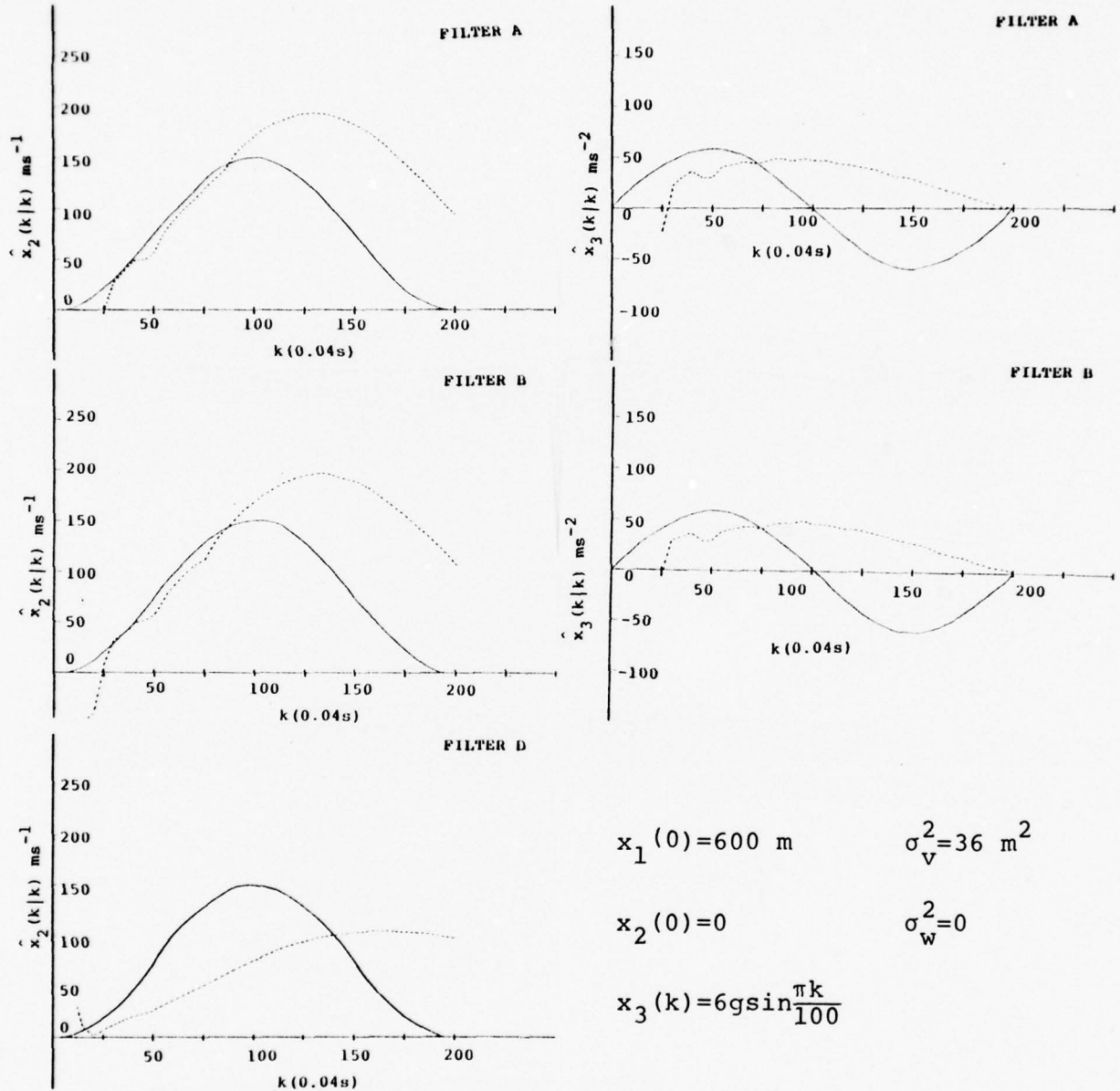


Figure A-26

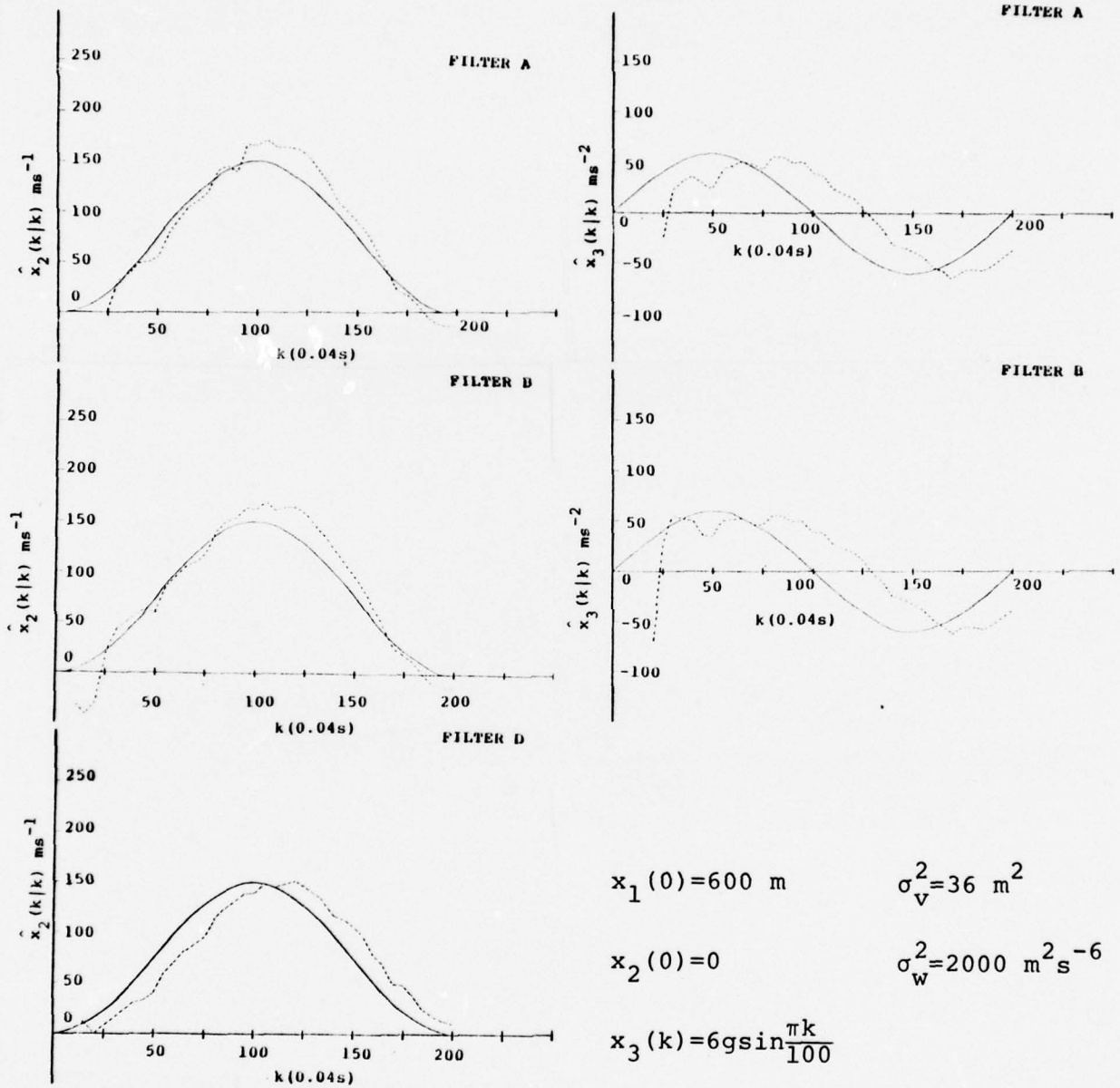


Figure A-28

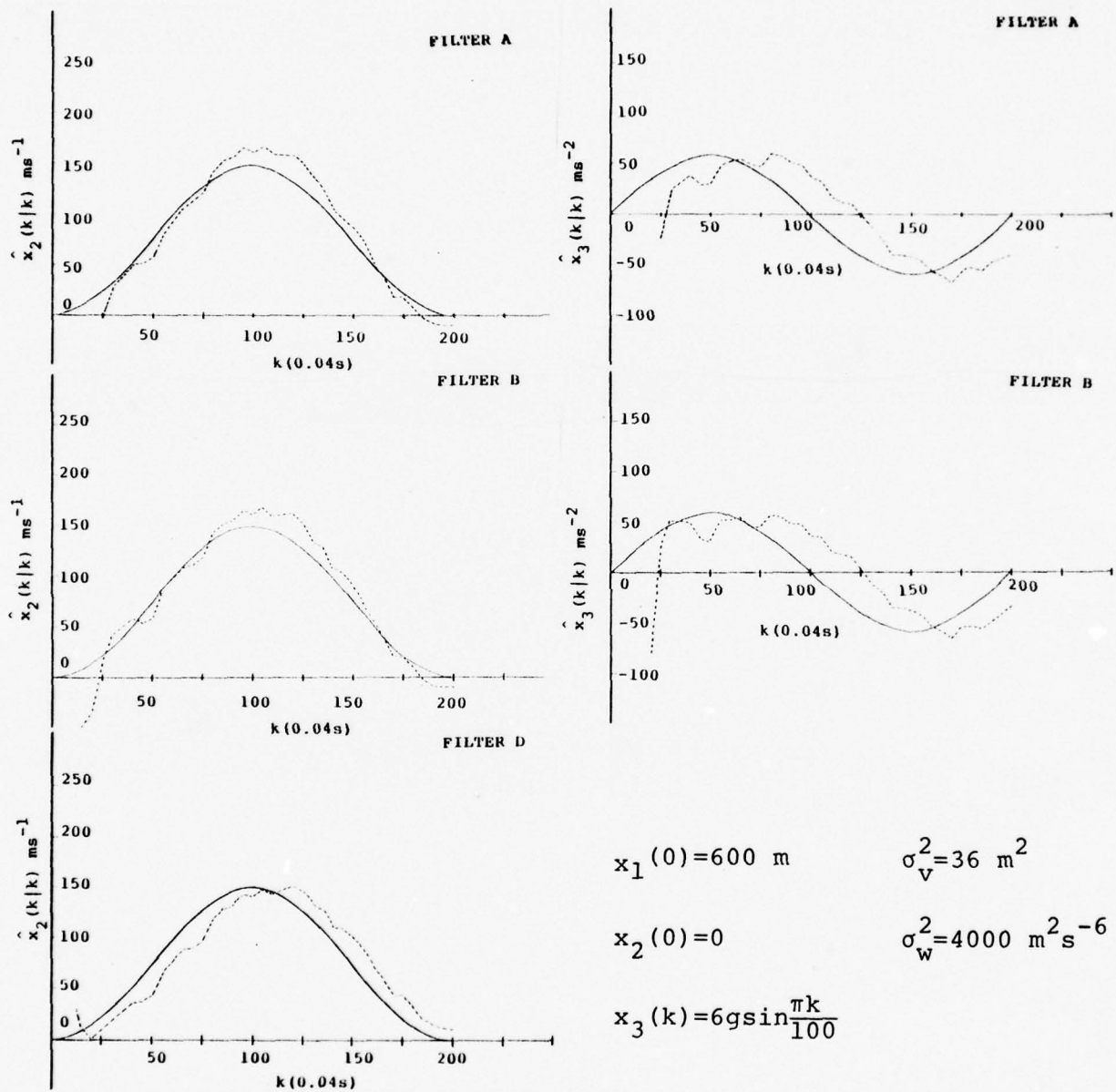


Figure A-29

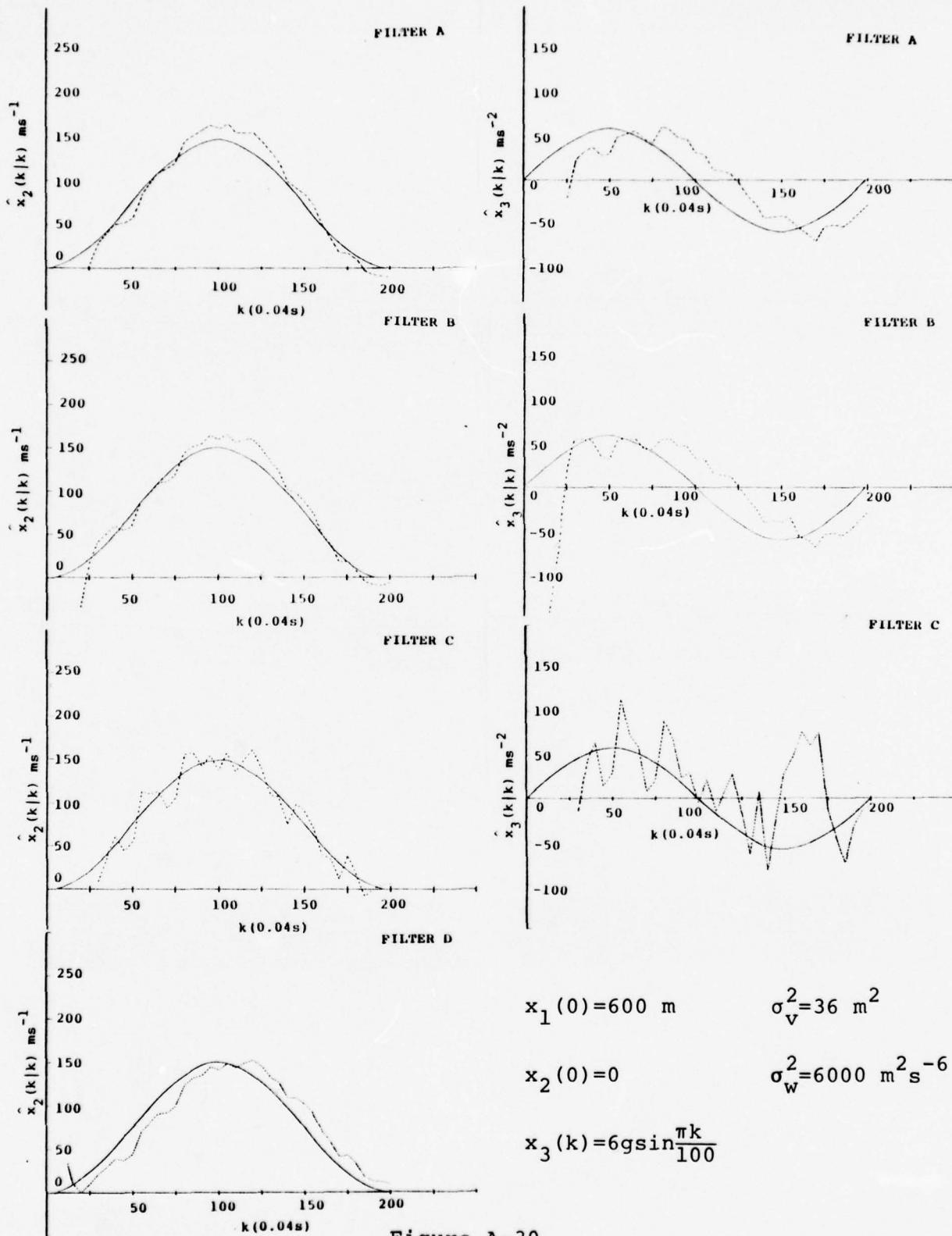


Figure A-30

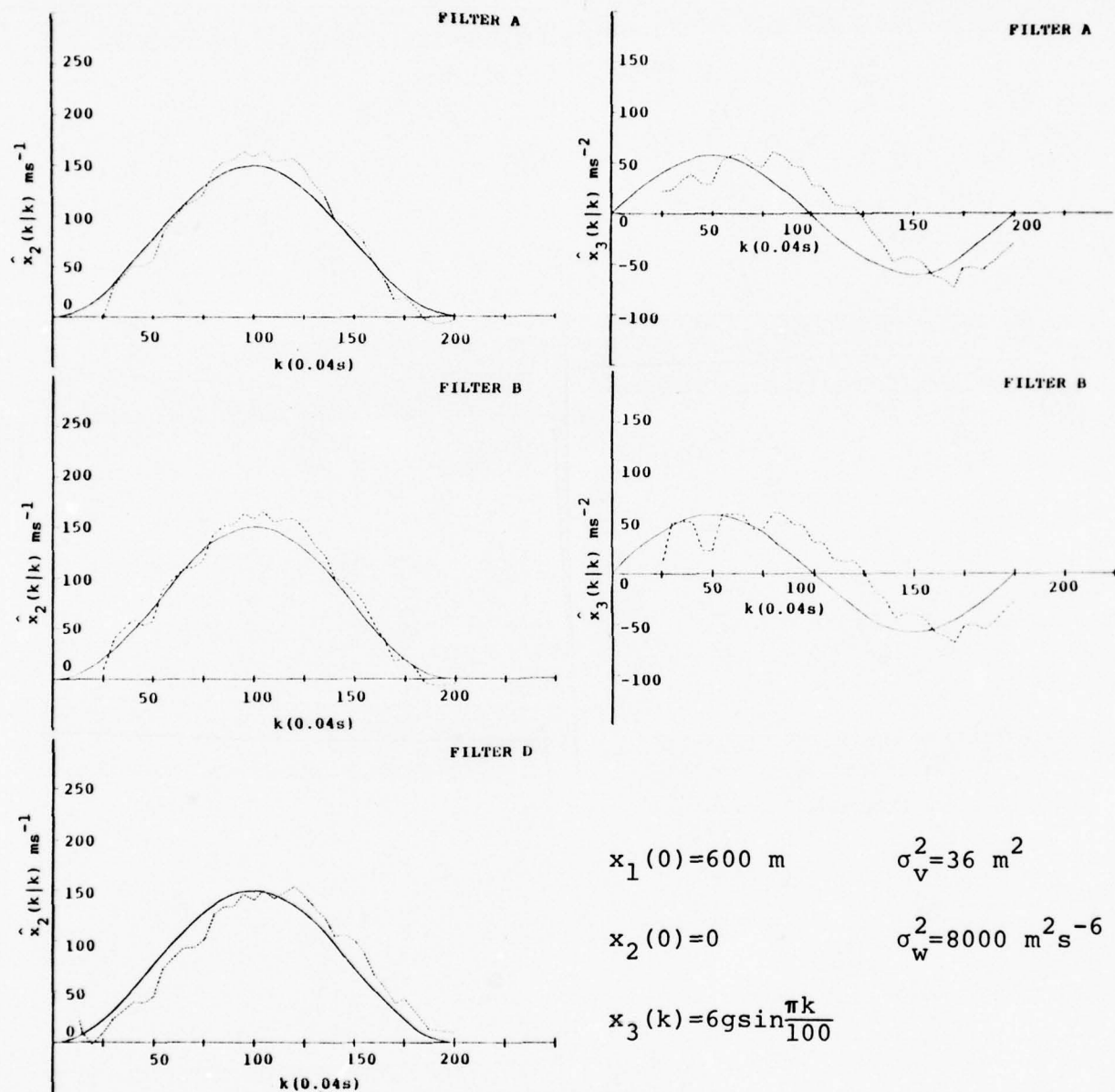


Figure A-31

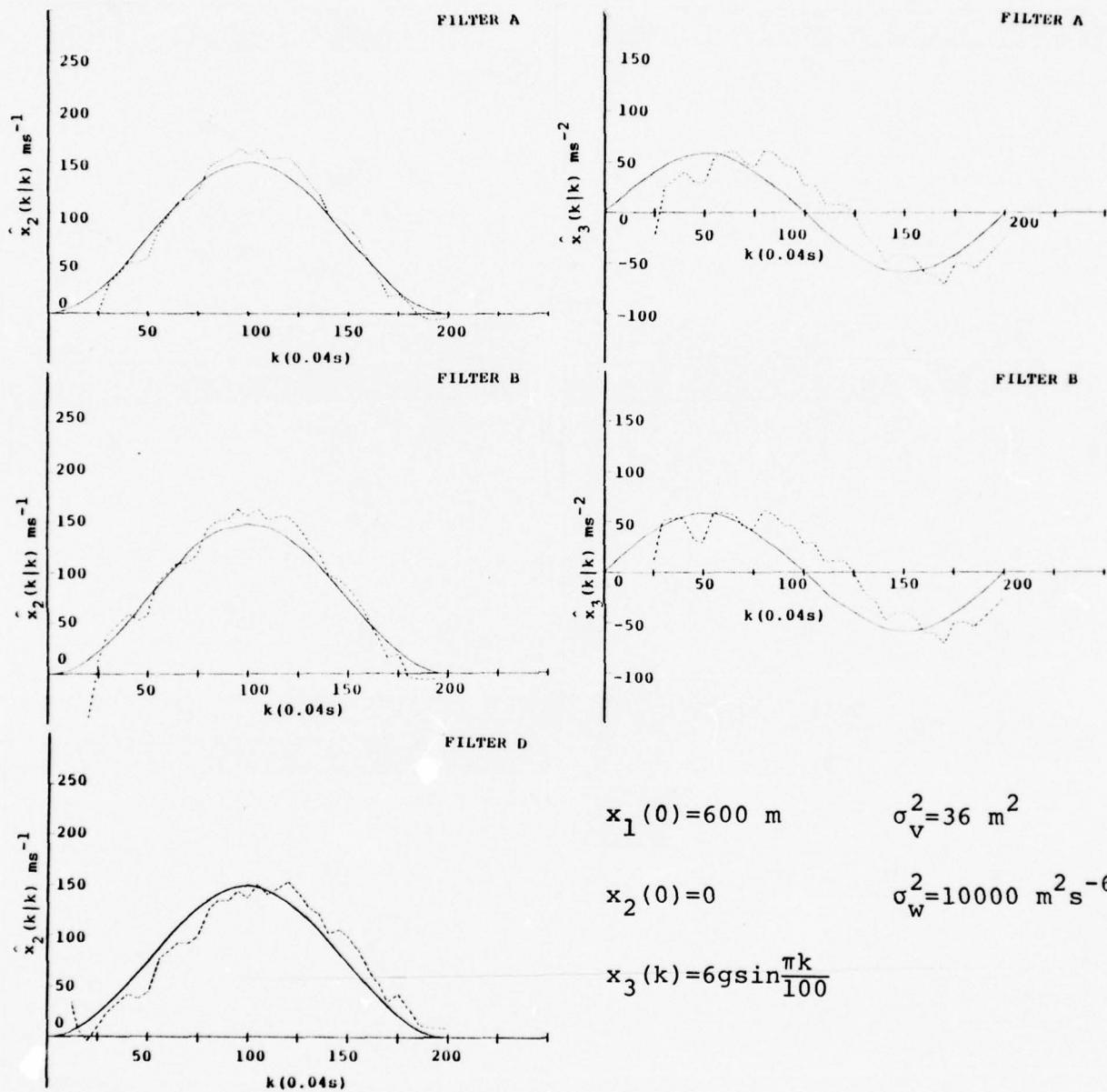


Figure A-32

APPENDIX B
PROGRAMS FOR KALMAN FILTERS

PART A - CONSTANT ACCELERATION FILTER

SECTION

PAGE NO.

DESCRIPTION

METHOD

INPUT

OUTPUT

PROGRAM LISTING

PART B - CONSTANT VELOCITY FILTER

DESCRIPTION

METHOD

INPUT

OUTPUT

PROGRAM LISTING*

*Listing is of the Straight Line Trajectory Model

DESCRIPTION

Computer program 'KALMAN' is a FORTRAN-coded range type Kalman filter. It contains the necessary equations to use one of three models; constant acceleration, sinusoidal acceleration (2G amplitude) and sinusoidal acceleration (6G amplitude). In addition, the Kalman gain may be computed in one of three ways; time varying gain (gain computed each pass as function of the filter parameter 'P'), synthetic time varying gain (gain computed each pass as function of time and input coefficients), and constant gain (gain is input).

The program computes statistics which can be used to compare range, velocity and acceleration with their estimated values.

The purpose of the model is two-fold:

- 1) To provide a means of evaluating several variations of the filter.
- 2) To enable the user to determine optimum values of some significant filter parameters

The program is not and never was intended to be the end product of the filter study.

METHOD

- (1) Calculate 'True' Values of Range, Velocity, and Acceleration (R , \dot{R} , \ddot{R}) According to One of Three Methods:

- k is an integer which takes on all values from 1 through NPTS (NPTS = duration of run/sampling rate)
- T = sampling rate, sec.

a - Constant Acceleration Model

$$R(k) = R_0 + V_0(kT) + \frac{1}{2} A(kT)^2$$

$$\dot{R}(k) = V_0 + A(kT)$$

$$\ddot{R}(k) = A$$

b - Sinusoidal Acceleration, 2G Amplitude

$$R(k) = R_0 + 24.955[(kT) - 1.27324 \sin(.031416 k)]$$

$$\dot{R}(k) = 24.955[1.0 - \cos(.031416 k)]$$

$$\ddot{R}(k) = 19.60 \sin(.031416 k)$$

c - Sinusoidal Acceleration, 6G Amplitude

$$R(k) = R_0 + 2.99466[k - 31.831 \sin(.031416 k)]$$

$$\dot{R}(k) = 74.8665[1.0 - \cos(.031416 k)]$$

$$\ddot{R}(k) = 58.8 \sin(.031416 k)$$

- (2) Generation of Gaussian Noise:

Generate 12 random numbers each having a uniform distribution between 0 and 1 (represented by RN_i)

Then the noise, $n(k) = \sigma_v \left[\sum_{i=1}^{12} RN_i - 6.0 \right]$ is a

Quasi-Gaussian random variable with zero mean and standard deviation $= \sigma_v$

- (3) The 'Measured' Value of Range is $Z(k) = R(k) + n(k)$

(4) X_1, X_2, X_3 = Estimates of R, \dot{R}, \ddot{R}

To initialize: $X_1 = Z(3)$

$$X_2 = 12.5[3.0Z(3) - 4.0Z(2) + (1)]$$

$$X_3 = 0.0$$

(5) Filter Equations

a) $P(k|k-1) = (\phi) P(k-1|k-1) (\phi^T) + S(k)$

$$\phi = \text{Constant Matrix} = \begin{vmatrix} 1 & T & T^2/2.0 \\ 0 & 1 & T \\ 0 & 0 & 1 \end{vmatrix}$$

ϕ^T = Transpose of ϕ

$$S(k) = \text{Maneuver Noise Term} = \sigma_w^2 T^2 / \sigma_v^2$$

$$\begin{vmatrix} T^4 & 3T^3 & 6T^2 \\ 3T^3 & 9T^2 & 18T \\ 6T^2 & 18T & 36.0 \end{vmatrix}$$

$$P \text{ is initialized as } \dots \sigma_v^2 \begin{vmatrix} 1 & (3/2T) & (1/T^2) \\ (3/2T) & (13/2T^2) & (6/T^3) \\ (1/T^2) & (6/T^3) & (6/T^4) + \sigma_w^2 \end{vmatrix}$$

b) Gain (Time Varying Gain)

$$\underline{K}(k) = \frac{1.0}{P_{1,1}(k|k-1) + \sigma_v^2} \begin{vmatrix} P_{1,1}(k|k-1) \\ P_{2,1}(k|k-1) \\ P_{3,1}(k|k-1) \end{vmatrix}$$

c) Estimates:

$$\hat{\underline{X}}(k|k) = (\phi) \hat{\underline{X}}(k|k-1) + \underline{K}(k) [Z(k) - (H) (\phi) \hat{\underline{X}}(k|k-1)]$$

where (H) = Row Matrix = $(1, 0, 0)$

d) $P(k|k) = [\underline{T} - \underline{K}(k)(H)] P(k|k-1)$

$$\text{where } \underline{T} = \text{Identity Matrix} = \begin{vmatrix} 1 & 0 & 0 \\ 0 & 1 & 0 \\ 0 & 0 & 1 \end{vmatrix}$$

* Note - For synthetic time varying gain and constant gain equations (a) and (d) are By-Passed for the constant gain case, K_i =input values for synthetic time varying gain, ...

$$\underline{K}_1 = \frac{C1}{k+C2} + C3; \underline{K}_2 = \frac{C4}{k^2+C5} + C6; \underline{K}_3 = \frac{C7}{k^3+C8} + C9$$

where C1, C2,---,C9 are input

(6) Statistics - The Following RMS Deviations are Calculated:

$$(\Delta X_1)_{RMS} = \sqrt{\frac{1.0}{(N2-N1+1)} \sum_{k=N1}^{N2} [R(k) - \hat{X}_1(k|k)]^2}$$

$$(\Delta X_2)_{RMS} = \sqrt{\frac{1.0}{(N2-N1+1)} \sum_{k=N1}^{N2} [\dot{R}(k) - \hat{X}_2(k|k)]^2}$$

$$(\Delta X_3)_{RMS} = \sqrt{\frac{1.0}{(N2-N1+1)} \sum_{k=N1}^{N2} [\ddot{R}(k) - \hat{X}_3(k|k)]^2}$$

N1, N2 are allowed to take on 3 sets of values, one of which is always N1=4; N2=NPTS. The other two sets are input.

PREPARATION OF INPUT CARDS

Note ... F.P.T. = Floating Point, I=Integer

CARD TYPE #1 (Mandatory)

Var.	MNEMONIC	COLS.	TYPE	DEFINITION
	IMEAS	5	I	Model Indicator: 0 = Constant Acceleration, R, \dot{R} , \ddot{R} computed 1 = Constant Acceleration, R Measurements Input 2 = Sinusoidal Acceleration, 2g Amplitude 3 = Sinusoidal Acceleration, 6g Amplitude
	IGAIN	10	I	Gain Indicator: 0 = Time Varying Gain 1 = Constant Gain 2 = Synthetic Time Varying Gain
	INTIA	11-15	I	Statistics Interval #1, First Point
	INTIB	16-20	I	Statistics Interval #1, Last Point
	INT2A	21-25	I	Statistics Interval #2, First Point
	INT2B	26-30	I	Statistics Interval #2, Last Point
T_R	TRATE	31-40	F.P.T.	Sampling Rate, Sec.
	SECS	41-50	F.P.T.	Total Time of Run, Sec. (SECS/TRATE = 250 Maximum)

CARD TYPE #2 (Mandatory)

σ_v^2	SVSQ	1-10	F.P.T.	Variance, Measurement Noise
σ_w^2	SWSQ	11-20	F.P.T.	Variance, Manuever Noise
r_o	RO	21-30	F.P.T.	Initial Range, Meters (Not required if IMEAS=1)
v_o	VO	31-40	F.P.T.	Initial Velocity, M/SEC. (Not required if IMEAS=2,3)

a	A	41-50	F.PT.	Acceleration, M/SEC ² (Not required if IMEAS=2,3)
K ₁	K ₁	51-60	F.PT.	Kalman Gain (Required for IGAIN=1 Only)
K ₂	K ₂	61-70	F.PT.	Kalman Gain (Required for IGAIN=1 Only)
K ₃	K ₃	71-80	F.PT.	Kalman Gain (Required for IGAIN=1 Only)

CARD TYPE #3 (This Card Required for Synthetic Time Varying Gain
Only --- IGAIN=2)

Var.	MNEMONIC	COLS.	TYPE	DEFINITION
C ₁	C1	1-10	F.PT.	Coefficients---See Equations On Page 3
C ₂	C2	11-20	F.PT.	
C ₃	C3	21-30	F.PT.	
C ₄	C4	31-40	F.PT.	
C ₅	C5	41-50	F.PT.	
C ₆	C6	51-60	F.PT.	
C ₇	C7	61-70	F.PT.	
C ₈	C8	71-80	F.PT.	
C ₉	C9	1-10, 2 nd CD.	F.PT.	

CARD TYPE #4 (This Card Required for IMEAS=1 Only)

Enter successive values of range measurements 8 per card,
8F10.1 Format. Use number of cards required, but number
of values must not exceed 250.

OUTPUT

The program output consists of three (3) parts:

- 1) Headings (type of run, values of input parameters, etc.). Plus the values of R , \dot{R} , \ddot{R} , \hat{X}_1 , \hat{X}_2 , \hat{X}_3 , K_1 , K_2 , K_3 at each point.
- 2) The measurement and noise at each point.
- 3) Statistics computed at three intervals, two of which are input and the last of which is for the range ($4 \rightarrow \text{NPTS}$).

BEST AVAILABLE COPY

PROGRAM KALMAN (INPUT, OUTPUT, TAPES=INPUT, TAPES=OUTPUT)

CALMAN FILE=--TIME VARYING, SYNTHETIC--TIME VARYING, OR CONSTANT GAIN

CONST ACCELERATION, RADIAL MANUEVER, OR INPUT TRAJECTORY

C=INPUT

C=IN=0, CONSTANT ACCELERATION

C=1, TRAJECTORY INPUT

C=2, 360 TURN

C=3, 36 TURN

C=4, TIME VARYING GAIN

C=5, CONSTANT GAIN

C=6, SYNTHETIC TIME VARYING GAIN

C=7, INITIAL PT, 1ST INTERVAL, STATISTICS

C=8, INITIAL PT, 1ST INTERVAL, STATISTICS

C=9, INITIAL PT, 2ND INTERVAL, STATISTICS

C=10, INITIAL PT, 2ND INTERVAL, STATISTICS

C=11, RATE SAMPLING RATE, SECONDS

C=12, TOTAL NUMBER OF SECONDS (USE 05, RATE=250 MAX)

C=13, SVS=0, MEASUREMENT NOISE

C=14, SVS=1, MEASUREMENT NOISE

C=15, INITIAL RANGE, METERS

C=16, INITIAL VELOCITY, M/SEC

C=17, ACCELERATION, M/SEC**2

C=18, GAIN (GAIN=1 ONLY)

C=19, GAIN COEFF FOR K(1) -- (IGAIN=2 ONLY)

C=20, GAIN COEFF FOR K(2) -- (IGAIN=2 ONLY)

C=21, GAIN COEFF FOR K(3) -- (IGAIN=2 ONLY)

C=22, RANGE MEASUREMENTS (IMASS=1 ONLY)

C=23, RANGE MEASUREMENTS (IMASS=1 ONLY)

C=24, RANGE MEASUREMENTS (IMASS=1 ONLY)

C=25, RANGE MEASUREMENTS (IMASS=1 ONLY)

C=26, RANGE MEASUREMENTS (IMASS=1 ONLY)

C=27, RANGE MEASUREMENTS (IMASS=1 ONLY)

C=28, RANGE MEASUREMENTS (IMASS=1 ONLY)

C=29, RANGE MEASUREMENTS (IMASS=1 ONLY)

C=30, RANGE MEASUREMENTS (IMASS=1 ONLY)

C=31, RANGE MEASUREMENTS (IMASS=1 ONLY)

C=32, RANGE MEASUREMENTS (IMASS=1 ONLY)

C=33, RANGE MEASUREMENTS (IMASS=1 ONLY)

C=34, RANGE MEASUREMENTS (IMASS=1 ONLY)

C=35, RANGE MEASUREMENTS (IMASS=1 ONLY)

C=36, RANGE MEASUREMENTS (IMASS=1 ONLY)

C=37, RANGE MEASUREMENTS (IMASS=1 ONLY)

C=38, RANGE MEASUREMENTS (IMASS=1 ONLY)

C=39, RANGE MEASUREMENTS (IMASS=1 ONLY)

C=40, RANGE MEASUREMENTS (IMASS=1 ONLY)

C=41, RANGE MEASUREMENTS (IMASS=1 ONLY)

C=42, RANGE MEASUREMENTS (IMASS=1 ONLY)

C=43, RANGE MEASUREMENTS (IMASS=1 ONLY)

C=44, RANGE MEASUREMENTS (IMASS=1 ONLY)

C=45, RANGE MEASUREMENTS (IMASS=1 ONLY)

C=46, RANGE MEASUREMENTS (IMASS=1 ONLY)

C=47, RANGE MEASUREMENTS (IMASS=1 ONLY)

C=48, RANGE MEASUREMENTS (IMASS=1 ONLY)

C=49, RANGE MEASUREMENTS (IMASS=1 ONLY)

C=50, RANGE MEASUREMENTS (IMASS=1 ONLY)

C=51, RANGE MEASUREMENTS (IMASS=1 ONLY)

C=52, RANGE MEASUREMENTS (IMASS=1 ONLY)

C=53, RANGE MEASUREMENTS (IMASS=1 ONLY)

C=54, RANGE MEASUREMENTS (IMASS=1 ONLY)

C=55, RANGE MEASUREMENTS (IMASS=1 ONLY)

C=56, RANGE MEASUREMENTS (IMASS=1 ONLY)

C=57, RANGE MEASUREMENTS (IMASS=1 ONLY)

C=58, RANGE MEASUREMENTS (IMASS=1 ONLY)

C=59, RANGE MEASUREMENTS (IMASS=1 ONLY)

C=60, RANGE MEASUREMENTS (IMASS=1 ONLY)

C=61, RANGE MEASUREMENTS (IMASS=1 ONLY)

C=62, RANGE MEASUREMENTS (IMASS=1 ONLY)

C=63, RANGE MEASUREMENTS (IMASS=1 ONLY)

C=64, RANGE MEASUREMENTS (IMASS=1 ONLY)

C=65, RANGE MEASUREMENTS (IMASS=1 ONLY)

C=66, RANGE MEASUREMENTS (IMASS=1 ONLY)

C=67, RANGE MEASUREMENTS (IMASS=1 ONLY)

C=68, RANGE MEASUREMENTS (IMASS=1 ONLY)

C=69, RANGE MEASUREMENTS (IMASS=1 ONLY)

C=70, RANGE MEASUREMENTS (IMASS=1 ONLY)

C=71, RANGE MEASUREMENTS (IMASS=1 ONLY)

C=72, RANGE MEASUREMENTS (IMASS=1 ONLY)

163

BEST AVAILABLE COPY

PAGE 4

09/19/77 18.56.43

FIN 4.5414

00751

PROGRAM KILMAN 7474

0*TEST PASS NUMBER

200 **((KX-3)+0.1)*210,220

210 X4(I)=7(I)

175 XH(2)=12.5*(THW0+7(I)*4.0*Z(2)+Z(1))

XH(3)=0.

160 IF(XH(1)-6.0)*160-10-410

P(1,1)=VSQ

150 P(2,1)=4000*VSQ/(TMO*11)

P(3,1)=VSQ/T2

P(4,1)=M(2,1)

140 P(2,2)=13.0*VSQ/(TMO*12)

P(3,2)=9.0*VSQ/T3

P(1,3)=P(3,1)

P(2,3)=P(3,2)

130 P(3,3)=9.0*VSQ/T4+VSQ

90-10-41

220 00 230 J=1,3

230 XH(3)=XH(1)

190 IF(GAIN-1)235,230,290

240 00 240 I=1,3

00 240 I=1,3

210 00 240 I=1,3

00 240 I=1,3

00 240 I=1,3

00 240 I=1,3

00 240 I=1,3

00 240 I=1,3

00 240 I=1,3

00 240 I=1,3

00 240 I=1,3

00 240 I=1,3

00 240 I=1,3

00 240 I=1,3

00 240 I=1,3

00 240 I=1,3

00 240 I=1,3

00 240 I=1,3

00 240 I=1,3

00 240 I=1,3

00 240 I=1,3

00 240 I=1,3

00 240 I=1,3

00 240 I=1,3

00 240 I=1,3

00 240 I=1,3

00 240 I=1,3

00 240 I=1,3

00 240 I=1,3

00 240 I=1,3

00 240 I=1,3

00 240 I=1,3

00 240 I=1,3

00 240 I=1,3

00 240 I=1,3

00 240 I=1,3

00 240 I=1,3

00 240 I=1,3

00 240 I=1,3

00 240 I=1,3

00 240 I=1,3

00 240 I=1,3

00 240 I=1,3

00 240 I=1,3

00 240 I=1,3

00 240 I=1,3

00 240 I=1,3

00 240 I=1,3

00 240 I=1,3

00 240 I=1,3

00 240 I=1,3

DESCRIPTION

Computer program 'CNVEL' is a FORTRAN coded range type constant velocity Kalman Filter. The program contains the necessary equations to implement one of three models (trajectories): constant accelerations, straight line, sinusoidal acceleration (2g amplitude), and a sinusoidal acceleration (6g amplitude).

The program computes statistics which can be used to compare range, velocity and acceleration with their respective estimated values.

The purpose of the program is twofold -

- 1) to provide a means of evaluating several variables of the filter,
- 2) to enable the user to determine optimum values of some significant filter parameters.

METHOD

(1) Calculate 'true' values of range velocity and acceleration (R , \dot{R} , \ddot{R}) according to one of three methods:

a. Constant acceleration, straight line trajectory

$$\begin{aligned} R_i &= X_1(k) = X_1(k-1) + TX_2(k-1) + \frac{T^2}{2} X_3(k-1) \\ \dot{R}_i &= X_2(k) = X_2(k-1) + TX_3(k-1) \\ \ddot{R}_i &= X_3(k) = \text{constant} \end{aligned}$$

b. Sinusoidal acceleration, 2g amplitude

$$\begin{aligned} R_i &= X_1(k) = 0.9982 [k - 31.831 \sin (.031416k)] + R_0 \\ \dot{R}_i &= X_2(k) = 24.955 [1.0 - \cos (.031416k)] \\ \ddot{R}_i &= X_3(k) = 19.60 \sin (.031416k) \end{aligned}$$

c. Sinusoidal acceleration, 6g amplitude

$$\begin{aligned} R_i &= X_1(k) = 2.9947 [k - 31.831 \sin (.031416k)] + R_0 \\ \dot{R}_i &= X_2(k) = 74.866 [1.0 - \cos (.031416k)] \\ \ddot{R}_i &= X_3(k) = 58.8 \sin (.031416k) \end{aligned}$$

where T = sampling rate, sec., and

k = is an integer which takes on all values 1 through NPTS

$$(NPTS = T_F - T_O) / \Delta t$$

(2) Generation of Gaussian noise:

Generate 12 random numbers each having a uniform distribution between 0 and 1 - represented by RN_i

Then - noise = $n(k) = \alpha_v \left[\sum_{i=1}^{12} RN_i - 6.0 \right]$ is a quasi-gaussian random variable with zero mean and standard deviation = α_v

(3) The range measurement is $Z(k) = R(k) + n(k)$

(4) $\hat{X}_1, \hat{X}_2, \hat{X}_3$ = estimates of R, \dot{R}, \ddot{R}

To initialize:

$$\hat{X}_1 = Z(2)$$

$$\hat{X}_2 = 25.0 [Z(2) - X(1)]$$

$$\hat{X}_3 = 0.0$$

(5) Filter Equations

a. Initialization

$$P(2/2) = 625 \sigma_v^2 \begin{vmatrix} .0016 & .04 \\ .04 & 2.0 \end{vmatrix}$$

b. Iteration

$$P(k+1|k) = \phi P(k|k) \phi' + Q'$$

where:

$$\phi = \begin{vmatrix} 1 & .04 \\ 0 & 1 \end{vmatrix}$$

$$\phi' = \begin{vmatrix} 1 & 0 \\ .04 & 1 \end{vmatrix}$$

$$Q' = \sigma_w^2 \begin{vmatrix} T^4/4 & T^3/2 \\ T^3/2 & T^2 \end{vmatrix}$$

$$K(k+1) = \frac{1}{P_{11}(k+1|k) + \sigma_v^2} \begin{bmatrix} P_{11}(k+1|k) \\ P_{21}(k+1|k) \end{bmatrix}$$

$$\hat{X}(k+1|k+1) = \phi \hat{X}(k|k) + K(k+1) Z(k+1) - (1.04) \hat{X}(k|k)$$

$$P(k+1|k+1) = \begin{bmatrix} 1-K_1(k+1) & 0 \\ -K_2(k+1) & 1 \end{bmatrix} P(k+1|k)$$

The following RMS deviations are computed:

$$(\Delta X_1)_{\text{RMS}} = \sqrt{\frac{1.0}{(N2-N1+1)} \sum_{k=N1}^{N2} \left[R(k) - \hat{X}_1(k|k) \right]^2}$$

$$(\Delta X_2)_{\text{RMS}} = \sqrt{\frac{1.0}{(N2-N1+1)} \sum_{k=N1}^{N2} \left[\dot{R}(k) - \hat{X}_2(k|k) \right]^2}$$

where $N1 \neq N2$ = initial and final indices of the points to be utilized in the computations of statistics

INPUT PREPARATION

CARD TYPE #1

VARIABLE	COLS.	TYPE	DEFINITION
R_o	1-10	F.Pt.	Initial range, meters
\dot{R}_o	11-20	F.Pt.	Initial velocity, meters/sec
\ddot{R}_o	21-30	F.Pt.	Initial acceleration, m/sec ²
T_o	31-40	F.Pt.	Initial time, sec
T_F	41-50	F.Pt.	Final time, sec
Δ_t	51-60	F.Pt.	Time increment, sec

CARD TYPE #2

σ_w^2	1-10	F.Pt.	Variance, maneuver noise
σ_v^2	11-20	F.Pt.	Variance, measurement noise
NEND	21-25	Int.	Value of index of highest point to be printed

CARD TYPE #3

NOST	1-5	Int.	Number of sets of statistics to be computed (3 in most cases)
------	-----	------	---

CARD TYPE #4 (1 card per statistics set)

NST	1-5	Int.	Initial and final 'K' indices of points to be used in
NFN	6-10	Int.	computation of statistics set

OUTPUT

- (1) Input values of R_o , R_o , R_o , σ_v^2 , σ_w^2
- (2) Iterative output at each 'k'
 k , $R(k)$, $\dot{R}(k)$, $\ddot{R}(k)$, $\hat{x}_1(k)$, $\hat{x}_2(k)$, $\hat{x}_3(k)$,
 xkA , xkB (Kalman gain constants),
 $z(k)$ = measurement of range
 $xN(k)$ = noise
- (3) Statistics: RMS deviations for position and velocity

```

PROGRAM CHVEL,TEMPUT,OUTTOTL,K,RDTS=1000,F,PAPRPA=2000,FOUTI,
EXTENSION R(300),RB(300),ROB(300),Z(300),XA(300),XB(300),
1TT(300),XM(300)
DATA JJ//1111111117776/
TTF=0.1
DO N=0.0
CIV=TIME(TTI)
ICAND(TTD,JJ)
1 READ(5,2)KOD,RODD,RO,TF,DELT
2 FORCAT(810.0)
ICUK=EOF(5)
IF (ICUK.NE.0) GO TO ZOOO
READ(5,401)ALF,BET,MEND
301 FORMAT(2F10.0,15)
GO TO 1
IF (ALF.LT.-.5)
IX=3468714927
XX=FLOAT(IX)
CALL KANDET(XX)
WRITE(6,11)
11 WRITE(6,11) RO,ZOD,RODD,ALF,BET
140FORMAT(3H R=E13.6,6H V=E13.6,6H A=E13.6,
111H SIGVSO,E13.6,11H SIGVSO,E13.6)
SN=(TF-TO)/DELT
N=SN+1.0
IF (M.GT. 300) M=300
IF (M.LT. MEND) GO TO 400
DO 3 I=1,M
XI=XI*DELT
T=T+DELT
RD(I)=RODD
RD(I)=RODD*(T-TO)+ROD
R(I)=RO+RODD*(T-TO)+0.5*RODD*(T-TO)*2
RNROT=0.0
DO 6 J=1,12
RN=RANF(DUM)
RNROT=RNROT+RN
6 CONTINUE
RNROT=6.*0*(RNROT-6..0)
XN(I)=RNROT
Z(JA,I)=R(I)*ZN(I)
3 CONTINUE
PA=DEF
PB=25.0*BET
PC=25.0*BET
PD=1250.0*BET
XA(1)=Z(1)
XA(2)=Z(1)
XB(1)=0.0
XB(2)=0.0
ZB(2)=(Z(2)-Z(1))/DELT
X=N-1
WRITE(6,12)
120FORMAT(3H EK,12X,10H,12X,10H,11X,4H Z(1),9X,4HX(2),3X,
15HX(1),3X,5HX(2),10X,10H2,10X,SINNOISE)
XKA=0.0
XKB=0.0
DO 4 K=1,N
IF (K.EQ.1) GO TO 25
WRITE(6,13)K,XB(K),RO(K),XA(K),XKA,XKB,Z(K),XN(N)
13 FORMAT(5X,13,5X,E13.6)
25 CONTINUE
IP(K,EQ.1) GO TO 4
QA=PA+0.04*PB+0.04*PC+0.01*PD+0.000000664*ALP
QB=PB+0.04*PD+0.000012*ALP
QC=PC+0.04*PD+0.000012*ALP
QD=PD+0.0016*ALP
XKA=QA/(QA+BET)
XKB=QB/(QA+BET)
L=K+1
XA(L)=XA(K)+0.04*XB(K)+XKA*Z(L)-XKA*(XA(K)+0.04*XB(K))
XB(L)=XB(K)+XKB*Z(L)-XKB*(XA(K)+0.04*XB(K))
PA=(1.0-XKA)*QA
PB=(1.0-XKA)*QB
PC=YAB*QA*QC
PD=-XKB*QB+QD
4 CONTINUE
HEAD(5,49) HOUT
FORNAT(15)
DO 41 K=1,NOST

```



```

      READ(5,42)NST,NFN
42  FORMAT(2I5)
      RMR=C.0
      DEN=NFN-NST+1
      DO 43 J=NST,NFN,1
      RMR=(R(J)-XA(J))*2/DEN+RMR
      RMV=(RD(J)-XB(J))*2/DEN+RMV
43  CONTINUE
      RMR=SORT(RMR)
      RMV=SORT(RMV)
      WRITE(6,44) K,RMR,RMV,NST,NFN
44  FORMAT(11H STAT. SET ,I5,6H POS RM5,E13.6,6H VEL RM3,E13.6,
14H K=,I5,3H TO,I5)
41  CONTINUE
      GO TO 400
2000 WRITE(6,2001)
2001 FORMAT(18H NORMAL COMPLETION )
      STOP
      END

```

APPENDIX C
PROGRAM FOR TARGET STATE MEASUREMENT

The attached documentation pertains to the program 'ERRORV' (velocity). The decks for two additional programs; 'ERROR' (acceleration) and 'ERRORR' (range) are also attached. The three programs are very similar. The following is a list of the distributions utilized in each of the three programs -

PROGRAM	VARIABLES	TYPE	DISTRIBUTION
'ERRORV'	v_t, v_a	uniform	range: 200, 600 KTS
	v_t & v_a errors	normal	$\sigma = 4.0$ KTS, $\bar{x}=0$
	α_t, α_a	uniform	range: $-5^\circ, +20^\circ$
	α_t & α_a errors	normal	$\sigma = 0.1^\circ, \bar{x}=0$
	roll angle(ϕ)	uniform	range: $-90^\circ, -60^\circ$ & $+60^\circ, +90^\circ$
	pitch angle(θ)	uniform	range: $-30^\circ, +45^\circ$ (75%) $-90^\circ, -30^\circ$ (12.5%) $+45^\circ, +90^\circ$ (12.5%)
	yaw angle(ψ)	uniform	range: $-180^\circ, +180^\circ$
	sine, cosine errors	normal	$\alpha = 0.005, \bar{x}=0$
	at_x, aa_x	uniform	$\sigma = 32.16, \bar{x}=0$
	at_y, aa_y	uniform	$\sigma = 8.0, \bar{x}=0$
'ERROR'	a-comp errors	normal	pdf= $-8.0+4e^{(x/2)}$ where x =normal dist, $\sigma=1.0$ & $\bar{x}=0$
	ϕ, θ, ψ	(same as above)	
	sine, cosine errors	(same as above)	
	ε, η	uniform	range: $-15^\circ, +15^\circ$
	ε, η errors	normal	$\sigma = .0691^\circ, \bar{x}=0$
'ERRORR'	range	uniform	range: 0, 2500 ft.
	range error	normal	$\sigma = 4.0$ ft., $\bar{x}=0$

COMPUTER PROGRAM 'ERRORV' CONTAINS THE
MONTE CARLO CALCULATION OF THE ERROR
DISTRIBUTION OF THE VELOCITY OF THE
TARGET RELATIVE TO THE ATTACKER IN THE
ATTACKERS BODY FRAME OF REFERENCE.

Page 2	Description of Input/Output
Pages 3, 4, 5	Explanation of program cross-referenced to line numbers on compilation listing
Pages 6,7,8	Purpose and method used in each subroutine

The Program Requires 56000 Words (Octal)
of Storage on the CDC 6600.

INPUT

Variable	Card Cols.	Type	Definition
XX	1-10	Floating Point	Seed for Random Number Generator
NPASS	11-15	Interger	No. of Passes

OUTPUT

The Output Consists of Four Columns of Data.

Col 1	$(V_x' - V_x)$	}	Primed values include error terms, unprimed values = No Error Terms
2	$(V_y' - V_y)$		
3	$(V_z' - V_z)$		
4	$(V_{tot}' - V_{tot})$		

LINE NOS.COMMENTS

7-11 Define Constants
12 READ: Seed for random number generator
and number of passes
15 Test for end of file on Input Tape 5
16-18 If last case has been processed, print
'NORMAL TERMINATION' and stop-if another
case is to be processed, proceed to
statement No. 30
20-21 Print Input Values
23 Initialize Random Number Generator
25 Start Main Execution Loop
27-29 Select airspeeds v_t & v_a from a uniform
distribution having the range 200-600 KTS
31-33 Select airspeed errors from a normal
distribution having a $\sigma=4.0$ KTS and a
MEAN=0
35-37 Select angles of attack α_t & α_a from a
uniform distribution having a range
-5° to +20° (convert to radians)
39-41 Select angle of attack errors from a
normal distribution having a $\sigma=0.1^\circ$
and MEAN=0. (Convert to radians)
43-48 Compute airspeed components, target
and attacker
$$\begin{pmatrix} v_{tx} \\ v_{ty} \\ v_{tz} \end{pmatrix} = \begin{pmatrix} \cos \alpha_t \\ 0 \\ \sin \alpha_t \end{pmatrix} v_t \quad \begin{pmatrix} v_{ax} \\ v_{ay} \\ v_{az} \end{pmatrix} \quad \begin{pmatrix} \cos \alpha_a \\ 0 \\ \sin \alpha_a \end{pmatrix} v_a$$

50-52 Select yaw angles from a uniform distri-
bution with the range -180° to 180°
(convert to radians)
53-59 Select roll angles from a uniform distri-
bution with the range =90° to -60° and
+60° to +90° (convert to radians)

<u>LINE NOS.</u>	<u>COMMENTS</u>												
60-71	Select pitch angles from uniform distribution with the range: -90° to +90° where												
	<table border="0"> <tr> <td>-90° to -30°</td> <td>Occurs</td> <td>12 1/2 %</td> <td>of the time</td> </tr> <tr> <td>-30° to +45°</td> <td>"</td> <td>75%</td> <td>" " "</td> </tr> <tr> <td>+45° to +90°</td> <td>"</td> <td>12 1/2%</td> <td>" " "</td> </tr> </table>	-90° to -30°	Occurs	12 1/2 %	of the time	-30° to +45°	"	75%	" " "	+45° to +90°	"	12 1/2%	" " "
-90° to -30°	Occurs	12 1/2 %	of the time										
-30° to +45°	"	75%	" " "										
+45° to +90°	"	12 1/2%	" " "										
	(convert to radians)												
73-80	Select sine & cosine errors from a normal distribution with $\sigma = .005$, MEAN=0.												
82-84	Set-up 'Y' matrix terms												
85	Compute elements of 'Y' matrix												
91	Solve matrix equation, no error terms----												
93-95	Set-up 'Y' matrix terms (errors included)												
96	Compute elements of 'Y' matrix												
97-99	Set-up 'X' matrix terms (error included)												
100	Compute elements of 'X' matrix												
101-110	Add error terms:												
	$\begin{aligned} v_t' &= v_t + \epsilon & ; & & v_a' &= v_a + \epsilon \\ \alpha_t' &= \alpha_t + \epsilon & & & \alpha_a' &= \alpha_a + \epsilon \\ v_{tx}' &= \cos \alpha_t' v_t' & , & & v_{ax}' &= \cos \alpha_a' v_a' \\ v_{ty}' &= 0 & , & & v_{ay}' &= 0 \\ v_{tz}' &= \sin \alpha_t' v_t' & , & & v_{az}' &= \sin \alpha_a' v_a' \end{aligned}$												
112	Solve matrix equation (with error terms)---												
	$V_v' = [X'] [Y'] [v_t'] - [v_a']$												
114-115	Difference velocity components ($v_v' - v_v$)												
116	Compute total velocity difference from sum of squares												
117-119	Store ($v_{vx}' - v_{vx}$) , ($v_{vy}' - v_{vy}$) , ($v_{vz}' - v_{vz}$) and ($v_{vtot}' - v_{vtot}$) in output array												
120	End Main Execution Loop												
122-125	Print Output												
126	Return to statement No. 1 for next case												

SUBROUTINE 'RANDOM'

Purpose: To compute 'NRN' random numbers from either a uniform or normal distribution. Subroutine 'RANF' is utilized to generate a uniformly distributed random number (0 → 1)

IDIST=0 Uniform Distribution
C1 = Additive Term (To Scale Range)
C2 = Multiplier Term (To Scale Range)

IDIST=1 Normal Distribution
C1 = σ = STD Deviation
C2 = \bar{X} = Mean

Method:

a) Uniform Distribution

Start Loop 'A'
i=1, NRN
↓
RN=RANF(DUM)
↓
RNS_i = (RN+C1) C2
↓
End Loop 'A'

b) Normal Distribution

Start Loop 'B'
i=1, NRN
↓
RNTOT=0
↓
Start Loop 'C'
j=1, 12
↓
RN=RANF(DUM)
↓
RNTOT=RNTOT+RN
↓
End Loop 'C'
180
↓
RNS_i = C1 (RNTOT=6.0) + C2
↓
End Loop 'B'

SUBROUTINE 'ELEM'

Purpose: To compute matrix elements in one of two ways specified by 'N'

Method: N=0

```
x(1,1) = cos(ψ) cos(θ)
x(2,1) = -sin(ψ) cos(φ) + cos(ψ) sin(θ) sin(φ)
x(3,1) = sin(ψ) sin(φ) + cos(ψ) sin(θ) cos(φ)
x(1,2) = sin(ψ) cos(θ)
x(2,2) = cos(ψ) cos(φ) + sin(ψ) sin(θ) sin(φ)
x(3,2) = -cos(ψ) sin(φ) + sin(ψ) sin(θ) cos(φ)
x(1,3) = -sin(θ)
x(2,3) = cos(θ) sin(φ)
x(3,3) = cos(θ) cos(φ)
```

N=1

```
x(1,1) = cos(ψ) cos(θ)
x(2,1) = sin(ψ) cos(θ)
x(3,1) = -sin(θ)
x(1,2) = -sin(ψ) cos(φ) + cos(ψ) sin(θ) sin(φ)
x(2,2) = cos(ψ) cos(φ) + sin(ψ) sin(θ) sin(φ)
z(3,2) = cos(θ) sin(φ)
x(1,3) = sin(ψ) sin(φ) + cos(ψ) sin(θ) cos(φ)
x(2,3) = -cos(ψ) sin(φ) + sin(ψ) sin(θ) cos(φ)
x(3,3) = cos(θ) cos(φ)
```


SUBROUTINE 'SOLVE'

Purpose: Given the matrices X, Y, AT, AA--Solve
for A:

$$A = X*Y*AT-AA \quad \text{Where}$$

$$\begin{aligned} X &= 3 \times 3 \\ Y &= 3 \times 3 \\ AT &= 3 \times 1 \\ AA &= 3 \times 1 \end{aligned}$$

Method:

$$\left. \begin{aligned} \text{a) } C_i &= Y_{i,1} AT_1 + Y_{i,2} AT_2 + Y_{i,3} AT_3 & (i=1,3) \\ \text{b) } D_i &= X_{i,1} C_1 + X_{i,2} C_2 + X_{i,3} C_3 & (i=1,3) \\ \text{c) } A_i &= D_i - AA_i & (i=1,3) \end{aligned} \right\}$$

10/20/77 18.06.39

FTN 4.5+14

PROGRAM ERRORV 74/74 CPI=1

```

1  PROGRAM ERRORV(INPUT,OUTPUT,TAF5=INPUT,TAF6=OUTPUT)
   COMMON RNS(10),DUM
   DIMENSION VELT(3),VELA(3),ANGT(3),XANG(2),ESA(3),ECA(3),
1  EST(3),EOT(3),T(6),S(6),VV(3),WVE(3),ADIF(3),ADUT(306,4),
2  X(3,3),Y(3,3)
   C*
   DUM=0.
   RAD=0.017453293
   G=32.16
10  X1=0.14285714
   X2=0.89285714
   READ(5,1) XX,NPASS
10  FORMAT(F10.1,I5)
   C*TEST END OF FILE
15  IF(EOT(5).EQ.0)GO TO 30
   WRITE(6,20)
20  FORMAT(11H//10X,24H**NORMAL TERMINATION***)
   STOP
   C*PRINT INPUT
21  30 WRITE(6,10)XX,NPASS
   40 FORMAT(11H//5X,12HSEED FOR RNS=E13.6,5X,13HNU OF PASSES=,I5)
   C*INITIALIZE
   C*MAIN EXECUTION LOOP
25  DO 500 K=1,NPASS
   C*SELECT AIRSPEEDS
   CALL RANDOM(0,2,0.5,400.)
   VT=RNS(1)
   VA=RNS(2)
30  C*SELECT AIRSPEED ERRORS
   CALL RANDOM(1,2,4.0,0.)
   VTE=RNS(1)
   VAE=RNS(2)
   C*SELECT ANGLES OF ATTACK
   CALL RANDOM(0,2,-0.2,25.0)
   ALPT=RNS(1)*RAD
   ALPA=RNS(2)*RAD
   C*SELECT ANG OF ATTCK ERRORS
40  CALL RANDOM(1,2,4.1,0.)
   ALPTE=RNS(1)*RAD
   ALPAE=RNS(2)*RAD
   C*COMPUTE V-COMPS
   VELT(1)=COS(ALPT)*VT
   VELT(2)=0.0
   VELT(3)=SIN(ALPT)*VT
   VELA(1)=COS(ALPA)*VA
   VELA(2)=0.0
   VELA(3)=SIN(ALPA)*VA
   C*SELECT FOLLOW PITCH,YAW
50  CALL RANDOM(0,2,-0.5,360.)
   ANGT(3)=RNS(1)*RAD
   ANGA(3)=RNS(2)*RAD
   CALL RANDOM(0,2,-0.5,1.)
   DO 65 L=1,2
   XS=1.0
   IF(RNS(L).LT.0.) XS=-1.0
65  XANG(L)=60.*(RNS(L)+XS)

```

10/20/77 14.00.39

FTN 4.5*414

PROGRAM ERKCRV 74/74. OPI=1

```

60  ANG(1)=XANG(1)*RAD
    ANGA(1)=XANG(2)*RAD
    CALL RANDOM(0,2,0.1.)
    DO 69 I=1,2
    IF (RNS(I).LT.X1) GO TO 67
    IF (RNS(I).GE.X2) GO TO 69
    XANG(I)=100.*(RNS(I)-X1)-30.0
    GO TO 69
65  XANG(I)=60.0*RNS(I)/X1-90.0
    GO TO 69
67  XANG(I)=45.0*(RNS(I)-X2)/0.10714286+45.0
    GO TO 69
68  XANG(I)=45.0*(RNS(I)-X2)/0.10714286+45.0
69  CONTINUE
70  ANG(2)=XANG(1)*RAD
    ANGA(2)=XANG(2)*RAD
    C*SELECT ERRORS--SIN,COS
    CALL RANDOM(1,6,0.005,0.)
    DO 70 I=1,3
    ESA(I)=RNS(I)
70  ECA(I)=RNS(I+3)
    CALL RANDOM(1,6,0.005,0.)
    DO 80 I=1,3
    EST(I)=RNS(I)
    ECT(I)=RNS(I+3)
80  C*SET-UP MATRIX--NO ERROR
    DO 100 I=1,3
    T(I)=COS(ANG(I))
    Y(I+3)=SIN(ANG(I))
85  CALL ELEM(T,Y,1)
    DO 110 I=1,3
    K(I)=COS(ANGA(I))
    R(I+3)=SIN(ANGA(I))
    CALL ELEM(R,X,0)
90  C*SOLVE MATRIX EQUATION--NO ERROR
    CALL SOLVE(X,Y,VELT,VELA,VV)
    C*SET-UP MATRIX--ERROR TERMS
    DO 120 I=1,3
    T(I)=T(I)+ECT(I)
    Y(I+3)=Y(I+3)+EST(I)
95  CALL ELEM(T,Y,1)
    DO 130 I=1,3
    R(I)=R(I)+ECA(I)
    F(I+3)=R(I+3)+ESA(I)
    CALL ELEM(R,X,0)
    VT=VT+VTE
    VA=VA+VAE
    ALPT=ALPT+ALPTE
    ALPA=ALPA+ALPAE
    VELT(1)=COS(ALPT)*VT
    VELT(2)=0.0
    VELT(3)=SIN(ALPT)*VT
    VELA(1)=COS(ALPA)*VA
    VELA(2)=0.0
    VELA(3)=SIN(ALPA)*VA
100  C*SOLVE MATRIX EQUATION--ERROR TERMS
    CALL SOLVE(X,Y,VELT,VELA,VVE)
    C*DIFFERENCE
    DO 150 I=1,3

```

```
115      150  A0IF(I)=VVE(I)-VV(I)
          ASUM=SUM(A0IF(I)+A0IF(1)+A0IF(2)+A0IF(3)+A0IF(3))
          DO 170 I=1,3
            170  AOUT(K,I)=A0IF(I)
            AOUT(K,4)=ASUM
          500  CONTINUE
          C*
          WRITE(6,600)
          600  FORMAT(1H1//5X,26HX-COMP,Y-COMP,Z-COMP,TOTAL/)
          WRITE(6,610) (AOUT(K,I),I=1,4),K=1,NPASS)
          610  FORMAT(5X,4E16.7)
          GO TO 1
          END
```

FTN 4.5+414

1 SUBROUTINE ELEM(TA,X,N)

C*COMPUTE MATRIX ELEMENTS

C*INPUT*****

C*TA(1)=COS(PHI)

C*TA(2)=COS(THETA)

C*TA(3)=COS(PSI)

C*TA(4)=SIN(PHI)

C*TA(5)=SIN(THETA)

C*TA(6)=SIN(PSI)

C*****

10 DIMENSION TA(5),X(3,3)

IF(N.EQ.1)GO TO 10

C*

X(1,1)=TA(3)*TA(2)

X(2,1)=-TA(6)*TA(1)+TA(3)*TA(5)*TA(4)

X(3,1)=TA(6)*TA(4)+TA(3)*TA(5)*TA(1)

X(1,2)=TA(6)*TA(2)

X(2,2)=TA(3)*TA(1)+TA(6)*TA(5)*TA(4)

X(3,2)=-TA(3)*TA(4)+TA(6)*TA(5)*TA(1)

X(1,3)=-TA(5)

X(2,3)=TA(2)*TA(4)

X(3,3)=TA(2)*TA(1)

GO TO 100

C*

10 X(1,1)=TA(3)*TA(2)

X(2,1)=TA(6)*TA(2)

X(3,1)=-TA(5)

X(1,2)=-TA(6)*TA(1)+TA(3)*TA(5)*TA(4)

X(2,2)=TA(3)*TA(1)+TA(6)*TA(5)*TA(4)

X(3,2)=TA(2)*TA(4)

X(1,3)=TA(6)*TA(4)+TA(3)*TA(5)*TA(1)

X(2,3)=-TA(3)*TA(4)+TA(6)*TA(5)*TA(1)

X(3,3)=TA(2)*TA(1)

100 RETURN

END

35

186

10/20/77 10.06.39

FTN 4.5+414

SUBROUTINE RANDOM 74/74 GPI=1

```

1      SUBROUTINE RANDOM(I0IST,NRN,C1,C2)
      C** INPUT*****
      C* NRN=NO. OF RN'S TO BE GENERATED*****
      C* IF UNIFORM DISTRIBUTION---
      5      C* I0IST=0
      C* C1=ADDITIVE TERM
      C* C2=MULTIPLIER TERM
      C* IF NORMAL DISTRIBUTION ---
      10     C* I0IST=1
      C* C1=STD DEV OF DISTRIBUTION
      C* C2=MEAN OF DISTRIBUTION
      C*****
      COMMON RNS(10),DUM
      C*TEST DISTRIBUTION TYPE
      IF(I0IST.EQ.1)GO TO 50
      C*UNIFORM DIST
      DO 20 I=1,NRN
      RN=RANF(DUM)
      RNS(I)=(RN+C1)*C2
      20   GO TO 100
      C*NORMAL DIST
      30   DO 70 I=1,NRN
      RNTOT=0.
      DO 60 J=1,12
      RN=RANF(DUM)
      60   RNTOT=RNTOT+RN
      RNS(I)=C1*(RNTOT-6.0)+C2
      70   CONTINUE
      100  RETURN
      30   END

```


10/20/77 14.06.39

FTN 4.5+414

OPT=1

74/74

SUBROUTINE SOLVE

```
1      SUBROUTINE SOLVE (X,Y,AT,AA,A)
      C*TO SOLVE THE MATRIX EQUATION:
      C*      A(3)=X(3,3)*Y(3,3)+AT(3)-AA(3)
      C*
      DIMENSION X(3,3),Y(3,3),AT(3),AA(3),C(3),D(3)
      C*
      DO 10 I=1,3
      10  C(I)=Y(I,1)*AT(1)+Y(I,2)*AT(2)+Y(I,3)*AT(3)
      DO 20 I=1,3
      20  D(I)=X(I,1)*C(1)+X(I,2)*C(2)+X(I,3)*C(3)
      DO 30 I=1,3
      30  A(I)=D(I)-AA(I)
      C*
      RETURN
      END
```

15

APPENDIX D

RADAR LAG PROGRAM

The SDATA program requires two cards of input for each pass which is to be analyzed. The first data card contains the following input which directs the reading of the Sight Eval tape being used.

F10.1 - XMISN - The mission number
I10 - IPAS - The pass to be analyzed from the above mission
I10 - ITME - That time during the pass at which computations are to begin (msec)
I10 - NPTS - The number of data time intervals over which SDATA is to perform computations

Twenty-five Sight Eval data arrays are required as input to SDATA. Each of these arrays is smoothed by SDATA. The number of points to be used in each smooth must be specified. This is read in on the second data card.

25I2 - NFIT(I), I=1,25 - The number of points to be used in smoothing each of the 25 Sight Eval variable arrays input to SDATA.

BEST AVAILABLE COPY

PROGRAM DATA	74/7-	OP1=1	FTS 11-11-11	11/ 5/77	11-12-57	PAGE	1
1	1	1	1	1	1	1	1
2	2	2	2	2	2	2	2
3	3	3	3	3	3	3	3
4	4	4	4	4	4	4	4
5	5	5	5	5	5	5	5
6	6	6	6	6	6	6	6
7	7	7	7	7	7	7	7
8	8	8	8	8	8	8	8
9	9	9	9	9	9	9	9
10	10	10	10	10	10	10	10
11	11	11	11	11	11	11	11
12	12	12	12	12	12	12	12
13	13	13	13	13	13	13	13
14	14	14	14	14	14	14	14
15	15	15	15	15	15	15	15
16	16	16	16	16	16	16	16
17	17	17	17	17	17	17	17
18	18	18	18	18	18	18	18
19	19	19	19	19	19	19	19
20	20	20	20	20	20	20	20
21	21	21	21	21	21	21	21
22	22	22	22	22	22	22	22
23	23	23	23	23	23	23	23
24	24	24	24	24	24	24	24
25	25	25	25	25	25	25	25
26	26	26	26	26	26	26	26
27	27	27	27	27	27	27	27
28	28	28	28	28	28	28	28
29	29	29	29	29	29	29	29
30	30	30	30	30	30	30	30
31	31	31	31	31	31	31	31
32	32	32	32	32	32	32	32
33	33	33	33	33	33	33	33
34	34	34	34	34	34	34	34
35	35	35	35	35	35	35	35
36	36	36	36	36	36	36	36
37	37	37	37	37	37	37	37
38	38	38	38	38	38	38	38
39	39	39	39	39	39	39	39
40	40	40	40	40	40	40	40
41	41	41	41	41	41	41	41
42	42	42	42	42	42	42	42
43	43	43	43	43	43	43	43
44	44	44	44	44	44	44	44
45	45	45	45	45	45	45	45
46	46	46	46	46	46	46	46
47	47	47	47	47	47	47	47
48	48	48	48	48	48	48	48
49	49	49	49	49	49	49	49
50	50	50	50	50	50	50	50
51	51	51	51	51	51	51	51
52	52	52	52	52	52	52	52
53	53	53	53	53	53	53	53
54	54	54	54	54	54	54	54
55	55	55	55	55	55	55	55
56	56	56	56	56	56	56	56
57	57	57	57	57	57	57	57
58	58	58	58	58	58	58	58
59	59	59	59	59	59	59	59
60	60	60	60	60	60	60	60
61	61	61	61	61	61	61	61
62	62	62	62	62	62	62	62
63	63	63	63	63	63	63	63
64	64	64	64	64	64	64	64
65	65	65	65	65	65	65	65
66	66	66	66	66	66	66	66
67	67	67	67	67	67	67	67
68	68	68	68	68	68	68	68
69	69	69	69	69	69	69	69
70	70	70	70	70	70	70	70
71	71	71	71	71	71	71	71
72	72	72	72	72	72	72	72
73	73	73	73	73	73	73	73
74	74	74	74	74	74	74	74
75	75	75	75	75	75	75	75
76	76	76	76	76	76	76	76
77	77	77	77	77	77	77	77
78	78	78	78	78	78	78	78
79	79	79	79	79	79	79	79
80	80	80	80	80	80	80	80
81	81	81	81	81	81	81	81
82	82	82	82	82	82	82	82
83	83	83	83	83	83	83	83
84	84	84	84	84	84	84	84
85	85	85	85	85	85	85	85
86	86	86	86	86	86	86	86
87	87	87	87	87	87	87	87
88	88	88	88	88	88	88	88
89	89	89	89	89	89	89	89
90	90	90	90	90	90	90	90
91	91	91	91	91	91	91	91
92	92	92	92	92	92	92	92
93	93	93	93	93	93	93	93
94	94	94	94	94	94	94	94
95	95	95	95	95	95	95	95
96	96	96	96	96	96	96	96
97	97	97	97	97	97	97	97
98	98	98	98	98	98	98	98
99	99	99	99	99	99	99	99
100	100	100	100	100	100	100	100

PROGRAM DATA	7470	OP1=1	FTN 4.54-14	11/05/77	10.12.37	PAGE	3
115	IFLAG=			ORIG	115		
	IFIXMIN=0.0,XHDF)IFLAG=1			ORIG	117		
	GO TO 117			ORIG	118		
	CAPACITY ERROR			ORIG	119		
120	IFIXFLG=0.2160 TO 130			ORIG	120		
				ORIG	121		
	185 WRITE(6,IN)			ORIG	122		
	187 FORMAT(//1X,20CAPACITY ERROR IGNORED)			ORIG	123		
	GO TO 10			ORIG	124		
125				ORIG	125		
	190 IFIXOF=0.0,OP'SIG TO 180			ORIG	125		
	NOI=NOI+1			ORIG	127		
	GO TO 100			ORIG	128		
				ORIG	129		
	END			ORIG	130		

192

BEST AVAILABLE COPY

BEST AVAILABLE COPY

BEST AVAILABLE COPY


```

      CALL TRANS (FA,FB,FC,ED,PSI,PCH,FOLI)
      ENP=DEL*DEL
      X=X+XD*DEL+0.5*XDD*TEMP
      Y=Y+YD*DEL+0.5*YDD*TEMP
      Z=Z+ZD*DEL+0.5*ZDD*TEMP
      XD=XD+XDD*DEL
      YD=YD+YDD*DEL
      ZD=ZD+ZDD*DEL
      UA=A(19,I)
      VA=A(20,I)
      WA=A(21,I)
      VDD=SD*TXD+XDD+YDD+ZDD
      CALL B*OT (UA,VA,WA,XDD,YDD,ZDD)
      ZDD=ZDD+G
      QD=SD*TXD+XDD+YDD+ZDD
      TX=QA(1,I)
      TD=QA(2,I)
      RA=QA(3,I)
      ED=QA(4,I)
      RE=QA(5,I)
      RD=QA(6,I)
      FA=QA(7,I)
      FC=QA(8,I)
      FE=QA(9,I)
      FE=QA(10,I)
      TEMP=COS(PE)
      PTJ=TX*TEMP+COS(FA)
      TJ=TX*TEMP+SIN(PE)
      TK=RA*SIN(PE)
      CALL B*OT (PTJ,PTK,PTX,PTY,PTZ)
      TPX=PTX+TX
      PTY=PTY+TY
      PTZ=PTZ+TZ
      TEN1=COS(FA)
      TEN2=SIN(FA)
      TEN3=SIN(PE)
      TVJM=RTAU+TEMP+T.M1-FTG+TEMP*(EM2*FAJ-RTJ+TEM3+T.M1-RE)
  
```

BEST AVAILABLE COPY

[illegible]

BEST AVAILABLE COPY

[illegible]

BEST AVAILABLE COPY

[illegible]

BEST AVAILABLE COPY

SUBROUTINE NAME	74/74	CP1=1	F*H 4.54.14	11/05/77	1.12.37	PAGE	1
SUBROUTINE X103							
COMMON/ITERATE(3,3)							
V1=1+(1,1)*XIN+1+(2,1)*V1+1+(3,1)*7 N							
V2=1+(1,2)*XIN+1+(2,2)*V1+1+(3,2)*7 N							
V3=1+(1,3)*XIN+1+(2,3)*V1+1+(3,3)*7 N							
END							
END							

SUBROUTINE NAME	74/74	CP1=1	F*H 4.54.14	11/05/77	1.12.37	PAGE	1
SUBROUTINE X103							
COMMON/ITERATE(3,3)							
V1=1+(1,1)*XIN+1+(2,1)*V1+1+(3,1)*7 N							
V2=1+(1,2)*XIN+1+(2,2)*V1+1+(3,2)*7 N							
V3=1+(1,3)*XIN+1+(2,3)*V1+1+(3,3)*7 N							
END							
END							

208

SUBROUTINE NAME	74/74	CP1=1	F*H 4.54.14	11/05/77	1.12.37	PAGE	1
SUBROUTINE X103							
COMMON/ITERATE(3,3)							
V1=1+(1,1)*XIN+1+(2,1)*V1+1+(3,1)*7 N							
V2=1+(1,2)*XIN+1+(2,2)*V1+1+(3,2)*7 N							
V3=1+(1,3)*XIN+1+(2,3)*V1+1+(3,3)*7 N							
END							
END							